PEPITEM, A REGULATOR OF LEUKOCYTE TRAFFICKING IN AGEING

by

Sophie Jo Hopkin

A thesis submitted to the University of Birmingham for the degree of

DOCTOR OF PHILOSOPHY

Institute of Cardiovascular Sciences

College of Medical and Dental Sciences

University of Birmingham

May 2023

ABSTRACT

With the continued advancement of modern medicine, the global ageing population is expanding. Although lifespan has been dramatically extended since the mid-1800s, preserving an individual's healthspan remains a challenge. Chronic inflammatory diseases are increasing within the older population and is in part driven by the age-related changes to the immune system (e.g. inflammageing, immunesenescence). Growing evidence suggests that ageing is associated with dysregulated leukocyte trafficking processes, which may contribute to the development of age-related inflammatory diseases. The PEPtide Inhibitor of TransEndothelial Migration (PEPITEM) is an immunoregulatory peptide that suppresses T-cell transmigration, but its ability to control T-cell trafficking in aged systems is currently unknown.

In this thesis we explored age-related and sex-specific changes to leukocyte trafficking patterns *in vivo* and *in vitro*. We found that ageing was associated with increased numbers of leukocytes within the peritoneal cavity under steady state, particularly in female mice, suggesting increased homeostatic leukocyte trafficking to this tissue. An increased inflammatory environment within the cavity and increased permeability of the peritoneal membrane vasculature likely supported increased leukocyte trafficking to this tissue in aged mice.

Using *in vitro* and *in vivo* models of acute inflammation, we next explored age-related changes to inflammatory leukocyte trafficking. We found that ageing did not affect peripheral blood lymphocyte (PBL) adhesion to nor migration across inflamed endothelial cells *in vitro,* however, changed the composition of migrating PBL. Using a model of zymosan-induced peritonitis, we found that aged mice, particularly female mice, had an exacerbated inflammatory response to zymosan challenge where

significantly more leukocytes were recruited to the peritoneal cavity. Following on from this, we demonstrated the ability of PEPITEM to control leukocyte trafficking in older mice and humans using these *in vitro* and *in vivo* models of inflammation. However, the PEPITEM pathway was evidently dysfunctional in older adults as adiponectin (initiator of the PEPITEM pathway) failed to control the transendothelial migration of PBL from older donors *in vitro*. We found that age-related changes to peripheral blood B-cells, including reduced expression of signalling components downstream of the adiponectin receptors (e.g. APPL1), led to reduced production of the PEPITEM parent protein, 14-3-3ζ, in response to adiponectin.

Thus, within this thesis, we report that age-related changes to leukocyte trafficking dynamics *in vivo* are sexually dimorphic. Using models of inflammation, we have demonstrated that PEPITEM can control the trafficking of leukocytes from older hosts. Finally, we have identified that the PEPITEM pathway is dysfunctional in older adults, which may contribute to the dysregulated leukocyte trafficking processes observed in ageing.

ACKNOWLEDGEMENTS

Firstly, thank you to the Royal Society for funding this project and supporting a costed extension to ensure this work could be carried out.

A huge thank you to Myriam Chimen for firstly allowing me the opportunity to take on this project, and then for the years of support and supervision you provided me with during the PhD. Your presence was sorely missed after your departure from UoB, but your continued support in the project was still felt. Another huge thank you goes to Asif Iqbal and Helen McGettrick for taking over the reins in the last year of the PhD. Your supervision, pressing me to write regularly, and your endless support helped me pull this thesis together. A thank you also goes to Dean Kavanagh for the many IVM studies you performed for me over the years, even with your insanely busy schedule you always found the time.

Thank you to all the blood donors who volunteered for these studies, none of the work in this thesis could have been completed without your help.

To all the people I have worked alongside in the LTG group, past and present, thank you for all your help and for the memories you have given me. Whilst this PhD has been particularly tough for me at times, your friendship and support have gotten me through it. It will be so strange not to work alongside you anymore, please know that I will miss you all dearly. Although there are too many people to name, I'd like to acknowledge a few. Thank you, Poppy, for your endless support in lab techniques (cytokine arrays, western blots), and for the entertaining lab chats during those long lab days. Jenefa, thank you so much for being my phlebotomist and for just generally helping me out so much. Abbey, without your 'put the world to rights' conversations and emotional support, I don't think I could have finished this PhD with my sanity still intact. Julia, I feel like we have ridden this PhD roller coaster together, and I thank you for all the memories you have given me (even those involving Halloween parties!).

Most importantly, I'd like to thank my family. A thank you goes to my siblings, Becky and Llyn, for always being there for me. I wouldn't be where I am today without you. Thank you, Becky, for attempting to read through this thesis before submission, it was a valiant attempt. Thank you, Jane, for your endless support and words of encouragement throughout this PhD, it has meant the world to me. Finally, a huge thank you to Jonnie – your love and friendship have seen me through the toughest of times. Plus, without you I'd probably still be manually moving cells in Excel!

Lastly, I'd just like to say that I truly put my blood, sweat and tears into this thesis!

OUTPUTS FROM THIS THESIS

First author manuscripts (accepted for publication)

Hopkin, S. J., Pezhman, L., Begum, J., Kavanagh, D., McGettrick, H. M., Iqbal, A. J., Chimen, M. (2022) Ageing modulates homeostatic leukocyte trafficking to the peritoneal cavity in a sex-specific manner. Submitted to JLB in December 2022, accepted for publication.

Other contributions to manuscripts (published or submitted)

Bourne, J., Campos, J., **Hopkin, S.**, Whitworth, K., Palis, J., Senis, Y., Rayes, J., Iqbal, A., Brill, A. (2023) Megakaryocyte NLRP3 hyperactivation induces anemia and potentiates inflammatory response in mice. Submitted to Cellular & Molecular Immunology in May 2023.

Pezhman, P., **Hopkin, S.**, Begum, J., Heising, S., Nasteska, D., Wahid, M., Rainger, G. E., Hodson, D., Iqbal, A., Chimen, M., McGettrick, H. (2023) PEPITEM modulates leukocyte trafficking to reduce obesity-induced inflammation. *Clinical & Experimental Immunology*, 212(1): 1-10

Reviews

Hopkin, S. J., Lewis, J. W., Krautter, F., Chimen, M., McGettrick, H. M. (2019) Triggering the resolution of immune mediated inflammatory diseases: Can targeting leukocyte migration be the answer? *Frontiers in Pharmacology*, 10: 184

Hopkin, S., Lord, J. M., Chimen, M. (2021) Dysregulation of leukocyte trafficking in ageing: Causal factors and possible corrective therapies. *Pharmalogical Research,* 163: 105323

Oral Presentations

BMVBS Virtual Conference, Age-associated impairment of the PEPITEM pathway: Implications for lymphocyte transendothelial migration, UK (2021)

BIRA Virtual Conference, Age-associated impairment of the PEPITEM pathway: Implications for lymphocyte transendothelial migration, UK (2021)

WCI, Age-associated dysregulation of leukocyte trafficking during acute inflammation: A potential therapeutic role for PEPITEM?, Italy (2022)

MIDAS, Age-associated dysregulation of leukocyte trafficking during acute inflammation: A potential therapeutic role for PEPITEM?, UK (2022)

PEPITEM Symposium, The role of PEPITEM in ageing, UK (2023)

Poster Abstracts

BSI 2019, Regulation of leukocyte trafficking during acute inflammation: Implications of advancing age on the PEPITEM pathway, UK (2019)

CSHL – Mechanisms of Aging, Implications of ageing on homeostatic leukocyte trafficking, USA (virtual, 2020)

BSI B-cell Meeting, Age-associated impairment of the PEPITEM pathway: Implications for lymphocyte trafficking, UK (2022)

BSI 2022, Age-associated dysregulation of leukocyte trafficking: A potential therapeutic role for PEPITEM?, UK (2022)

COVID-19 MITIGATION STATEMENT

The COVID-19 pandemic significantly impacted the research originally planned for this thesis. Following the commencement of the pandemic, the *in vitro* studies were severely delayed due to the complete lack of (March 2020 - June 2020) or limited access (June 2020-July 2021) to the laboratory, the need to modify ethics and risk assessments to allow blood collection, and waiting for our older donors to complete their vaccination courses. Furthermore, the planned complementary *in vivo* studies using aged mice were severely delayed by more than 7-months, as we were forced to cull our ageing mice prior to the first lockdown (March 2020) to avoid non-compliance of the PPL. New batches of mice were purchased following the first lockdown, however, we had to wait until they reached the appropriate age (21months) before recommencing these studies. This thesis focuses on the effects of ageing on leukocyte trafficking; as such, the research relies heavily upon blood samples from older humans and *in vivo* studies utilising aged mice. The reasons stated above, and the ongoing implications of COVID-19 on donor recruitment, laboratory access, working hours within the laboratory and self-isolation periods severely delayed research needed for this thesis between March 2020 and July 2021.

CONTENTS

LIST OF FIGURES

LIST OF TABLES

ABBREVIATIONS

ABC	Age-associated B-cells
AdipoR1/2	Adiponectin receptor 1/2
AMPK	Adenosine monophosphate-activated protein kinase
APC	Antigen-presenting cells
APPL1	Adaptor protein phosphotyrosine interacting with PH domain and leucine zipper 1
AQ	Adiponectin
ATF	Activating transcription factor
BAFF	B-cell activating factor of the TNF family
BCA	Bicinchoninic acid
BCR	B-cell receptor
BEGM	Basal endothelial growth MV
BM	Bone marrow
BMDC	Bone marrow-derived dendritic cells
BMI	Body mass index
BSA	Bovine serum albumin
CAMKK	Calcium/calmodulin-dependent protein kinase kinase
cAMP	Cyclic adenosine monophosphate
CCR/CCL	C-C chemokine receptor/ligand
CD	Cluster of differentiation
CM	Central memory T-cells
CREB	cAMP response element-binding protein
CTL	Cytotoxic lymphocytes
CX3CR	C-X3-C chemokine receptor
CXCR/CXCL	C-X-C chemokine receptor/ligand
(d)LN	(draining) lymph node
DC	Dendritic cell
DMVEC	Dermal microvascular endothelial cells
EC	Endothelial cells
EDTA	Ethylenediaminetetraacetic acid
ELISA	Enzyme-linked immunosorbent assay
EM	Effector memory T-cells
ERK	Extracellular signal-regulated kinase
FCS	Fetal calf serum
FITC	Fluorescein isothiocyanate
FLT	FMS-like tyrosine kinase
FSC/SSC	Forward/side scatter
GC	Germinal centre
GCs	Germinal centres
GPCR	G-protein coupled receptor
HDBEC	Human dermal blood endothelial cells
HEV	High endothelial venules
HUVEC	Human umbilical vein endothelial cells
ICAM	Intercellular adhesion molecule
IFNγ	Interferon gamma
Ig	Immunoglobulin
IL	Interleukin
IP	Intraperitoneal

IVM	Intravital microscopy
JCV	John Cunningham virus
KLRG1	Killer cell lectin-like receptor subfamily G member 1
KO	Knock out
LAT	Linker for activation of T-cells
LC/MS	Liquid chromatography-mass spectrometry
Lck	Lymphocyte-specific protein tyrosine kinase
LFA	Lymphocyte function-associated antigen
LMW/MMW/HMW	Low/medium/high molecular weight
LPAM	Lymphocyte Peyer patch adhesion molecule
LPS	Lipopolysaccharide
MAPK	Mitogen-activated protein kinase
M-CSF	Macrophage colony-stimulating factor
MFI	Median fluorescent intensity
MHC	Major histocompatibility complex
NF-κB	Nuclear factor kappa B
NK/NKT	Natural killer cells/Natural killer T-cells
NO	Nitric oxide
nrPML	Natalizumab-related progressive multifocal leukoencephalopathy
OVA	Ovalbumin
PBL	Peripheral blood lymphocyte
PBMC	Peripheral blood mononuclear cells
PBS	Phosphate buffered saline
PBSA	PBS containing BSA
PBST	PBS-Tween
PECAM1	Platelet endothelial cell adhesion molecule 1
PEPITEM	PEPtide Inhibitor of TransEndothelial Migration
PHA	Phytohaemagglutinin
PLF	Peritoneal lavage fluid
PM	Peritoneal membrane
PPAR	Peroxisome-proliferator-activated-receptor
PSGL1	P-selectin glycosylated ligands
RA	Rheumatoid arthritis
RBC	Red blood cell
RNA	Ribonucleic acid
RT	Room temperature
S1P(R)	Sphingosine-1-phosphate (receptor)
SASP	Senescence-associated secretory phenotype
SEM	Standard error of the mean
SLE	Systemic lupus erythematosus
SLOs	Secondary lymphoid organs
SPHK	Sphingosine kinase
SPNS	Shingosine-1-phosphate transporter protein spinster homolog
STAT	Signalling transducer and activator of transcription
T1DM	Type 1 diabetes mellitus
TCR	T-cell receptor
TEMRA	Terminally differentiated effector memory T-cells re-expressing CD45RA
TF	Transcription factor
Th	Helper T-cells

TLR	Toll-like receptors
TNFα	Tumor necrosis factor alpha
Treg	Regulatory T-cell
TRITC	Tetramethylrhodamine isothiocyanate
VCAM	Vascular cell adhesion molecule
VE-cadherin	Vascular endothelial-cadherin
VLA	Very late antigen
WNV	West Nile virus
ZIP	Zymosan-induced peritonitis

FORWARDS

Chapter 1: *The material in this chapter (especially Section 1.3) draws heavily on my previously published literature review (Hopkin, Lord and Chimen, 2021) and has been adapted for this thesis.*

Chapter 3: *This chapter is an expanded version of the manuscript submitted to JLB, "Ageing modulates homeostatic leukocyte trafficking to the peritoneal cavity in a sex-specific manner".*

Chapter 6: *Some of this material draws on my previously published review (Hopkin, Lord and Chimen, 2021) and has been adapted for this thesis.*

CHAPTER 1 – GENERAL INTRODUCTION

As we age, our risk of developing inflammatory diseases increases (Yang *et al.*, 2016). Although the reasons for this remain uncertain, and are likely multi-factorial, it is known that the ageing process has a significant impact on the human immune system (Montecino-Rodriguez, Berent-Maoz and Dorshkind, 2013). Ageing is associated with the development of low-grade systemic inflammation, often referred to as 'inflammageing' (Montecino-Rodriguez, Berent-Maoz and Dorshkind, 2013), however, we do not fully understand how this affects the trafficking of leukocytes. Does the ageing process affect leukocyte trafficking patterns during health? Do these trafficking patterns change in the context of inflammation? Is there a way to re-establish younger leukocyte trafficking patterns in older hosts? As it is well known that the immune system is sexually dimorphic (Marquez *et al.*, 2020; Klein and Flanagan, 2016), do these age-related changes occur in a sex-specific manner? These are the fundamental questions that led to the establishment of this project.

This thesis investigates leukocyte trafficking under homeostatic and inflammatory conditions *in vitro* and *in vivo*, and determines how biological sex and ageing affect these processes. Within this, the question of whether regulated immune cell trafficking can be re-established in aged hosts using the immunoregulatory PEPtide Inhibitor of TransEndothelial Migration (PEPITEM) pathway is also explored.

1.1 AGEING

Ageing is defined as the gradual deterioration of physiological processes that leads to an increased risk of mortality (Jayanthi, Joshua and Ranganathan, 2010). The characteristics of ageing include a loss of skin elasticity, cognitive decline, organ dysfunction, and increased frailty (Balcombe and Sinclair, 2001). Ageing is, almost, a

universal phenomenon that is the cumulative result of environmental, genetic, and epigenetic events over time (Jayanthi, Joshua and Ranganathan, 2010; Franceschi and Campisi, 2014).

In 2019, the number of adults aged 65 years or over reached 703 million worldwide, a number expected to increase to over 1.5 billion by 2050 (United Nations, 2019). In the UK, approximately ⅕th of the population is currently aged 65 years or over, which is expected to increase to ¼ by 2043 (UK Parliament, 2021). Sexual dimorphism exists within the ageing process of humans, as women tend to outlive men (Hossin, 2021; Naghavi *et al.*, 2015). As older adults have an increased risk of developing debilitating diseases (Yang *et al.*, 2016; Syed *et al.*, 2022), especially older women (Crimmins *et al.*, 2019), there is a great need to further our understanding of the biological mechanisms of ageing in both male and female systems, and how this can impede on the healthspan of an individual.

Chronological ageing is defined as the passage of time from birth onwards, whilst biological age relates to the establishment of pathological cellular processes (Balcombe and Sinclair, 2001). In 2013, nine hallmarks of biological ageing were proposed for mammals, which contribute to, and collectively determine, the chronological ageing phenotype (Lopez-Otin *et al.*, 2013). These hallmarks relate to the accumulation of genetic damage (genomic instability, telomere attrition, epigenetic alterations), the dysfunction of metabolic processes (loss of proteostasis, deregulated nutrient-sensing, mitochondrial dysfunction) and the changes to cellular responses (cellular senescence, stem cell exhaustion, altered intracellular communication) that occur during ageing (Lopez-Otin *et al.*, 2013). In 2023, a further three hallmarks of ageing have been proposed, namely disabled macroautophagy, chronic inflammation,

and dysbiosis (**Figure 1-1**) (Lopez-Otin *et al.*, 2023). Indeed, several studies have reported an age-related decline in autophagic activity in yeast, nematodes, flies and mammals, likely contributing to the accumulation of damaged macromolecules in ageing (Barbosa, Grosso and Fader, 2018). Importantly, the accumulation of damaged molecular material can drive the establishment of neurodegenerative disease and cancer in older hosts (Mehrpour *et al.*, 2010). Improving the autophagic activity of cells may therefore mitigate some of the effects of ageing. In agreement with this, Pyo and colleagues reported that overexpression of Atg5, a protein involved in autophagosome formation, in 18-month transgenic C57Bl6 mice promoted autophagy across multiple tissue types, improved insulin sensitivity, and extended lifespan compared to wildtype controls (Pyo *et al.*, 2013).

Another major hallmark of ageing is the development of cellular senescence (Lopez-Otin *et al.*, 2023). Senescence is an anti-tumour mechanism originally described in human fibroblasts in 1961 when it was observed that cells in culture were unable to replicate indefinitely, therefore reducing the risk of malignant transformations (Hayflick and Moorhead, 1961). Senescent cells are quiescent but metabolically highly active, secreting a mix of pro-inflammatory cytokines, matrix metallopeptidases and growth factors termed the senescence associated secretory phenotype (SASP), and contribute to the development of inflammageing (Lopez-Otin *et al.*, 2013; Coppe *et al.*, 2010; Xu and Larbi, 2017). The accumulation of senescent cells is well documented (van Deursen, 2014), with treatments that target senescent cells (senolytics/senomorphics) proving to be effective anti-ageing agents (Di Micco *et al.*, 2021). Ultimately, each of these hallmarks of ageing contribute to the age-related

decline in immune system function, reducing both the healthspan and lifespan of older individuals (Lopez-Otin *et al.*, 2013; Fulop *et al.*, 2017; Lopez-Otin *et al.*, 2023).

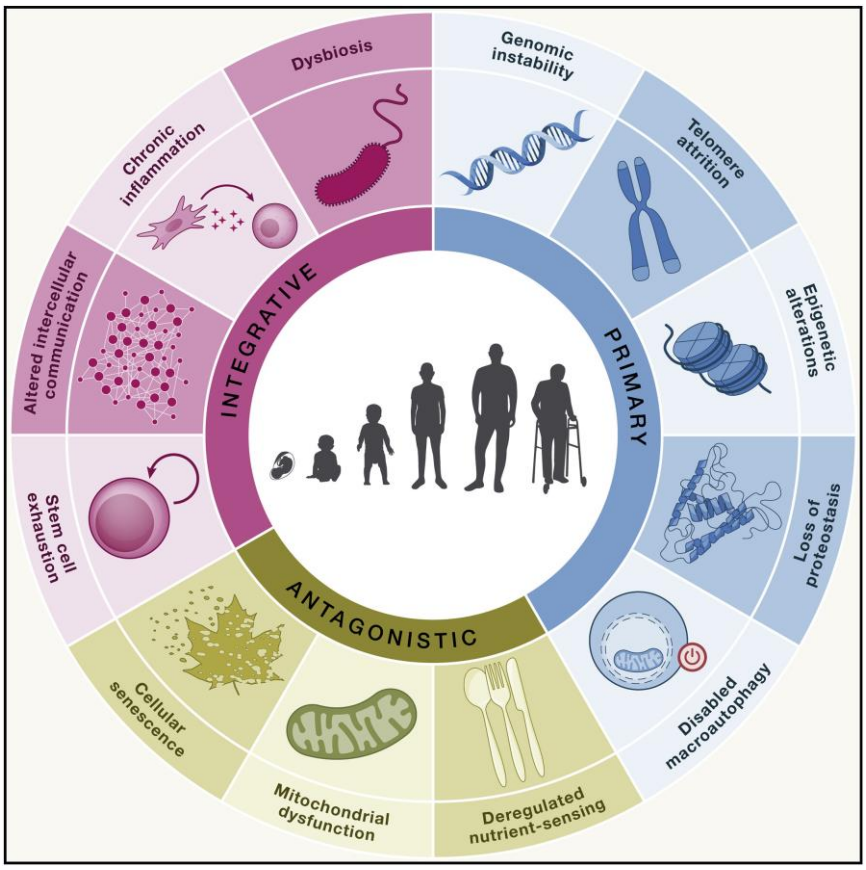

Figure 1-1 The twelve hallmarks of ageing

A schematic depicting the twelve hallmarks of ageing. These include primary (genomic instability, telomere attrition, epigenetic alterations, loss of proteostasis, disabled macroautophagy), antagonistic (cellular senescence, mitochondrial dysfunction, deregulated nutrient-sensing), and integrative (stem cell exhaustion, altered intercellular communication, chronic inflammation, dysbiosis) hallmarks. Taken from Lopez-Otin *et al.*, 2023 .

1.2 OVERVIEW OF THE AGEING ADAPTIVE IMMUNE SYSTEM

To protect the host from a range of biological threats and to maintain normal homeostasis, the immune system has evolved two arms of defence; the innate and adaptive immune systems (Chaplin, 2010). Whilst the innate immune system is operational from birth and provides broad immunity, the focus of this thesis will be on the adaptive immune system; a system that develops over the course of the host's lifetime and provides targeted immunity to specific pathogens (Simon, Hollander and McMichael, 2015).

Ageing profoundly affects the mammalian immune system. Older mice and humans exhibit increased circulating levels of pro-inflammatory mediators (Fagiolo *et al.*, 1993; Ershler and Keller, 2000; Hu *et al.*, 2017), and changes to immune cell function (Pereira *et al.*, 2020; Nakajima *et al.*, 2002; Nicoletti *et al.*, 1991; Mogilenko *et al.*, 2021) compared to their younger counterparts. Although it has been well established that immune responses are sexually dimorphic in both humans and mice (Marquez *et al.*, 2020), the majority of *in vivo* studies underpinning immunological research to date either use a mixture of male and female participants or solely use male participants in their investigations (Lee, 2018); therefore, how sex specifically affects age-related changes to the immune system has been severely under-researched. Whether age-related changes to the immune system are more pronounced in male or female systems is still debated (Gubbels Bupp, 2015; Rubtsov *et al.*, 2011), and it is not known to what extent hormones, sex chromosomes, or gender-dependent environmental cues influence the ageing immune system (Gubbels Bupp, 2015).

Although inflammatory responses are necessary for the protective and tissue regenerative effects of the immune system, the chronic yet dysfunctional inflammatory responses that occur as a result of the ageing process can lead to tissue damage and disease (Chung *et al.*, 2019). Indeed, older adults present with immune system dysfunction as they exhibit vaccine hyporesponsiveness, and are at greater risk of developing infections, malignancies and inflammatory diseases compared to younger adults (Derhovanessian *et al.*, 2008; Goncalves, Mitchell and Lord, 2016; Lord, 2013). Ultimately, the immunesenescence that is associated with the ageing process impedes the healthspan and lifespan of the individual (Hazeldine and Lord, 2015; Fulop *et al.*, 2017). How ageing specifically affects the adaptive immune system is described below.

1.2.1 LYMPHOCYTES

The major cellular players of the adaptive immune system are T- and B-cells, a group of white blood cells that are collectively known as lymphocytes along with natural killer cells (NK) and NKT-cells (Chaplin, 2010). In health, lymphocytes account for approximately 70-90% of peripheral blood mononuclear cells (PBMC) in young adults (Kleiveland, 2015). Within the circulating lymphocyte population of young adults, 70-85% are $CD3^+$ T-cells, 5-10% are $CD19^+$ B-cells and 5-20% are $CD56^+$ NK cells (Kleiveland, 2015).

It has been well-established that ageing modulates the circulating proportions of major lymphocyte populations (**Table 1-1**). Several cross-sectional studies using multiple methodologies including single-cell RNA sequencing, mass cytometry, and flow cytometry report an age-associated reduction in the frequency of B-cells, naïve $CD4^+$ and $CD8^+$ T-cells, and an increased frequency of NK cells and monocytes in the

blood of older individuals compared to younger individuals (Zheng *et al.*, 2020; Le Garff-Tavernier *et al.*, 2010; Sansoni *et al.*, 1993; Huang *et al.*, 2021). Using single-cell RNA sequencing and mass cytometry, Zheng *et al.* reported a reduced frequency of circulating T- and B-cells in the blood of older (>60 years) adults compared to young (<45 years), and an increased frequency of circulating monocytes (Zheng *et al.*, 2020). Huang *et al.* found that the frequency of circulating NK cells, $CD4^+$ and $CD8^+$ naïve T-cells was reduced, and the frequency of circulating monocytes was increased in the blood of older (>60 years) adults compared to young (<30 years) adults following single-cell RNA sequencing analysis of the PBMC populations (Huang *et al.*, 2021). Using flow cytometric analysis, Le Garff-Tavernier *et al.* reported reduced numbers of B-cells, but not T-cells, in the blood of older (>60 years) adults compared to young (<60 years) adults (Le Garff-Tavernier *et al.*, 2010).

In contrast, a longitudinal study reported no effect of ageing on proportions of circulating lymphocytes using flow cytometric analysis, however, this study was relatively short with only 5 years between baseline and follow-up sample collection (Lin *et al.*, 2016). Indeed, by using mass cytometric analysis, the longitudinal IMM-AGE study reported an increased frequency of circulating monocytes and a reduced frequency of circulating lymphocytes in the blood of older (60-96 years) men and women over the course of 7 years (Alpert *et al.*, 2019). Additionally, many of the studies mentioned so far did not consider the sex of the subjects (Le Garff-Tavernier *et al.*, 2010; Sansoni *et al.*, 1993) or used mixed-sex subjects (Zheng *et al.*, 2020; Lin *et al.*, 2016; Alpert *et al.*, 2019) when investigating the impact of ageing on circulating PBMC populations. The age-related changes to lymphocyte populations in the blood may be sex-dependent as the reported age-related reduction in the frequency of circulating B-

cells is only statistically significant for older men (Marquez *et al.*, 2020; Yan *et al.*, 2010; Colonna-Romano *et al.*, 2002; Hirokawa *et al.*, 2013). Using flow cytometric analysis of the PBMC populations, Marquez *et al.* reported an age-related reduction in the frequency of $CD19^+$ B-cells in the blood of older (>65 years) men compared to young (<40 years), whilst Yan *et al.* and Hirokawa *et al.* reported an age-related decline in the proportion of circulating $CD20^+$ B-cells in men aged 20-80^+ years (Marquez *et al.*, 2020; Yan *et al.*, 2010; Hirokawa *et al.*, 2013). Additionally, Huang *et al.* found that older men had increased proportions of monocytes within the PBMC compartment compared to older women (Huang *et al.*, 2021). To determine the impact of chronological age and sex on circulating lymphocyte populations, a longer longitudinal study stratified according to the sex of the subjects is needed.

Lymphocytes undergo several rounds of extensive cell division to exert their protective immune functions, however, this ultimately drives lymphocytes towards cellular senescence (Heath and Grant, 2020). Senescent lymphocytes accumulate with age in mice and humans (Shimatani *et al.*, 2009; Hao *et al.*, 2011; Effros *et al.*, 1994; Colonna-Romano *et al.*, 2009), and possess altered immune functions that impede protective immunity (reviewed by Akbar, Henson & Lanna, 2016, and Frasca, 2018). How ageing affects the function and trafficking patterns of different lymphocyte populations, including senescent lymphocytes, is described below.

Table 1-1 The reported effects of ageing on different PBMC populations

PBMC population	Effect of ageing	For which sex	Methodology used	Reference
Monocytes	Increased frequency	Men and women	Mass cytometry and scRNA seq	Alpert *et al.*, 2019; Zheng *et al.*, 2020
	Increased frequency	Men only	scRNA seq	Huang *et al.*, 2021
	No effect	Men and women	Flow cytometry and scRNA seq	Marquez *et al.*, 2020
NK cells	Increased frequency	Men and women	Flow cytometry and scRNA seq	Zheng *et al.*, 2020; Marquez *et al.*, 2020; Le Garff-Tavernier *et al.*, 2010
	Increased frequency	Men only	Flow cytometry	Yan *et al.*, 2010
	Increased frequency	Women only	Flow cytometry	Hirokawa *et al.*, 2013
	No effect	Men and women	Flow cytometry and mass cytometry	Alpert *et al.*, 2019; Lin *et al.*, 2016
T-cells	Reduced frequency	Men and women	Flow cytometry, scRNA seq and mass cytometry	Alpert *et al.*, 2019; Zheng *et al.*, 2020; Marquez *et al.*, 2020
	Reduced frequency	Men only	Flow cytometry	Hirokawa *et al.*, 2013
	No effect	Men and women	Flow cytometry	Le Garff-Tavernier *et al.*, 2010; Yan *et al.*, 2010; Lin *et al.*, 2016
B-cells	Reduced frequency	Men and women	Flow cytometry and scRNA seq	Zheng *et al.*, 2020; Le Garff-Tavernier *et al.*, 2010
	Reduced frequency	Men only	Flow cytometry and scRNA seq	Marquez *et al.*, 2020; Yan *et al.*, 2010; Hirokawa *et al.*, 2013
	No effect	Men and women	Flow cytometry and mass cytometry	Alpert *et al.*, 2019; Lin *et al.*, 2016
	No effect	Women only	Flow cytometry and scRNA seq	Marquez *et al.*, 2020

A summary of the observed age-related changes to different PBMC populations in men and women along with the methodology used. scRNA seq, single-cell RNA sequencing.

1.2.2 T-CELLS

T-cells play a fundamental role in adaptive immunity, through orchestrating highly specific and long-lasting immune responses to pathogens and malignancies (Chaplin, 2010). To achieve this, each T-cell is equipped with a unique antigen-specific receptor,

namely the T-cell receptor (TCR), which is able to provide targeted immunity towards specific immune stimuli (Fabbri, Smart and Pardi, 2003). T-cells play various roles in the progression of adaptive immune responses and can be divided into several subsets depending on specific immune functions, antigen experience, exposure to specific cytokines, and the distinct patterns of Cluster of Differentiation (CD) proteins expressed on the extracellular surface (Chaplin, 2010; Jameson and Masopust, 2018; Kumar, Connors and Farber, 2018).

Although all mature T-cells express CD3 (Germain and Stefanova, 1999), the immune properties of T-cells can be largely distinguished based on CD4 and CD8 expression. $CD4^+$ T-cells largely confer immunity through coordinating the immune responses of other leukocytes, whilst $CD8^+$ T-cells provide immunity through their cytotoxic functions (Kumar, Connors and Farber, 2018). The five major T-cell subsets discussed in this thesis are $CD4^+$ and $CD8^+$ naïve, central memory (CM), effector memory (EM), regulatory (Treg), and senescent T-cells where the CD markers used to identify each T-cell subset is listed in **Table 1-2**. The functions, trafficking patterns of and age-related changes to each T-cell subset are described below.

1.2.2.1 NAÏVE T-CELLS

T-cells originate from hematopoietic stem cells found in the bone marrow (BM), which differentiate into lymphoid progenitors and relocate to the thymus for maturation (Moroy and Karsunky, 2000; Germain, 2002). During this process, T-cells acquire an antigen-specific TCR and the ability to distinguish between self from non-self, ensuring the establishment of self-tolerance in conjunction with antigen-specificity (Moroy and Karsunky, 2000; Germain, 2002). Mature T-cells exit the thymus as antigen-inexperienced $CD4^+$ or $CD8^+$ naïve T-cells, where they recirculate between the blood,

secondary lymphoid organs (SLOs), and the lymphatic network every 12-24 hours to maximise their chances of encountering cognate antigen (Gowans, 1959; Mackay, Marston and Dudler, 1990).

Thymic involution is an inevitable part of the ageing process, which consequently results in reduced naïve T-cell output (Mackall *et al.*, 1995). The drivers of thymic involution are varied and include the presence of sex steroids, adipocyte expansion, and changes to the balance of intrathymic cytokines (Lynch *et al.*, 2009; Dooley and Liston, 2012). For example, increased thymic levels of IL-6 and leukemia inhibitory factor (LIF), and reduced IL-7 levels have been associated with thymic involution in older mice and humans (Sempowski *et al.*, 2000; Sempowski *et al.*, 2002; Thomas, Wang and Su, 2020). As a consequence of age-related thymic involution, older adults (>60 years) exhibit reduced frequencies of naïve T-cells in the circulation compared to younger (<45 years) adults (Yan *et al.*, 2010; Zheng *et al.*, 2020). The importance of maintaining thymic function is obvious from studies utilising athymic mice, which under normal living conditions had a reduced lifespan (De Sousa, Parrott and Pantelouris, 1969; Flanagan, 1966). Additionally, naïve T-cells isolated from older hosts appear dysfunctional (Kohler *et al.*, 2005; Naylor *et al.*, 2005; Haynes *et al.*, 2003; Kang *et al.*, 2004; Goronzy *et al.*, 2015; Clise-Dwyer *et al.*, 2007). Naïve $CD4^+$ T-cells isolated from older (>18 months) mice were more prone to apoptosis *ex vivo* following antigen stimulation compared to those isolated from young (<3 months) mice, which led to defective cytokine responses and a poorer ability to transition into memory T-cells (Mattoo *et al.*, 2009). Indeed, in response to a tick-borne encephalitis virus vaccine, $CD8^+$ naïve T-cells derived from older (>70 years) adults displayed reduced priming capabilities compared to those isolated from middle-aged (20-50 years)

individuals *in vitro*, which was associated with altered naïve-memory T-cell differentiation and poorer antibody responses (Briceno *et al.*, 2016). Several studies have also indicated that the post-thymic proliferation of $CD4^+$ and $CD8^+$ naïve T-cells in older humans and mice causes the contraction of the TCR repertoire (Kohler *et al.*, 2005; Naylor *et al.*, 2005; Ahmed *et al.*, 2009), contributing to the age-related decline in T-cell function (Goronzy *et al.*, 2015). Thymic involution and, in turn, the contraction in the size and diversity of the naïve T-cell pool that occurs with ageing impedes both the cellular and humoral arms of the adaptive immune response and increases the risk of host mortality (Lischner and DiGeorge, 1969).

1.2.2.2 EFFECTOR T-CELLS

T-cell activation is triggered upon TCR engagement with its cognate antigen (**Figure 1-2**). Once activated, naïve $CD4^+$ and $CD8^+$ T-cells differentiate into their corresponding effector T-cells, namely helper T-cells (Th) and cytotoxic T-lymphocytes (CTL), respectively (Luckheeram *et al.*, 2012; Zhang and Bevan, 2011). Effector T-cells undergo clonal expansion during the early phase of inflammation and exert their effector functions to facilitate immune responses and clearance of the inflammatory stimulus (Luckheeram *et al.*, 2012; Zhang and Bevan, 2011). Th cells polarise the immune response against specific pathogens through secretion of particular cytokines e.g. Th1 cells secrete interferon gamma (IFNγ) to promote anti-viral responses (Romagnani, 2000; Luckheeram *et al.*, 2012), whilst CTL elicit direct killing and removal of infected, damaged or malignant cells through exerting cytotoxic functions (Zhang and Bevan, 2011).

Newly formed effector T-cells exit SLOs and traffic to sites of inflammation where they can exert their effector functions (Groom *et al.*, 2012; Agace, 2006). The

specific trafficking patterns of effector T-cells is largely dictated by the site of priming (Iwata *et al.*, 2004; Dudda, Simon and Martin, 2004; Ferguson and Engelhard, 2010). For example, in mice, administration of ovalbumin (OVA)-specific BM-derived dendritic cells (BMDC) via the intraperitoneal route gave rise to lymphocyte Peyer patch adhesion molecule (LPAM)-1^{+} P-selectin ligand^{+} CD8^{+} T-cells which homed to the mesenteric lymph nodes (LN) (Ferguson and Engelhard, 2010). However, administration of the same OVA-specific BMDC via the intravenous route gave rise to LPAM-1^{-} P-selectin ligand^{+} CD8^{+} T-cells which homed to the spleen (Ferguson and Engelhard, 2010). Therefore the phenotype, functions and trafficking patterns of activated T-cells depend on the specific activation signals received by the T-cell and the route of antigen entry into the body.

The age-associated decline in naïve T-cell output and functionality (see section 1.2.2.1) results in a reduced pool of T-cells that can differentiate into effector T-cells in older hosts (Thome *et al.*, 2016; Pfister *et al.*, 2006; Nikolich-Zugich, 2008). Consequently, the frequency of effector T-cells in the circulation of older (>61 years) adults is reduced compared to younger (<40 years) adults (van der Geest *et al.*, 2014). These processes are reflected in murine models, as the ability of naïve T-cells to give rise to effector T-cells is evidently impaired in older mice (Haynes *et al.*, 1999; Garcia and Miller, 2001). For example, the number of naïve CD4^{+} T-cells isolated from older (>18 months) mice that can form immunological synapses with antigen-presenting cells (APC) was two-fold lower than those isolated from younger (<8 months) mice, thus leading to reduced levels of T-cell activation (Garcia and Miller, 2001). Reduced activation of older naïve T-cells is, in part, due to defective intracellular signalling downstream of the TCR and shorter telomere lengths (Garcia and Miller, 2002).

Indeed, naïve T-cells isolated from older mice exhibited altered cytoskeletal arrangements, and delayed recruitment of lymphocyte-specific protein tyrosine kinase (Lck) and linker for activation of T-cells (LAT), signalling molecules downstream of the TCR, to lipid rafts compared to younger mice (Garcia and Miller, 2002). Furthermore, naïve T-cells isolated from older (>18 months) mice have been observed to undergo apoptosis in response to anti-CD3 and anti-CD28 monoclonal antibody activation signals *in vitro* (Mattoo *et al.*, 2009). Finally, the homeostatic proliferation of effector T-cell populations in the periphery drive telomere attrition and modulated T-cell responses in older hosts (den Braber *et al.*, 2012; Westera *et al.*, 2015; Rufer *et al.*, 1999; Goronzy and Weyand, 2019). Indeed, $CD45RA^{+}CCR7^{-}CD57^{+}$ T-cells derived from younger (<60 years) adults had shorter telomeres and produced less IFNγ following *in vitro* stimulation with phytohaemagglutinin (PHA) compared to $CD45RA^{+}CCR7^{-}CD57^{-}$ T-cells (Verma *et al.*, 2017). Collectively these data support the notion that, following the attrition of the naïve T-cell pool in ageing, the remaining naïve T-cells are dysfunctional and exhibit a reduced ability to differentiate into effector T-cells upon activation (**Figure 1-2**); consequently impeding the immunoprotective functions of the immune system in older hosts.

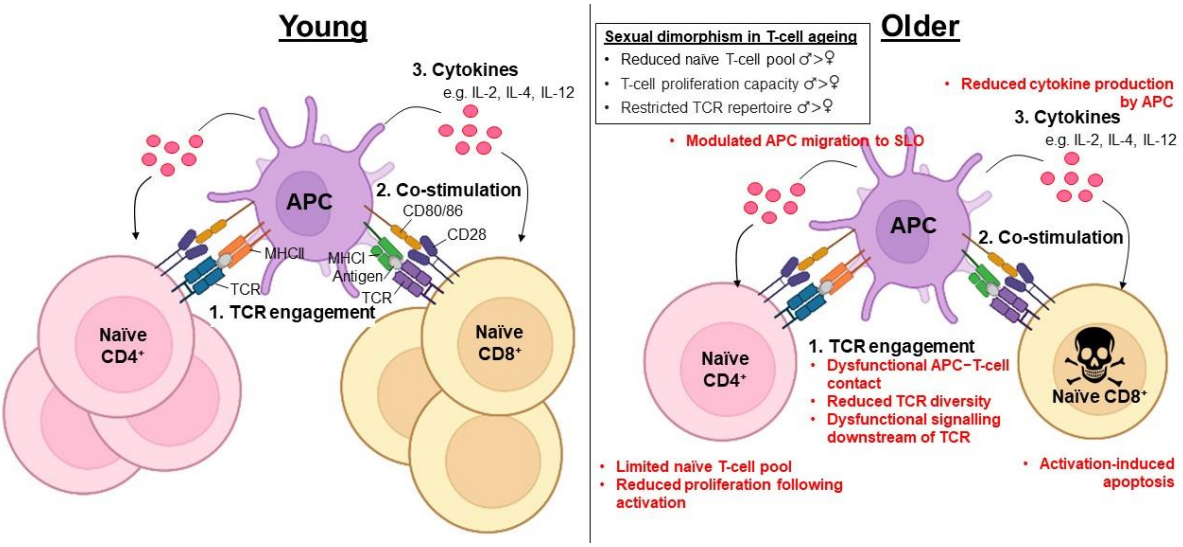

Figure 1-2 Effects of ageing and sex on T-cell activation

T-cell activation primarily consists of three steps: 1) T-cell receptor (TCR) engagement with antigen bound to major histocompatibility complex I or II on the surface of antigen presenting cells (APC); 2) Engagement of co-stimulatory molecules e.g. CD28 (T-cell) and CD80/86 (APC); 3) Cytokine signals from the APC programme T-cell activation and skew T-cell differentiation towards a particular phenotype e.g. IL-4 promotes $CD4^+$ T-cell differentiation into Th2 cells. The effects of ageing on T-cell activation are depicted and include an age-related decline in the naïve T-cell pool, a restricted TCR repertoire, and modulated APC functions. Sexual dimorphism is evident in some of these age-related changes to T-cell activation. Created using Biorender.com

1.2.2.3 MEMORY T-CELLS

Once the inflammatory response subsides, for example after the successful clearance of a pathogen, a period of T-cell contraction ensues where most effector T-cells undergo apoptosis (Chaplin, 2010). However, a small proportion of antigen-specific effector T-cells survive and differentiate into EM and CM T-cells (Kumar, Connors and Farber, 2018; Kaech, Wherry and Ahmed, 2002). Memory T-cells represent the major circulating population in adult blood and serve an important immune function: to provide rapid, long-lasting, and specific immunity against previously encountered pathogens (Kumar, Connors and Farber, 2018).

Whilst both EM and CM T-cells become activated and exert their immune functions upon re-encounter with their cognate antigens, they differ in terms of their trafficking patterns (Masopust and Schenkel, 2013). CM T-cells populate SLOs, whilst EM T-cells circulate between the blood and peripheral tissues (Masopust and Schenkel, 2013). EM T-cells are therefore more likely to recognise their cognate antigen following re-infection with a previously encountered pathogen, and thus exhibit more diverse effector functions compared to CM T-cells (Hamann *et al.*, 1997). However, despite a shift towards a memory phenotype within the ageing immune system (Lerner, Yamada and Miller, 1989; Ernst *et al.*, 1990; Linton *et al.*, 2005), antigen-specific EM T-cell numbers decline with age (Willinger *et al.*, 2005). To ensure that immunological memory against specific pathogens prevails over time, CM T-cells exhibit strong survival traits, such as an increased proliferative capacity and a resistance to apoptosis, to ensure CM T-cell numbers are maintained within lymphoid tissues (Willinger *et al.*, 2005; Martin and Badovinac, 2018).

In humans, there is a third memory T-cell subset: the terminally differentiated effector memory T-cells re-expressing CD45RA (TEMRA; $CD45RA^{+}CCR7^{-}$) (Pilling *et al.*, 1996; Faint *et al.*, 2001). The majority of TEMRA are $CD8^{+}$ with heightened cytotoxic abilities (Rufer *et al.*, 2003; Hamann *et al.*, 1997) and senescence-like traits, including a SASP (Callender *et al.*, 2018), shortened telomeres and a reduced proliferative capacity (Kumar, Connors and Farber, 2018; Geginat, Lanzavecchia and Sallusto, 2003; Verma *et al.*, 2017). The precise trafficking patterns of TEMRA have not been extensively studied, however, they are believed to behave similarly to EM T-cells (Tian *et al.*, 2017) and recirculate between the blood and peripheral tissues (Buggert *et al.*, 2020; Setoguchi, 2016). Indeed, as well as expressing high levels of PD-1 signifying cellular exhaustion (Parry *et al.*, 2021; Henson *et al.*, 2015), TEMRA express high levels of lymphocyte function-associated antigen 1 (LFA-1) and low levels of C-C chemokine receptor 7 (CCR7) facilitating their trafficking within the periphery (Faint et al 2001). Although our understating of TEMRA is currently limited, including an understanding of their developmental origins and effector immune functions, TEMRA are believed to be an adapted memory T-cell subset that serves to control persistent viral infections and is a population that accumulates with age in humans (Weltevrede *et al.*, 2016).

With age, the memory T-cell pool expands (Lerner, Yamada and Miller, 1989; Ernst *et al.*, 1990; Nikolich-Zugich, 2008). The increasing number of memory T-cells in aged mice and humans are primarily $CD8^{+}$, as the reactivation of persistent viral infections is one of the major age-related drivers of memory T-cell expansion (Solana *et al.*, 2012; Fulop, Larbi and Pawelec, 2013). Furthermore, memory T-cells in older hosts exhibit functional changes (Nagel *et al.*, 1988; Haynes *et al.*, 2003; Roberts, Ely

and Woodland, 2005). Memory T-cells generated from naïve T-cells isolated from older (>14 months) mice proliferated less, generated fewer cytokines upon activation, and had a reduced cognate helper function compared to memory T-cells generated from naïve T-cells isolated from young (<4 months) mice (Haynes *et al.*, 2003). Additionally, memory T-cells isolated from older (>60 years) individuals were less responsive to interleukin 2 (IL-2) stimulation, the cytokine which promotes T-cell growth and proliferation in response to antigen, *in vitro* compared to those isolated from younger (<40 years) individuals (Nagel *et al.*, 1988). Therefore, although memory T-cells accumulate with age, they are functionally distinct from their younger counterparts.

1.2.2.4 REGULATORY T-CELLS

Treg are an immunoregulatory population of T-cells that modulate the immune responses of other leukocytes to maintain peripheral tolerance, limit chronic inflammation and prevent the establishment of autoimmune diseases (reviewed by Vignali, Collison and Workman, 2008). Following their development in the thymus or induction in the periphery, activated Treg suppress other T-cells through mopping up pro-proliferative cytokine IL-2 (Tang and Bluestone, 2008), secreting anti-inflammatory cytokines and inducing apoptosis in effector T-cells (Shevach, 2009).

Upon emigration from the thymus, Treg, equipped with CCR7 and L-selectin, follow a C-C chemokine ligand 19 (CCL19) gradient and traffic to SLOs to exert their immune suppressive functions (Lim, Hillsamer and Kim, 2004; Ochando *et al.*, 2005). Mature Treg can migrate to and take up residency within peripheral tissues (Curiel *et al.*, 2004; Stephens *et al.*, 2001; Zou *et al.*, 2004), although the exact chemotactic mechanisms for this under homeostatic conditions is unclear.

In ageing, the frequency of Treg increases in the circulation of humans (Lages *et al.*, 2008; Gregg *et al.*, 2005) and within multiple tissues of mice (Zhao *et al.*, 2007; Fulop *et al.*, 2017). The accumulation of Treg in ageing plays a deleterious role in the inflammatory responses of older hosts as Treg impair anti-tumour immunity (Ruby and Weinberg, 2009; Sharma, Dominguez and Lustgarten, 2006) and immune responses following vaccination (van der Geest *et al.*, 2014) in older mice and humans. Indeed, Treg appear to be hyperactive in older hosts and possess increased immunosuppressive capabilities (Garg *et al.*, 2014; Lages *et al.*, 2008; Rosenkranz *et al.*, 2007). Treg isolated from older (>18 months) C57Bl6 mice had a greater ability to suppress effector T-cells *in vitro* through reducing extracellular cysteine availability and secreting higher levels of IL-10 compared to Treg isolated from younger (<4 months) mice (Garg *et al.*, 2014). The depletion of $CD25^+$ cells, including Treg, in 18-20 month BALB/c mice by intravenous delivery of an anti-CD25 monoclonal antibody improved anti-tumour immune responses in the aged host, including T-cell cytotoxicity and the generation of immunological memory (Sharma, Dominguez and Lustgarten, 2006). In humans, $CD25^+$ cell depletion from T-cells isolated from the blood of older (>70 years) donors improved T-cell proliferation in response to PHA, indicating improved effector T-cell activation (Lages *et al.*, 2008). The age-related accumulation of Treg in older individuals is therefore detrimental to the protective functions of the immune system and targeting these cells may prove beneficial in restoring protective immune responses, at least in the short term.

1.2.2.5 AGE-ASSOCIATED AND SENESCENT T-CELL POPULATIONS

Ageing profoundly affects T-cells as they are driven towards cellular senescence (reviewed by Chou and Effros, 2013; Pangrazzi and Weinberger, 2020; Mittelbrunn

and Kroemer, 2021). At birth, most T-cells express the co-stimulatory receptor, CD28 (Azuma, Phillips and Lanier, 1992). However, by 80 years of age, CD28 expression is drastically reduced on T-cells, especially on $CD8^+$ T-cells (Brzezinska *et al.*, 2004; Weyand *et al.*, 1998; Fagnoni *et al.*, 1996). Ageing T-cells also lose CD27 expression, an additional costimulatory molecule (Larbi and Fulop, 2014), and gain many NK markers, such as CD57, an NK maturity antigen, and killer cell lectin-like receptor subfamily G member 1 (KLRG1), a co-inhibitory receptor that serves to inhibit NK function (Brenchley *et al.*, 2003; Voehringer, Koschella and Pircher, 2002). KLRG1 expression on circulating $CD8^+$ T-cells rises significantly from approximately 40% in young adults to over 90% in the older population (Voehringer, Koschella and Pircher, 2002; Ouyang *et al.*, 2003), whilst CD57 expression on $CD8^+CD28^-$ T-cells is positively correlated with age (Merino *et al.*, 1998).

The loss of co-stimulatory molecules and acquisition of NK markers have functional consequences for ageing T-cells, as they have a diminished capacity to upregulate activation and proliferation pathways (Topp *et al.*, 2003; Valenzuela and Effros, 2002; Henson and Akbar, 2009), are more prone to activation-induced cell death (Borthwick *et al.*, 2000), display increased cytotoxic activity (Chattopadhyay *et al.*, 2009; Pereira *et al.*, 2020) and have the shortest telomere lengths (Plunkett *et al.*, 2007; Borthwick *et al.*, 2000) compared to more youthful T-cells. Furthermore, $CD28^-$ $CD8^+$ T-cells exhibit modified gene expression of chemokines and their receptors compared to $CD28^+CD8^+$ T-cells, including increased transcription of CCL4, CCR5 and C-X3-C chemokine receptor 1 (CX3CR1) and reduced transcription of CCR6 and CCR7 (Fann *et al.*, 2005; Czesnikiewicz-Guzik *et al.*, 2008; Lazuardi *et al.*, 2009), which may limit their trafficking to sites of inflammation and SLOs. However, the point

at which these T-cells are defined as senescent according to their pattern of extracellular markers is unclear.

Currently, there is no standardisation for the definition of senescent T-cells in humans or mice using extracellular markers. Most studies to date utilise the presence or absence of the markers listed above in addition to CD45RA and CCR7 to define human senescent T-cells by flow cytometry; including $CD28^{-}CD57^{+}$ (Duggal *et al.*, 2018; Onyema *et al.*, 2015), $CD27^{-}CD28^{-}$ (Pereira *et al.*, 2020), $CD45RA^{+}CD27^{-}$ (Callender *et al.*, 2020; Riddell *et al.*, 2015; Henson *et al.*, 2015), and $CCR7^{-}CD45RA^{+}$ (Lau *et al.*, 2019) gating strategies. Although murine senescent T-cells have not been as extensively characterised as human senescent T-cells, CD153, PD-1 (Shirakawa *et al.*, 2016; Yi *et al.*, 2019; Yoshida *et al.*, 2020), and KLRG1 (Voehringer *et al.*, 2001; Beyersdorf *et al.*, 2007) have been suggested as markers for this population. The discrepancy between markers used for humans and mice could be explained by interspecies differences, and the significantly lower burden of immune challenges mice face in germ-free housing compared to humans (Masopust, Sivula and Jameson, 2017). Despite a great need for consistency in the definition of senescent T-cells between studies, no combination of extracellular markers has been proven to be the best to define this T-cell population (Rodriguez *et al.*, 2020; Xu and Larbi, 2017). To that end, in this thesis, human senescent T-cells will be identified as $CD28^{-}CD27^{-}$ or $CD57^{+}KLRG1^{+}$ cells, whilst murine senescent T-cells will be identified by positive expression of KLRG1.

Table 1-2 Extracellular markers used to define CD4+ and CD8+ T-cell subsets in humans and mice

T-cell subsets	Extracellular markers	References
Human		
Naïve	$CCR7^+CD45RA^+$	Okada *et al.*, 2008 Koch *et al.*, 2008
EM	$CCR7^-CD45RA^-$	
CM	$CCR7^+CD45RA^-$	
TEMRA	$CCR7^-CD45RA^+$	
Treg	$CD4^+CD25^+$	Wing *et al.*, 2002 ; Bryl *et al.*, 2009
Senescent T-cells	$CD27^-CD28^-$ $CD57^+KLRG1^+$	Pereira *et al.*, 2020 Ramello *et al.*, 2021
Mice		
Naïve	$CD62L^+CD44^-$	Gerberick *et al.*, 1997
EM	$CD62L^-CD44^+$	Gerberick, Cruse and Ryan, 1999
CM	$CD62L^+CD44^+$	
Treg*	$CD4^+CD25^+$	Kuniyasu *et al.*, 2000
Senescent T-cells	$KLRG1^+$	Voehringer *et al.*, 2001; Beyersdorf *et al.*, 2007

*Treg were only identified in the $CD4^+$ T-cell population.

1.2.2.6 EFFECTS OF SEX ON AGEING T-CELL POPULATIONS

The effect of biological sex on T-cell subset composition and function in older hosts has not been extensively investigated, with the majority of immunological studies generating male-biased data (reviewed by Dodd and Menon, 2022). Of the existing literature, sexual dimorphism appears to exist within the ageing T-cell compartment (Nacka-Aleksić *et al.*, 2020; Barrat *et al.*, 1997b; Hirokawa *et al.*, 2013; Goetzl *et al.*, 2010; Heng *et al.*, 2005). In dark agouti rats, older (>22 months) males exhibited more pronounced changes to $CD4^+/CD8^+$ T-cell ratios, naïve/memory T-cell ratios, and increased oxidative damage in the peripheral LN compared to older females in the context of natural ageing (Nacka-Aleksić *et al.*, 2020). In C57Bl6 mice, old (23 months) female mice had increased memory/naïve T-cell ratios in the spleen compared to old

male mice, determined by flow cytometry (Barrat *et al.*, 1997b). In humans, the age-related decline in circulating naïve T-cells (Hirokawa *et al.*, 2013; Gubbels Bupp, 2015) and increase in circulating senescent $CD8^+$ effector T-cells is greater in older men (>60 years) compared to older women (Ritzel *et al.*, 2016). Furthermore, poorer T-cell proliferative responses to anti-CD3 monoclonal antibody stimulation *in vitro* (Hirokawa et al., 2013), poorer IFNγ and IL-17 cytokine production (Goetzl *et al.*, 2010), and a greater restriction in the TCR repertoire (Yager *et al.*, 2008) was observed in T-cells isolated from older men (>60 years) compared to older women. However, T-cells isolated from older (>60 years) women exhibited poorer production of IL-2 and increased production of IFNγ in response to anti-CD3 and anti-CD28 monoclonal antibodies *in vitro* compared to T-cells isolated from older men (Goetzl *et al.*, 2010; Barrat *et al.*, 1997a). Therefore, both biological sex and chronological ageing affect T-cell subset composition within tissues of humans and mice, and more importantly, both variables affect T-cell activation/responses.

Interestingly, there is a series of studies describing the benefits of sex-steroid ablation on improving thymic regeneration and T-cell responses in older mice and humans (Sutherland *et al.*, 2005; Heng *et al.*, 2005; Heng *et al.*, 2012). Heng *et al.* demonstrated that sex-steroid ablation by means of surgical castration or ovariectomy increased thymic cell population numbers, specifically T-cells, in aged (24 months) male and female mice, respectively, after just two weeks (Heng *et al.*, 2012). What more, surgical castration of aged male mice resulted in increased frequencies of naïve T-cells in the spleen after 6 weeks and restored $CD8^+$ T-cell anti-influenza A and anti-tumour immune responses to more youthful levels (Heng *et al.*, 2012).

Both male and female sex steroids have been reported to influence thymic involution in mice and humans (Sutherland *et al.*, 2005). Androgens and oestrogens interact with thymic epithelial cells via their reciprocal receptors to promote thymic development but also to drive thymic atrophy (Staples *et al.*, 1999; Olsen *et al.*, 2001). Using selective androgen receptor knock-out (ARKO) mice, Lai *et al.* reported normal thymic involution in thymocyte ARKO and fibroblast ARKO mice but increased thymic size in thymic epithelial cell ARKO mice (Lai *et al.*, 2013). Similarly, oestrogen receptor α knock-out mice were partially protected from thymic atrophy after 8 days of exogenous oestrogen administration compared to wildtype controls (Wang *et al.*, 2008a). Interestingly, sexual dimorphism in thymic atrophy is evident from mouse studies, where female mice are reported to be more resistant to thymic involution and retain thymic cellularity compared to male mice, highlighting the major role for androgens in thymic atrophy (Pido-Lopez, Imami and Aspinall, 2001; Aspinall and Andrew, 2001; Hun *et al.*, 2020).

Although the association between sex steroid levels and thymic involution has been well described, sex steroid levels are not believed to play a direct role in thymic involution. This is due to several observations, including the positive effects of sex steroid ablation on non-aged thymus function (Papadopoulou *et al.*, 2011), the lack of increased thymic involution in response to increased sex steroid levels (Morley, 2003), and the initiation of thymic involution prior to puberty where sex steroid levels are low (Shanley *et al.*, 2009). Nevertheless, studies investigating the effects of sex steroids on thymic involution highlight the importance of considering biological sex in age-related changes to the T-cell compartment.

1.2.3 B-CELLS

B-cells are key players of the adaptive immune system, as they form the crux of the humoral response and serve as APC for T-cells (Hoffman, Lakkis and Chalasani, 2016). Conventional B-cells (also referred to as B2 cells) are formed from haematopoietic progenitor cells in the BM (Pieper, Grimbacher and Eibel, 2013), where they acquire CD19 expression and a unique antigen-specific B-cell receptor (BCR), formed from the immunoglobulin (Ig) M (Tonegawa, 1983). Immature B-cells leave the BM and enter SLOs, such as the spleen, as transitional regulatory cells to complete maturation into naïve, follicular, or marginal-zone B-cells (Sims *et al.*, 2005).

Activation of mature naïve B-cells occurs in SLOs, where they can recognise their cognate antigen, but B-cells only become fully activated when T-cell help is provided (Engel *et al.*, 2011). Activated effector B-cells form germinal centre (GC) reactions, where key processes of the humoral response occur, including antibody affinity maturation (MacLennan *et al.*, 2003; Engel *et al.*, 2011), class-switching (Engel *et al.*, 2011) and B-cell differentiation (MacLennan *et al.*, 2003). To provide immediate humoral immunity, activated B-cells first differentiate into weak antibody-secreting short-lived cells, known as plasma blasts, via extrafollicular responses (Nutt *et al.*, 2015), and subsequently differentiate into strong antibody-secreting long-lived plasma cells within GC (Shlomchik and Weisel, 2012). Plasma cells secrete high levels of antigen-specific antibodies and either reside in SLOs or migrate to the BM (Hargreaves *et al.*, 2001). Alternatively, activated B-cells may differentiate into memory cells to provide lifelong immunity (Shlomchik and Weisel, 2012).

Several subsets exist within the B-cell population, each with specific immunological functions (Sanz *et al.*, 2019). B1 cells are a small and unique subpopulation of conventional B-cells that spontaneously secrete antimicrobial and homeostatic antibodies to aid immunosurveillance (Stall, Wells and Lam, 1996; Baumgarth *et al.*, 2000; Lalor, 1991). These cells mostly occupy anatomical cavities, such as the pleural and peritoneal cavities, and are virtually absent from SLOs such as the spleen, LN and Peyer's patches (Stall, Wells and Lam, 1996; Lalor, 1991). B10 cells are a regulatory subset of conventional B-cells which suppress T-cell activation through secretion of IL-10 (Yanaba *et al.*, 2008; Matsushita *et al.*, 2008). B10 cells primarily reside in the peritoneal cavity, with a small subset occupying the spleen (DiLillo, Matsushita and Tedder, 2010). The B-cell subsets considered in this thesis, along with the extracellular markers used to define them by flow cytometric analysis, are listed in **Table 1-3**.

Table 1-3 Extracellular markers used to define human and murine CD19+ B-cells

B-cell subsets	Extracellular markers	References
Human		
Transitional regulatory	$CD38^{hi}CD24^{hi}$	Sanz *et al.*, 2019 ; Kaminski *et al.*, 2012
Mature naïve	$IgD^{+}CD27^{-}CD38^{-}IgM^{+}$	
Effector	$IgD^{+}CD27^{+}CD38^{-}$	
Memory	$IgD^{-}CD27^{+}CD38^{-}$	
B1	$CD70^{-}CD43^{+}CD27^{+}$	Griffin, Holodick and Rothstein, 2011
B10	$CD5^{+}CD1d^{hi}$	Karim and Wang, 2019
Senescent	$IgD^{-}CD27^{-}$	Colonna-Romano *et al.*, 2009; Frasca *et al.*, 2017
Mouse		
Age-associated B-cells	$CD21/35^{-}CD23^{-}CD93^{-}CD43^{-}$	Hao *et al.*, 2011; Ratliff *et al.*, 2013

1.2.3.1 EFFECTS OF AGEING ON B-CELL SUBSETS

B-cell output from the BM is greatly reduced with ageing (Riley, Kruger and Elia, 1991; Stephan, Sanders and Witte, 1996; Rossi *et al.*, 2003). Although an age-associated reduction in B-cell lymphopoiesis is well documented, the number of peripheral B-cells are maintained with age (Johnson, Rozzo and Cambier, 2002; Stephan, Sanders and Witte, 1996) due to the extended lifespan of B-cells in older hosts compared to younger hosts (Kline, Hayden and Klinman, 1999). These long-lived B-cells display characteristics of memory B-cells, and so maintained B-cell numbers throughout life could be explained by the shift of the B-cell compartment from naïve toward a memory phenotype during ageing (reviewed in Bulati, Caruso and Colonna-Romano, 2017). Indeed, the balance between different B-cell subsets is changed with age (Chong *et al.*, 2005; Yanaba *et al.*, 2009; Colonna-Romano *et al.*, 2008; Hao *et al.*, 2011). Circulating numbers of naïve B-cells, transitional regulatory B-cells and B1 cells were reduced in the blood of older (>60 years) adults compared to younger (<40 years) adults, whilst the number of circulating memory B-cells were increased (Chong *et al.*, 2005; Rodriguez-Zhurbenko *et al.*, 2019; Duggal *et al.*, 2013). Ageing is also

associated with an expansion of regulatory B10 cells, as the frequency of this particular subset was increased in the spleens of aged (6 months) mice compared to younger (3-10 days) mice (Yanaba *et al.*, 2009). The accumulation of long-lived antigen-experienced B-cells (Rubtsova *et al.*, 2015; Rubtsov *et al.*, 2011), namely age-associated B-cells (ABC) and senescent B-cells (Colonna-Romano *et al.*, 2008; Hao *et al.*, 2011), also occurs with ageing (see Section 1.2.3.2).

1.2.3.2 EFFECTS OF SEX ON B-CELL POPULATIONS

Although not many studies have considered biological sex when investigating age-related changes to the B-cell compartment, sexual dimorphism is evident in the few studies that have (Hao *et al.*, 2011; Rubtsov *et al.*, 2011; Huang *et al.*, 2021; Arsenovic-Ranin *et al.*, 2019). Older (>15 months) female C57Bl6 mice presented with increased frequencies of ABC in the spleen compared to older male mice, suggesting that the rate of accumulation of these cells in ageing occurs in a sex-dependent manner (Hao *et al.*, 2011; Rubtsov *et al.*, 2011). Indeed, older (30-60 years) women have increased frequencies of ABC in the circulation compared to age-matched men (Keller *et al.*, 2021). In BALB/c mice, old (18 months) female mice had increased numbers of GC B-cells in the spleen following intramuscular administration of a trivalent mixture of influenza virus antigens compared to older male mice, which led to improved anti-viral immune responses (Arsenovic-Ranin *et al.*, 2019). Interestingly, sex steroids play a role in the age-associated contraction of B-cell lymphopoiesis (Dudakov *et al.*, 2009). The ablation of sex steroids by means of surgical castration reversed the age-related decline in B-cell lymphopoiesis in the BM and led to increased numbers of B-cells in the spleens of 9 month C57Bl6 male mice (Dudakov *et al.*, 2009); whether sex steroid ablation reverses B-cell lymphopoiesis in old female mice has not been explored.

Therefore, biological sex, including sex hormones, should not be overlooked when studying age-related changes to the B-cell compartment of older hosts.

The antibody responses formed in youth are robust and persist into old age (Yu *et al.*, 2008). However, the ability of aged hosts to generate high-affinity antibodies to new antigens is greatly reduced in ageing (Goidl, Innes and Weksler, 1976; Kosco *et al.*, 1989), and is the cumulative result of impaired GC formation (Szakal *et al.*, 1990; Miller and Kelsoe, 1995), reduced levels of somatic hypermutations during BCR generation (Miller and Kelsoe, 1995), and decreased T-cell help during B-cell activation (Eaton *et al.*, 2004; Yang and Wilson, 1996). The dramatic collapse in the B-cell repertoire of older individuals is associated with poorer health outcomes (Gibson *et al.*, 2009). Interestingly, age-related changes to antibody responses in the context of vaccination exhibits sexual dimorphism and depends on vaccine type. Older women exhibited improved antibody responses to viral vaccines, such as the seasonal influenza vaccine, compared to men (Falsey *et al.*, 2009; Voigt *et al.*, 2019), but poorer antibody responses to bacterial vaccines such as tetanus diphtheria/pertussis (Hainz *et al.*, 2005; Stark *et al.*, 1999; Marlovits *et al.*, 2000) and pneumococcal vaccines (Brandao *et al.*, 2004; Goldblatt *et al.*, 2009). Indeed, biological sex as well as chronological ageing affect the B-cell composition and function in hosts.

1.3 LEUKOCYTE TRAFFICKING AND THE AGEING PROCESS

1.3.1 LEUKOCYTE TRAFFICKING DURING HOMEOSTASIS AND INFLAMMATION

1.3.1.1 THE LEUKOCYTE ADHESION CASCADE

During homeostasis and inflammation, leukocytes traffic from the blood into tissues by interacting with, and crossing through, endothelial cells (EC) lining blood vessel walls (reviewed by Ley and Reutershan, 2006). Traditionally, leukocyte migration was characterised by a 3-step process, comprising of leukocyte rolling along inflamed EC, chemokine-mediated activation of the leukocyte, and finally, firm adhesion of the leukocyte to the endothelium (Butcher, 1991; von Andrian *et al.*, 1991). However, as our knowledge of leukocyte recruitment has grown, the leukocyte adhesion cascade has expanded to incorporate additional steps such as margination, slow rolling, and intraluminal crawling (Ley *et al.*, 2007; Nourshargh and Alon, 2014).

To initiate leukocyte egress from blood, circulating leukocytes move from the central blood stream to the blood stream flowing over the single layer of vascular EC (Langer and Chavakis, 2009). This process is termed margination and positions leukocytes close to the endothelial lining of blood vessels in anticipation of the leukocyte-endothelial interactions that facilitate the leukocyte adhesion cascade (Langer and Chavakis, 2009). Leukocyte capture is the first step in the cascade and is primarily mediated by selectins. Local pro-inflammatory cytokines, including tumor necrosis factor alpha (TNFα) and IL-1β, activate vascular EC, inducing the upregulation of adhesion molecule expression on the vasculature (True, Rahman and Malik, 2000; Deisher *et al.*, 1993). Peripheral blood leukocytes can interact with

cytokine-activated EC via L-, P- and E-selectins, binding with their glycosylated ligands. P- and E-selectins are found on inflamed EC and bind to P-selectin glycosylated ligand 1 (PSGL1) on circulating leukocytes (Ley *et al.*, 2007). Despite its name, PSGL1 can interact with all three selectins, and is expressed on most leukocytes as well as some EC (Carlow *et al.*, 2009; Rivera-Nieves *et al.*, 2006; da Costa Martins *et al.*, 2007). The interaction between P- or E-selectin and PSGL1 is therefore one of the major mechanisms that facilitates leukocyte capture and rolling on inflamed endothelium. Leukocytes that express L-selectin but lack ligands for P- and E-selectins are indirectly recruited to activated EC through interactions with PSGL1 on adhered leukocytes (Sundd *et al.*, 2011). L- and P-selectins are dependent upon the sheer stress generated by blood flow to maintain adhesion with their ligands, highlighting the importance of physiological forces in leukocyte recruitment (Finger *et al.*, 1996; Lawrence *et al.*, 1997).

Following capture, leukocytes proceed to roll along the EC before establishing firm adhesion (Ley *et al.*, 2007). Leukocyte arrest is established by endothelial-expressed chemokines interacting with G-protein coupled receptors on the surface of rolling leukocytes, triggering intracellular signalling cascades that result in the activation of integrins (Campbell *et al.*, 1998b). Integrins are heterodimer cell surface receptors formed of α and β chains of type I transmembrane glycoproteins, and are usually expressed in the non-activate confirmation (reviewed by Mould and Humphries, 2004). Upon chemokine-activation of the leukocyte, integrins are modulated into an extended, activated conformation which increases the affinity of the integrin for its ligands e.g. matrix proteins and Ig superfamily members (Geiger *et al.*,

2001). Activated integrins then cluster within the cell membrane (Miyamoto *et al.*, 1995) to facilitate the firm adhesion of the leukocyte on the endothelium.

Upon adhesion, leukocytes may crawl along the blood vessel using adhesion molecules, such as macrophage-1 antigen and intercellular adhesion molecule 1 (ICAM-1), until they have reached a location that permits transmigration, either via the paracellular or transcellular route (Schenkel, Mamdouh and Muller, 2004; Phillipson *et al.*, 2006; Voisin, Probstl and Nourshargh, 2010; Yadav *et al.*, 2003). Permissible sites depend on the structure formed by endothelial-pericyte interactions, composition of the endothelial basement membrane and availability of chemokine and adhesion molecules (Ley *et al.*, 2007; Alon and Nourshargh, 2013). The paracellular route of transmigration requires a reduced affinity of interendothelial contacts to permit transmigration of leukocytes between EC. Rho GTPase activation increases intracellular calcium concentrations in EC which in turn facilitates the redistribution of molecules, such as vascular endothelial (VE)-cadherin within EC junctions, to aid in the opening of cell junctions and allow paracellular leukocyte transmigration (Millan and Ridley, 2005; Huang *et al.*, 1993; Shaw *et al.*, 2001). Transmigrating leukocytes relocalise their nuclei to the lamellipodia to push through the endothelia barrier (Barzilai *et al.*, 2017). Many molecules within endothelial junctions actively assist transmigrating leukocytes, albeit in a leukocyte- as well as cytokine-specific fashion (Reglero-Real *et al.*, 2016; Bradfield *et al.*, 2007). Such molecules include platelet EC adhesion molecule 1 (PECAM1; also known as CD31), which facilitates leukocyte transmigration in the presence of IL-1β but not TNFα, and EC-selective adhesion molecule, which assists transmigrating neutrophils but not T-cells (Nourshargh, Krombach and Dejana, 2006; Wegmann *et al.*, 2006; Kishore *et al.*, 2012).

Paracellular transmigration is facilitated by sequential molecular interactions, as disruption or blockade of certain molecules, such as PECAM1 and CD99, hinders the transmigration of leukocytes in a cumulative manner (Schenkel *et al.*, 2002; Lou *et al.*, 2007). Transcellular leukocyte migration is a reportedly minor route of leukocyte extravasation, with a 5-20% occurrence observed *in vitro* (Carman and Springer, 2004). The process is instigated by the extension of leukocyte protrusions into the EC (Millan *et al.*, 2006), and involves membranous passageways through the EC, termed vesiculo-vacuolar organelles (Dvorak and Feng, 2001).

Following transendothelial migration, leukocytes must cross the basement membrane as well as the pericyte sheath before entering tissues (reviewed by Nourshargh, Hordijk and Sixt, 2010). The expression of basement membrane constituents, such as laminin-10 and collagen type IV, is low in certain locations and co-localises with gaps in the pericyte sheath (Wang *et al.*, 2006; Sixt *et al.*, 2001). These low-expression sites grow upon cytokine stimulation, permitting the transendothelial migration of leukocytes (Wang *et al.*, 2006). Once in tissue, leukocytes may migrate in a random fashion (chemokinesis) in the absence of chemoattractants, or if a strong chemoattractant gradient is available, leukocytes will move in a directional manner (chemotaxis) towards the area with the highest concentration of chemoattractants (Gaylo *et al.*, 2016). In the context of inflammation, leukocytes utilise a chemokine gradient to migrate towards the source of infection/injury.

1.3.1.2 T-CELL TRAFFICKING DURING HOMEOSTASIS

Although heavily associated with inflammatory responses, the trafficking of T-cells into and out of tissues is an essential part of steady state homeostasis to provide ongoing immunosurveillance (Reglero-Real, Rolas and Nourshargh, 2019). Homeostatic T-cell

trafficking occurs in a time-dependent manner, with peak T-cell extravasation from the blood into tissues occurring in the day for humans and in the night for mice (Casanova-Acebes *et al.*, 2013; Scheiermann, Kunisaki and Frenette, 2013). To determine whether this circadian control of T-cell trafficking in mice was due to an oscillating expression of adhesion molecules within tissues, He *et al.* collected several murine tissues at different time points of the day and assessed the expression of ICAM-1, vascular cell adhesion molecule 1 (VCAM-1), and P-selectin using quantitative fluorescence microscopy (He *et al.*, 2018). Throughout the 24 hour cycle, ICAM-1 and VCAM-1 exhibited oscillating expression patterns in the spleen, LN and Peyer's patches whilst P-selectin expression oscillated in the thymus and the spleen (He *et al.*, 2018). Furthermore, He *et al.* assessed chemokine receptor and adhesion molecule expression on leukocytes using flow cytometry. The expression of PSGL-1, L-selectin, CD11a, CD49d adhesion molecules and CCR7, CXCR4 chemokine receptors displayed oscillating expression on circulating $CD4^+$ and $CD8^+$ T-cells throughout the 24 hour cycle. The diurnal control of homeostatic T-cell trafficking is therefore at least partly imposed by the oscillating expression of adhesion molecules within tissue and on T-cells themselves, as well as through the oscillating expression of T-cell chemokine receptors.

T-cells are not only trafficked between the circulatory system and peripheral tissues, but also within the lymphatic network (Jackson, 2019; Hampton and Chtanova, 2019). Lymphatic vessels facilitate the trafficking of antigen-loaded APC to draining LN (dLN) in order to initiate adaptive immune responses during acute inflammation, and also the trafficking of T-cells that mediate immunoregulation and immunosurveillance during homeostasis (Jackson, 2019). T-cells enter dLN from high endothelial venules

(HEV) (Kansas *et al.*, 1993). Glycoprotein peripheral node addressins are abundantly expressed on HEV, which interact with L-selectin (CD62L) on naïve T-cells to assist their homing to SLOs (Kansas *et al.*, 1993; Ley, Tedder and Kansas, 1993). CCR7 and LFA-1 on the surface of naïve T-cells also aid their homing to SLOs by binding to CCL21 and ICAM-1/2, respectively (Weninger *et al.*, 2001; Gunn *et al.*, 1998; Campbell *et al.*, 1998a; Campbell *et al.*, 1998b). T-cells eventually exit the lymphatic network and enter tissues through extravasation within efferent lymphatic vessels (Hampton and Chtanova, 2019).

The trafficking patterns of T-cells during homeostasis are also dependent on the specific subset of T-cell considered. For example, EM and CM T-cell subsets differ in their expression of L-selectin and CCR7 to reflect their different trafficking patterns (Kaech, Wherry and Ahmed, 2002). CM T-cells express high levels of L-selectin and CCR7 to facilitate their entry into SLOs, whilst EM T-cells express low levels of L-selectin and lack CCR7 expression to remain in the periphery (Kaech, Wherry and Ahmed, 2002). Treg are primarily located in the circulation and in SLOs, including the thymus, LN, spleen and BM, in the steady state (Shevach, 2002; Sakaguchi, 2005; Zou *et al.*, 2004) despite the fact that not all Treg express the SLO-homing molecules CCR7 and L-selectin (Thornton and Shevach, 2000; Ermann *et al.*, 2005). The mechanisms of Treg homing to SLOs remains to be delineated (Wei, Kryczek and Zou, 2006). The homeostatic trafficking patterns of T-cells is therefore specific to the T-cell subset and relies on a plethora of adhesion molecules and chemokine receptors.

1.3.1.3 T-CELL TRAFFICKING DURING INFLAMMATION

T-cell trafficking patterns are modulated during inflammation (Hamann and Syrbe, 2000). Newly formed effector T-cells downregulate L-selectin and CCR7 and

upregulate integrins (LFA-1; very late antigen-1/4, VLA-1,-4) and homing molecules (CCR5, CCR6, CCR8, CCR9, CXCR3) so that they may egress from SLOs and enter the circulation to traffic to sites of inflammation (Groom *et al.*, 2012; Bromley, Mempel and Luster, 2008). In the steady state, all T-cells express PSGL-1 which interacts with CCL19/21 and mediates T-cell homing to SLOs, and possibly peripheral tissues (Carlow *et al.*, 2009). However, T-cell activation results in the O-glycosylation of PSGL-1 on the T-cell surface, increasing its affinity for P- and E-selectins expressed on inflamed endothelium to facilitate T-cell rolling (Carlow *et al.*, 2009).

Once captured by the inflamed endothelium, T-cells interact with endothelial-expressed chemokines, such as CXCL9-11, which induces the activation of T-cell integrins including LFA-1 and VLA-4 (Bromley, Mempel and Luster, 2008). Integrin activation enhances the affinity of LFA-1 and VLA-4 for their endothelial-expressed ligands ICAM-1 and VCAM-1, respectively, and facilitates the firm adhesion of T-cells to inflamed EC (Walling and Kim, 2018; Shamri *et al.*, 2005; McGettrick *et al.*, 2009b). Once firmly adhered, T-cells primarily utilise LFA-1 to facilitate intraluminal crawling and to resist blood flow-mediated detachment from the vessel wall (Shulman *et al.*, 2009) whilst seeking a permissible site to facilitate transendothelial migration. T-cell transmigration across the endothelial monolayer is a dynamic process, as T-cells have been observed to migrate back and forth along the inflamed endothelial layer *in vitro* (McGettrick *et al.*, 2009a), and is assisted by active lipid compounds, such as prostaglandin D2 (Ahmed *et al.*, 2011).

For successful recruitment and entry into inflamed tissue, T-cells must be able to negotiate the endothelial barrier using an arsenal of molecules, including cell adhesion molecules, chemokine receptors and lipid mediators, which differ depending

on the inflammatory stimulus, T-cell subset and vascular bed involved in the migration process. Importantly, the adhesion molecules involved in T-cell trafficking also influence T-cell effector functions, such as the involvement of integrin signalling in T-cell activation, differentiation, and proliferation (Bertoni *et al.*, 2018). Importantly, the relationship between T-cells and EC is not unidirectional, as T-cells can hinder the ability of EC to support leukocyte migration through cell-cell contact (James *et al.*, 2003). Any age-related changes to T-cells or EC can affect T-cell trafficking processes, ultimately impeding protective immune responses.

1.3.2 AGE-RELATED CHANGES TO LEUKOCYTE TRAFFICKING PROCESSES

1.3.2.1 AGE-RELATED ENDOTHELIAL CELL ACTIVATION

1.3.2.1.1 ADHESION MOLECULES

Several studies have investigated the effect of ageing on the endothelial expression of adhesion molecules under homeostatic conditions and found their expression to be increased on the aged vasculature (Rom and Scalia, 2013; Zou *et al.*, 2006; Miguel-Hidalgo *et al.*, 2007; Yousef *et al.*, 2019; Ketani *et al.*, 2016; Li *et al.*, 1999). Older (>32 months) F1-F344xBN rats had increased expression of endothelial ICAM-1, P-selectin and VCAM-1 within the mesenteric microcirculation under basal conditions compared to younger (<6 months) rats, which led to enhanced leukocyte rolling, adhesion and transmigration within the mesentery (Rom and Scalia, 2013). In the human orbitofrontal cortex, increased endothelial ICAM-1 expression was observed in post-mortem tissue derived from older (60-80 years) individuals compared to younger (27-54 years) individuals (Miguel-Hidalgo *et al.*, 2007). Similarly, there was increased expression of VCAM-1 in the hippocampus of old (18 months) C57Bl6 mice under basal conditions

compared to younger (3 months) mice as determined by quantitative fluorescent microscopy (Yousef *et al.*, 2019).

Soluble adhesion molecules in serum and plasma are an easily accessible measure of endothelial expressed adhesion molecules, however, their presence may signify elevated levels of EC activation, proteolytic activity, or EC damage (Kjaergaard *et al.*, 2013). Several studies to date have reported increased levels of soluble ICAM-1 and VCAM-1 in the circulation of older (>50 years) adults compared to younger (<50 years) adults (Yousef *et al.*, 2019; Morisaki *et al.*, 1997; Richter *et al.*, 2003; Miles *et al.*, 2008; Miles *et al.*, 2001). The age-associated increase in endothelial expression of adhesion molecules under basal conditions could be due to the increased levels of systemic pro-inflammatory cytokines in older hosts (Chung *et al.*, 2019). TNFα and IL-6, two of the most extensively studied cytokines released as part of the SASP, are increased in the serum of older adults (Bruunsgaard *et al.*, 1999; Wei *et al.*, 1992) and older mice (Daynes *et al.*, 1993; Spaulding, Walford and Effros, 1997), and can modulate the expression of adhesion molecules on EC (Wang *et al.*, 2014; Luu, Rainger and Nash, 2000; Chimen *et al.*, 2017; Watson *et al.*, 1996). For instance, *in vitro*, TNFα treatment increased the expression of VCAM-1 (Ahmad *et al.*, 1995; Lechleitner *et al.*, 1998), ICAM-1 (Burke-Gaffney and Hellewell, 1996) and E-selectin (Bevilacqua *et al.*, 1987) on human umbilical cord EC (HUVEC) and increased E-selectin expression on pulmonary artery EC (Rahman *et al.*, 1998); whilst IL-6 treatment increased the expression of ICAM-1, VCAM-1 and E-selectin on HUVEC (Watson *et al.*, 1996). The increasing pro-inflammatory environment of older hosts in the absence of infection or tissue damage is therefore modulating leukocyte trafficking under homeostatic conditions through altering the expression of adhesion molecules

within tissues and on EC. However, whether there is sexual dimorphism in the expression of adhesion molecules in ageing is largely unknown as the studies mentioned in this section only considered male subjects or mixed-sex subjects.

1.3.2.1.2 JUNCTIONAL ADHESION MOLECULES

VE-cadherin is a classical cadherin expressed on EC and is involved in regulating vascular permeability (Gavard, 2014). Ageing is associated with increased internalisation and degradation of arterial VE-cadherin in the tails of aged (>24 months) male F344 rats compared to younger (<4 months) rats, determined by quantitative florescence microscopy (Chang, Flavahan and Flavahan, 2017). Increased arterial VE-cadherin degradation disrupted endothelial barrier integrity and contributed to the observed age-associated increase in vascular permeability in the jejunal microcirculation and aortas of aged (>24 months) male rats (Belmin *et al.*, 1993; Chen, Zhang and Duan, 2003). The reduced expression of junctional proteins such as VE-cadherin in aged tissues under homeostatic conditions may be due to the age-related changes in the inflammatory status of the tissue, therefore modulating leukocyte trafficking and vascular permeability in the steady state.

1.3.2.1.3 ENDOTHELIAL CELLULAR SENESCENCE

Vascular EC provide a surface for the exchange of materials between the blood and tissues (Baldwin and Thurston, 2001). Besides their role in instigating pro-inflammatory responses (see section 1.3.1.1), EC serve as important regulators of vascular homeostasis including the regulation of vascular tone, blood fluidity and the extravasation of solutes, macromolecules, and hormones (Kruger-Genge *et al.*, 2019). For example, EC support many anticoagulation pathways, such as the protein C/protein S pathway, to maintain blood fluidity (Stern *et al.*, 1991). However, the ageing

process negatively affects vascular EC as they are driven towards cellular senescence (Jia *et al.*, 2019).

EC ageing and, in turn, senescence are associated with a loss of typical EC functions, and a progressive shift of EC towards a pro-inflammatory state (Uryga and Bennett, 2016). Indeed, late passage (passage 50) HUVEC displayed reduced nitride oxide (NO) production (Sato *et al.*, 1993), an important soluble gas involved in EC homeostasis (reviewed in Tousoulis *et al.*, 2012), *in vitro* compared to an earlier passage (passage 8) (Sato *et al.*, 1993). Reduced NO production consequently leads to impaired EC functions, such as those involving vasodilation, the regulation of local cell growth and the protection of EC from circulating leukocytes (Tousoulis *et al.*, 2012). Senescent EC also exhibit a pro-inflammatory phenotype (Maier *et al.*, 1990; Mun and Boo, 2010; Donato *et al.*, 2008). Highly passaged HUVEC (passage >18) displayed increased gene and protein expression of CD44 compared to younger (passage 4) HUVEC, which facilitated increased monocyte adhesion to EC *in vitro* (Mun and Boo, 2010). EC isolated from the antecubital vein of older (>62 years) adults displayed increased intracellular expression of nuclear factor kappa B (NF-κB) p65 protein and reduced expression of inhibitor of kappa Bα compared to EC isolated from young (<24 years) adults, signifying upregulated NF-κB activation in older EC (Donato *et al.*, 2008). Further analysis using quantitative fluorescence microscopy confirmed that the older EC expressed increased levels of intracellular IL-6, TNFα, and CCL2, a monocyte chemoattractant, compared to the younger EC (Donato *et al.*, 2008).

Whilst the term ‘senescent’ has been used to describe older EC (i.e. late passage EC, or EC derived from older hosts) in earlier studies, such as those mentioned above, the precise definition and robust characterisation of truly senescent

EC wasn't established until the early 2010s as our understanding of senescent cells improved (Kuilman *et al.*, 2010). Nowadays, a variety of techniques, such as quantifying p16 expression, measuring telomere lengths and assessing telomerase activity, are used to define truly senescent EC (Noren Hooten and Evans, 2017; Biran *et al.*, 2017). Despite the advances in the classification of senescent EC, most of the findings concerning 'senescent' EC mentioned above have been confirmed to be features unique to truly senescent EC (Bhayadia *et al.*, 2016; Silva *et al.*, 2017; Kim *et al.*, 2021). How the ageing process triggers EC senescence is unclear and is likely to be multifactorial (Jia *et al.*, 2019). Indeed, oxidative stress (Abbas *et al.*, 2017), hyperuricemia (Puddu *et al.*, 2012) and vascular inflammation (Khan *et al.*, 2017; Franceschi and Campisi, 2014) have all been linked to the progression of senescence in EC. Nonetheless, it is clear that the gradual accumulation of pro-inflammatory senescent EC during ageing influences leukocyte trafficking in the steady state.

1.3.2.2 AGE-RELATED CHANGES TO SYSTEMIC CYTOKINE AND CHEMOKINE LEVELS

As a consequence of ageing, the circulating levels of pro-inflammatory mediators, including cytokines, chemokines and chemoattractants, are increased in older mice (Daynes *et al.*, 1993; Spaulding, Walford and Effros, 1997; Jeon, Mun and Boo, 2012; Yousefzadeh *et al.*, 2018) and humans (Bruunsgaard *et al.*, 1999; Wei *et al.*, 1992; Mariani *et al.*, 2006; Miles *et al.*, 2008; Allen *et al.*, 2021). For example, IL-8, CXCL10, and CCL2 chemoattractants, as well as IL-6 and TNFα cytokines, are increased in the blood of older (>85 years) adults compared to younger (<60 years) adults (Mariani *et al.*, 2006; Inadera *et al.*, 1999; Miles *et al.*, 2008; Antonelli *et al.*, 2006). Interestingly, there was no effect of sex on the levels of circulating IL-6, IL-8, CCL2, and TNFα in

older adults (Mariani *et al.*, 2006; Inadera *et al.*, 1999). In mice, ageing is associated with increased circulating levels of CCL11, an eosinophil chemoattractant, CCL2, and CCL17, a T-cell chemoattractant, in old (20 months) male and female C57Bl6 mice compared to younger (2 months) mice under resting conditions (Jeon, Mun and Boo, 2012; Yousefzadeh *et al.*, 2018).

Although the source of the circulating cytokines and chemokines in the circulation of older hosts in the steady state has not been elucidated, the mediators are likely to be produced by several cell types including senescent cells as part of the SASP (Coppe *et al.*, 2010), and also by PBMC themselves (Pulsatelli *et al.*, 2000; Clark and Peterson, 1994; Chen *et al.*, 2003). Intriguingly, PBMC from older (>86 years) adults spontaneously secrete IL-8, CCL2, CCL3, and CCL5 under unstimulated conditions *in vitro* whilst PBMC from younger (>85 years) adults do not (Pulsatelli *et al.*, 2000). The extent to which increased circulating chemokine/chemoattractant and cytokine levels influence leukocyte trafficking processes in older hosts in the steady state has not been extensively studied.

1.3.2.3 AGE-RELATED CHANGES TO ADHESION MOLECULE AND CHEMOKINE RECEPTOR EXPRESSION ON LEUKOCYTES

Ageing is also associated with modified adhesion molecule expression on leukocytes (Ritzel *et al.*, 2016; Orme and Roberts, 1998; Ginaldi *et al.*, 2000). In C57Bl6 mice, the expression of LFA-1 and VLA-4 integrins was increased on circulating $CD8^+$ T-cells derived from aged (>18 months) male mice compared to younger (<3 months) mice, and was associated with a higher incidence of $CD8^+$ T-cell recruitment to peripheral tissues such as the brain (Ritzel *et al.*, 2016). In female B6D2F1 mice, there was increased expression of the integrin subunit α_5 and LFA-1, as well as reduced

expression of ICAM-1 and L-selectin on circulating $CD4^+$ T-cells isolated from older (24 months) mice compared to younger (4 months) mice (Orme and Roberts, 1998). In humans, the percentage of circulating monocytes expressing LFA-1 and T-cells expressing L-selectin was significantly reduced in older (>75 years) adults compared to younger (<50 years) adults (Ginaldi *et al.*, 2000; Chiricolo *et al.*, 1995). Although several studies have noted an age-related alteration in adhesion molecule expression by circulating T-cells in mice and humans, an air of caution must be implemented when interpreting the data as the changes in frequencies of T-cells expressing some adhesion molecules such as L-selectin may simply be a reflection of the reduced pool of circulating naïve T-cells that accompanies the ageing process (see section 1.2.2.1).

Many studies have also shown that advancing age affects the surface expression of chemokine receptors on T-cells (Mo *et al.*, 2003; Yung and Mo, 2003; Cane, Ponnappan and Ponnappan, 2012a; Gomez *et al.*, 2003). Splenic $CD4^+$ T-cells isolated from aged (>20 months) C57Bl6 mice exhibited higher levels of gene and protein expression of CCR1, 2, 4, 5, 6, 8 and CXCR2-5, and lower levels of CCR7 and 9 compared to their younger counterparts (<4 months), as determined by Western blot analysis (Mo *et al.*, 2003). In humans, circulating PBMC and $CD4^+$ T-cells isolated from older (>60 years) adults had increased expression of CCR1-5 compared to cells isolated from younger (<40 years) adults (Yung and Mo, 2003). However, it is important to note that the pattern of chemokine receptors expressed on a given T-cell is unique to a particular T-cell subset, and so any age-related changes observed in overall chemokine receptor expression within pools of T-cells may just reflect age-related changes in the proportion of T-cell subsets.

Importantly, differential chemokine receptor expression on old T-cells is functionally relevant. Splenic $CD4^+$ T-cells isolated from aged mice demonstrated increased chemotactic responses to CXCL12 and CCL3 *in vitro* compared to those isolated from younger mice (Mo *et al.*, 2003). Similarly, in humans, circulating $CD4^+$ T-cells isolated from older adults (>65 years) exhibited enhanced chemotactic responses to CXCL12 compared to T-cells derived from younger (<30 years) adults, facilitated by an increased surface expression of CXCR4 on old T-cells (Cane, Ponnappan and Ponnappan, 2012b; Cane, Ponnappan and Ponnappan, 2012a). The age-related modulation of adhesion molecule and chemokine receptor expression therefore affects leukocyte trafficking in the steady state. Once again, the extent to which biological sex affects these processes has not been extensively studied.

1.3.2.4 AGE-RELATED CHANGES TO LYMPHOCYTE TRAFFICKING

The ageing process significantly impacts the trafficking processes of leukocytes in both humans and mice during inflammation (**Figure 1-3**), however, the extent to which biological sex affects these processes has largely been overlooked (**Table 1-4** and **Table 1-5**). What is more, murine studies specifically investigating the age-related changes to homeostatic trafficking of lymphocytes are lacking. Instead, most studies to date have utilised single-cell RNA sequencing techniques to determine age-related changes to lymphocyte population counts within tissues. Single-cell RNA sequencing has revealed age-related changes in the abundance of B- and T-cells in various murine tissues under homeostatic conditions, albeit in a tissue-specific manner (Tabula Muris, 2020; Schaum *et al.*, 2020). The proportion of B-cells in the spleen and anterior tibialis muscles of aged (>18 months) male and female C57BL/6 mice is reduced compared to younger (<3 months) mice, whilst the proportion of T-cells in the thymus, spleen and

mammary glands are decreased (Tabula Muris, 2020). Indeed, by using adoptive transfer studies, Wols *et al.* showed that fewer immature B-cells migrated from the blood to the spleen in old (>20 months) female BALB/c mice due to age-related changes in CXCL13 expression and distribution within the spleen (Wols *et al.*, 2010). In another study, single-cell RNA sequencing revealed increased B- and T-cell infiltration of the gonadal adipose tissue in aged (24 months) male and female C57Bl6 mice compared to young mice (3 months), along with increased levels of VCAM-1 in the serum, kidney and heart of the aged animals (Schaum *et al.*, 2020).

Other methodologies, including quantitative fluorescent microscopy, have revealed increased numbers of T-cells in the retina of old (>24 months) male rats (Chan-Ling *et al.*, 2007) and the brains of old (>12 months) male mice (Stichel and Luebbert, 2007; Ritzel *et al.*, 2016) compared to younger counterparts under basal conditions. What more, Ritznel *et al.* noted that aged (>18 months) female C57Bl6 mice exhibited increased numbers of T-cells within the brain compared to aged male mice, however, the authors did not pursue investigating the sexual dimorphism of T-cell recruitment to the brain during ageing (Ritzel *et al.*, 2016). Nonetheless, the studies mentioned above suggest that under homeostatic conditions lymphocytes are drawn away from SLOs and enter peripheral tissues in older hosts; perhaps in a sex-specific manner. As of such, determining the effects of chronological age and biological sex on leukocyte population numbers within lymphoid and peripheral tissues is a major aim of this thesis.

Table 1-4 Effects of ageing on innate immune cell trafficking in the context of acute inflammation

	Effect of ageing on immune cell trafficking	Potential mechanisms	Species investigated	Sex considered	Reference
Innate cells					
DC	↓DC recruitment to lung-dLN post-burn injury in mice	↑Prostoglandin D_2 levels leading to ↓ CCR7 expression on old DC	Mice	Not mentioned	Zhao *et al.*, 2011
	Delayed DC recruitment to the lungs of influenza A-infected mice	Delayed local IL-8 production	Mice	Females	Toapanta and Ross, 2009
	↓CCL21-directed chemotaxis *in vitro*, ↓popliteal dLN-homing *in vivo*	Defective signal transduction pathways	Mice	Not mentioned	Grolleau-Julius *et al.*, 2008
	↓CCL19-directed chemotaxis *in vitro*	Defective PI3K-AKT signalling	Humans	Not mentioned	Agrawal *et al.*, 2007
Neutrophils	↑Chemokinesis and ↓CXCL1-directed chemotaxis *in vitro*, ↑neutrophil recruitment to the lung post-burn injury in mice	↑ICAM-1 expression in aged lung and ↑neutrophil chemokinesis	Mice	Females	Nomellini *et al.*, 2012
	↑Neutrophil recruitment to peritoneum during *C. albicans* infection	No mechanisms described	Mice	Females	Murciano *et al.*, 2008
	↓Neutrophil infiltration into wounds infected with *S. aureus*	↓ICAM-1 expression in wounds of aged mice	Mice	Not mentioned	Brubaker *et al.*, 2013
	↓Neutrophil trafficking to spleen and mesenteric LN during *S. Typhimurium* infection	No mechanisms described	Mice	Males	Ren *et al.*, 2009
	↑Neutrophil recruitment to the peritoneal cavity during zymosan-induced peritonitis	↓Specialised pro-resolving mediators within the aged peritoneal cavity	Mice	Males	Arnardottir *et al.*, 2014
	↓fMLP-directed chemotaxis *in vitro*	Defective intracellular calcium signalling	Humans	Mixed	Wenisch *et al.*, 2000
	↓fMLP- and PAF-directed chemotaxis *in vitro*	No mechanisms described	Humans	Mixed	Niwa *et al.*, 1989
	↓fMLP-, CXCL8-, and CXCL1-directed chemotaxis *in vitro*	Defective PI3K-signalling	Humans	Mixed	Sapey *et al.*, 2014; Wilson *et al.*, 2020
	↑Neutrophil reverse transendothelial migration (rTEM) resulting in remote organ damage	↑Mast cell-derived CXCL1 sensitising the CXCR2 on neutrophils	Mice	Mostly males	Barkaway *et al.*, 2021
Monocytes	Inappropriate recruitment to the skin in response to harmless stimuli	CCL2 secretion by senescent fibroblasts in skin	Humans	Mixed	Chambers *et al.*, 2021

A summary of the studies investigating the age-related changes of innate immune cell trafficking in humans and mice along with the potential mechanisms that drive the changes. The sex investigated is also noted.

Table 1-5 Effects of ageing on adaptive immune cell trafficking in the context of acute inflammation

	Effect of ageing on immune cell trafficking	Potential mechanisms	Species investigated	Sex considered	Reference
Adaptive cells					
T-cells	Delayed recruitment to the lungs of influenza A-infected mice	Delayed local IL-8 and MIP-1β production	Mice	Females	Toapanta and Ross, 2009
	↓T-cell recruitment to popliteal LN during West Nile virus infection in mice	↓CCL2 production, ↓ability of old T-cells to extravasate	Mice	Not mentioned	Richner *et al.*, 2015
	↓T-cell recruitment to tumours	No mechanisms described	Mice	Females	Norian and Allen, 2004
	↓CD4+ T-cell recruitment to the spleen following OVA immunization	↓CCL19 and CCL21 in the aged spleen	Mice	Not mentioned	Lefebvre *et al.*, 2012
	↓T-cell recruitment to the skin in response to recall antigens	↓E-selectin, ICAM-1, and VCAM-1 expression on endothelial cells in old skin	Humans	Not considered	Agius *et al.*, 2009
	↓CD27-CD8+ T-cell chemotaxis towards autologous serum *in vitro*	Impaired mitochondrial function leading to inadequate ATP production	Humans	Not considered	Callender *et al.*, 2020
B-cells	Retention within marginal zones of spleens	↑CXCR5 expression on aged B-cells	Mice	Females	Turner and Mabbott, 2017

A summary of the studies investigating the age-related changes of adaptive immune cell trafficking in humans and mice along with the potential mechanisms that drive the changes. The sex investigated is also noted.

Several models of inflammation, including infection, immunisation, and tissue injury, have been used to study age-related changes to lymphocyte trafficking in mice (Norian and Allen, 2004; Toapanta and Ross, 2009; Lefebvre *et al.*, 2012; Richner *et al.*, 2015). Induction of subcutaneous West Nile virus (WNV) infection led to reduced trafficking of T-cells and NK cells, as well as macrophages and DC, to the popliteal dLN of aged (>18 months) C57Bl6 mice compared to younger (<4 months) mice (Richner *et al.*, 2015). Reduced leukocyte trafficking to the dLN was associated with an increased viral burden in the blood, spleen, and brain of aged animals compared to young, suggesting that dysfunctional leukocyte trafficking in the aged mice impeded anti-viral responses (Richner *et al.*, 2015). Impaired naïve $CD4^+$ T-cell trafficking into the dLN of WNV-infected aged mice was partly attributed to intrinsic cellular defects, as the adoptive transfer of naïve $CD4^+$ T-cells derived from aged mice into young recipients experiencing WNV infection did not improve T-cell trafficking to youthful levels (Richner *et al.*, 2015). Intravital two-photon microscopy revealed that leukocyte capture and rolling along HEV is unaffected by age, however, aged naïve $CD4^+$ T-cells extravasated less efficiently into dLN (Richner *et al.*, 2015).

Defective naïve $CD4^+$ T-cell trafficking in WNV-infected aged mice was also partly attributed to age-related changes to the microenvironment, as both young and aged naïve $CD4^+$ T-cells displayed lower levels of migration into dLN when adoptively transferred into infected aged recipient animals (Richner *et al.*, 2015). Indeed, aged mice had significantly lower levels of CCL21, a chemoattractant for naïve T-cells, in the dLN after 2 days of infection compared to young mice, determined by ELISA analysis. This was also true in models of immunization (Lefebvre *et al.*, 2012). Intraperitoneal delivery of OVA (50µg) resulted in reduced recruitment of $CD4^+$ T-cells

to the spleens of aged (>20 months) C57Bl6 mice compared to young (<3 months) mice, and correlated with a reduced expression of CCL19 and CCL21 T-cell chemoattractants in the aged spleen (Lefebvre *et al.*, 2012). Collectively, the literature suggests T-cell trafficking during acute inflammation is dysregulated in older mice.

One of the most extensively used and simple models of acute inflammation to study leukocyte trafficking in young mice is zymosan-induced peritonitis (Cash, White and Greaves, 2009). The peritoneal cavity is a fluid-filled space that contains the abdominal organs, and is an easily accessible immunological niche comprising of several populations of leukocytes, primarily macrophages and B1 cells (reviewed by Liu *et al.*, 2021). Dating back to the 1890s (Steven, 1892), the induction of acute peritoneal inflammation, known as peritonitis, through use of irritants (thioglycolate, polyacrylamide), pro-inflammatory cytokines (IL-1) and pathogenic materials (zymosan A) has been used to study mechanisms of inflammation (Chen *et al.*, 2008; Henderson *et al.*, 2003; Bursill *et al.*, 2003; Paul-Clark *et al.*, 2004; Rao *et al.*, 1994).

Zymosan A is an insoluble polysaccharide derived from the cell walls of *Saccharomyces cerevisiae* and has been used to induce self-resolving peritonitis since 1985 (Doherty *et al.*, 1985). Peritoneal inflammation is initiated by Zymosan A binding to toll-like receptors (TLR)-2/6 (Ozinsky *et al.*, 2000) and dectin-1 (Brown *et al.*, 2002; Brown *et al.*, 2003) receptors on large peritoneal macrophages, which subsequently secrete inflammatory mediators that attract a plethora of leukocytes to the cavity at specific time intervals (Newson *et al.*, 2014). The dose of zymosan (Rajakariar *et al.*, 2008; Newson *et al.*, 2014) and sex of the host organism (Kay *et al.*, 2015; Scotland *et al.*, 2011) shapes the course of the inflammatory response. But to date, only a finite number of studies have used this extensively characterised model to study leukocyte

trafficking in aged mice (Arnardottir *et al.*, 2014). Here, Arnardottir *et al.* used a self-resolving model of peritonitis to study neutrophil recruitment to the peritoneal cavity of male BALBc mice after 4, 12 and 24 hours and found that aged (20 months) mice recruited more neutrophils at each time point compared to young (2 months) mice (Arnardottir *et al.*, 2014). However, to date, no one has used the peritonitis model to specifically study T-cell trafficking in aged mice or to determine if there is sexual dimorphism within this model in aged animals. As of such, these became two major aims of this thesis.

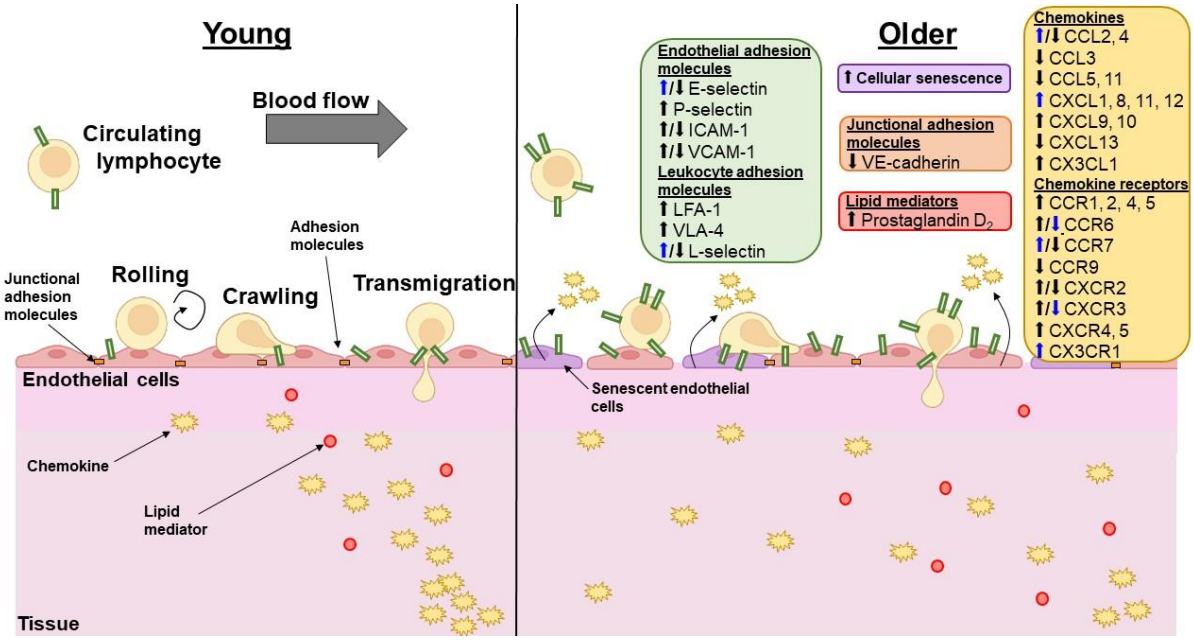

Figure 1-3 How the ageing process influences the leukocyte adhesion cascade

A schematic depicting age-related changes to the leukocyte adhesion cascade. The trafficking of lymphocytes into and out of tissue is modulated by the ageing process under homeostatic and inflammatory conditions. The direct consequences of ageing (depicted by bold black arrows, ⬆/⬇) on leukocyte trafficking include: changes to the expression of adhesion molecules on the endothelium, changes to the expression of adhesion molecules and chemokine receptors on circulating lymphocytes, reduced expression of junctional molecules between endothelial cells, and increased production of lipid mediators and chemokines within tissue. The indirect consequences of ageing (depicted by bold blue arrows, ⬆/⬇) that influence leukocyte trafficking dynamics stem from the accumulation of senescent cells in tissue that express increased levels of adhesion molecules and secrete pro-inflammatory mediators, including chemokines. The age-related dysregulation of lymphocyte trafficking is therefore multifactorial and a direct, as well as indirect, consequence of ageing.

1.4 THE PEPITEM PATHWAY

In 2015, a novel B-cell-mediated immunoregulatory pathway involved in the regulation of T-cell trafficking into tissues was identified (Chimen *et al.*, 2015). This homeostatic pathway, centred around PEPITEM, served to inhibit T-cell migration across, but not adhesion to, vascular endothelium (Chimen *et al.*, 2015). The pathway is initiated by adiponectin (AQ) binding adiponectin receptors 1 and 2 (AdipoR1/2) on circulating B-cells, resulting in the release of a small peptide named PEPITEM (Chimen *et al.*, 2015). PEPITEM then interacts with vascular endothelium via cadherin-15, stimulating the release of sphingosine-1-phosphate (S1P) (Chimen *et al.*, 2015). S1P binds S1P receptors on adhered T-cells and, through intracellular signalling cascades, results in integrin LFA-1 inactivation; in turn leading to inhibited T-cell transendothelial migration (Chimen *et al.*, 2015). A schematic depiction of the PEPITEM pathway can be found in **Figure 1-4**. One of the major aims of this thesis is to understand whether ageing is associated with PEPITEM pathway dysfunction, and in turn, whether this pathway plays a role in dysregulated leukocyte trafficking in older hosts. The known molecular mechanisms of the PEPITEM pathway components are described below along with a summary of the reported sex-specific differences of and age-related changes to each signalling component.

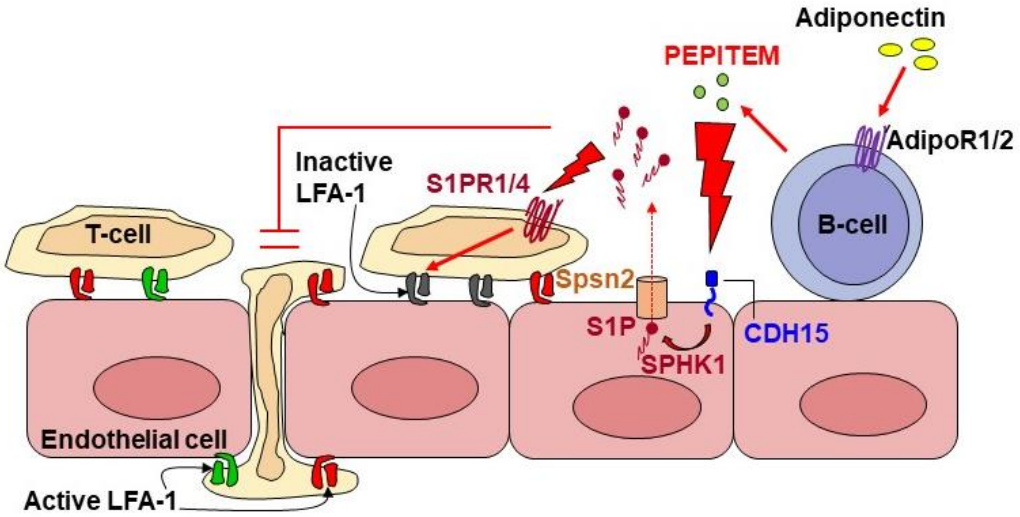

Figure 1-4 Schematic of the PEPITEM pathway

Circulating adiponectin binds adiponectin receptors 1 and 2 (AdipoR1/2) on B-cells, resulting in the release of PEPITEM. PEPITEM binds cadherin-15 (CDH15) on vascular endothelial cells, stimulating the activation of sphingosine kinase 1 (SPHK1) and secretion of sphingosine-1-phosphate (S1P) via spinster homolog 2 (Spsn2). S1P binds S1P receptors 1 and 4 (S1PR1/4) on circulating T-cells, resulting in LFA-1 integrin inactivation. In turn, this pathway prevents T-cells from performing transendothelial migration. Adapted from Chimen *et al.*, 2015.

1.4.1 ADIPONECTIN

AQ is a 30kDa adipokine released by adipocytes and other tissues (Diez and Iglesias, 2003; Berner *et al.*, 2004; Yoda-Murakami *et al.*, 2001; Delaigle *et al.*, 2004) that serves to regulate glucose levels, lipid metabolism and insulin sensitivity by binding its receptors and instigating intracellular signalling cascades in metabolic tissues such as the kidneys and liver (Nguyen, 2020; Esmaili, Hemmati and Karamian, 2020). It is encoded by the AdipoQ gene located on chromosome 3q21 (Kissebah *et al.*, 2000) and its structure is comprised of a carboxy terminal globular head and a collagenous tail (Shapiro and Scherer, 1998; Yokota *et al.*, 2000). AQ exists in the circulation as the globular domain or full-length multimeric isoforms, including a low-molecular weight (LMW) trimer, a medium molecular weight (MMW) hexamer, and the biologically most active form based on blood glucose studies, a high molecular weight (HMW) multimer (Pajvani *et al.*, 2003; Tsao *et al.*, 2003). Globular forms of AQ are produced from cleavage of the collagenous tails by leukocyte elastase (Waki *et al.*, 2005) whilst non-covalent linkage of the collagenous tails form LMW dimers and trimers (Pajvani *et al.*, 2003), and additional disulphide bridges/post-translational modifications form MMW and HMW multimers (Tsao *et al.*, 2003; Richards *et al.*, 2006).

Circulating levels of total AQ range between 2-20µg/ml in young healthy individuals (Arita *et al.*, 1999; Ouchi *et al.*, 1999), although the circulating concentrations of AQ appear to be sex-specific (Adamczak *et al.*, 2005; Ouchi *et al.*, 1999). Indeed, multiple studies have reported that young (<50 years) men have significantly lower levels of circulating AQ (approximately 9.6µg/ml) compared to young (<50 years) women (approximately 11.2µg/ml) after controlling for body mass index

(BMI), though the average concentration of AQ per sex varied between studies (Adamczak *et al.*, 2005; Ouchi *et al.*, 1999; Isobe *et al.*, 2005). The sex-specific differences in circulating AQ levels is believed to be due to the inhibitory effects of testosterone on AQ release from adipose tissue, leading to lower levels of AQ in the circulation of men (Wang *et al.*, 2008b).

The ageing process evidently affects circulating AQ levels in a sex-specific manner, as increased levels of total AQ were observed in the serum of older (>70 years) men (14μg/ml) compared to younger men, but were unchanged in the serum of older (>70 years) women (11.7μg/ml) compared to younger women (Song *et al.*, 2014; Adamczak *et al.*, 2005). These changes could be explained by the age-related decline in testosterone levels in men (Stanworth and Jones, 2008), which would release the inhibitory effects of testosterone on AQ secretion. Intriguingly, despite higher circulating AQ levels being linked with frailty in older individuals (Tsai *et al.*, 2013; Nagasawa *et al.*, 2018), increased levels of AQ in the plasma of centenarians, individuals who live longer than 100 years, has been reported (Bik *et al.*, 2006). Several studies have suggested that AQ is able to promote longevity (Iwabu *et al.*, 2015; Atzmon *et al.*, 2008) through inducing signalling cascades mimicking exercise, such as the calcium/calmodulin-dependent protein kinase β-dependent pathways and the phosphorylation of peroxisome proliferator-activated receptor γ coactivator 1α in skeletal muscle (Iwabu *et al.*, 2010), as well as alleviating oxidative stress in metabolic tissues such as the liver through inducing the expression catalase and superoxide dismutase genes (Yamauchi *et al.*, 2007). Any age-related changes to circulating AQ levels may affect the function of the PEPITEM pathway.

1.4.1.1 IMMUNOREGULATORY PROPERTIES OF ADIPONECTIN

Many immunoregulatory properties of AQ have been reported, including broad anti-inflammatory effects (Yamaguchi *et al.*, 2005; Ohashi *et al.*, 2010; Ouchi *et al.*, 1999; Ajuwon and Spurlock, 2005). *In vitro*, the culturing of primary human monocytes, monocyte-derived DC, and monocyte-derived macrophages in the presence of 20µg/ml AQ for 7 days led to IL-10 and IL-1RA production in the absence of immune stimuli; although the exact isoform of adiponectin used was not stated (Wolf *et al.*, 2004). Furthermore, 20µg/ml AQ treatment reduced IFNγ production by lipopolysaccharide (LPS)-stimulated primary macrophages, dampening LPS-induced pro-inflammatory responses (Wolf *et al.*, 2004). AQ-deficient C57Bl6 mice displayed an impaired ability to clear apoptotic thymocytes in response to dexamethasone treatment, and to clear apoptotic Jurkat T-cells administered directly into the peritoneal cavity; a phenotype that was rescued upon intraperitoneal administration of recombinant AQ (Takemura *et al.*, 2007).

Interestingly, the anti-inflammatory effects of AQ affect leukocyte-endothelial interactions (Ouchi *et al.*, 1999; Ouedraogo *et al.*, 2007; Cao *et al.*, 2009). Pre-treatment of human aortic endothelial cells with various concentrations (1-50µg/ml) of recombinant AQ *in vitro* before a 6 hour TNFα treatment led to reduced endothelial expression of VCAM-1, ICAM-1 and E-selectin, and reduced adhesion of THP-1 cells, a human monocytic cell line, to the EC (Ouchi *et al.*, 1999). In agreement with this, increased levels of leukocyte rolling and adhesion were observed in the peri-intestinal venules of AQ-deficient C57Bl6 mice compared to wildtype controls using intravital microscopy (Ouedraogo *et al.*, 2007). Quantitative fluorescent microscopy revealed increased expression of VCAM-1 and E-selectin in the peri-intestinal venules of AQ-

deficient mice (Ouedraogo *et al.*, 2007), signifying that AQ-deficiency influences endothelial expression of adhesion molecules which in turn affects leukocyte trafficking processes. Indeed, AQ influences leukocyte-endothelial interactions and is the initiating component of the PEPITEM pathway (Chimen *et al.*, 2015).

However, there are confounding data in the literature as many studies have also reported pro-inflammatory properties of AQ (Song, Chan and Rovin, 2009; Zhang *et al.*, 2020a; Cheng *et al.*, 2012; Frommer *et al.*, 2010). Overnight treatment of PBMC (0.01-1µg/ml) and dermal microvascular EC (DMVEC; 5-20µg/ml) with HMW AQ promoted a dose-dependent production of CCL2 and IL-8 by both cell types *in vitro* (Song, Chan and Rovin, 2009). However, this response appeared to be specific to the isoform of AQ used, as LMW AQ at similar concentrations did not elicit the production of these cytokines/chemokines from either cell type (Song, Chan and Rovin, 2009). In PBMC from healthy donors, 5µg/ml AQ treatment induced the production of pro-inflammatory CXCL1, CXCL5, CCL3, CCL4, CCL17, IL-6, TNFα and anti-inflammatory IL-10 (Zhang *et al.*, 2020a). However, these PBMC were isolated from adults of various ages (25-72 years) and were frozen for an unspecified amount of time before use which could have affected their functional responses to AQ (Ramachandran *et al.*, 2012). Although there is some literature describing the pro-inflammatory properties of AQ, most of the literature to date describes the broad-acting anti-inflammatory properties of AQ in healthy individuals (Ouchi and Walsh, 2007; Choi, Doss and Kim, 2020). Importantly, the observed pro-inflammatory properties of AQ appear to be context dependent and vary depending on the isoform of AQ used (Song, Chan and Rovin, 2009), the inflammatory state of the cell/blood donors (Kitahara *et al.*, 2009; Kusunoki *et al.*, 2010) and the experimental design (Zhang *et al.*, 2020a).

Of the studies that have investigated the immunoregulatory properties of AQ, very few have considered the effects of chronological ageing (Li *et al.*, 2021) on the system and none have considered sexual dimorphism. In mice, quantitative fluorescence microscopy revealed that 23-32 month AQ-knock out (KO) male mice exhibited an increased abundance of pro-inflammatory macrophages in the epididymal fat compared to age-matched control mice, which was associated with increased levels of TNFα, CCL2 and C-reactive protein in the tissue (Li *et al.*, 2021). Whether high levels of circulating AQ are beneficial or detrimental to older individuals is currently unknown (Stott *et al.*, 2009; Oh *et al.*, 2018; Hansen *et al.*, 2009; Kizer *et al.*, 2012). Higher levels of total AQ in the circulation of older adults was associated with a lower risk of ischemic stroke (Stott *et al.*, 2009), but was also associated with an increased incidence of depression (Oh *et al.*, 2018), atherosclerosis (Hansen *et al.*, 2009) and cardiovascular disease (Kizer *et al.*, 2012). As AQ has metabolic as well as immunoregulatory functions, the conflicting data regarding circulating AQ levels in older individuals may be due to the fact that these are correlation studies and changes in circulating AQ levels in these older adults may be independent of their disease states.

1.4.2 ADIPONECTIN RECEPTORS

In the context of the PEPITEM pathway, AQ primarily acts via two seven transmembrane receptors that bear resemblance to G-protein coupled receptors (GPCR), namely AdipoR1 and AdipoR2 (Yamauchi *et al.*, 2003; Chimen *et al.*, 2015). Although both receptors are expressed on multiple cell types throughout the body, including on pancreatic beta-cells (Kharroubi *et al.*, 2003), osteoblast-like cells (Berner *et al.*, 2004) and PBMC such as NK cells and B-cells (Pang and Narendran, 2008), AdipoR1 is primarily found in skeletal muscle and AdipoR2 in the liver (Polito *et al.*,

2019). They also differ in their specificity for AQ isoforms (Polito *et al.*, 2019), with AdipoR1 preferentially binding globular AQ and AdipoR2 preferentially binding multimeric isoforms of AQ (Yamauchi *et al.*, 2014).

The signalling cascade downstream of the AdipoR has not been characterised in B-cells specifically but has been delineated in metabolic tissues such as the liver, skeletal muscle, and heart (Yamauchi *et al.*, 2002; Iwabu *et al.*, 2010; Tsuchida *et al.*, 2004; Cui *et al.*, 2012). In these tissues, AdipoR1/2 stimulation by AQ resulted in calcium influx into the cells (Iwabu *et al.*, 2010) and the activation of adenosine monophosphate-activated protein kinase (AMPK), peroxisome-proliferator-activated-receptor α (PPARα), p38 mitogen-activated protein kinase (p38 MAPK), NF-κβ, extracellular signal-regulated kinase 1/2 (ERK-1/2), signalling transducer and activator of transcription 3 (STAT3) and ceramidase pathways (Yamauchi *et al.*, 2003; Yamauchi *et al.*, 2007; Tang *et al.*, 2007; Obeid and Hebbard, 2012; Holland *et al.*, 2011). Interestingly, sexual dimorphism exists within the signalling cascades downstream of the AdipoR as the presence of oestrogen receptor α confers the preferential activation of the MAPK pathway rather than the AMPK pathway following adiponectin stimulation (Mauro *et al.*, 2015). The intracellular signalling component immediately downstream of the AdipoR was discovered in the mid-2000s, namely the adaptor protein phosphotyrosine interacting with pH domain and leucine zipper 1 (APPL1) (Cheng *et al.*, 2007; Mao *et al.*, 2006). Specifically how APPL1 interacts with AdipoR1/2 is currently unknown (Deepa and Dong, 2009), but is believed to be due to the dimerization of the receptors upon AQ-stimulation, allowing the phosphotyrosine-binding domain of APPL1 to interact with the intracellular NH_2-terminus of AdipoR1/2 (Yamauchi *et al.*, 2003; Nechamen *et al.*, 2004).

1.4.2.1 AGE-RELATED CHANGES TO SIGNALLING COMPONENTS DOWNSTREAM OF THE ADIPONECTIN RECEPTORS

Ageing profoundly affects the signalling components downstream of the AdipoR in several tissue types (Salminen and Kaarniranta, 2012; Iwabu *et al.*, 2015). In male Fischer 344 rats, activation of AMPK-α_2 by 5'-aminoimidazole-4-carboxamide-1-β-D-ribofuranoside was reduced in the skeletal muscle of old (28 months) rats compared to young (3 months) rats (Reznick *et al.*, 2007). A similar observation was made by Ljubicic *et al.*, whereby phosphorylated AMPKα levels were reduced in the tibialis anterior muscle of old (36 months) Fischer 344 rats following artificial muscle contractions *in situ* compared to young (6 months) rats (Ljubicic and Hood, 2009). PPARα signalling is also influenced by the ageing process as baseline gene and protein expression of PPARα is reduced in the kidneys of old (31 months) male Fischer 344 rats compared to younger (13 months) male rats (Sung *et al.*, 2004), and is reduced in the spleens of 18 month female Fischer 344 rats compared to 3 month female rats (Gelinas and McLaurin, 2005). The activation of ERK-1/2 and MAPK pathways are also blunted during the ageing process as reduced phosphotransferase activities of ERK-1/2 and p38 MAPK isolated from the cerebrocortex of old (>12 months) male Fischer 344 rats were observed *in vitro* compared to younger (6 months) rats (Zhen *et al.*, 1999).

Importantly, the age-related downregulation of signalling components downstream of the AdipoR1/2 is evident in leukocytes (Wang *et al.*, 2021; Douziech *et al.*, 2002; Tortorella *et al.*, 2004). The gene and protein expression of PPARα was reduced in circulating monocytes derived from old (>18 months) female C57Bl6 mice compared to younger (<2 months) mice. PPARα protein expression was also reduced

in circulating monocytes isolated from older (>60 years) adults compared to younger (<30 years) adults (Wang *et al.*, 2021). The activation of ERK and p38 MAPK pathways was reduced in T-cells isolated from older (>65 years) adults following anti-CD3 monoclonal antibody stimulation *in vitro* compared to T-cells isolated from younger (<30 years) donors (Douziech *et al.*, 2002). Furthermore, the stimulation of neutrophils isolated from older (>65 years) adults with GM-CSF resulted in reduced levels ERK-1/2 phosphorylation compared to neutrophils isolated from younger (<35 years) adults (Tortorella *et al.*, 2004). Collectively, these studies highlight the negative effect chronological ageing has on the downstream signalling components of the AdipoR in various tissues including leukocytes.

1.4.2.2 TRANSCRIPTION FACTORS DOWNSTREAM OF THE ADIPONECTIN RECEPTORS

The activation of p38 MAPK and PPARα pathways (Yamauchi *et al.*, 2003; Tang *et al.*, 2007), as well as the calcium/calmodulin-dependent protein kinase kinase (CAMKK)-dependent pathways (Iwabu *et al.*, 2010), that occur downstream of AdipoR1/2 stimulation leads to the activation of cAMP response element-binding protein (CREB) (Di Giacomo *et al.*, 2009; Kim *et al.*, 2018; Chen *et al.*, 1998; Roy *et al.*, 2013) and activating transcription factor 1 (ATF-1) (Wiggin *et al.*, 2002; Shimomura *et al.*, 1996) transcription factors (TF) (see **Figure 1-5**). CREB and ATF-1 belong to the CREB family of TF and regulate the transcription of a multitude of genes involved in various physiological process, such as cellular metabolism, growth-factor-dependent survival, and immune cell development (reviewed by Mayr and Montminy, 2001). Importantly, both CREB and ATF-1 regulate the transcription of the gene that encodes 14-3-3ζ/δ, the parent protein of PEPITEM, *YWHAZ* (Kasinski *et al.*, 2014).*YWHAZ is* located on

chromosome 8q22.3 and although there have been five reported transcript variants of *YWHAZ*, only one is dominant in its translation efficiency (Kasinski *et al.*, 2014).

A limited number of studies have suggested that the activation of CREB family TF is dampened by the ageing process, albeit the majority of studies to date have specifically focused on CREB activation in the brain (Porte, Buhot and Mons, 2008; Paramanik and Thakur, 2013). In 129T2/Sv mice, there was a reduced abundance of phosphorylated CREB in the brains of aged (>23 months) male mice compared to young (<6 months) mice following 15 minutes of a spatial memory reference task, which correlated with spatial memory deficits in the older mice (Porte, Buhot and Mons, 2008). A similar observation was made in Wistar rats, where a reduced abundance of phosphorylated CREB was observed in the hippocampus of aged (30 months) male rats compared to young (5 months) rats following conditioned fear (Monti, Berteotti and Contestabile, 2005). Furthermore, DMVEC isolated from older (66 years) adults displayed reduced levels of phosphorylated CREB in culture compared to DMVEC isolated from neonates and was associated with the impaired angiogenesis of older EC in response to VEGF treatment (Ahluwalia *et al.*, 2014). One of the aims of this thesis is to explore the impact of ageing on the intracellular signalling cascades downstream of the AdipoR in B-cells as this may influence PEPITEM production.

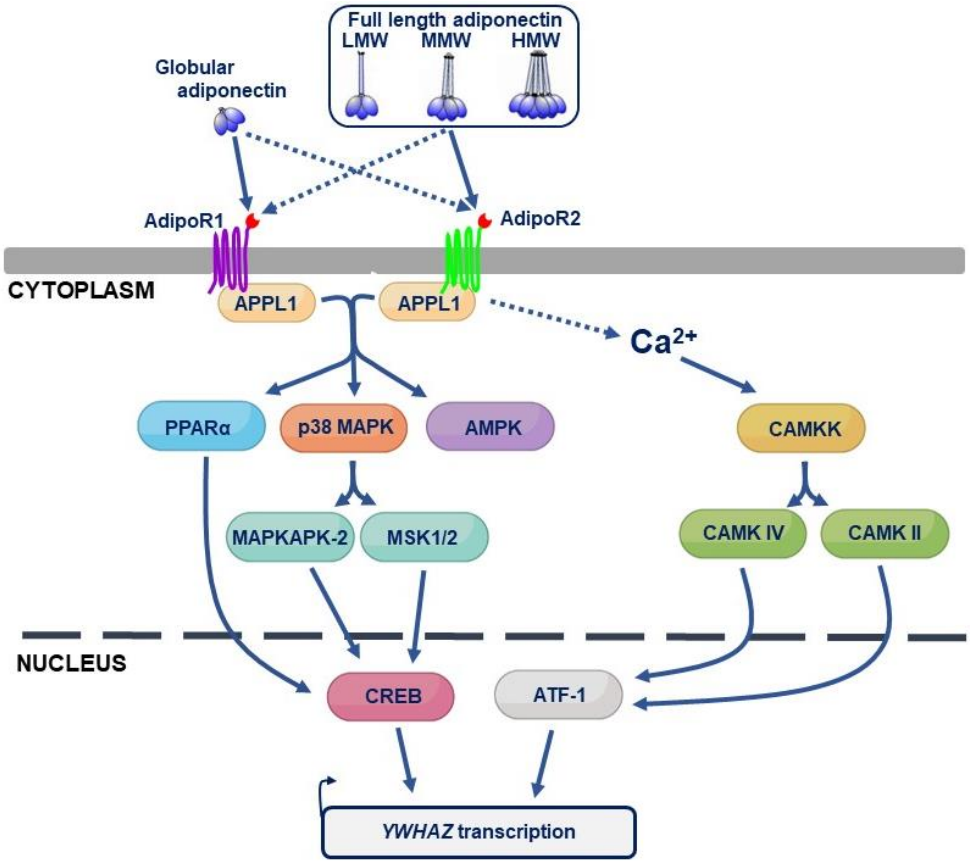

Figure 1-5 Schematic of the intracellular signalling cascades downstream of adiponectin receptor stimulation that lead to *YWHAZ* transcription

Globular adiponectin preferentially binds adiponectin receptor 1 (AdipoR1), whilst full length low (LMW), medium (MMW) and high (HMW) molecular weight adiponectin preferentially binds AdipoR2. AdipoR1/2 stimulation leads to adaptor protein phosphotyrosine interacting with pH domain and leucine zipper 1 (APPL1) activation, which stimulates peroxisome-proliferator-activated-receptor α (PPARα), p38 mitogen-activated protein kinase (p38 MAPK) and adenosine monophosphate-activated protein kinase (AMPK) pathways. p38 MAPK activation leads to MAPK-activated protein kinase 2 (MAPKAPK2) and mitogen- and stress-activated protein kinase 1 and 2 (MSK-1/2) activation. In turn, signalling downstream of APPL1 results in the activation of cAMP response element-binding protein (CREB) transcription factor, which leads to *YWHAZ* transcription. Reportedly, AdipoR1/2 engagement with adiponectin also leads to increased intracellular calcium levels, activating calcium/calmodulin-dependent protein kinase kinase (CAMKK)-dependent pathways and activating transcription factor 1 (ATF-1). ATF-1 activation also leads to *YWHAZ* transcription. Dotted lines represent possible/uncertain interactions.

1.4.3 14-3-3 PROTEINS

One of the critical steps in the PEPITEM pathway is the cleavage of PEPITEM from its parent protein, 14-3-3 ζ. The 14-3-3 family of proteins (28-33 kDa) are found in all eukaryotic organisms and are expressed in almost every tissue in multiple isoforms (Mhawech, 2005). In mammals, seven highly homologous and conserved isoforms exist, namely the beta (β), epsilon (ε), gamma (γ), eta (η), sigma (σ), tau (τ) and zeta (ζ) isoforms (Mhawech, 2005). A further two isoforms are formed by the phosphorylation of 14-3-3β and 14-3-3ζ, namely the alpha (α) and delta (δ) isoforms, respectively (Fu, Subramanian and Masters, 2000). The monomeric structure of 14-3-3 proteins consists of nine anti-parallel alpha helices forming an amphipathic groove which binds phosphorylated serines and threonines on 14-3-3 binding partners such as mammalian target of rapamycin, AMPK, and MAPK (Liu *et al.*, 1995; Morrison and Cutler, 1997; Kuwana, Peterson and Karlsson, 1998; Hausser *et al.*, 1999; Muslin *et al.*, 1996; Pennington *et al.*, 2018). The 14-3-3 family of proteins are involved in a range of cellular processes including cellular metabolism, cell cycle regulation, apoptosis, autophagy, and protein trafficking (Mhawech, 2005; Fu, Subramanian and Masters, 2000; Bridges and Moorhead, 2005; Dougherty and Morrison, 2004).

1.4.3.1 ROLE OF 14-3-3 PROTEINS IN LEUKOCYTE TRAFFICKING

Importantly, 14-3-3 proteins are involved in cell adhesion and migration processes (Han, Rodriguez and Guan, 2001; Rodriguez and Guan, 2005; Garcia-Guzman *et al.*, 1999; Wilker and Yaffe, 2004). *In vitro*, macrophage stimulating protein activation of keratinocytes led to 14-3-3τ binding to the integrin laminin receptor, $\alpha_6\beta_4$, invoking the redistribution of $\alpha_6\beta_4$ away from hemidesmosomes to lamellipodia in support of

keratinocyte spreading and migration (Santoro, Gaudino and Marchisio, 2003). In fibroblasts, cell adhesion to fibronectin *in vitro* was supported by 14-3-3β binding to the cytoplasmic domain β1 integrins via a non-phosphoserine mechanism (Han, Rodriguez and Guan, 2001; Rodriguez and Guan, 2005), and by 14-3-3ζ/δ binding to Cas, an integrin signalling adaptor protein, in a phosphoserine-dependent manner (Garcia-Guzman *et al.*, 1999). In mammary epithelial cells, the overexpression of 14-3-3ζ interfered with transforming growth factor-receptor 1 signalling and led to reduced levels of E-cadherin expression on the cell surface, which promoted cell migration *in vitro* (Lu *et al.*, 2009). It is therefore evident that 14-3-3 protein signalling is involved in the adhesion and migration of multiple cell types.

14-3-3 proteins are expressed by almost every immune cell type (monocytes, T-cells, B-cells, NK cells (BioGPS)) and are known to play an integral role in the inflammatory response (reviewed by Munier, Ottmann and Perry, 2021). In murine hybridoma T8.1 T-cells, TCR stimulation by anti-CD3 monoclonal antibodies *in vitro* led to 14-3-3ε and β binding to and activating the SH2 domain-containing leukocyte protein of 76 kD, a key signalling component for TCR activation (Di Bartolo *et al.*, 2007). In THP-1 monocytes, metabolic reprogramming through exposure to diabetic conditions led to the degradation of 14-3-3ζ and conversion of monocytes into hypermigratory, proatherogenic cells (Kim *et al.*, 2014a). B-cells isolated from 14-3-3σ-deficient mice exhibited reduced survival and proliferation in response to BCR-engagement *in vitro* compared to those isolated from wildtype mice (Su *et al.*, 2011). Interestingly, extracellular 14-3-3ζ treatment induced a range of immunoregulatory responses in PBMC *in vitro*, including cell proliferation, T-cell polarization towards Th1 and Th17 subsets and the production of IFNγ and IL-17 (McGowan *et al.*, 2019). The

14-3-3 family of proteins therefore appear to exert pro-inflammatory responses in leukocytes in both intracellular and extracellular formats.

1.4.3.2 AGE-RELATED CHANGES TO 14-3-3 PROTEINS

The 14-3-3 family of proteins have been heavily implicated with ageing and longevity (reviewed by Fan *et al.*, 2019). In *Saccharomyces cerevisiae*, deletion of the 14-3-3 protein, Bmh1, extended the lifespan of yeast cells through activating stress response TF and reducing intracellular levels of reactive oxygen species (Wang *et al.*, 2009). In glioblastoma cells, 14-3-3β depletion by the introduction of small interfering RNA resulted in the upregulation of senescence pathways and an inhibition in cell growth/proliferation pathways (Seo *et al.*, 2018). Indeed, ageing was associated with a reduced abundance of 14-3-3σ in the skin of nude mice (Fang *et al.*, 2016) and reduced 14-3-3ε in the skin of humans (Choi *et al.*, 2005), which corresponded with a loss of cell growth processes. Although studies specifically investigating the role of 14-3-3 proteins in ageing leukocytes are lacking, it is clear that 14-3-3 proteins play an integral role in the longevity and senescence processes that occur during ageing.

1.4.4 PEPITEM

PEPITEM is a small peptide (14 amino acids) that represents residues 28-41 of 14-3-3ζ/δ (Chimen *et al.*, 2015). The PEPITEM sequence is highly conserved between species, with the majority of mammals expressing the protein at 100% homology (Chimen, 2012). Although the peptide was first identified by Suri *et al.* in 2005 (Suri *et al.*, 2005), the biological function of PEPITEM was not described until 2015 by Chimen *et al.* (Chimen et al., 2015). The ability of PEPITEM to regulate T-cell trafficking has been confirmed in several murine models of acute inflammation, including ZIP,

systemic bacteraemia, and LPS-mediated uveitis (Chimen *et al.*, 2015), also in murine models of chronic inflammation, such as systemic lupus erythematosus (SLE; (Matsubara *et al.*, 2020) and obesity (Pezhman *et al.*, 2023). Whether PEPITEM exerts any immunoregulatory properties in the absence of inflammation is currently unknown.

The production of PEPITEM from 14-3-3ζ/δ is not yet fully understood but is believed to occur extracellularly (Apta, 2015). Apta showed that the treatment of PBL with 14-3-3ζ inhibited PBL transendothelial migration *in vitro* at comparable levels to PEPITEM treatment, and that these effects were abolished in the presence of a broad-spectrum protease inhibitor (Apta, 2015). Therefore, the current working hypothesis is that upon AdipoR stimulation by AQ, 14-3-3ζ is synthesised intracellularly and then secreted by peripheral blood B-cells. It is postulated that EC-derived proteases then cleave PEPITEM from 14-3-3ζ in the extracellular space. Following its generation, PEPITEM then proceeds to interact with vascular EC via cadherin-15 (Chimen *et al.*, 2015).

1.4.5 CADHERIN-15 AND SPHINGOSINE-1-PHOSPHATE

Cadherin-15 (also known as M-cadherin) is a calcium-dependent adhesion molecule that is predominantly expressed within skeletal muscle and the cerebellum (Bahjaoui-Bouhaddi *et al.*, 1997; Rose *et al.*, 1995; Irintchev *et al.*, 1994; Kaufmann *et al.*, 1999). Whilst the primary function of cadherins is to mediate homophilic cell-cell interactions, cadherin-15 specifically aids in muscle development and regenerative processes (Bornemann and Schmalbruch, 1994; Donalies *et al.*, 1991; Hollnagel *et al.*, 2002). Although cadherin-15 expression on EC has not been extensively documented, Chimen *et al.* reported the expression of cadherin-15 on unstimulated and TNFα+IFNγ-

stimulated human microvascular EC *in vitro* using confocal microscopy (Chimen *et al.*, 2015). Furthermore, Matsubara *et al.* reported cadherin-15 protein expression on the vascular EC of the kidneys, skin and peritoneal membrane of 22 week-old MRL/lpr mice (Matsubara *et al.*, 2020). The extent to which ageing affects cadherin-15 expression is currently unknown as the number of studies are limited. Lagerwaard *et al.* reported an age-related increase in the gene expression of cadherin-15 in *vastus lateralis* muscle biopsies of older (>67 years) men compared to younger (<24 years) men, which correlated with increased cell adhesion between muscle fibres in older men (Lagerwaard *et al.*, 2021). However, it would be of interest to investigate age-related changes to cadherin-15 protein expression by vascular endothelium to determine whether ageing affects this step in the PEPITEM pathway.

Following PEPITEM interactions with cadherin-15 on the EC surface, intracellular signalling events within the vascular cells result in the release of S1P into the extracellular space (Chimen *et al.*, 2015). S1P is a sphingolipid that is involved in a range of biological functions, such as suppressing apoptosis, promoting cell growth, and supporting immune cell migration (reviewed by Maceyka *et al.*, 2012; Spiegel and Milstien, 2011). S1P is generated by the phosphorylation of sphingosine by sphingosine kinase 1 and 2 (SPHK1/2) in the cytosol of numerous cell types including EC (Hla *et al.*, 2001). S1P is then transported across the cell membrane into the extracellular space by the S1P transporter protein spinster homolog 2 (SPNS2) (Kawahara *et al.*, 2009). Once secreted, S1P can then interact with its GPCRs, S1P receptors 1 to 5 (S1PR1-5), on target cells (Maceyka *et al.*, 2012).

1.4.5.1 SPHINGOSINE-1-PHOSPHATE, ENDOTHELIAL JUNCTIONS AND LEUKOCYTE TRAFFICKING

S1P is a pleiotropic lipid mediator that can modulate the function of multiple cell types, including EC and leukocytes (Xiong and Hla, 2014; Blaho and Hla, 2014). Through interacting with endothelial expressed S1PR1-3, S1P can modulate endothelial spreading, vascular maturation, and vessel permeability (Ancellin *et al.*, 2002; Hla, 2003). S1PR1 and 3 stimulation leads to the activation of Rac in EC, inducing cytoskeletal rearrangements and junctional molecule relocalisation leading to enhanced endothelial barrier integrity (Oo *et al.*, 2011; Blaho and Hla, 2011). Indeed, in HUVEC, S1P treatment (500nM) led to increased expression of VE-cadherin and β-catenin at cell-cell contact regions *in vitro* compared to vehicle controls (Lee *et al.*, 1999). Importantly, VE-cadherin redistribution was specifically a consequence of S1P signalling as the administration of oligonucleotides that disrupted S1P signalling suppressed this phenotype (Lee *et al.*, 1999). It is therefore possible that S1P plays an additional role in the PEPITEM pathway. It is possible that, following S1P production by EC (**Figure 1-4**), S1P may act in an autocrine fashion on EC via S1PR1-3 to enhance vascular integrity; thus promoting a physical barrier to inhibit T-cell transendothelial migration.

S1P plays a central role in the regulation of leukocyte trafficking (reviewed by Spiegel and Milstien, 2011). Regarding T-cells, S1P primarily signals via S1PR1-4 (reviewed by Garris *et al.*, 2014) and regulates T-cell trafficking from SLOs into the circulation (Matloubian *et al.*, 2004; Fukuhara *et al.*, 2012), but also retains T-cells within peripheral tissue during inflammation (Ledgerwood *et al.*, 2008; Roviezzo *et al.*, 2011). In mice that specifically lack S1PR1 expression on haematopoietic cells, mature

T-cells were retained in the thymus whilst B-cells were excluded from the blood and lymph (Matloubian *et al.*, 2004). What more, adoptive transfer of S1PR1-expressing B- and T-cells into the circulation rescued this phenotype as S1PR1-expressing lymphocytes were not restricted to lymphoid tissues (Matloubian *et al.*, 2004). In C57Bl6 mice, the treatment of T-cells with FTY720, a S1PR1 agonist, prevented T-cell egress from the site of administration into afferent lymphatic vessels under homeostatic and inflammatory conditions (Ledgerwood *et al.*, 2008). This was in part due to the interactions of T-cell expressed LFA-1 and VLA-4 with their ligands ICAM-1 and VCAM-1 on afferent lymphatics, respectively, as T-cells pre-treated with anti-LFA-1 and anti-VLA-4 antibodies were not retained at the site of administration (Ledgerwood *et al.*, 2008). Indeed, S1P-mediated signalling influences T-cell integrin activation states (Halin *et al.*, 2005; Ledgerwood *et al.*, 2008) and forms the crux of the PEPITEM pathway (Chimen *et al.*, 2015). Here, S1P interactions with S1PR1/4 on the surface of EC-adhered T-cells resulted in the inactivation of LFA-1 integrins, which, in turn, inhibited T-cells from performing transendothelial migration *in vitro* (Chimen *et al.*, 2015).

1.4.5.2 AGE-RELATED CHANGES TO SPHINGOSINE SIGNALLING

Whilst studies investigating sex-specific differences in leukocyte S1P-S1PR signalling are lacking (Al-Attar *et al.*, 2016), limited studies have reported age-related changes to S1P-S1PR signalling in lymphocytes (Turner and Mabbott, 2017; Huang *et al.*, 2011; Cattoretti *et al.*, 2009). Marginal zone B-cells derived from the spleens of old (20 months) female C57Bl6 mice exhibited increased chemotactic responses to S1P *in vitro* and increased expression of S1PR1 on the cell surface compared to B-cells derived from young (<12 months) mice, ultimately increasing B-cell retention within old

spleens (Turner and Mabbott, 2017). In a chemotactic assay, T-cells isolated from the blood of older (>65 years) adults exhibited diminished chemotactic responses to S1P *in vitro* compared to T-cells isolated from younger (<40 years) adults which could signify increased retention of T-cells in the SLOs or peripheral tissues of older adults (Huang *et al.*, 2011). Furthermore, dysregulated sphingosine metabolism in activated T-cells derived from older (18 months) C57Bl6 mice compared to young (2 months) mice is associated with mitochondrial dysfunction and poor anti-tumour immunity in ageing (Vaena *et al.*, 2021). Due to the limited studies, it is difficult to say whether these age-related changes to sphingosine signalling and metabolism in B- and T-cells is due to the different cell types considered, the different locations in which the cells were isolated, or the different species used in the studies. Nonetheless, the importance of S1PR signalling in anti-tumour immunity during ageing is evident from studies utilizing global S1PR2 KO mice (Cattoretti *et al.*, 2009). In these mice, S1PR2 deficiency led to the development of clonal B-cell lymphomas by 18-24 months of age compared to age-matched wildtype mice and was attributed to increased spontaneous GC formation in KO mice (Cattoretti *et al.*, 2009). Age-related changes to sphingosine signalling evidently hinders protective immunity, and is, in part, due to lymphocyte retention within tissues.

1.4.6 THE ROLE OF PEPITEM PATHWAY IN CHRONIC INFLAMMATORY DISEASES

In 2015, Chimen *et al.* proposed the dysregulation of the PEPITEM pathway in some chronic autoimmune diseases, such as type 1 diabetes mellitus (T1DM) and rheumatoid arthritis (RA) (Chimen *et al.*, 2015). The expression of AdipoR1/2 on the circulating B-cells of T1DM and RA patients was reduced compared to age-matched healthy control as determined by flow cytometric analysis (Chimen *et al.*, 2015). This

equated to a reduced ability of AQ to regulate the transendothelial migration of PBL derived from T1DM and RA patients *in vitro* (Chimen *et al.*, 2015). The dysregulation of the PEPITEM pathway in T1DM and RA patients could therefore contribute to the dysregulated trafficking of T-cells in these disease settings (reviewed by Mellado *et al.*, 2015; Sandor, Jacobelli and Friedman, 2019). Recently, Matsubara *et al.* described a role for PEPITEM in the control of lymphocyte infiltration of the kidneys during a mouse model of SLE (Matsubara *et al.*, 2020). In this model, PEPITEM treatment suppressed the enlargement of the kidneys, spleen, and axillary LN, and suppressed the development of nephritis (Matsubara *et al.*, 2020). It is clear that PEPITEM has therapeutic potential for multiple inflammation-driven diseases.

Importantly, data generated by this lab suggest that the PEPITEM pathway is dysregulated in older individuals (Chimen *et al.*, 2015). Chimen *et al.* observed an age-related reduction in AdipoR1/2 expression on peripheral blood B-cells derived from otherwise-healthy adults, which may signify reduced PEPITEM production by older B-cells (Chimen *et al.*, 2015). To that end, the focus of this thesis is to determine whether the PEPITEM pathway is dysregulated in older hosts, and whether the presence of exogenous PEPITEM restores regulated leukocyte trafficking in an aged context.

1.5 AIMS AND HYPOTHESIS

Age-related inflammatory diseases account for a considerable proportion of morbidity and mortality rates within the older population in the UK and worldwide (Yang *et al.*, 2016; Collaborators, 2022). Leukocyte trafficking is necessary for effective immunity, however, age-related changes to leukocyte trafficking processes drive the establishment of age-related inflammatory diseases (Chung *et al.*, 2019; Hopkin, Lord and Chimen, 2021).

It was hypothesised that the ageing process would modulate the trafficking of leukocytes under homeostatic and inflammatory conditions, and that this was in part due to the age-related dysfunction of the PEPITEM pathway. The administration of PEPITEM, or the downstream mediators of the pathway, into *in vitro* and *in vivo* models of inflammation was hypothesised to restore regulated leukocyte trafficking in aged systems.

Therefore, the main aims of this thesis were as follows:

1. To determine age-related, as well as sex-specific, changes to leukocyte populations within murine tissues under homeostatic conditions (Chapter 3).

2. To determine whether age-related changes to leukocyte population numbers in murine tissues is associated with to age-related changes to the structure and/or the integrity of the vasculature (Chapter 3).

3. To determine age-related and sex-specific changes to leukocyte trafficking under inflammatory conditions in humans and mice (Chapter 4).

4. To determine whether administration of PEPITEM can regulate leukocyte trafficking under inflammatory conditions in aged humans and mice (Chapter 5).

5. To determine whether the PEPITEM pathway is dysfunctional in older adults (Chapter 5). If the pathway is indeed dysfunctional, the factors driving age-related PEPITEM pathway impairment will be assessed (Chapter 5).

CHAPTER 2 – MATERIALS AND METHODS

2.1 MATERIALS

2.1.1 LIST OF MAIN REAGENTS

Table 2-1 List of main reagents

Reagent	Supplier	Catalogue Number	Working concentration /dilution	Use/application
Histopaque 1077	Sigma-Aldrich	10771-100ml	1x	PBMC isolation
PBS with magnesium/calcium	Sigma-Aldrich	14040-091	1x	Washes, *in vitro* and *in vivo* studies, flow cytometry
PBS without magnesium/calcium	Sigma-Aldrich	14190-094	1x	Washes, *in vitro* and *in vivo* studies, flow cytometry
EDTA, 0.02%	Sigma-Aldrich	E8008-100ml	0.1mM or 0.02%	Washes, MACS buffer, RBC lysis buffer
EDTA, 0.5M	Sigma-Aldrich	03690-100ml	5mM	Lavaging peritoneal cavity
BSA, 7.5%	Gibco	15260-037	0.15-2%	M199+BSA buffer, MACS buffer, PBSA
FCS	Sigma-Aldrich	F9665-500ml	1-20%	Enzyme neutralisation buffers
M199, 1x	Gibco	31150-022	1x	*In vitro* studies
M199, 10x	Sigma-Aldrich	M0650-100ml	170:830	Making collagen matrices
Rat-tail type I collagen	First Link	60-30-810	830:170	Making collagen matrices
EasySep Human B-cell Enrichment kit	StemCell	19054	/	Isolating B-cells from PBMC
Basal Endothelial Growth Medium MV	Promocell	C-22220	1x	HDBEC culture, *in vitro* assays
Trypsin	Gibco	25300-054	0.05%	HDBEC culture
Cryo-SFM	Promocell	C-29910	1x	HDBEC culture
TNFα	R&D Systems	210-TA	100U/ml	HDBEC activation
IFNγ	PeproTech	300-02	10ng/ml	HDBEC activation
Adiponectin	Enzo Life Sciences	ALX-522-063-C050	10µg/ml	PBL or B-cell treatments
SVTEQGAELSNEER	Cambridge Research Biosciences	Batch 39225 (Quote CP20896)	20ng/ml	PBL treatments
SVTEQGAELSNEER-[PEG6]-amide	Cambridge Research Biosciences	Batch 41521 (Quote CP19800/1)	300µg	*In vivo* studies
Dispase type II	Sigma-Aldrich	D4693	1mg/ml	Static adhesion assays
Collagenase type III	StemCell	07423	2mg/ml	Static adhesion assays
EasyPep Mini MS Sample Prep kit	ThermoFisher	A40006	/	LC/MS

Reagent	Supplier	Catalogue Number	Working concentration /dilution	Use/application
Pierce BCA Protein Assay kit	ThermoFisher	23225	/	Western blot, LC/MS
Protease inhibitor cocktail	Sigma-Aldrich	P8340	10%	Western blot, LC/MS
Laemmli Sample buffer	BioRad	1610747	1:5	Western blot
PageRuler Plus Prestained protein ladder	Invitrogen	26616	1x	Western blot
Tween 20	Sigma-Aldrich	P1379-100ml	1x	Western blot
MES SDS Running Buffer, 20x	Invitrogen	NP0002	1x	Western blot
Clarity Western ECL substrate	BioRad	170-5060	1x	Western blot
Restore Western Blot Stripping Buffer	Thermo Scientific	21059	1x	Western blot
Zymosan	Merck	Z4250-250mg	0.1mg	ZIP studies
20 kDa dextran-TRITC	Sigma-Aldrich	73766-1G	50mg/ml	IVM studies
70 kDa dextran-FITC	Sigma-Aldrich	46945-100MG-F	50mg/ml	IVM studies
Mouse FcR block	Miltinyi Biotec	130-092-575	1:50	Flow cytometry
Human FcR block	Miltinyi Biotec	130-059-901	1:50	Flow cytometry
Formaldehyde 36%	TAAB	F003	2%	Flow cytometry
CountBright beads	ThermoFisher	C36950	1:15	Flow cytometry
Mouse XL Cytokine Array kit	R&D Systems	ARY028	/	Cytokine array
CCL21/6Ckine DuoSet ELISA	Bio-Techne	DY457	/	ELISA
CXCL13/BLC/BCA-1 DuoSet ELISA	Bio-Techne	DY470	/	ELISA
DuoSet Ancillary Reagent Kit 2	Bio-Techne	DY008	/	ELISA

- List of main reagents used in the experimental methods of this thesis
- /, not applicable

2.1.2 ANTIBODIES

The unconjugated primary antibodies and peroxidase-conjugated secondary antibodies used for western blotting are described in Section 2.2.1.5. The antibodies used for the flow cytometric analysis of human samples are in **Table 2-2** and **Table 2-3**, whilst the antibodies for the flow cytometric analysis of murine samples are in **Table 2-4** and **Table 2-5**.

2.2 METHODS

2.2.1 HUMAN STUDIES

2.2.1.1 PARTICIPANT RECRUITMENT

Informed written consent was obtained from all participants prior to collecting blood samples for this project. Ethical approval was awarded by the University of Birmingham Local Ethical Review Committee (ERN_12-0079). Healthy volunteers were recruited from the University of Birmingham or from the Birmingham 1000 Elders cohort. All participants were seen at the Institute for Biomedical Research (IBR; Birmingham, UK) where participants filled out consent forms and provided a blood sample. Volunteers were required to be aged 18 years or over, to not have any underlying conditions that affect the immune system, and to not have any on-going infections.

2.2.1.2 PBMC, B-CELL AND PBL ISOLATION FROM WHOLE BLOOD

Human blood was obtained by venepuncture and collected into Potassium-Ethylenediaminetetraacetic acid (K_3EDTA)-coated vacuettes for collection of PBMC (BD Biosciences, UK). In a 15ml falcon tube, 5ml blood was layered on top of 5ml Histopaque-1077 (Sigma-Aldrich, UK), as previously described (Apta, Chimen and McGettrick, 2017). Tubes were then centrifuged at 800 *g* for 30 minutes with no acceleration and no brake at room temperature (RT). The buffy-coat containing PBMC was collected and placed into a fresh 15ml falcon tube. The cells were diluted 1:15 with phosphate buffered saline (PBS) without magnesium/calcium ($PBS^{-/-}$; Sigma-Aldrich) and centrifuged at 300 *g* for 5 minutes at RT to wash the cells. The supernatant was discarded, and the wash step was repeated once more. The PBMC pellet was then resuspended in MACS buffer (0.1mM ethylenediaminetetraacetic acid (EDTA),

0.6% bovine serum albumin (BSA) in $PBS^{-/-}$; all Sigma-Aldrich) for B-cell isolation (see below) or flow cytometric based analysis (see Section 2.2.3), or in medium 199 (M199; Gibco, UK) with 0.15% BSA to isolate PBL (see below).

To isolate B-cells from PBMC, the EasySep Human B-cell Enrichment kit (StemCell, UK) was used according to the manufacturer's instructions. In a polystyrene round-bottom tube (StemCell), PBMC ($50x10^6$/ml) were incubated 1:20 with enrichment antibody cocktail or 10 minutes at RT. Magnetic particles were then vortexed and added to the sample (1:13) for 5 minutes at RT. PBMC were diluted to 4ml using MACS buffer and the tube was placed into a magnet (StemCell) for 5 minutes at RT. The enriched B-cell supernatant (~75% purity) was then poured into a fresh 15ml falcon tube and centrifuged at 300 *g* for 10 minutes. Pelleted B-cells were counted using the Cellometer Auto T4 (Nexcelom Bioscience, UK) and aliquoted at $2x10^5$ B-cells/tube into 12x75 mm polystyrene tubes (BD Biosciences) using MACS buffer for flow cytometric analysis (Section 2.2.3), or aliquoted at $2x10^6$ B-cells/tube into eppendorfs for liquid chromatography-mass spectrometry (LC/MS; Section 2.2.1.4) or western blot (Section 2.2.1.5) analysis.

To isolate PBL, PBMC in 5ml M199 0.15% BSA were transferred into a T25 flask and incubated (37°C, 5% CO_2) for 45 minutes to allow the monocytes to adhere to culture plastic, an amendment of the previously described methodology (Rainger *et al.*, 2001). The non-adherent PBL were then collected, washed with M199 0.15% BSA pre-warmed to 37°C and centrifuged at 300 *g* for 5 minutes. The pellet was resuspended in 1ml M199 0.15% BSA before cells were counted using the Cellometer. The PBL (~92% purity) concentration was adjusted to $1x10^6$ cells/ml using M199

0.15% BSA and the cells were kept at RT prior to the static adhesion assay (see Section 2.2.1.3).

2.2.1.3 IN VITRO STATIC ADHESION AND MIGRATION ASSAYS

2.2.1.3.1 GENERATING COLLAGEN MATRICES

In an ice-cold 15ml round bottomed tube, rat-tail type I collagen (First Link, UK) was mixed with 10x M199 media (Sigma-Aldrich) in a 830:170 ratio to achieve a final concentration of 1.6mg/ml, as previously described (McGettrick *et al.*, 2017). The tube was slowly inverted three times before the collagen mixture was titrated with cold 1N sodium hydroxide (Thermo Scientific, UK) to neutralise the acetic acid. The tube was kept on ice and inverted in between additions of sodium hydroxide to ensure thorough mixing. Titration was completed upon colour change of the collagen mixture from yellow to orange-pink, indicating a neutral pH. In a 12-well plate, 500µl of the collagen mixture was pipetted into a well, ensuring no air bubbles formed during the transfer. The plate was then slowly rocked to ensure even coverage of the well and the plate was placed into an incubator set at 37°C for 15 minutes to allow the collagen mixture to set. To matrix was equilibrated with fully supplemented Basal Endothelial Growth Medium MV (BEGM) media (fetal calf serum (FCS) 0.05ml/ml, endothelial cell growth supplement 0.004ml/ml, recombinant human epidermal growth factor 10ng/ml, heparin 90µg/ml, hydrocortisone 1µg/ml; all from Promocell, Germany) media for 24 hours before the addition of human dermal blood endothelial cells (HDBEC).

2.2.1.3.2 CULTURING AND SEEDING OF ENDOTHELIAL CELLS

2.2.1.3.2.1 DEFROSTING ENDOTHELIAL CELLS

All reagents were pre-warmed to 37°C unless otherwise stated. For these studies, HDBEC ($6x10^5$ cells) were purchased from Promocell (Lot #423Z004; Germany) at passage one and were subsequently expanded to passage six before use in assays, as previously described (Apta, Chimen and McGettrick, 2017). The HDBEC were derived from a 22 year old female donor. Once received, the HDBEC were placed into liquid nitrogen for long-term storage. To passage the HDBEC, the cells were transported on dry ice and placed into a water bath set to 37°C for 2 minutes to defrost the cells (Apta, Chimen and McGettrick, 2017). HDBEC were then resuspended in 10ml BEGM media with 100U/ml penicillin and 100µg/ml streptomycin (P4333-100ml, Sigma-Aldrich) and transferred into a T25 flask as passage two. The flask was placed into the incubator (37°C, 5% CO_2) until the cells reached 90% confluency (approximately 48 hours).

2.2.1.3.2.2 TRYPSINISATION OF THE ENDOTHELIAL CELLS

Once 90% confluent, the media was aspirated and the flask was washed with 0.02% EDTA (Sigma-Aldrich) for 10 seconds. The EDTA was aspirated and trypsin 0.05% (Gibco) warmed to RT was then added to the flask for 2 minutes to detach the HDBEC from culture plastic. The flask was tapped on the bench to assist dislodging and was checked using an upright Primo Vert microscope (Zeiss, Germany) to ensure HDBEC detachment. M199 with 20% FCS (Sigma-Aldrich) was then added to the flask to neutralise the trypsin, as previously described (Apta, Chimen and McGettrick, 2017). HDBEC were collected into a 15ml falcon tube using a stripette, and the walls of the flask were then washed six times with fresh M199 20% FCS to collect any remaining

EC. HDBEC were centrifuged at 250 *g* for 5 minutes at RT. The pelleted cells were resuspended in BEGM media and split between two T25 flasks for passage three. This process was repeated until HDBEC reached passage six.

2.2.1.3.2.3 FREEZING THE ENDOTHELIAL CELLS

Upon reaching passage six, HDBEC received a final round of trypsinisation and centrifugation (see above), followed by resuspension in cold Cryo-SFM (Promocell). HDBEC from one T75 flask were split into three CryoVials and placed into a pre-cooled Nalgene Mr Frosty Cryo 1°C freezing container (Thermo Scientific), as previously described (Apta, Chimen and McGettrick, 2017). The freezing container was then placed into a -80°C freezer overnight. The following day CryoVials were transferred into liquid nitrogen for long-term storage.

2.2.1.3.2.4 SEEDING THE ENDOTHELIAL CELLS

Frozen HDBEC at passage six were defrosted, cultured and trypsinised as described above. Once pelleted, HDBEC were resuspended in 1ml BEGM media and the cells were counted using the Cellometer. The HDBEC concentration was adjusted to $2x10^5$ cells/ml using BEGM media and 1ml HDBEC was carefully added to a collagen matrix (1ml/well). The plate was gently tilted back and forth to ensure even coverage of the HDBEC on the collagen matrix, and then placed back into an incubator (37°C, 5% CO_2) for 24 hours.

2.2.1.3.3 CYTOKINE STIMULATION OF THE ENDOTHELIAL CELLS

HDBEC were checked under an upright microscope to ensure a complete endothelial monolayer had formed on top of the collagen matrix. The spent media was aspirated, and replaced with BEGM media containing 100U/ml TNFα (R&D Systems, UK) and 10ng/ml IFNγ (PeproTech, UK) for 24 hours (37°C, 5% CO_2), which was based on previously published work (Piali *et al.*, 1998; Bahra *et al.*, 1998; Curbishley *et al.*, 2005).

2.2.1.3.4 PBL TREATMENTS

For AQ stimulation, PBL ($1x10^6$ cells) were centrifuged at 300 *g* for 5 minutes, resuspended in 100µl M199 0.15% BSA and treated with 10µg/ml recombinant AQ (Enzo Life Sciences, UK) for 1 hour under agitation at RT. Following pre-treatment, PBL were then washed with 1ml M199 0.15% BSA, centrifuged at 300 *g* for 5 minutes and resuspended in 1ml M199 0.15% BSA before immediate use (see Section 2.2.1.3.5). For PEPITEM treatment, $1x10^6$ PBL were added to the TNFα+IFNγ-treated HDBEC in conjunction with 20ng/ml native PEPITEM (Cambridge Research Biochemicals (CRB), UK) for the duration of the static adhesion assay (see Section 2.2.1.3.5).

2.2.1.3.5 STATIC ADHESION ASSAY

Cytokine-treated HDBEC monolayers (see Section 2.2.1.3.3) were washed twice with M199 0.15% BSA to remove excess cytokines before the addition of $1x10^6$ untreated or treated PBL (see above). PBL were allowed to migrate for 20 minutes, 2 hours, or 24 hours at 37°C. Between timepoints, non-adherent PBL were then removed by gentle washing with M199 0.15% BSA and each well was imaged/recorded using a phase-contrast Olympus IX70 microscope (Olympus, UK) in a Perspex box to maintain a temperature of 37°C. At the 20 minute, 2 hour and 24 hour time points each well was

imaged as follows. Firstly, five fields of view within each well were imaged at random to quantify the number of PBL that had adhered to the EC monolayer and to measure the percentage of PBL transendothelial migration. This was followed by the acquisition of five digitised z-stack sequences in random fields of view. Z-stack sequences were captured at 2µm intervals from the surface of the HDBEC monolayer to the bottom of the collagen matrix to measure average depth of PBL penetration. Finally, a 5 minute sequence of a single field of view on the EC surface was recorded to measure PBL migration velocities.

2.2.1.3.6 COLLECTION OF MIGRATED PBL FOR FLOW CYTOMETRIC ANALYSIS

After imaging, the media was aspirated from the wells and the endothelial surface was washed twice with $PBS^{-/-}$. Dispase type II (1mg/ml; Sigma-Aldrich) was then added to the wells, and the plate was incubated at 37°C for 30 minutes under agitation to lift of adhered PBL and HDBEC from the collagen matrix. PBS containing 2% BSA (PBSA) was added to neutralise the dispase, and the adhered cells were washed off the collagen matrix using $PBS^{-/-}$. Once all adhered cells were removed, the collagen matrix was scooped up using a pipette tip and placed into a 15ml falcon tube containing 2mg/ml collagenase type III (StemCell) for 20 minutes at 37°C under agitation to digest the collagen. PBSA was then added to neutralise the digestion and the freed PBL were centrifuged for 5 minutes at 300 *g*. The supernatant was aspirated and the PBL were resuspended in 100ul MACS buffer and placed on ice prior to flow cytometric analysis (see Section 2.2.3).

2.2.1.3.7 ANALYSIS OF THE IMAGES AND SEQUENCES

The images and sequences were analysed off-line using Image-Pro 6.2 software (Media Cybernetics; Maryland, USA). The field dimensions of the microscope were calibrated by imaging a graticule and setting the scale on the image analysis software.

2.2.1.3.7.1 PBL ADHESION AND MIGRATION

In the images, adhered and transmigrated PBL were classified as previously described (Apta, Chimen and McGettrick, 2017; McGettrick *et al.*, 2009a). The phase bright PBL on the surface of the HDBEC (rounded morphology and slowly migrating along the EC monolayer) were classified as adhered cells, whilst the phase dark PBL underneath the HDBEC (spread and migrating beneath the EC monolayer) were classed as transmigrated cells. Phase grey PBL were classified as adhered cells if they exhibited rounded morphology and over 50% of the cell appeared to be on top of the EC monolayer, whilst phase grey PBL that exhibited an irregular morphology with less than 50% of the cell appearing on top of the HDBEC were classified as transmigrated (Apta, Chimen and McGettrick, 2017). In the z-stack sequences, migrated PBL within the collagen matrix appeared as rounded phase bright cells.

Both adhered and transmigrated populations were counted in the images and z-stack sequences. Total PBL adhesion to the EC monolayer was the sum of adhered and transmigrated PBL, expressed as cells per mm^2 per number of PBL added. The percentage of PBL transmigration across the EC monolayer was calculated by expressing the number of transmigrated PBL as a percentage of the total number of adhered PBL. The percentage of AQ and PEPITEM inhibition (**Figure 5-3**) is the percentage change in the proportion of PBL transmigration between the control group

and the AQ and PEPITEM groups, respectively. This was calculated for each blood donor.

2.2.1.3.7.2 AVERAGE DEPTH OF PBL PENETRATION INTO THE COLLAGEN MATRIX

The average depth of PBL penetration into the collagen matrix was calculated as previously described (Apta, Chimen and McGettrick, 2017). The number of cells within 20µm slices were counted and assigned the midpoint depth of that slice. The midpoint depth was then multiplied by the number of cells found within the slice. These values were then summed and divided by the total number of cells in the stack to give the average depth of PBL penetration into the matrix per z-stack. These values were then averaged across the five z-stacks to provide the average depth of PBL penetration into the collagen matrix per time point. To ensure that shrinkage of the collagen gel was not occurring over time, the depth of the gel was also measured at each time point using the z-stack setting on the phase-contrast microscope.

2.2.1.3.7.3 PBL MIGRATION VELOCITIES

To calculate average migration velocities, the centroids of individual migrating PBL were recorded for each minute of the 5-minute sequence and analysed as previously described (Munir *et al.*, 2015; Apta, Chimen and McGettrick, 2017). The X and Y position values of PBL from minute 0 were subtracted from the values in minute 1 of the sequence. This was repeated for each minute of the sequence. The X and Y values were then squared and summed. The resulting value was then square rooted to provide the distance travelled by an individual PBL over the course of 1 minute, a method based on Pythagoras' theorem. The distance travelled by a singular PBL over the course of five minutes was averaged and divided by 5 to calculate the migration

velocity (i.e. µm/minute). The migration velocities of all PBL within the frame of view were then averaged to provide the average PBL migration velocity of that time point.

2.2.1.4 LC/MS ANALYSIS OF B-CELL LYSATES

B-cells were isolated from blood as described in Section 2.2.1.2. Using B-cells isolated from a single blood donor, half of the B-cells were left untreated and half were treated with 10µg/ml AQ for 15 minutes at RT under agitation. B-cells were then centrifuged at 300 *g* for 8 minutes where the supernatant was collected and stored at -80°C for future analysis and the cell pellet was washed twice with $PBS^{+/+}$. Pelleted B-cells were then prepared for LC/MS analysis using the EasyPep Mini MS Sample Prep kit (ThermoFisher) according to the manufacturer's instructions. Pelleted B-cells were lysed using the kit's lysis buffer containing 0.5kU universal nuclease and 10% protease inhibitor cocktail (Sigma-Aldrich).

2.2.1.4.1 BCA ASSAY

Total protein content of the B-cell lysates was determined using the bicinchoninic acid (BCA) assay, using the Pierce BCA Protein Assay kit (ThermoFisher) according to the manufacturer's instructions. Briefly, 1,500-0µg/ml BSA standards were prepared by diluting the BSA in $PBS^{+/+}$, whilst samples were diluted 1:4. In a 96-well flat-bottomed plate, 25µl/well of standards and sample were added in duplicate. The working solution was prepared by diluting Reagent B 1:50 in Reagent A, and was added at a volume of 200µl/well to the standards and samples. The plate was placed on a shaker at RT for 30 seconds to mix the solutions, and then incubated at 37°C for 30 minutes. The plate was then cooled to RT and read at 562 nm using a BioTek Synergy HT plate reader (BioTek, USA). The numerical data was exported into a table, where the average absorbance value of the blank wells was deducted from the absorbance values of the

standards and samples. The absorbance values for each standard were averaged and a standard curve was generated. The protein concentration (µg/ml) of the samples was determined using the y-intercept and slope derived from the standard curve ((average fluorescence − y-intercept) ÷ slope), and multiplied by the dilution factor of the sample.

2.2.1.4.2 COLLECTION OF INTRACELLULAR PROTEINS

Once the protein concentration had been determined, 70µg of B-cell lysate protein was then transferred into an Eppendorf and subjected to the EasyPep Mini MS Sample Prep kit as per the manufacturer's instructions. Briefly, 50µl of Reduction solution and 50µl Alkylation solution was added to the sample prior to incubation at 95°C for 10 minutes. Once cooled to RT, 10µg Trypsin/Lys-C Protease Mix was added to the sample for 2 hours at 37°C under agitation to digest the proteins. The digest was stopped by the addition of 50µl Digestion Stop solution. The peptide solution was then transferred into a Peptide Clean-up column and centrifuged at 1,500 *g* for 2 minutes (reagents from EasyPep Mini MS Sample Prep kit). The column was washed once with 300µl Wash Solution A and twice with Wash Solution B, where samples were centrifuged at 1,500 *g* for 2 minutes between washes. Peptides were eluted by the addition of 300µl Elution Solution into the column and centrifugation at 1,500 *g* for 2 minutes. The eluted peptides were placed into a Concentrator 5301 vacuum centrifuge (Eppendorf, UK) and dried overnight. Peptides were stored at -80°C until they were transported to the Advanced Mass Spectrometry unit (Birmingham, UK) for LC/MS analysis.

2.2.1.4.3 LC/MS

LC/MS analysis of B-cell peptides was performed by the Advanced Mass Spectrometry Unit (University of Birmingham). Peptides were resuspended in 10µl 0.1% formic acid

diluted in LC/MS grade water, and 5µl of each sample was analysed using LC/MS. A gradient of 3-44% v/v acetonitrile in 0.1% formic acid was run at 350 nl/min for 30 minutes in a Dionex Ultimate 3000 liquid chromatography (LC) system to facilitate the separation of peptides. A low concentration of solvent at the beginning of the run allows the peptides within the sample to bind to the column, whilst the increasing concentration of solvent over the course of the run permits the elution of peptides based on hydrophobic properties. Highly hydrophobic peptides are retained longer on the column and are the last to be eluted. Using a nanospray source, the samples were then sprayed into the Thermo Q Exactive HF Orbitrap mass spectrometer (ThermoFisher) from the LC instrument. With the sample now in gas phase, the electrostatic attraction of the sample draws the peptides into the ion-trap and separates ions based on their mass to charge ratio (m/z). A mass spectrometry survey of 380 to 1800 m/z was performed and automatic gain control for selecting ions was set at MS1 $3x10^6$ and MS2 $1x10^5$. The m/z peaks generated by Thermo Xcalibur software (ThermoFisher) were then identified using the Proteome Discoverer 2.2 software (ThermoFisher) with the Uniprot protein database. The relative abundance of a specific peptide within a sample was equivalent to its peak intensity normalised by the sum of intensities of all other peptides. The relative abundance of proteins in AQ-treated B-cell samples (AQ) compared to control B-cell samples (C) of a single donor was calculated as a ratio: AQ/C and is expressed as fold change.

2.2.1.5 WESTERN BLOT ANALYSIS OF B-CELL PROTEINS

B-cells were isolated from whole blood as described in Section 2.2.1.2. B-cells were then treated, lysed, and subjected to a BCA assay to determine protein concentration, as described in Section 2.2.1.4.

2.2.1.5.1 WESTERN BLOT

To denature the proteins, 5µg B-cell lysate was diluted 1:5 with Laemmli Sample buffer (BioRad, USA) and then incubated at 95°C for 10 minutes. Samples and 4µl of the PageRuler Plus Prestained protein ladder (Invitrogen, UK) were then loaded into a NuPAGE 4-12 % Bis-Tris mini protein gel (Invitrogen) and electrophoresed at 100 V for 90 minutes. Proteins were transferred onto a PVDF Midi 0.2mm membrane (BioRad) using the Trans Blot Turbo system (BioRad) for 10 minutes at 25 V. The membrane was then blocked with 5% milk diluted in PBS-Tween 0.1% (blocking buffer; reagents from Sigma-Aldrich) for 1 hour at RT under agitation. The membrane was then incubated with 1:4,000 rabbit anti-APPL1 (12639-1-AP, ProteinTech, UK) primary antibody, diluted in blocking buffer, overnight at 4°C under agitation. The membrane received three rounds of 10-minute washes using 0.1% PBS-Tween (PBST), and was then incubated with 1:10,000 goat anti-rabbit IgG peroxidase conjugate (401393, EMD Millipore Corp, UK) secondary antibody, diluted in blocking buffer, for 90 minutes at 4°C under agitation. The membrane received three 10-minute washes with PBST prior to the addition of 2ml Clarity Western ECL chemi reagent substrate (BioRad) for 1 minute. Excess chemi reagent was removed by touching the edge of the membrane onto paper towel. The membrane was then wrapped in clingfilm, ensuring no air bubbles or creases formed, and placed into an autoradiography cassette (Amersham Life Science, UK). The membrane was exposed to X-ray film for 30 seconds and developed using the Compact X4 Automatic X-ray Film Processor (Xograph, UK).

Following development, the membrane was washed using PBST as described above and incubated with 20ml Restore Western Blot Stripping Buffer (Thermo Scientific) at 37° for 30 minutes under agitation to strip the antibody from the

membrane. The membrane was re-probed with 1:4,000 rabbit anti-actin (A2066, Sigma-Aldrich) primary antibody and subsequently 1:10,000 goat anti-rabbit peroxidase conjugate secondary antibody as described above to assess actin abundance.

2.2.1.5.2 ANALYSIS OF THE BLOTS

After developing the X-ray film, blots were scanned and analysed offline using ImageJ (version 2.1.0, Cambridge). To quantify protein abundance, the area under the peak method was employed (Alonso Villela *et al.*, 2020; Gassmann *et al.*, 2009; ImageJ, 2012). Briefly, a region of interest (ROI) comprising of 260 x 290 pixels was drawn around each protein band and grey-pixel intensity plots were generated by ImageJ. A horizontal line was drawn underneath the peak to eliminate background noise, and the area under the peak was measured. The size and intensity of the protein band directly corresponded to the area under the peak value: the larger and darker the protein band, the larger the area under the peak value. These measurements were determined for APPL1 and actin protein bands for each sample. To normalise the data according to total protein abundance of the sample, the actin data were normalised to the lowest actin value and the corresponding normalisation ratios were applied to the APPL1 data. The data in this thesis are presented as normalised APPL1 abundance.

2.2.2 IN VIVO STUDIES

2.2.2.1 MICE

Animal studies were regulated by the Animals (Scientific Procedures) Act 1986 of the United Kingdom and were performed under Personal Project Licence P379E5607. Approval was granted by the University of Birmingham's Animal Welfare and Ethical

Review Body and all ethical guidelines were adhered to whilst carrying out these studies.

Wildtype male and female C57Bl6J mice aged 2 months (young) and 18 months (aged) were purchased from Charles River (UK) and housed in the animal facilities located at the University of Birmingham until they reached the appropriate age for our studies. We had initially planned to use 3 month-old mice for the young cohort and 21 month-old mice for the aged cohort. However, due to the COVID-19 pandemic, we were required to cull a cohort of 18 month-old male and female mice and so we included this data in **Chapter 3**. In line with UK Home Office regulations, mice were maintained under a controlled 12-hour light/12-hour dark cycle and received food and water *ad libitum*.

2.2.2.2 BASELINE STUDIES

Naïve mice were sacrificed via cardiac puncture from the side of the ribcage under terminal anaesthesia to collect blood. Blood was aliquoted into EDTA-coated tubes (Starstedt, Germany) for flow cytometric analysis, and into Eppendorfs to collect serum. Subsequently, the peritoneum was lavaged by injecting 5ml of 5mM EDTA (Sigma-Aldrich) diluted in $PBS^{-/-}$ into the peritoneal cavity and massaging the peritoneal membrane to detach adherent cells. The peritoneal lavage fluid (PLF) was collected using a 19 G 2-inch needle and 5ml syringe and stored on ice. The inguinal LN, spleen, and the right hind leg were each collected into separate 15ml falcon tubes containing $PBS^{+/+}$ and transported on ice. All tissues were processed immediately as described below (Section 2.2.2.4).

2.2.2.3 ZYMOSAN-INDUCED PERITONITIS (ZIP) STUDIES

Peritonitis was induced by intraperitoneal (IP) injection of 0.1mg zymosan A (Merck, UK) from *Saccharomyces cerevisiae*, as previously described (Rajakariar *et al.*, 2008; Newson *et al.*, 2014). Control mice received an IP injection of $PBS^{-/-}$ only. Some mice received 300µg pegylated PEPITEM, SVTEQGAELSNEER-[PEG6]-amide (CRB), concurrently with zymosan administration, and again at the 24 hour timepoint (Chimen *et al.*, 2015). After 48 hours, mice were sacrificed and tissues were collected as described above (Section 2.2.2.2).

2.2.2.4 TISSUE PROCESSING FOR FLOW CYTOMETRIC ANALYSIS

2.2.2.4.1 BLOOD

To lyse red blood cells (RBC), formulated RBC lysis buffer (155mM NH_4Cl, 12mM $NaHCO_3$, 0.1mM EDTA; all from Sigma-Aldrich) was added to blood samples in a 10:1 ratio for 10 minutes at room temperature. Cells were then washed twice by diluting cells with 10ml $PBS^{+/+}$ followed by centrifugation at 300 *g* for 5 minutes. Pelleted cells were resuspended in MACS buffer and stored on ice prior to flow cytometric analysis. Serum samples were collected by centrifuging the blood at 750 *g* for 10 minutes and were stored at -80°C for future analysis.

2.2.2.4.2 PERITONEAL LAVAGE FLUID

PLF samples were centrifuged at 300 *g* for 5 minutes to pellet cells. PLF supernatants were collected and stored at -80°C for future analysis. Peritoneal cells were then resuspended in MACS buffer and stored on ice prior to analysis by flow cytometry (Section 2.2.3).

2.2.2.4.3 SPLEEN AND INGUINAL LYMPH NODES

Spleens were weighed using Pioneer weighing scales (Ohaus, Switzerland). Excess adipose tissue surrounding the inguinal LN was removed using tweezers. Spleens and LN were then placed onto separate 40µm cell strainers (Grenier Bio-One, Austria). Using the plunger of a 5ml syringe, the tissue was mashed and washed through the cell strainer into the collection tube with $PBS^{+/+}$. Cells were pelleted by centrifugation at 300 *g* for 5 minutes. RBC in the spleen samples were then lysed as described in Section 2.2.2.4.1. Cells of the spleen or LN were then resuspended in MACS buffer and stored on ice prior to analysis by flow cytometry (Section 2.2.3).

2.2.2.4.4 BONE MARROW

Tissue was dissected away from the tibia and the femur of the right hind leg, which were then separated and the ends of each bone removed to expose the BM. A hole was made at the bottom of a 0.5ml Eppendorf using a 19 G needle into which the bones were then placed. The 0.5ml Eppendorf was nested into a larger 1.5ml Eppendorf and centrifuged at 10,000 *g* for 30 seconds to extract the BM. The BM was filtered through a 40µm cell strainer before RBC were lysed as described in Section 2.2.2.4.1. Cells of the BM were then resuspended in MACS buffer and stored on ice prior to analysis by flow cytometry (Section 2.2.3).

2.2.2.5 INTRAVITAL MICROSCOPY OF THE PERITONEAL MEMBRANE VASCULATURE

2.2.2.5.1 INTRAVITAL MICROSCOPY

All intravital microscopy studies were conducted by Dr Dean Kavanagh (Intravital imaging suite, Birmingham, UK). Three-month (22.04±1 gram) and 21-month (30.08±1 gram) female mice were anaesthetised by IP injection of ketamine hydrochloride

(100mg/kg; Pfizer, USA) and medetomidine hydrochloride (10mg/kg; Pfizer) diluted in $PBS^{-/-}$. The trachea and right common carotid artery were cannulated and the peritoneal membrane was exposed. Prior to imaging, 50µl tetramethylrhodamine isothiocyanate (TRITC) conjugated 20 kDA dextran (50mg/ml; Sigma-Aldrich) and 50µl fluorescein isothiocyanate (FITC) conjugated 70 kDa dextran (50mg/ml; Sigma-Aldrich) were administered via the carotid artery. A 60 second sequence of the peritoneal membrane vasculature was recorded at 0- and 60-minutes post-dextran administration using an Olympus IX81 inverted microscope (Olympus, UK) through a 10X objective. After imaging, the mice were sacrificed via cervical dislocation and the peritoneal cavity was lavaged as described in Section 2.2.2.2.

2.2.2.5.2 ANALYSIS OF THE SEQUENCES

The sequences were analysed offline using Fiji ImageJ. Five still images were extracted from each sequence (0-minute and 60-minute sequences) at random, ensuring the vasculature was in focus. To measure the average extravascular fluorescence, the mean grey values of five regions of interest (20 x 20 pixels) within the background of an image were obtained and averaged. The mean grey values obtained from the five different images of the same timepoint were then averaged. The average mean grey value of the 0-minute images was then subtracted from the average mean grey value of the 60-minute images, and this value was used as the final measure of extravascular fluorescence for the 60-minute timepoint.

To analyse the structure of the vasculature, the vasculature network was manually mapped onto the image using the paintbrush feature in ImageJ. The threshold was then adjusted to 13 – 255 pixels to capture the vasculature outline, the image was inverted and analysed using the Angiogenesis Analyzer plug-in (Carpentier

et al., 2020). A schematic of the workflow is depicted in **Figure 2-1**. The Angiogenesis Analyzer plug-in labelled points of bifurcation as ‘nodes’, which were identified by pixels connecting with three neighbouring pixels, and labelled looping structures within the vasculature as ‘meshes’, which were identified as areas completely enclosed by vessels (**Figure 2-2**). The ‘mesh index’ is a measure of the mean distance between nodes within a mesh structure, ultimately conveying the average number of vessels involved in a mesh structure within a set area of vasculature. The lower the mesh index, the more vessels involved in mesh structures within the vasculature. Measurements were scaled using a graticule.

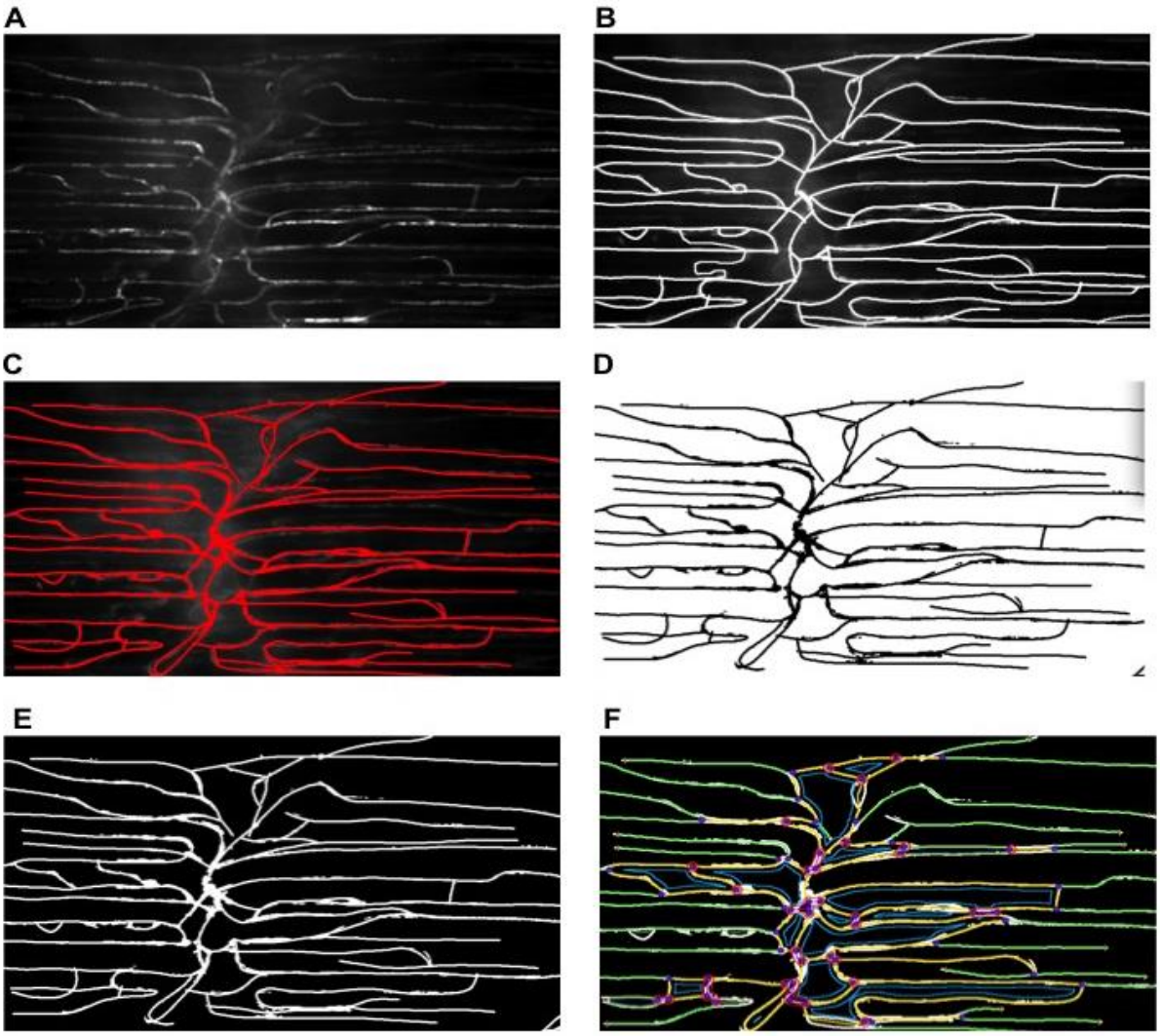

Figure 2-1 Schematic of intravital microscopy sequence analysis

(A) An image was extracted from the intravital microscopy sequence, and **(B)** the vasculature was manually outlined using the brush tool in Fiji ImageJ. **(C-D)** The threshold of the image was adjusted to 13 – 255 pixels, **(E)** the image was inverted and **(F)** the vasculature structure was analysed using the Angiogenesis Analyzer plug-in on Fiji ImageJ.

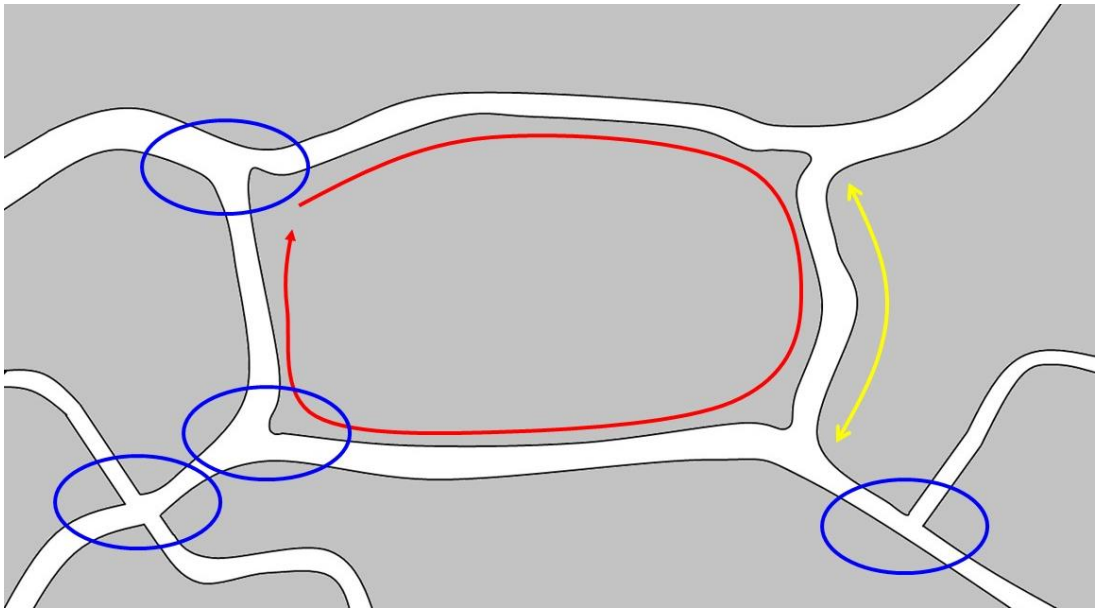

Figure 2-2 Schematic depicting vasculature structure terms

A schematic depicting the different structure terms for vasculature used in this thesis, as defined by the Angiogenesis Anlayzer plug-in for ImageJ. A ‘node’ (blue circle) is a point of bifurcation within the vasculature, determined by a single pixel connected to at least three neighbouring pixels. A ‘mesh’ (red circle) is a looping structure in the vasculature, determined by multiple nodes connected by vessels in a circular fashion. A ‘mesh index’ (yellow arrow) is a measure of the mean distance between nodes within a mesh structure.

2.2.2.5.3 MEASURING FLUORESCENT DEXTRANS IN PERITONEAL LAVAGE FLUID

A two-fold serial dilution of the 20 kDa dextran-TRITC and 70 kDa dextran-FITC was performed to generate standards. The PLF samples, standards, and blanks (5mM EDTA-PBS) were placed into a 96-well plate (Grenier Bio-One) in triplicate and read using the BioTek Synergy HT plate reader. Different excitation and emission wavelengths were used to obtain fluorescent measurements for the different fluorochromes (excitation: 530/25 nm, emission: 590/35 nm for 20 kDa dextran-TRITC; 485/20 nm, emission: 528/20 nm for 70 kDa dextran-FITC). The fluorescent values for each set of standards were averaged and two standard curves were generated (**Figure 2-3**). The fluorescent values of the samples and blanks were averaged, and the fluorescent value of the blank was deducted from the sample values. The 20 kDa and 70 kDa dextran concentrations within the samples were then determined using the y-intercept and slope derived from the standard curves ((average fluorescence − y-intercept) ÷ slope). The data were plotted as weight of dextran per ml of PLF (µg/ml).

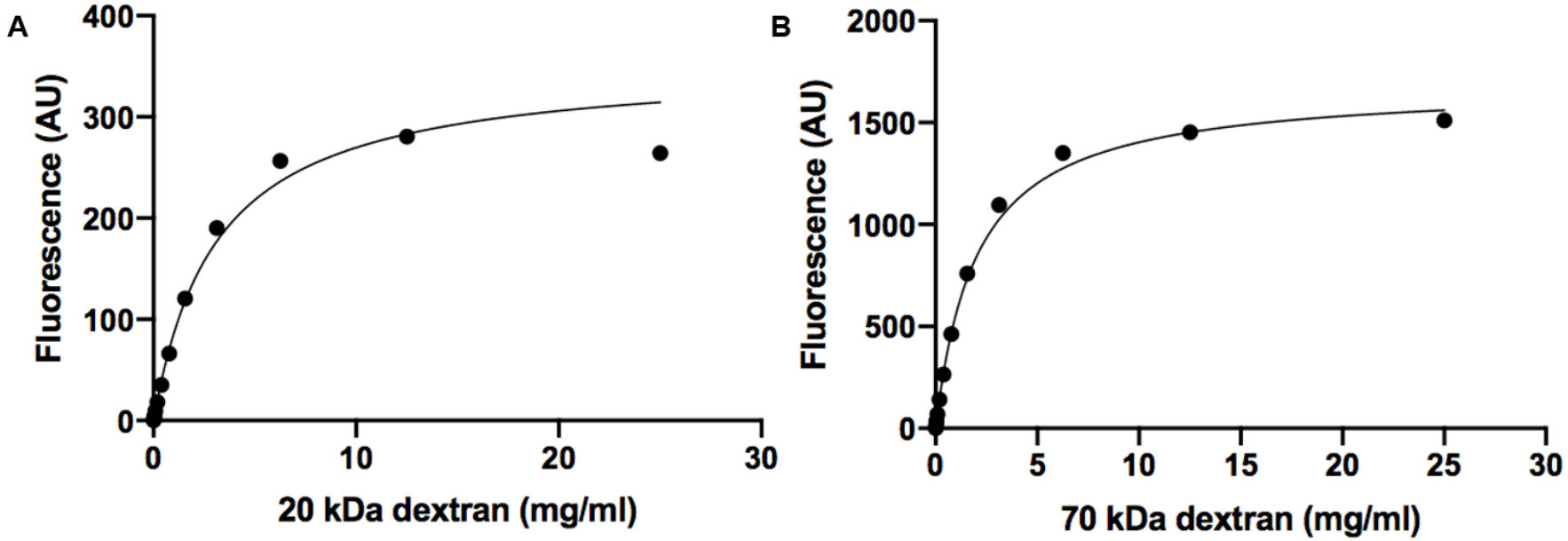

Figure 2-3 Standard curves for dextran quantification

To generate standard curved for (A) 20 kDa dextran-TRITC and (B) 70 kDa dextran-FITC, standards ranging 25-0 mg/ml were generated and plated in triplicate. The arbitrary unit (AU) of fluorescence was measured using a plate reader. An excitation wavelength of 530/25 nm and emission wavelength of 590/35 nm was used for 20 kDa dextran-TRITC. An excitation wavelength of 485/20 nm and emission wavelength of 528/20 nm was used for 70 kDa dextran-FITC.

2.2.2.6 CYTOKINE ARRAY

Soluble proteins within PLF supernatant samples were measured using the Mouse XL Cytokine Array Kit (R&D systems) according to the manufacturer's instructions. Each Mouse XL Cytokine Array membrane was incubated with 2ml Array Buffer 6 for 1 hour at RT under agitation to block non-specific binding of analytes. To prepare samples, equal volumes (333µl) of PLF supernatant from 3 separate mice were mixed to measure soluble proteins within a cohort of mice. PLF samples were then topped up to 1.5ml using Array Buffer 4 prior to addition to the membrane and incubation overnight at 4°C under agitation. Each membrane underwent three 10-minute washes using 1X Wash Buffer prior to incubation with the Detection Antibody Cocktail (1:50) for 1 hour at RT under agitation. The membranes were then washed as described above prior to the addition of 2ml 1X Streptavidin-HRP for 30 minutes at RT under agitation. One final round of membrane washing preceded the addition of 1ml Chemi Reagent Mix for 1 minute at RT. The membranes were then wrapped in clingfilm and placed into an autoradiography cassette (Amersham Life Science). The membranes were exposed to X-ray film for 1 minute (Chapter 3) and developed using the Compact X4 Automatic X-ray Film Processor (Xograph).

The developed membrane was scanned, and the images were analysed offline using ImageJ. Each analyte spot was present in duplicate on the membrane, and so one ROI (36 x 36 pixels) was created for each analyte spot. The image was then inverted so that and the mean grey pixel value could be measured as a numerical quantification of the relative abundance of each analyte within the sample. The numerical data was then exported into a table. The values of each set of analyte spots were averaged and the background signal was removed by subtracting the average

value of the negative control spots from each analyte spot value. The aged data were then normalised to the young data and expressed as fold-change in analyte abundance based on the sex of the mice (Chapter 3).

2.2.2.7 ELISA

The concentration of soluble CCL21 and CXCL13 was measured in PLF samples from 3-month, 18-month, and 21-month male and female mice using an ELISA. The Mouse CCL21/6Ckine DuoSet ELISA and Mouse CXCL13/BLCA/BCA-1 DuoSet ELISA in conjunction with the DuoSet Ancillary Reagent Kit 2 (all from Bio-Techne) were used according to the manufacturer's instructions. All reagents and materials listed below were provided in the specific ELISA kit or the DuoSet Ancillary Reagent Kit 2. In brief, two 96-well plates were incubated with the appropriate capture antibody (1µg/ml; 100µl/well) overnight at RT. The plates were then washed by aspirating the wells prior to the addition of wash buffer (400µl/well); this process was repeated three times to complete the wash step. The plates were then blotted on paper towel to ensure complete removal of any remaining liquid from the wells.

Following washing, the plates were blocked with block buffer (300µl/well) for 1 hour at RT. After an additional round of washing (described above), neat PLF samples and standards (15.6-1,000 pg/ml) were added (100µl/well) in duplicate to the plates, which were then incubated at RT for 2 hours. The plates were washed again (described above) prior to the addition of the detection antibody (25ng/ml; 100µl/well) and incubation for 2 hours at RT. The plates were washed once more (described above) prior to the addition of streptavidin-HRP (100µl/well) for 20 minutes at RT in the dark. A final round of plate washing (described above) preceded the addition of substrate solution (100µl/well) for 20 minutes at RT in the dark. Stop

solution (50µl/well) was then added to each well, and the plates were tapped to ensure gentle mixing of the solutions. The optical density of each well at 450 nm (OD_{450}) was measured using the BioTek Synergy HT plate reader, and the numerical values were exported into a table.

To quantify the levels of CCL21 and CXCL13 in the PLF samples, the background signal was deducted from the OD_{450} values of the samples for each plate. As they were in duplicate, the OD_{450} values of the standards and samples were then averaged and standard curves were generated for each chemoattractant. The concentration of CCL21 and CXCL13 in each PLF sample was then interpolated by using the y-intercept and slope derived from the appropriate standard curve ((average fluorescence − y-intercept) ÷ slope). Data are presented as pg chemoattractant per ml PLF.

2.2.3 PHENOTYPING LEUKOCYTE POPULATIONS BY FLOW CYTOMETRY

2.2.3.1 SAMPLE PREPARATION AND STAINING

Single cell suspensions were aliquoted into 12x75 mm polystyrene FACS tubes. Unless otherwise stated, cells were stained for 20 minutes at 4°C, then washed with 3ml $PBS^{+/+}$ and centrifuged at 300 *g* for 5 minutes between rounds of staining/fixation.

2.2.3.1.1 STAINING OF HUMAN SAMPLES

PBMC ($1x10^6$/tube), PBL ($1x10^6$/tube), or B-cells ($2x10^5$/tube) were incubated 1:50 with human FcR block (Miltenyi Biotec) for 2 minutes at RT and then stained with the human T-cell panel (HTP), human B-cell/monocyte panel (HBMP) or human B-cell subset panel (HBSP) shown in **Table 2-2**.

For CCR7 staining as part of the HTP, PBMC or PBL were incubated with 1:50 anti-human CCR7 BV421 for 20 minutes at 37°C (**Table 2-2**). Cells were then washed, centrifuged, and stained with either the HBMP or HTP of antibodies (see **Table 2-2**). Cells were then washed, centrifuged, and fixed as described below (Section 2.2.3.1.3). The compensation antibodies (C) used were the primary antibodies listed in **Table 2-2**, whilst the isotype antibodies used can be found in **Table 2-3**.

To measure AdipoR1/2 expression on B-cell subsets, enriched B-cells were first stained with 1:100 unconjugated rabbit anti-human antibodies specific to either AdipoR1 or AdipoR2 (**Table 2-2**). B-cells were then washed, centrifuged, resuspended in MACS buffer and stained with the HBSP, including 1:250 of the Alexa fluor 488-conjugated secondary goat anti-rabbit antibody (see **Table 2-2**). Control tubes received the HBSP and secondary antibody only. A list of compensation and isotype antibodies can be found in **Table 2-2** and **Table 2-3**, respectively. After staining, B-cells were washed, centrifuged, and fixed as described below (Section 2.2.3.1.3).

2.2.3.1.2 STAINING OF MURINE SAMPLES

A proportion of the single-cell suspension of each murine tissue was placed into a polystyrene tube (⅓ PLF, ⅓ LN, ⅓ BM, ⅓ blood, ⅕ spleen cells per tube) and incubated 1:50 with mouse FcR block (Miltenyi Biotec) for 2 minutes at RT. Cells were then stained with either the mouse T-cell (MTP), mouse B-cell (MBP), or mouse myeloid (MP) antibody panel for 20 minutes at 4°C to label extracellular markers (see **Table 2-4**). After staining was completed, cells were washed, centrifuged and fixed as described below. A list of compensation and isotype antibodies can be found in **Table 2-4** and **Table 2-5**, respectively.

2.2.3.1.3 SAMPLE FIXATION AND ACQUISITION

All samples were fixed using 400µl 2% formaldehyde (TAAB, UK) diluted in $PBS^{+/+}$ for 10 minutes at 4°C. Cells were then washed, centrifuged, and resuspended in a fixed volumed of 300µl $PBS^{+/+}$. All samples were spiked with CountBright beads (1:15; ThermoFisher) and acquired on a 4-laser Fortessa X20 flow cytometer.

Table 2-2 Primary antibody panels used for human PBMC, PBL and B-cell samples

Antibodies								
Target	**Clone**	**Conjugate**	**Isoform**	**Manufacturer**	**Catalogue #**	**Concentration (µg/ml)**	**Dilution**	**Panel**
CD3	OKT3	PerCPCy5.5	IgG2a, κ	ThermoFisher	45-0037-42	50	1:50	HTP, HBMP, C
CD4	RPA-T4	Alexa fluor 700	IgG1, κ	ThermoFisher	56-0049-42	50	1:50	HTP, C
CD8	RPA-T8	BV786	IgG1, κ	BD Biosciences	563824	N/A	1:50	HTP
CD8	OKT8	eFluor450	IgG2a, κ	ThermoFisher	48-0086-42	25	1:50	C
CD45RA	HI100	PECy5	IgG2b, κ	ThermoFisher	15-0458-42	25	1:50	HTP, C
CCR7	150503	BV421	IgG2a	BD Biosciences	562555	N/A	1:50	HTP
CD28	CD28.2	PE	IgG1, κ	ThermoFisher	12-0289-42	50	1:50	HTP, C
CD27	O323	APC-eFluor 780	IgG1, κ	ThermoFisher	47-0279-42	50	1:50	HTP
CD27	O323	eFluor 450	IgG1, κ	BioLegend	423101	N/A	1:500	HTP, HBMP
KLRG1	MAFA	Alexa fluor 647	IgG2a, κ	BioLegend	367704	N/A	1:100	HTP, HBMP
CD57	QA17A04	BV605	IgG1, κ	BioLegend	393304	N/A	1:100	HTP, HBMP
CD25	CD25-4E3	PE-eFluor 610	IgG2b, κ	ThermoFisher	61-0257-42	25	1:100	HTP
CD19	HIB19	PECy7	IgG1, κ	ThermoFisher	25-0199-42	50	1:50	HTP, HBMP, C
CD19	HIB19	Alexa fluor 700	IgG1, κ	ThermoFisher	56-0199-42	25	1:100	HBSP
CD24	ML5	BV711	IgG2a, κ	BD Biosciences	563371	N/A	1:100	HBSP
CD20	2H7	PerCPCy5.5	IgG2b, κ	ThermoFisher	45-0209-42	50	1:100	HBSP
CD38	HIT2	APC	IgG1, κ	ThermoFisher	17-0389-42	50	1:40	HBSP
IgD	IA6-2	PECy7	IgG2a, κ	BD Biosciences	561314	N/A	1:100	HBSP
IgD	IA6-2	Super Bright 702	IgG2a, κ	ThermoFisher	67-9868-42	50	1:50	C
CD43	1G10	BV650	IgG1, κ	BD Biosciences	743613	200	1:100	HBSP, C
CD5	UCHT2	PECy5	IgG2a, κ	ThermoFisher	15-0058-42	12	1:100	HBSP
CD1d	CD1d42	PE	IgG2a, κ	ThermoFisher	15-0058-42	12	1:40	HBSP
CD56	R19-760	BV711	IgG1, κ	BD Biosciences	744221	200	1:50	HBMP

Target	Clone	Conjugate	Isoform	Manufacturer	Catalogue #	Concentration (µg/ml)	Dilution	Panel
CD14	61D3	eFluor 450	IgG1, κ	ThermoFisher	48-0149-42	100	1:100	HBMP
CD14	61D3	APC	IgG1, κ	ThermoFisher	17-0149-42	50	1:50	C
CD41	HIP8	Pacific Blue	IgG1, κ	BioLegend	303714	N/A	1:50	HBMP
AdipoR1	/	Unconjugated	IgG	Pheonix Pharmaceuticals	G-001-44	200	1:100	HBSP
AdipoR2	/	Unconjugated	IgG	Pheonix Pharmaceuticals	G-001-23	200	1:100	HBSP
Goat anti-rabbit IgG	/	Alexa fluor 488	IgG	ThermoFisher	A11008	2000	1:250	HBSP
Viability dye								
Zombie aqua	/	/	**/**	BioLegend	423101	N/A	1:500	HTP, HBMP, HBSP, C

- The concentration listed is the concentration the antibody was supplied at and the dilution is the working dilution the antibody was used at per experiment.
- The antibodies were used in 3 separate panels: Human T-cell panel (HTP), human B-cell/monocyte panel (HBMP), and human B-cell subset panel (HBSP)
- C, compensation antibody; N/A, not available; /, not applicable.

Table 2-3 List of primary human antibodies and corresponding isotype controls

Primary antibody	Isotype	Manufacturer	Catalogue #	Concentration (µg/ml)	Dilution	Panel
CD45RA PECy5	IgG2b, κ PECy5	ThermoFisher	15-4732-42	6	1:50	Isotype panel for HTP
CCR7 BV421	IgG2a BV421	BD Biosciences	562439	200	1:100	Isotype panel for HTP
CD28 PE	IgG1, κ PE	ThermoFisher	12-4714-42	200	1:100	Isotype panel for HTP
CD27 APC-eFluor 780	IgG1, κ APC-eFluor 780	ThermoFisher	47-4714-82	200	1:100	Isotype panel for HTP
CD57 BV605	IgG1, κ BV605	BD Biosciences	562652	200	1:100	Isotype panel for HTP
KLRG1 Alexa fluor 647	IgG2a, κ Alexa fluor 647	ThermoFisher	51-4724-81	200	1:100	Isotype panel for HTP
CD24 BV711	IgG2a, κ BV711	BD Biosciences	563345	200	1:100	Isotype panel for HBP
CD27 eFluor 450	IgG1, κ eFluor 450	ThermoFisher	48-4714-82	200	1:800	Isotype panel for HBP
CD20 PerCPCy5.5	IgG2b, κ PerCPCy5.5	ThermoFisher	45-4724-82	200	1:400	Isotype panel for HBP
CD38 APC	IgG1, κ APC	ThermoFisher	17-4714-42	100	1:160	Isotype panel for HBP
IgD PECy7	IgG2a, κ PECy7	ThermoFisher	25-4724-81	200	1:100	Isotype panel for HBP
CD43 BV650	IgG1, κ BV650	BD Biosciences	563231	200	1:100	Isotype panel for HBP
CD5 PECy5	IgG2a, κ PECy5	ThermoFisher	15-4724-81	200	1:500	Isotype panel for HBP
CD1d PE	IgG2a, κ PE	ThermoFisher	12-4724-82	200	1:200	Isotype panel for HBP

- Each primary antibody and immunoglobulin (Ig) isotype antibody is listed followed by the corresponding isotype control concentration and dilutions.
- N/A, not available.

Table 2-4 List of primary antibodies used for murine tissue samples

Antibodies								
Target	**Clone**	**Conjugate**	**Isoform**	**Manufacturer**	**Catalogue #**	**Concentration (µg/ml)**	**Dilution**	**Panel**
CD45.2	104	BV605	IgG2a, κ	BioLegend	109841	200	1:100	MTP, MBP,
CD45.2	104	APC-eFluor 780	IgG2a, κ	ThermoFisher	47-0454-82	200	1:200	MMP, C
CD3ξ	145-2C11	PECy7	IgG	ThermoFisher	25-0031-82	200	1:50	MTP, MBP, C
CD4	GK1.5	eFluor450	IgG2b, κ	ThermoFisher	48-0041-82	200	1:100	MTP, C
CD8	5H10	PE-Texas Red	IgG2b	ThermoFisher	MCD0817	N/A	1:200	MTP, C
CD62L	MEL-14	PE	IgG2a, κ	ThermoFisher	12-0621-82	200	1:500	MTP
CD44	IM7	FITC	IgG2b, κ	ThermoFisher	11-0441-82	500	1:500	MTP
CD25	PC61.5	Alexa fluor 700	IgG1, κ	ThermoFisher	56-0251-82	200	1:50	MTP
KLRG1	2F1	APC-eFluor 780	IgG2a, κ	ThermoFisher	47-5893-82	200	1:100	MTP
CD19	1D3	APC	IgG2a, κ	ThermoFisher	17-0193-82	200	1:50	MTP, MBP
CD21/35	7G6	PE	IgG2b, κ	BD Biosciences	552957	200	1:100	MBP
CD23	B3B4	BV421	IgG2a, κ	BD Biosciences	562929	200	1:100	MBP
CD93	AA4.1	BV650	IgG2b, κ	BD Biosciences	563807	200	1:100	MBP
CD43	S7	PerCPCy5.5	IgG2a, κ	BD Biosciences	562865	200	1:100	MBP
F4/80	BM8	FITC	IgG2b	ThermoFisher	MA5-16628	100	1:50	MMP
CD11c	N418	PECy7	IgG	ThermoFisher	25-0114-82	200	1:50	MMP
Siglec F	E50-2440	PE-CF594	IgG2a, κ	BD Biosciences	562757	200	1:50	MMP
Ly6G	1A8	APC	IgG2a, κ	BD Biosciences	560599	200	1:50	MMP
CD3ξ	145-2C11	PE	IgG	ThermoFisher	12-0031-82	200	1:100	C
CD3ξ	145-2C11	FITC	IgG	ThermoFisher	11-0031-82	500	1:100	C
CD45.2	30-F11	Alexa fluor 700	IgG2b, κ	ThermoFisher	56-0451-82	200	1:100	C
CD3ξ	17A2	BV650	IgG2b, κ	BD Biosciences	100229	N/A	1:100	C
CD3ξ	17A2	BV605	IgG2b, κ	BD Biosciences	100237	N/A	1:100	C
CD3ξ	145-2C11	PerCPCy5.5	IgG	ThermoFisher	45-0031-82	200	1:100	C

Target	Clone	Conjugate	Isoform	Manufacturer	Catalogue #	Concentration (µg/ml)	Dilution	Panel
CD3ξ	17A2	APC	IgG2b, κ	ThermoFisher	17-0032-82	200	1:100	C
Viability dye								
Zombie aqua	/	/	/	BioLegend	423101	N/A	1:500	MTP, MBP, MMP

- The concentration listed is the concentration the antibody was supplied at and the dilution is the working dilution the antibody was used at per experiment.
- The antibodies were used in 5 separate panels: Mouse T-cell panel (MTP), mouse B-cell panel (MBP), mouse myeloid panel (MMP).
- C, compensation; N/A, not available; /, not applicable.

Table 2-5 List of primary mouse antibodies and corresponding isotype controls

Primary antibody	Isotype	Manufacturer	Catalogue #	Concentration (µg/ml)	Dilution	Panel
CD25 Alexa fluor 700	IgG1, κ Alexa fluor 700	ThermoFisher	56-4301-80	200	1:50	Isotype panel for MTP
KLRG1 APC-eFluor 780	IgG2a, κ APC-eFluor 780	ThermoFisher	47-4321-82	200	1:100	Isotype panel for MTP
CD21/35 PE	IgG2b, κ PE	ThermoFisher	12-4031-82	200	1:100	Isotype panel for MBP
CD23 BV421	IgG2a, κ BV421	BD Biosciences	562602	200	1:100	Isotype panel for MBP
CD93 BV650	IgG2b, κ BV650	BD Biosciences	563233	200	1:100	Isotype panel for MBP
CD43 PerCPCy5.5	IgG2a, κ PerCPCy5.5	ThermoFisher	45-4321-80	200	1:100	Isotype panel for MBP

- Each primary antibody and immunoglobulin (Ig) isotype antibody is listed followed by the corresponding isotype control concentration and dilutions.

2.2.3.2 ANALYSIS OF FLOW CYTOMETRY DATA

Gates were set up on FACSDiva (version 7; BD Biosciences) to gate for cells and CountBright beads (approximately 1,000 beads/µl) using forward (FSC) and side (SSC) scatter profiles. Doublets and dead cells were excluded using forward scatter area versus height (FSC-A and FSC-H), and positive zombie aqua signal, respectively (**Figure 2-3**). After acquisition, data were exported from FACSDiva as Flow Cytometry Standard (FCS) files and analysed using Flow Jo (version 10.7.1, BD Biosciences). Individual populations were gated on as described below (Sections 2.2.3.2.1 and 2.2.3.2.2). The absolute number of each leukocyte population listed below was quantified using the CountBright beads (ThermoFisher) according to the manufacturer's instructions. The number of bead events and the number of cell events per leukocyte population within a sample were exported into a table. The number of beads added per sample was calculated using the bead concentration stated on the CountBright beads, which varied between lots. The absolute number of different leukocyte populations within the sample was then calculated using the following equation:

$$\text{Total number of cells} = \frac{\text{Number of cell events x Number of beads}}{\text{Number of bead events x Volume of sample (µl)}} \text{ x Volume of sample (µl)}$$

For murine samples, this value was then multiplied by the denominator of the fraction of tissue added to the tube to provide the total number of leukocyte populations within the tissue. Flow cytometry data in this thesis are expressed as either absolute counts, percentage of the parent population, or median fluorescence intensity (MFI) values.

2.2.3.2.1 HUMAN LEUKOCYTE POPULATIONS

The standard gating strategy used for human PBMC samples is shown in **Figure 2-4**. Within the live cell population, T-cells ($CD3^+CD19^-$), B-cells ($CD3^-CD19^+$), NK $CD56^{lo}$

($CD3^-CD56^{lo}$), NK $CD56^{hi}$ ($CD3^-CD56^{hi}$) and monocytes ($CD14^+$) were selected (**Figure 2-4A-C**). T-cells were further distinguished based on $CD4^+$ and $CD8^+$ expression (**Figure 2-4D**). Treg were identified as $CD4^+CD25^+$ T-cells (**Figure 2-4E**). $CD4^+$ and $CD8^+$ T-cells were identified as naïve ($CCR7^+CD45RA^+$), EM ($CCR7^-CD45RA^-$), CM ($CCR7^+CD45RA^-$) and TEMRA ($CCR7^-CD45RA^+$) T-cells (**Figure 2-4F**). $CD4^+$ and $CD8^+$ senescent T-cells were identified based on lack of CD27 and CD28 expression (**Figure 2-4G**), or positive CD57 and KLRG1 expression (**Figure 2-4H**).

The standard gating strategy used for human B-cell samples is shown in **Figure 2-5**. Within the live cells gate, B-cells were selected based on $CD19^+$ and $CD20^+$ expression (**Figure 2-5A**). B1 cells ($CD43^+CD27^+$) were gated out, followed by B10 cells ($CD5^+CD1d^+$) (**Figure 2-5B+C**). The remaining B-cells were identified as naïve ($IgD^+CD27^-CD38^-$), transitional regulatory ($IgD^+CD27^-CD38^+CD24^+$), effector ($IgD^+CD27^+CD38^-$), class-switched memory ($IgD^-CD27^+CD38^-$) and senescent (IgD^-CD27^-) cells (**Figure 2-5D+E**).

To measure AdipoR1/2 expression on B-cell subsets, the MFI and the percentage of positive and negative populations of the Alexa fluor 488 channel were extracted for each B-cell subset and exported into a table. The positive Alexa fluor 488 signal of the isotype control was subtracted from the positive Alexa fluor signal within the sample to determine the percentage of B-cells expressing AdipoR1/2 (**Figure 2-5F**).

The flow cytometric analysis of migrated PBL populations in Chapter 4 was normalised to the circulating population of the donor. To achieve this, the number of

different lymphocyte populations within the PBL ($1x10^6$) pool and the migrated PBL sample were quantified using flow cytometry. These values were then used to calculate the percentage of migrated cells relative to the number of circulating cells of a given lymphocyte population per donor.

2.2.3.2.2 MURINE LEUKOCYTE POPULATIONS

The standard gating strategy used for murine samples is shown in **Figure 2-6**. Within the live cell population, leukocytes were selected using CD45 expression (**Figure 2-6A)**. Leukocytes were then identified as T-cells ($CD3^+CD19^-$), B-cells ($CD3^-CD19^+$) macrophages ($F4/80^{hi}CD11c^-$), DC ($F4/80^-CD11c^+$), eosinophils (Siglec F^+), and neutrophils ($Ly6G^+$) (**Figure 2-6B-E**). T-cells were further distinguished based on CD4 and CD8 expression (**Figure 2-6F**), then identified as naïve ($CD62L^+CD44^-$), EM ($CD62L^-CD44^+$), and CM ($CD62L^+CD44^+$) T-cells (**Figure 2-6G+H**). Treg were defined as $CD4^+CD25^+$ cells (**Figure 2-6I**). Senescent T-cells were identified based on positive expression of KLRG1 (**Figure 2-6J**). Age-associated B-cells were identified as $CD19^+CD21/35^-CD23^-CD43^-$ cells (**Figure 2-6K**).

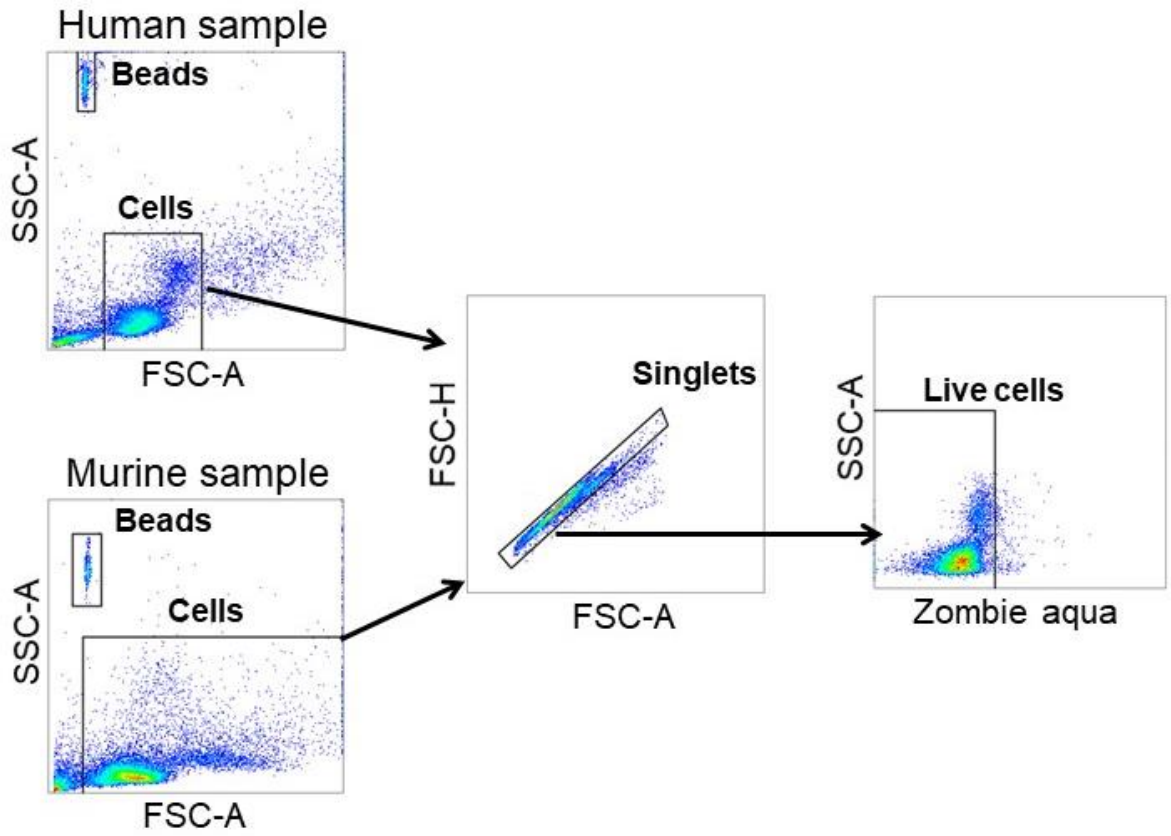

Figure 2-3 Initial flow cytometry gating strategy for human and murine samples
Human and murine samples were collected and processed for flow cytometric analysis. Firstly, cells and CountBright beads were selected based on forward (FSC) and side scatter (SSC) profiles. Doublets were excluded based on cell circularity, and dead cells were excluded based on positive zombie aqua staining.

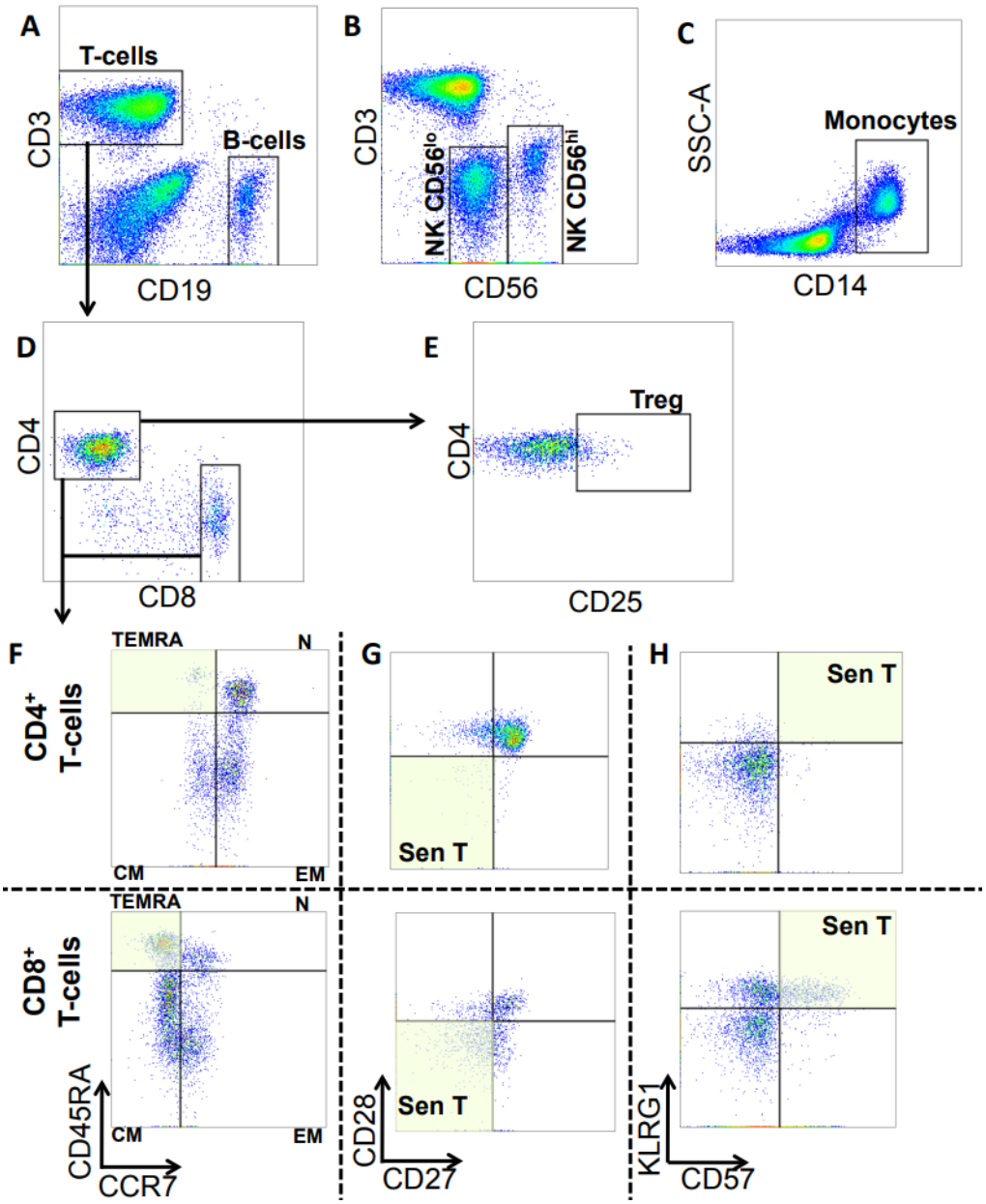

Figure 2-4 Extended flow cytometry gating for human PBMC samples

PBMC or PBL were isolated from fresh blood and migrated PBL were collected from collagen gels before flow cytometric analysis. Live cells were identified as **(A)** T-cells ($CD3^+CD19^-$), B-cells ($CD3^-CD19^+$), **(B)** NK $CD56^{lo}$ ($CD3^-CD56^{lo}$), NK $CD56^{hi}$ ($CD3^-CD56^{hi}$) and **(C)** monocytes ($CD14^+$). **(D)** T-cells were further distinguished based on CD4 and CD8 expression. **(E)** Regulatory T-cells (Treg) were identified as $CD4^+CD25^+$ cells. **(F)** CD45RA and CCR7 were used to identify $CD4^+$ and $CD8^+$ naïve (N), effector memory (EM), central memory (CM) and TEMRA T-cells. Senescent T-cells (Sen T) were either identified based on **(G)** lack of CD28 and CD27 expression, or **(H)** positive KLRG1 and CD57 expression. NK, Natural killer cells.

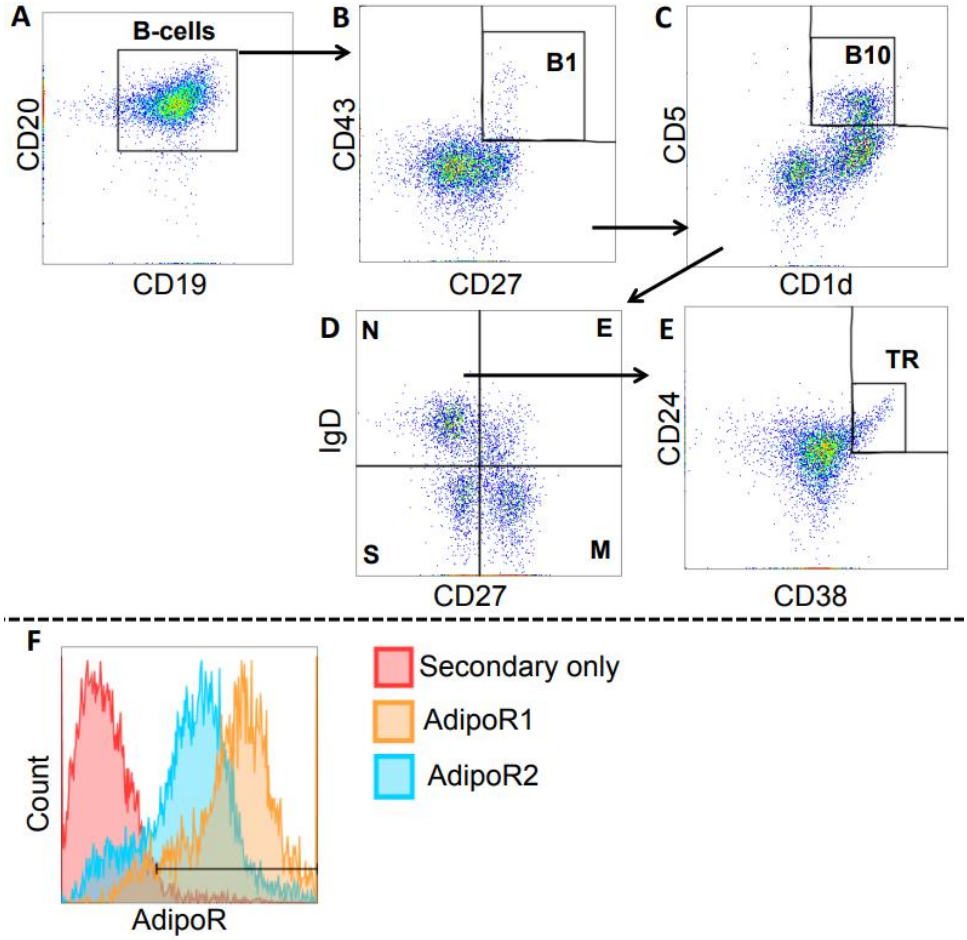

Figure 2-5 Extended flow cytometry gating for human B-cell samples

B-cells were isolated from the blood of young and older donors prior to flow cytometric analysis. **(A)** Live cells were identified as B-cells ($CD19^+CD20^+$), and then identified as individual B-cell subsets: **(B)** B1 ($CD43^+CD27^+$), **(C)** B10 ($CD5^+CD1d^+$), **(D)** naïve (N; $IgD^+CD27^-CD38^-$), effector (E; $IgD^+CD27^+CD38^-$), class-switched memory (M; $IgD^-CD27^+CD38^-$) and senescent (S; IgD^-CD27^-) cells. **(E)** Transitional regulatory (TR) B-cells were identified as $IgD^+CD27^-CD38^+CD24^+$ cells. **(F)** Representative histogram depicting positive expression of AdipoR1/2 on B-cell subsets in comparison to the secondary antibody-only control.

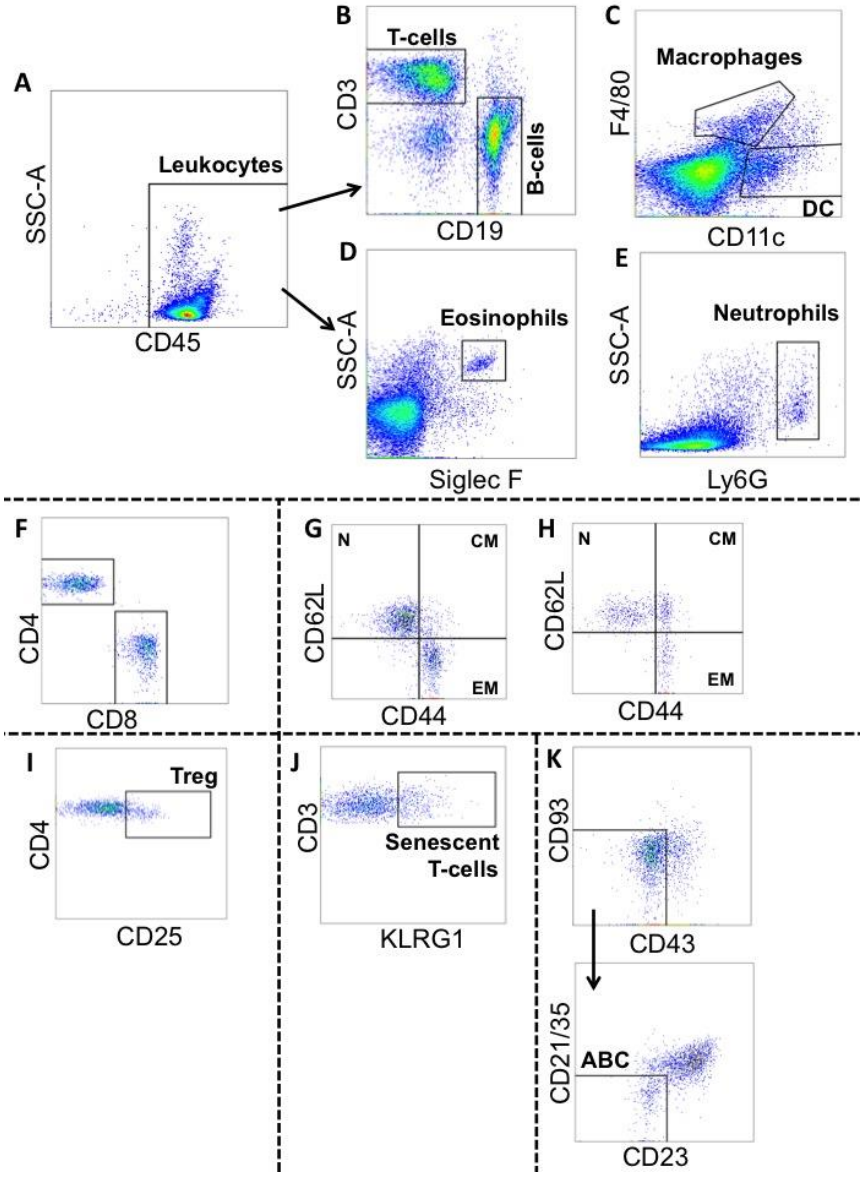

Figure 2-6 Extended flow cytometry gating for murine samples

Murine tissues were processed into single-cell suspensions prior to flow cytometric analysis. **(A)** First, live cells were identified as leukocytes based on CD45 expression. Leukocytes were then identified as **(B)** T-cells ($CD3^+CD19^-$), B-cells ($CD3^-CD19^+$), **(C)** macrophages ($F4/80^+CD11c^-$), dendritic cells (DC; $F4/80^-CD11c^+$), **(D)** eosinophils (Siglec F^+), and **(E)** neutrophils ($Ly6G^+$). **(F)** T-cells were further distinguished based on CD4 and CD8 expression, and then CD62L and CD44 expression to identify naïve (N), effector memory (EM), and central memory (CM) $CD4^+$ **(G)** and $CD8^+$ **(H)** T-cell subsets. **(I)** Regulatory T-cells (Treg) were defined as $CD4^+CD25^+$ cells. **(J)** Senescent T-cells were identified as $CD3^+KLRG1^+$ cells. **(K)** Age-associated B-cells (ABC) were identified as $CD93^-CD43^-CD21/35^-CD23^-$ cells.

2.3. STATISTICS

Data analysis was performed using GraphPad Prism software (version 8.4.3; GraphPad Software Inc., USA). All data are expressed as mean ± standard error of the mean (SEM) unless otherwise stated. Data were first assessed for normal distribution using the Shapiro-Wilk test, where a p-value <0.05 was considered normally distributed. For *in vitro* experiments a paired t-test, unpaired t-test, line regression analysis, one-way or two-way ANOVA with Bonferroni or Dunnett's multiple comparison test was used. For *in vivo* experiments an unpaired t-test, one-way, two-way, or three-way ANOVA with Bonferroni multiple comparison test was used.

In all cases, a p-value <0.05 was considered statistically significant.

CHAPTER 3 – AGE-RELATED CHANGES TO HOMEOSTATIC LEUKOCYTE TRAFFICKING

3.1 INTRODUCTION

There is growing evidence to suggest that ageing negatively influences leukocyte trafficking processes during varying models of inflammation (reviewed by Hopkin, Lord and Chimen, 2021), however less is known about age-related changes to leukocyte trafficking in the steady state. Homeostatic leukocyte trafficking is necessary for immunosurveillance and tissue homeostasis (Reglero-Real, Rolas and Nourshargh, 2019), and so understanding how advancing age influences this process is important in the context of an individual's healthspan. Importantly, there is an abundance of evidence demonstrating the impact of biological sex on immunological processes (Klein and Flanagan, 2016; Marquez *et al.*, 2020), yet most studies to date regarding age-related changes to leukocyte trafficking processes have overlooked this variable. Here we investigated age-related and sex-specific changes to leukocyte populations across multiple murine tissues, with a specific focus on the peritoneal cavity, to infer age-related changes to homeostatic leukocyte trafficking.

3.2 RESULTS

3.2.1 AGEING IS ASSOCIATED WITH INCREASED NUMBERS OF PERITONEAL LEUKOCYTES IN VIVO

To investigate the impact of ageing on homeostatic leukocyte trafficking patterns we quantified the number of leukocyte subsets in the peritoneum, spleen, BM, inguinal LN, and blood of 3-month, 18-month, and 21-month male and female wildtype mice using flow cytometry **(Figure 3-1)**. As ageing is associated with chronic low-grade inflammation (Franceschi and Campisi, 2014), it was hypothesised that older mice would have different numbers of leukocytes within tissues compared to young mice to

reflect age-relate9d changes to leukocyte generation, maintenance, and trafficking patterns.

Surprisingly, age was associated with increased numbers of leukocytes in the peritoneal cavity in a sex-specific manner. Twenty-one-month female mice had significantly more $CD45^+$ leukocytes within the peritoneal cavity compared to 3 month (>5-fold change) and 18 month (>11-fold change) females **(Figure 3-2)**. Increased numbers of peritoneal leukocytes were observed in 21-month male mice compared to the 3 month and 18-month males, although this did not reach statistical significance **(Figure 3-2)**. Ageing was associated with significant changes to innate immune cell populations within the peritoneal cavity, such as a significant decline in macrophage numbers **(Figure 3-3A)** and a significant increase in neutrophil numbers **(Figure 3-3B)** within the cavity of 21-month male and female mice compared to young mice. DC were also increased in the peritoneum of 21-month mice compared to younger mice, although this only reached statistical significance for the male mice **(Figure 3-3C)**. Together these data suggest that ageing significantly changes the number of innate immune cells within the peritoneal cavity of resting wildtype mice in a sex-independent manner.

As for lymphocyte populations, B-cell numbers were significantly increased in the peritoneum of 21-month female, but not male, mice compared to 3-month and 18-month mice **(Figure 3-4A)**. T-cell numbers were significantly increased in the peritoneal cavity of 21-month male and female mice compared to young animals **(Figure 3-4B)**. Increased numbers of age-related lymphocyte populations were also observed in the peritoneum of 21-month mice **(Figure 3-5)**. ABC numbers were significantly increased >4-fold in the peritoneal cavity of 21-month female mice

compared to younger females **(Figure 3-5A)**, whilst no expansion of ABCs was observed for 21-month males compared to younger males. Senescent T-cell population numbers were significantly increased in the peritoneum of 21-month male and female mice compared to 3-month and 18-month counterparts **(Figure 3-5)**. The impact of ageing on the number of multiple peritoneal T-cell subsets can be found in **Table 3-1**. Collectively, these data suggest that ageing expands peritoneal lymphocyte populations in aged mice, with females exhibiting a stronger age-related phenotype compared to males.

Leukocyte numbers in the spleen, BM, iLN and blood were also affected by ageing **(Figure 3-6)**. The number of leukocytes in the spleen of 21-month male mice was significantly reduced (>2-fold) compared to 3 month and 18-month males **(Figure 3-6A)**; whereas no age-related changes to splenic leukocyte numbers were observed for the females. Interestingly, the number of age-associated lymphocyte populations, ABC and senescent T-cells, were significantly increased in the spleens of 21-month female mice, but not male mice, compared to 3-month counterparts **(Table 3-2)**. No age-related changes to leukocyte numbers were observed in the BM of wildtype mice **(Figure 3-6B)**, but a significant reduction (>4-fold) in inguinal LN leukocyte numbers was observed in 18 month and 21-month male and female mice compared to 3-month mice **(Figure 3-6C)**. The number of T- and B-cells in the inguinal LN of 21-month male and female mice was significantly reduced compared to 3-month mice **(Table 3-3)**. An age-related increase in the number of circulating leukocytes was observed in 21-month male and female mice compared to younger mice, however, this increase only reached statistical significance for the male mice **(Figure 3-6D)**. Indeed, the circulating number of DC, eosinophils, neutrophils, and B-

cells was significantly increased for 21-month male mice compared to 3-month mice **(Table 3-2)**. These data suggest that the ageing process affects leukocyte population numbers in multiple tissues in a sex-specific manner.

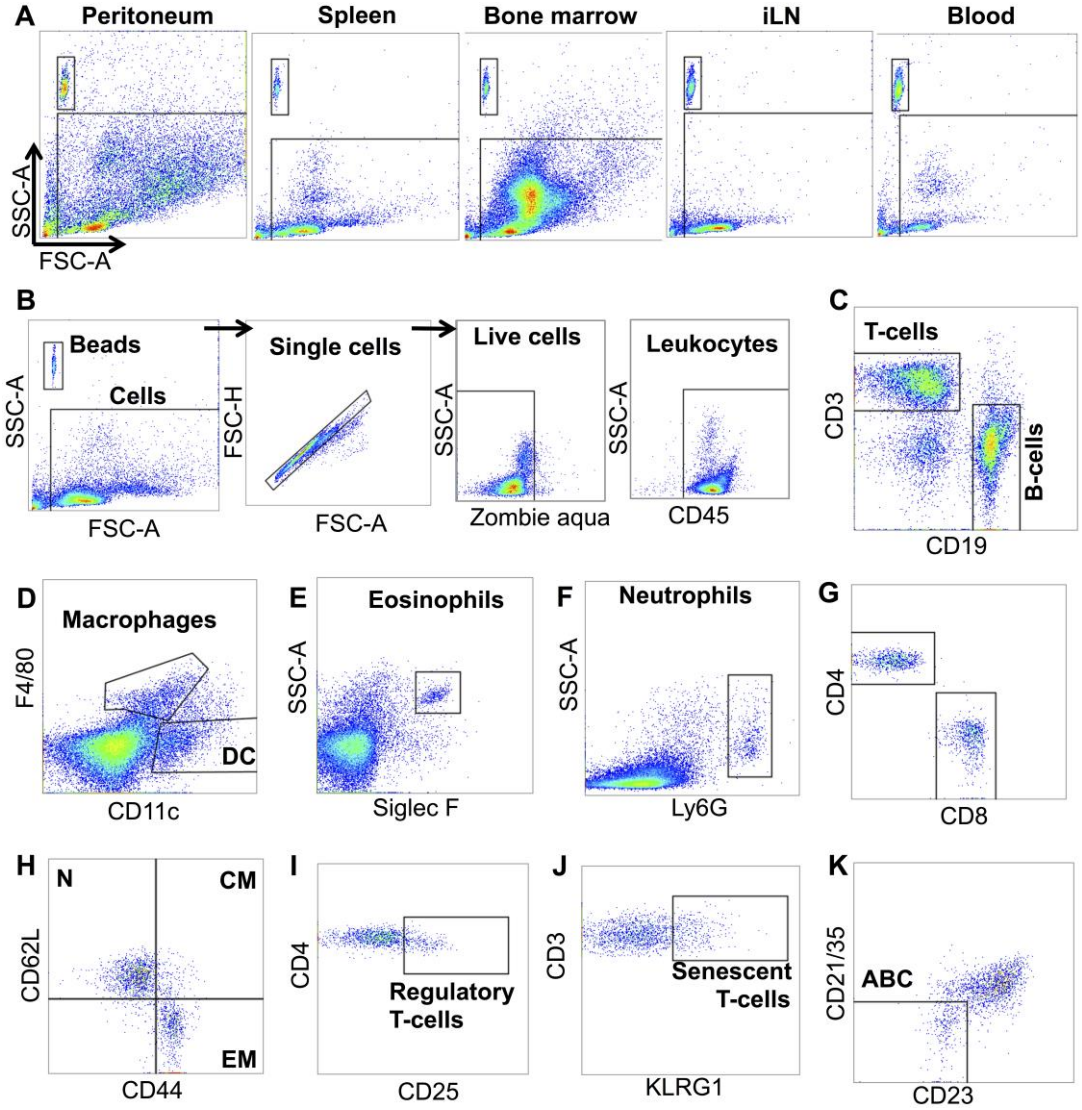

Figure 3-1 Gating strategy to identify murine leukocytes using flow cytometry

Tissues were collected from naïve 3-month, 18-month and 21-month male and female mice, and processed to single-cell suspension prior to flow cytometric analysis. **(A)** Representative forward (FSC) versus side (SSC) plots of cells derived from the peritoneum, spleen, bone marrow, inguinal lymph nodes (iLN) and blood. **(B)** Gating strategy to identify live, single leukocytes for all tissues. Subsequently, **(C)** T-cells, B-cells, **(D)** macrophages, dendritic cells (DC), **(E)** eosinophils and **(F)** neutrophils were identified. Within the T-cell gate, T-cells were distinguished based on **(G)** CD4 and CD8 expression, and then **(H)** CD44 and CD62L expression. **(I)** Regulatory T-cells were identified as $CD4^{+}CD25^{+}$ cells, whilst **(J)** senescent T-cells were identified as $CD3^{+}KLRG1^{+}$. **(K)** Age-associated B-cells (ABC) were identified as $CD19^{+}CD93^{-}CD43^{-}CD21^{-}CD23^{-}$ cells.

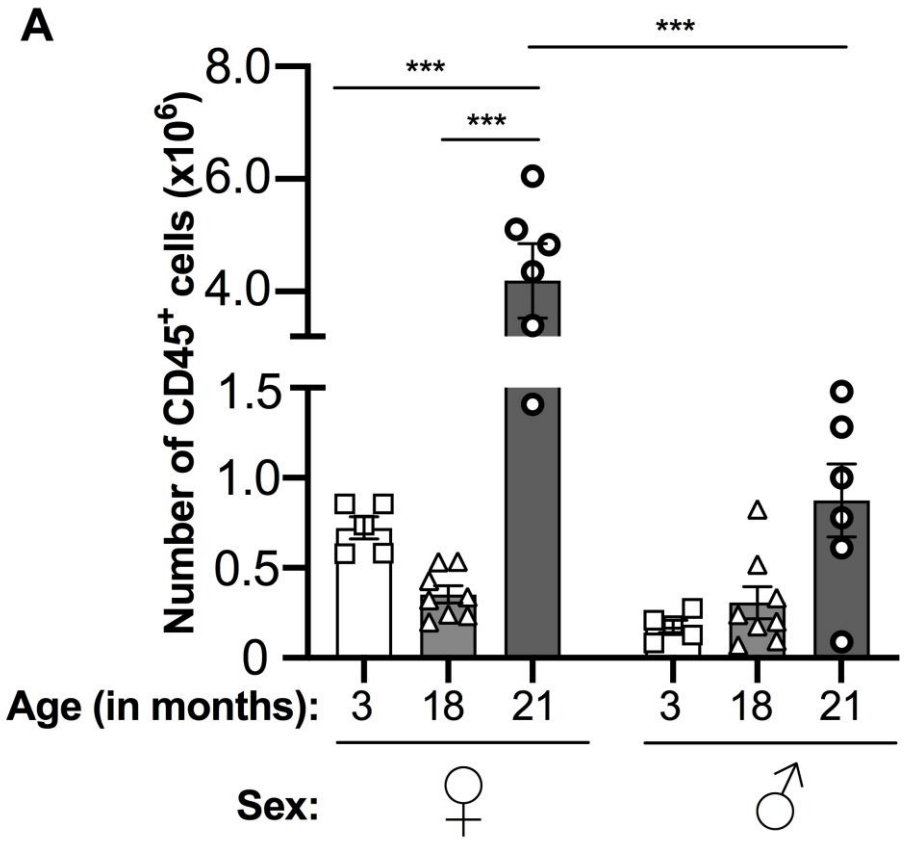

Figure 3-2 Ageing and sex influenced peritoneal leukocyte numbers *in vivo*

Exudate from the peritoneal cavity of naïve 3 month, 18 month and 21 month female (♀) and male (♂) C57Bl6 mice was collected and analysed using flow cytometry. The total number of peritoneal $CD45^+$ leukocytes was quantified using CountBright beads. Two-way ANOVA showed a significant effect of sex ($p<0.001$) and age ($p<0.001$) on peritoneal $CD45^+$ leukocyte numbers. Data are presented as mean±SEM for n=9 independent experiments using n=5 for 3 month mice, n=8 for 18 month mice and n=6 for 21 month mice. ***$p<0.001$ by Bonferroni multiple comparison post-test.

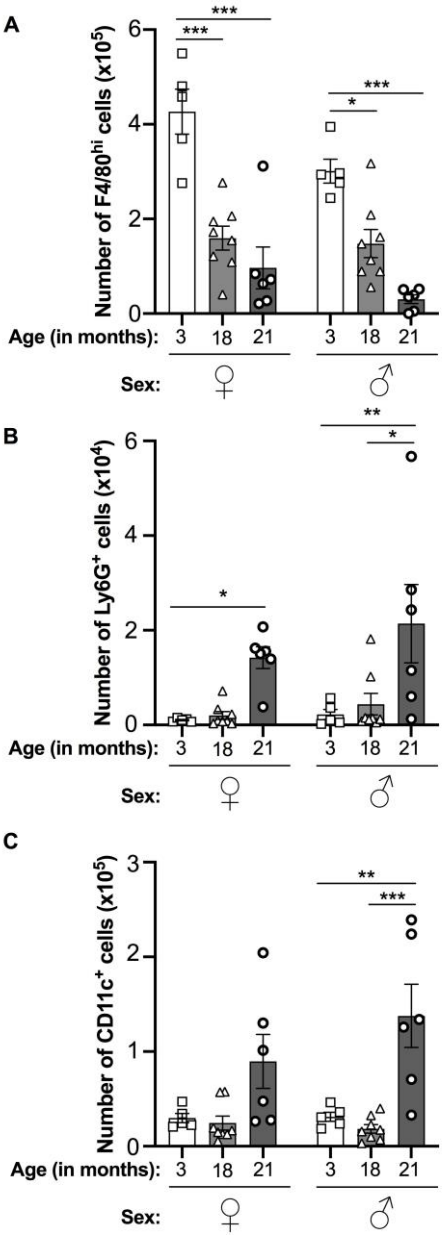

Figure 3-3 Ageing affected peritoneal myeloid population numbers

Exudate from the peritoneal cavity of naïve 3 month, 18 month and 21 month female (♀) and male (♂) C57Bl6 mice was collected and analysed using flow cytometry. Peritoneal **(A)** F4/80^{hi} macrophages, **(B)** Ly6G^{+} neutrophils, and **(C)** CD11c^{+} dendritic cells (DC) were quantified using CountBright beads. Two-way ANOVA showed a significant effect of age on macrophage, neutrophil, and DC numbers ($p>0.0.001$) and of sex on macrophage ($p<0.01$) numbers. Data are presented as mean±SEM for n = 9 independent experiments using n=5 for 3 month mice, n=8 for 18 month mice and n=6 for 21 month mice. ***$p<0.001$, **$p<0.01$, *$p<0.05$ by Bonferroni multiple comparison post-test.

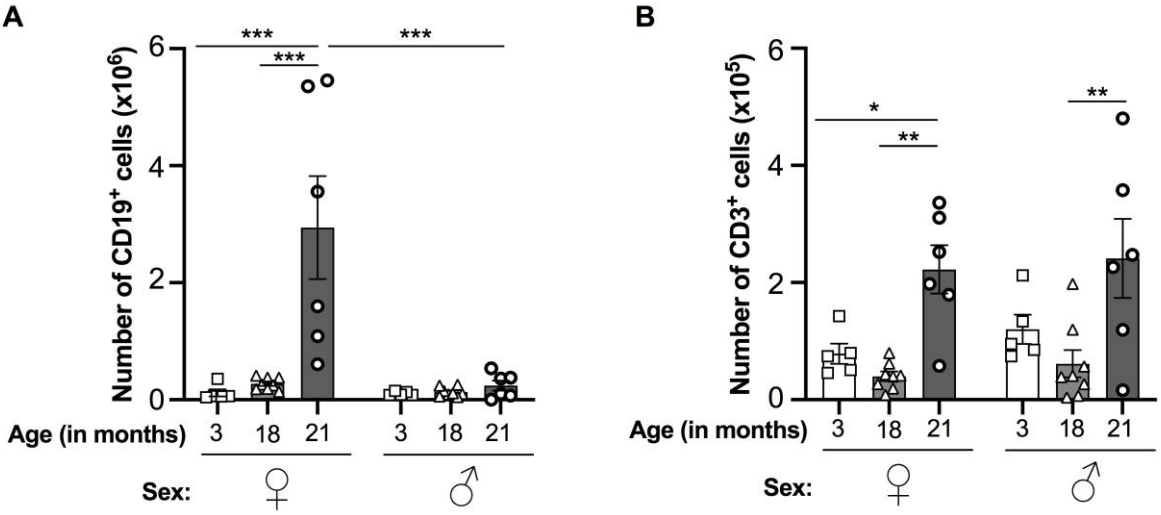

Figure 3-4 Ageing affected peritoneal lymphocyte populations in a sex-dependent manner

Exudate from the peritoneal cavity of naïve 3 month, 18 month and 21 month female (♀) and male (♂) C57Bl6 mice was collected and analysed using flow cytometry. Peritoneal **(A)** $CD19^+$ B-cells and **(B)** $CD3^+$ T-cells were quantified using CountBright beads. Two-way ANOVA showed a significant effect of age on B- and T-cell numbers ($p>0.0.01$) and of sex on B-cell ($p<0.05$) numbers. Data are presented as mean±SEM for n = 9 independent experiments using n=5 for 3 month mice, n=8 for 18 month mice and n=6 for 21 month mice. ***$p<0.001$, **$p<0.01$, *$p<0.05$ by Bonferroni multiple comparison post-test.

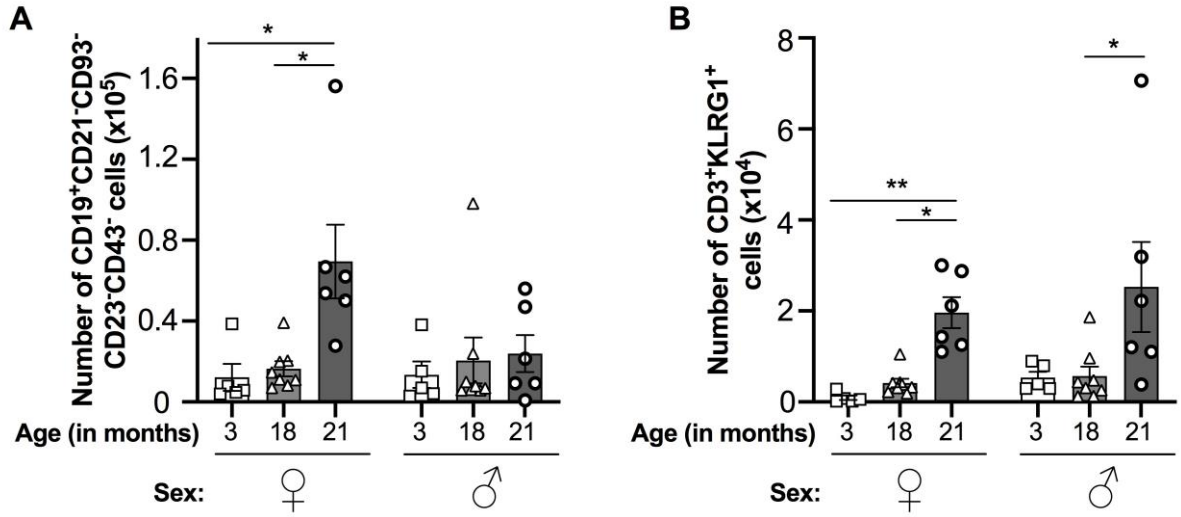

Figure 3-5 Ageing was associated with increased numbers of age-related lymphocytes in the peritoneal cavity, in a sex-specific manner

Exudate from the peritoneal cavity of naïve 3 month, 18 month and 21 month female (♀) and male (♂) C57Bl6 mice was collected and analysed using flow cytometry. Peritoneal **(A)** $CD19^+CD93^-CD43^-CD21/35^-CD23^-$ age-associated B-cells (ABCs) and **(B)** $CD3^+KLRG1^+$ senescent T-cells were quantified using CountBright beads. Two-way ANOVA showed a significant effect of age on ABCs and senescent T-cell numbers ($p>0.0.01$). Data are presented as mean±SEM for n = 9 independent experiments using n=5 for 3 month mice, n=8 for 18 month mice and n=6 for 21 month mice. **p<0.01, *p<0.05 by Bonferroni multiple comparison post-test.

Table 3-1 T-cell subsets in the peritoneum of young and aged wildtype mice

T-cell subset (total no.)	F 3mo (mean±SEM)	F 18mo (mean±SEM)	F 21mo (mean±SEM)	p-value (F 3mo v 18mo)	p-value (F 18mo v 21mo)	p-value (F 3mo v 21mo)	M 3mo (mean±SEM)	M 18mo (mean±SEM)	M 21mo (mean±SEM)	p-value (M 3mo v 18mo)	p-value (M 18mo v 21mo)
$CD4^+$ T-cells	45,079 ±6,181	27,505 ±5,334	114,617 ±26,256	>0.999	**0.002**	**0.024**	99,990 ±19,978	63,900 ±22,069	85,228 ±22,038	0.820	>0.999
$CD8^+$ T-cells	13,285 ±3,301	29,523 ±6,708	107,517 ±35,906	>0.999	**0.036**	**0.023**	35,365 ±4,392	45,170 ±11,087	147,904 ±46,468	>0.999	**0.036**
$CD4^+$ N T-cells	34,335 ±8,837	9,157 ±1,772	38,462 ±5,794	**0.012**	**0.002**	>0.999	40,054 ±10,520	16,780 ±5,357	23,428 ±7,978	0.139	>0.999
$CD4^+$ EM T-cells	11,338 ±5,580	2,433 ±667	38,878 ±12,915	>0.999	**0.007**	0.083	45,018 ±8,366	25,507 ±14,800	38,399 ±10,290	0.922	>0.999
$CD4^+$ CM T-cells	6,377 ±1,115	10,721 ±1,954	15,821 ±4,123	0.845	0.559	0.110	8,046 ±1,688	7,472 ±1,515	18,526 ±5,391	>0.999	0.069
Tregs	3,547 ±835	994.7 ±127	7,146 ±1,657	0.265	**0.009**	0.085	9,288 ±1,713	1,350 ±487	4,329 ±1,259	**0.003**	0.182
$CD8^+$ N T-cells	8,745 ±2,333	3,267 ±1,266	21,716 ±3,900	0.458	**0.002**	**0.012**	12,203 ±1,725	14,248 ±6,666	31,494 ±12,614	>0.999	0.465
$CD8^+$ EM T-cells	450.3 ±390	10,125 ±2,487	40,218 ±9,038	0.653	**0.002**	**0.004**	8,896 ±1,776	23,121 ±6,287	39,911 ±15,131	0.937	0.636
$CD8^+$ CM T-cells	3,975 ±570	8,252 ±2,109	96,820 ±15,067	>0.999	**<0.001**	**<0.001**	15,614 ±1,114	6,788 ±3,154	74986 ±26,531	>0.999	**0.010**

Peritoneal T-cell subsets of 3 (3mo), 18 (18mo) and 21 (21mo) month male (M) and female (F) wildtype mice. Data are shown as mean ± standard error of the mean (SEM) for lymphocyte subsets. Statistical analysis performed using two-way ANOVA to determine the effects of sex and age on the number of peritoneal lymphocyte subsets. N, naïve; EM, effector memory; CM, central memory; Tregs, regulatory T-cells.

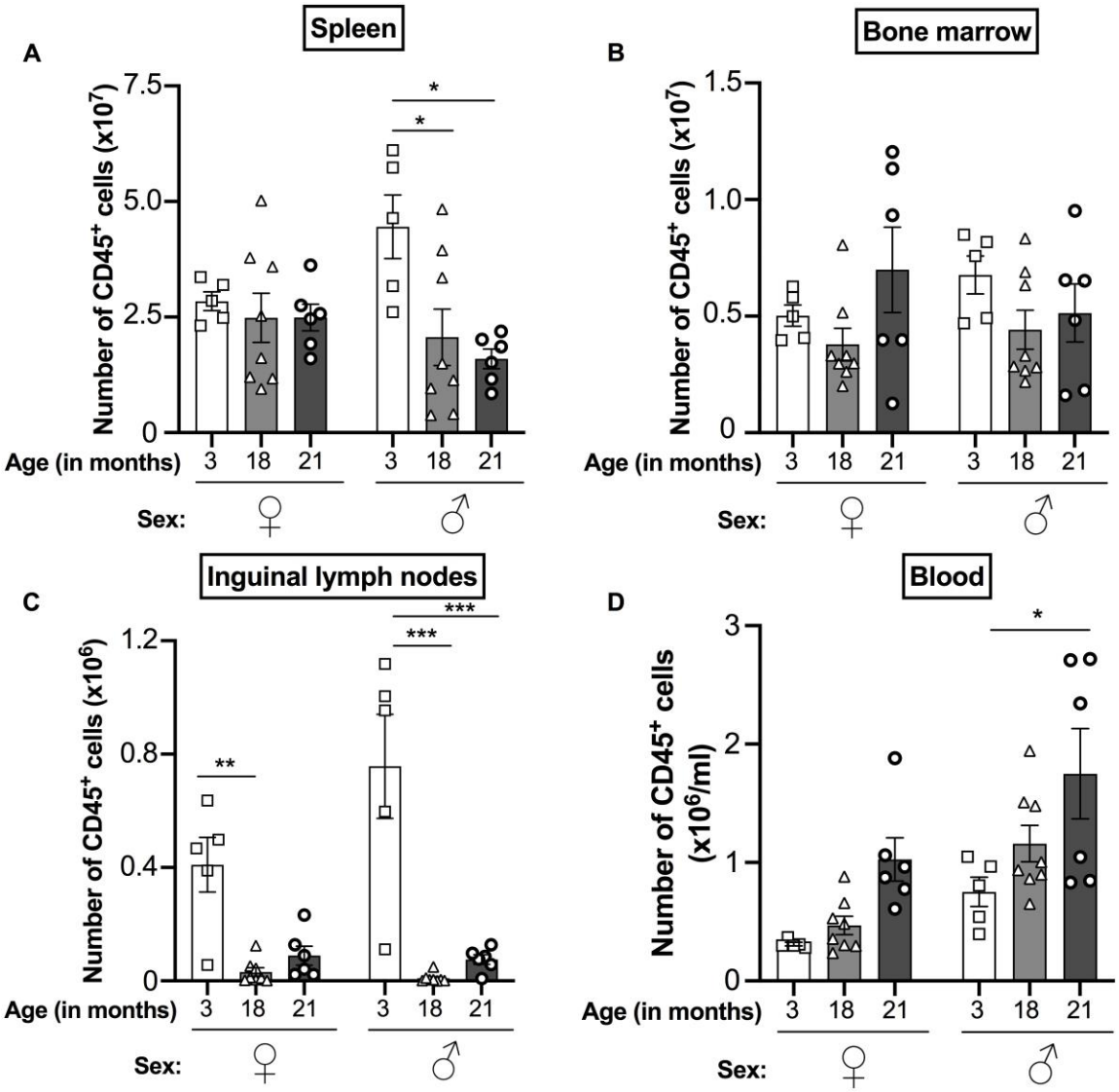

Figure 3-6 Ageing affected leukocyte numbers in various murine tissues

The **(A)** spleen, **(B)** bone marrow (BM), **(C)** inguinal lymph nodes (iLN) and **(D)** blood of naïve 3 month, 18 month and 21 month female (♀) and male (♂) C57Bl6 mice were collected, processed and analysed using flow cytometry to quantify the number of $CD45^+$ leukocytes. Two-way ANOVA showed a significant effect of age on the number of $CD45^+$ leukocytes in the blood, spleen and iLN ($p<0.05$), and of sex on $CD45^+$ leukocyte numbers in the blood ($p<0.001$). Data are presented as mean±SEM for n=9 independent experiments using n=5 for 3 month mice, n=8 for 18 month mice and n=6 for 21 month mice. ***$p<0.001$, **$p<0.01$, *$p<0.05$ by Bonferroni multiple comparison post-test.

Table 3-2 Innate and adaptive leukocyte population numbers in the blood and spleen of young and aged wildtype mice

		Leukocyte subset	F 3mo (mean±SEM)	F 18mo (mean±SEM)	F 21mo (mean±SEM)	p-value (F 3mo v 18mo)	p-value (F 18mo v 21mo)	p-value (F 3mo v 21mo)	M 3mo (mean±SEM)	M 18mo (mean±SEM)	M 21mo (mean±SEM)	p-value (M 3mo v 18mo)	p-value (M 18mo v 21mo)	p-value (M 3mo v 21mo)	p-value (3mo F v M)	p-value (18mo F v M)	p-value (21mo F v M)
Blood (no. cells/ml)	Innate	DC	26,677 ±5,224	31,875 ±5,007	113,608 ±26,658	>0.999	**0.003**	**0.005**	80,905 ±5,303	87,178 ±13,628	345,078 ±97,463	>0.999	**0.009**	**0.017**	>0.999	0.829	**0.001**
		Eosinophils	4,667 ±1,235	7,274 ±2,020	21,778 ±7,148	>0.999	0.066	0.050	13,895 ±3,551	19,013 ±5,207	81,357 ±23,705	>0.999	**0.011**	**0.015**	0.919	0.737	**0.008**
		Monocytes	13,516 ±3,712	22,296 ±3,929	114,893 ±22,822	>0.999	**0.002**	**0.003**	30,129 ±7,284	63,896 ±14,605	168,534 ±49,175	>0.999	0.052	**0.019**	>0.999	0.453	0.331
		Neutrophils	12,682 ±4,303	12,633 ±2,524	95,994 ±22,291	>0.999	**0.004**	**0.001**	24,507 ±10,814	39,522 ±8,281	532,786 ±38,345	>0.999	**<0.001**	**<0.001**	>0.999	0.734	**0.001**
	Adaptive	B-cells	60,674 ±17,999	65,529 ±13,455	544,802 ±137,801	>0.999	**0.008**	**0.002**	217,120 ±47,792	186,133 ±49,879	868,317 ±154,168	>0.999	**0.002**	**0.001**	0.778	0.813	**0.042**
		ABCs	6,664 ±1,855	5,176 ±1,097	57,110 ±12,891	>0.999	**0.002**	**0.008**	13,465 ±3,146	5,365 ±1,084	19,369 ±3,009	0.078	**0.001**	0.334	>0.999	>0.999	**<0.001**
		T-cells	64,915 ±17,102	55,048 ±6,602	143,365 ±24,127	>0.999	**0.003**	**0.016**	485,870 ±158,474	139,324 ±13,016	343,476 ±52,109	**0.018**	0.201	0.719	**0.001**	0.703	0.054
		Senescent T-cells	1,523 ±477	3,174 ±743	13,837 ±3,405	>0.999	**0.003**	**0.002**	8,455 ±2,293	7112 ±3,224	23,416 ±4,969	>0.999	**0.017**	0.056	0.465	0.909	0.104
Spleen (total no.)	Innate	DC	1,417,287 ±67,911	1,700,867 ±409,244	3,750,665 ±797,065	>0.999	**0.035**	**0.032**	951,194 ±332,608	1,646,629 ±344,362	1,711,769 ±155,124	0.403	>0.999	0.372	>0.999	>0.999	**0.008**
		Eosinophils	146,267 ±18,783	225,079 ±43,197	267,246 ±54,778	0.708	>0.999	0.282	111,268 ±42,057	137,807 ±46,420	87,671 ±8,414	>0.999	>0.999	>0.999	>0.999	0.329	**0.019**
		Macrophages	1,587,859 ±213,374	2,778,134 ±913,602	6,349,032 ±1,398,734	>0.999	0.062	**0.023**	1,551,970 ±922,143	1,565,264 ±489,383	1,757,760 ±340,848	>0.999	>0.999	>0.999	>0.999	0.766	**0.002**
		Neutrophils	286,217 ±66,137	816,679 ±319,199	1,003,620 ±294,744	0.652	>0.999	0.365	136,554 ±71,939	418,391 ±173,191	311,758 ±44,889	0.417	>0.999	>0.999	>0.999	0.544	0.124
	Adaptive	B-cells	8,507,685 ±1,966,429	8,228,260 ±1,339,769	15,367,843 ±2,109,164	>0.999	**0.026**	0.062	6,955,385 ±2,683,521	4,807,313 ±980,842	9,144,053 ±1,027,218	>0.999	0.150	>0.999	>0.999	0.318	**0.040**
		ABCs	207,910 ±43,480	619030 ±90,936	1,666,052 ±396,720	0.675	**0.011**	**0.002**	88,612 ±26,175	216,543 ±74,858	408,658 ±66,993	0.616	0.158	0.020	>0.999	0.195	**<0.001**
		T-cells	9,319,097 ±362,952	5,838,168 ±1,148,865	6,129,464 ±1,123,682	0.109	>0.999	0.199	10,809,573 ±1,818,844	3,578,705 ±670,828	6,150,467 ±280,582	**<0.001**	0.233	**0.018**	>0.999	**0.276**	>0.999
		Senescent T-cells	105,218 ±45,860	173,147 ±38,964	450,251 ±52,647	0.942	**0.001**	**0.004**	126,813 ±46,860	219,165 ±77,914	219,210 ±53,246	>0.999	>0.999	>0.999	>0.999	>0.999	**0.029**

Innate and adaptive leukocyte numbers in the blood and spleen of 3 (3mo), 18 (18mo) and 21 (21mo) month male (M) and female (F) wildtype mice. Data are shown as mean ± standard error of the mean (SEM) for leukocyte populations. Statistical analysis performed using two-way ANOVA to determine the effects of sex and age on the number of leukocytes in each tissue. DC, dendritic cells; ABCs, age-associated B-cells.

Table 3-3 Innate and adaptive leukocyte population numbers in the bone marrow and inguinal lymph nodes of young and aged wildtype mice

		Leukocyte subset	F 3mo (mean±SEM)	F 18mo (mean±SEM)	F 21mo (mean±SEM)	p-value (F 3mo v 18mo)	p-value (F 18mo v 21mo)	p-value (F 3mo v 21mo)	M 3mo (mean±SEM)	M 18mo (mean±SEM)	M 21mo (mean±SEM)	p-value (M 3mo v 18mo)	p-value (M 18mo v 21mo)	p-value (M 3mo v 21mo)	p-value (3mo F v M)	p-value (18mo F v M)	p-value (21mo F v M)
BM (total no.)	Innate	DC	192,098 ±20,380	277,230 ±21,118	307,953 ±66,770	0.490	>0.999	0.239	91,199 ±19,802	299,560 ±53,328	324,846 ±63,245	**0.045**	>0.999	**0.033**	0.570	>0.999	>0.999
		Eosinophils	275,460 ±25,805	534,146 ±68,610	303,959 ±77,903	**0.049**	0.069	>0.999	135,649 ±27,499	453,154 ±51,363	252,245 ±72,613	**0.004**	0.055	0.579	0.499	0.922	>0.999
		Macrophages	2,214,544 ±345,576	1,790,010 ±493,938	1,667,558 ±415,802	>0.999	>0.999	>0.999	921,604 ±258,709	2,502,318 ±570,090	2,681,608 ±678,255	0.218	>0.999	0.184	0.382	0.851	0.564
		Neutrophils	2,416,272 ±198,146	4,537,459 ±577,023	3,422,972 ±968,080	0.139	0.746	>0.999	467,185 ±148,652	5,896,720 ±1,584,220	1,874,224 ±422,997	**0.019**	0.077	>0.999	0.659	0.833	0.852
	Adaptive	B-cells	747,109 ±74,481	146,796 ±46,605	733,776 ±273,914	0.050	**0.042**	>0.999	2,822,387 ±936,581	646,378 ±151,409	504,602 ±203,399	**0.011**	>0.999	**0.011**	**0.001**	0.728	>0.999
		ABCs	10,272 ±4,003	19,017 ±3,430	51,464 ±19,474	>0.999	0.138	0.079	38,030 ±13,901	42,208 ±8,502	34,676 ±8,259	>0.999	>0.999	>0.999	0.319	0.266	**0.837**
		T-cells	244,596 ±49,807	311,525 ±26,408	286,555 ±59,486	0.909	>0.999	>0.999	70,467 ±15,994	289,533 ±19,148	205,535 ±35,457	**<0.001**	0.075	**0.008**	**0.013**	>0.999	0.384
		Senescent T-cells	5,968 ±696	7,849 ±1,527	46,983 ±16,277	>0.999	**0.016**	**0.025**	6,104 ±1,879	26,599 ±2,502	23,133 ±4,493	**0.007**	>0.999	**0.012**	>0.999	0.288	0.083
LN (total no.)	Innate	DC	12,766 ±3,840	780.7 ±228	5,885 ±1,085	**0.001**	0.165	0.072	28,724 ±2,587	670.2 ±370	5,968 ±1,371	**<0.001**	**0.039**	**<0.001**	**<0.001**	>0.999	>0.999
		Eosinophils	158.8 ±49	27.83 ±8	157 ±31	**0.018**	**0.013**	>0.999	258.5 ±99	14.69 ±7	47.5 ±11	**0.005**	>0.999	**0.021**	0.320	>0.999	0.163
		Macrophages	2,463 ±898	581.3 ±121	1,448 ±263	**0.024**	0.482	0.433	2,274 ±448	408.1 ±173	700.8 ±181	**0.003**	>0.999	**0.003**	>0.999	>0.999	0.476
		Neutrophils	143.9 ±33	126.8 ±31	172.3 ±42	>0.999	>0.999	>0.999	134.3 ±31	107.6 ±43	237.5 ±88	>0.999	0.366	0.829	>0.999	>0.999	>0.999
	Adaptive	B-cells	48,769 ±11,123	1,840 ±389	10,858 ±3,523	**<0.001**	0.688	**0.007**	177,639 ±28,761	2,323 ±1,417	18,196 ±5,240	**<0.001**	>0.999	**<0.001**	**<0.001**	>0.999	>0.999
		ABCs	185.2 ±60	282.3 ±71	290.3 ±41	0.914	>0.999	0.887	283.8 ±60	234.9 ±68	112.7 ±22	0.833	0.305	0.169	0.961	>0.999	0.165
		T-cells	214,885 ±63,344	11,826 ±8,678	23,022 ±3,667	**0.001**	>0.999	**0.002**	748,367 ±88,330	4,437 ±2,061	39,025 ±8,392	**<0.001**	>0.999	**<0.001**	**<0.001**	>0.999	>0.999
		Senescent T-cells	1,065 ±322	175.5 ±50	728.5 ±126	**0.005**	0.072	0.586	2,030 ±323	67.48 ±11	869.6 ±223	**<0.001**	**0.019**	**0.003**	**0.005**	>0.999	>0.999

Innate and adaptive leukocyte numbers in the bone marrow (BM) and inguinal lymph nodes (LN) of 3 (3mo), 18 (18mo) and 21 (21mo) month male (M) and female (F) wildtype mice. Data are shown as mean ± standard error of the mean (SEM) for leukocyte populations. Statistical analysis performed using two-way ANOVA to determine the effects of sex and age on the number of leukocytes in each tissue. DC, dendritic cells; ABCs, age-associated B-cells.

3.2.2 AGEING IS ASSOCIATED WITH AN ALTERED PERITONEAL SECRETOME

To understand why there was an increased number of leukocytes in the peritoneal cavity of aged mice, we assessed the relative abundance of chemokines/chemoattractants, leukocyte survival/growth factors, and soluble adhesion molecules in the PLF of young and aged mice using a cytokine array. We observed a ≥3-fold increase in the levels of CCL-2, 3, 5, 6, 11, 17, 21, CX3CL1, CXCL-1, 2, 13, 16 and chemerin in the peritoneal cavity of aged male and female mice compared to young, although this age-associated change was more pronounced in the female mice **(Figure 3-7)**. For some chemokines, the age-associated increase in their expression occurred in a sex-specific manner. For example, a ≥3-fold increase in the expression of CCL12, CCL19, CXCL10, CXCL11 and LIX was only observed in the PLF of aged female mice compared to young animals, but not in the PLF of aged male mice **(Figure 3-7)**. On the other hand, there was a ≥3-fold increase in the levels of CCL20 in the PLF of aged male mice compared to young males that was not evident in the PLF of aged female mice. Interestingly, CCL22 levels were increased >40-fold in the PLF of aged female mice compared to young females, but these levels were reduced >4-fold in the PLF of aged male mice compared to their younger counterparts. We validated some of these age-related observations by quantifying the levels of CCL21 and CXCL13, B-cell chemoattractants, in the PLF of 3-month, 18-month and 21-month male and female mice using an ELISA (**Figure 3-8**). We observed a significant increase in the concentration of CCL21 in the PLF of 21-month female, but not male, mice compared to 18-month and 3-month counterparts (**Figure 3-8A**). The concentration of CXCL13 was increased in the PLF of 21-month male and female mice

compared to 3-month mice (**Figure 3-8B**). Despite these sex-specific differences, the data suggest that ageing is associated with a dramatic increase in the chemokine/chemoattractant levels within the peritoneal cavity, which may support increased leukocyte recruitment in the steady state.

We also observed a ≥3-fold increase in the levels of BAFF (a B-cell survival factor) and FLT-3 (a hematopoietic cell growth/survival factor) in the PLF of aged male and female mice compared to young animals; although the age-associated change in expression was more pronounced for the female mice **(Figure 3-9A)**. Interestingly, we observed a >40-fold increase in the levels of M-CSF (a monocyte/macrophage differentiation/survival factor) in the PLF of aged female mice compared to young females, but observed a >7-fold reduction in M-CSF levels in the PLF of aged male mice compared to young males **(Figure 3-9A)**. There was a ≥3-fold increase in the abundance of soluble adhesion molecules P-selectin, ICAM-1, and VCAM-1 in the PLF of 21-month male and female mice compared to young mice, although the increase was more striking for the females **(Figure 3-9B)**. Interestingly, levels of soluble E-selectin were increased >40-fold in the PLF of aged female mice compared to young females, but were decreased by >8-fold in the PLF of aged male mice **(Figure 3-9B)**. Collectively these data indicate that ageing is associated with increased levels of immune cell growth and survival factors, as well as soluble adhesion molecules, within the peritoneal cavity under homeostatic conditions.

To understand whether the age-associated increase in peritoneal leukocyte numbers corroborated a pro-inflammatory environment, we assessed the relative abundance of pro- and anti-inflammatory mediators in the PLF of 21-month male and female mice compared to 3 month mice using a cytokine array **(Figure 3-10)**. We

observed a ≥3-fold increase in the pro-inflammatory cytokines IFNγ, IL-5, IL-12, IL-15, and IL-33 in the peritoneal cavity of aged male and female mice compared to young mice. Aged female PLF also presented with a ≥3-fold increase in the levels of pro-inflammatory cytokines IL-1α, IL-1β, IL-23, TNFα and the pleiotropic cytokines IL-4, IL-11, IL-13, IL-22, IL-27 compared to young females, although these levels were either reduced or unchanged in aged male PLF **(Figure 3-10)**. Interestingly, pleiotropic cytokines IL-6 and IL-7 were increased in the PLF of male and female mice compared to young mice **(Figure 3-10)**. We also observed an increase in the anti-inflammatory cytokines IL-1RA (>16-fold), IL-10 (>5-fold) and IL-28 (>15-fold) in the PLF of aged female mice compared to young females, although these levels were either reduced or unchanged in aged male PLF **(Figure 3-10)**. Collectively these data suggest that ageing alters the inflammatory environment within the peritoneal cavity in a sex-specific manner and, overall, skews it towards a more pro-inflammatory phenotype.

To determine if changes to the peritoneal membrane vasculature contributed to increased leukocyte recruitment to the peritoneal cavity, we assessed the relative abundance of pro-and anti-angiogenic factors in the PLF of 21 month male and female mice compared to young mice using a cytokine array. We observed a ≥3-fold increase in the levels of pro-angiogenic factors angiopoietin-2, angiopoietin-like 3, endoglin, PD-ECGF, and VEGF in the PLF of aged male and female mice compared to young mice **(Figure 3-11)**. We also observed an increase in the pro-angiogenic factors angiopoietin-1 (>3-fold) and Gas 6 (>40-fold) in the PLF of aged female mice compared to young females, but these levels were unchanged in the PLF of aged male mice **(Figure 3-11)**. Interestingly, we also observed a striking increase in the level of anti-angiogenic factor endostatin (>40-fold) in the PLF of aged male and female mice

compared to young mice. Collectively, these data suggested that ageing may influence the angiogenic processes within the peritoneal vasculature, which may affect vascular structure/integrity.

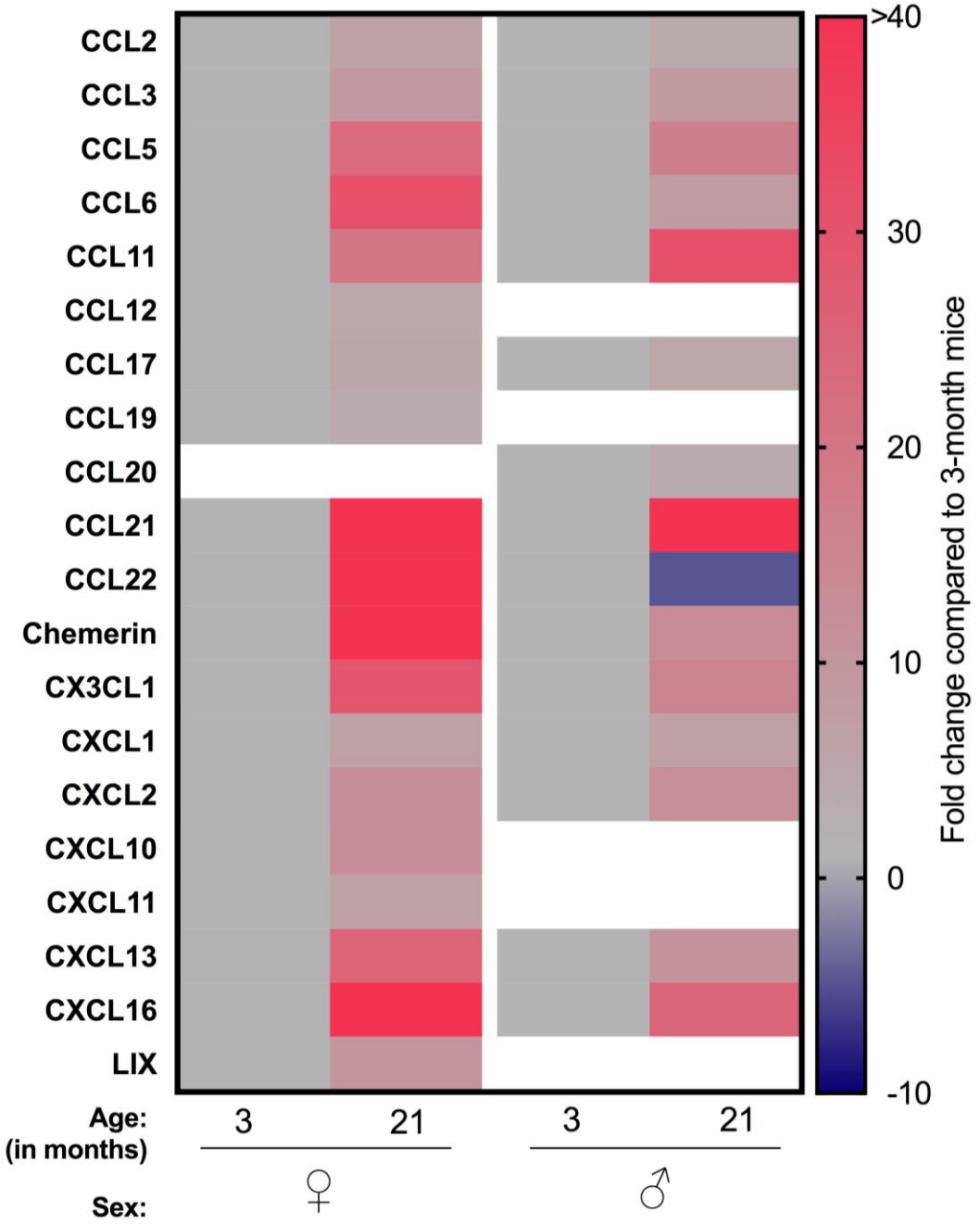

Figure 3-7 Ageing is associated with increased levels of chemokines and chemoattractants in the peritoneal cavity

Exudate from the peritoneal cavity of naïve 3 month and 21 month female (♀) and male (♂) C57Bl6 mice was collected and analysed using a cytokine array. The chemokines and chemoattractants that exhibited a ≥3-fold change within the peritoneal cavity of aged mice relative to young mice within a sex group are shown. Data was obtained from the mixing of exudate derived from three mice per group, n=1.

Figure 3-8 Ageing is associated with increased levels of B-cell chemoattractants, CCL21 and CXCL13, in the peritoneal cavity

Exudate from the peritoneal cavity of naïve 3 month, 18 month, and 21 month female (♀) and male (♂) C57Bl6 mice was collected and analysed using an ELISA to quantify levels of **(A)** CCL21 and **(B)** CXCL13. ANOVA showed a significant effect of age ($p<0.001$) and sex ($p<0.001$) on the concentration of CCL21 in the peritoneal fluid, and of age ($p<0.001$), but not sex, on the concentration of CXCL13. Data are presented as mean ± SEM using n=4-5 per age group, from n = 1 independent experiment. *$p<0.05$, **$p<0.01$, and ***$p<0.001$ by Bonferroni multiple comparison post-test.

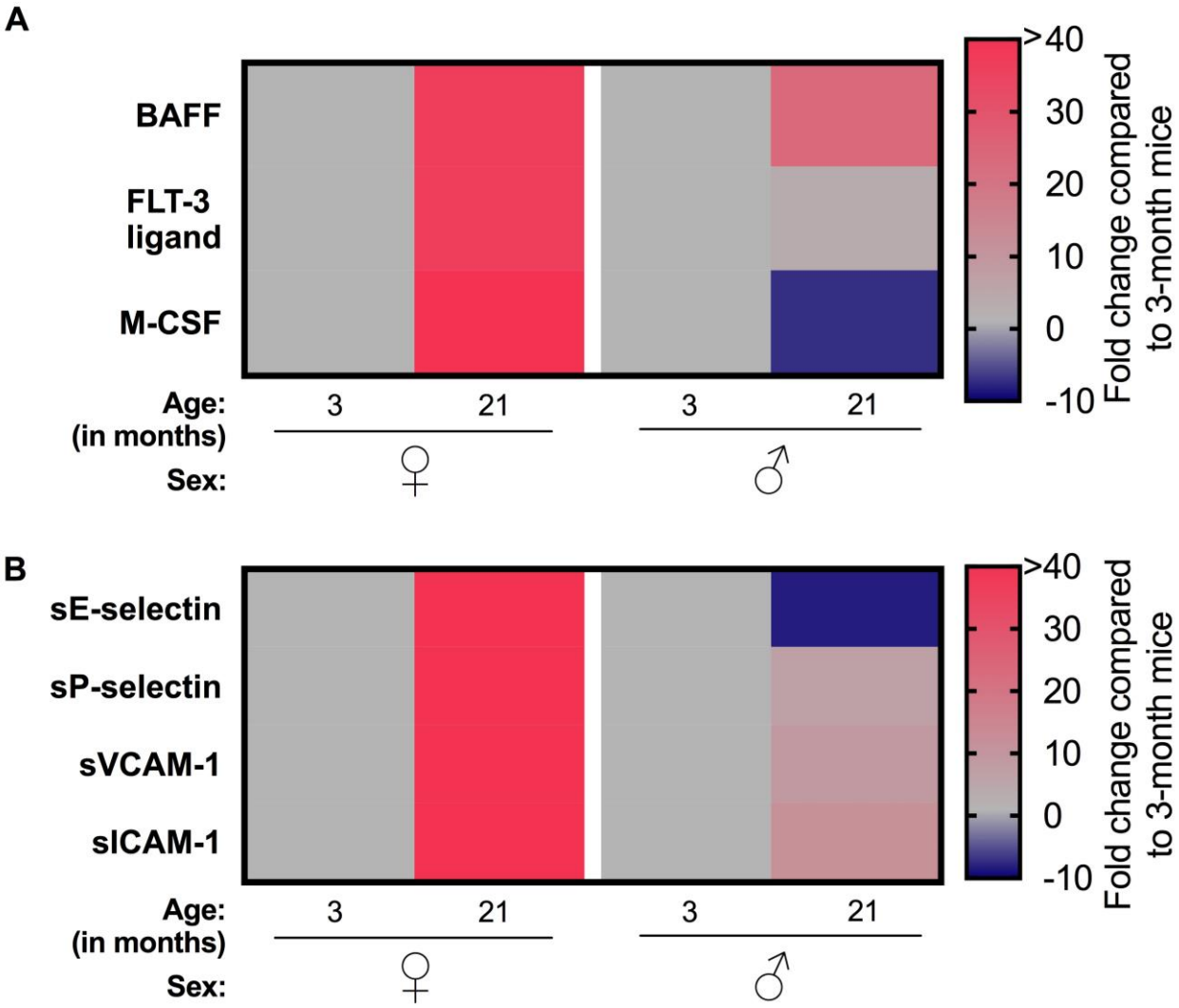

Figure 3-9 Ageing is associated with increased levels of leukocyte growth/survival factors and soluble adhesion molecules in the peritoneal cavity
Exudate from the peritoneal cavity of naïve 3 month and 21 month female (♀) and male (♂) C57Bl6 mice was collected and analysed using a cytokine array. The **(A)** leukocyte growth and survival factors and **(B)** soluble adhesion molecules that exhibited a ≥3-fold change within the peritoneal cavity of aged mice relative to young mice within a sex group are shown. Data was obtained from the mixing of exudate derived from three mice per group, n=1.

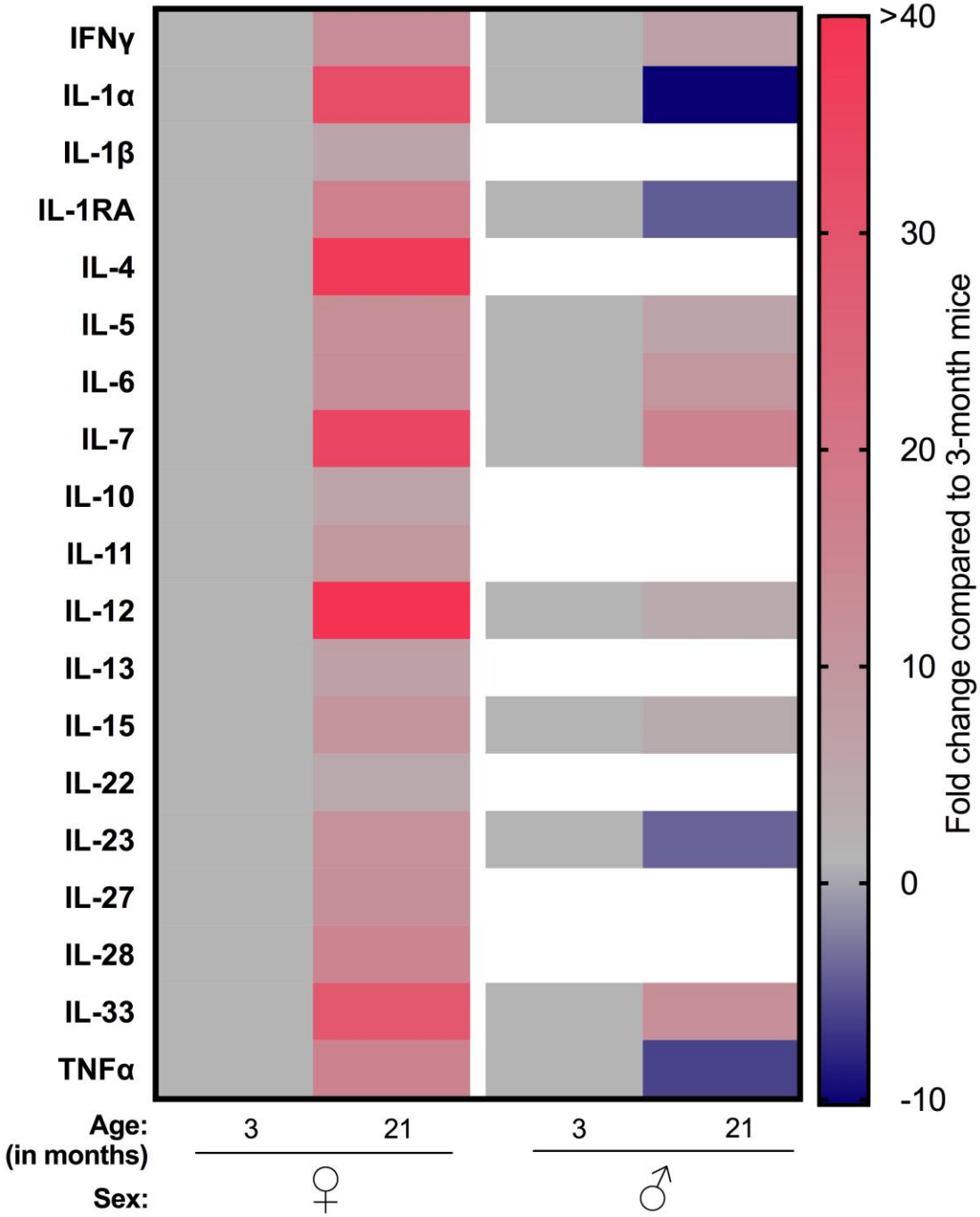

Figure 3-10 Ageing is associated with increased levels of pro-inflammatory mediators in the peritoneal cavity

Exudate from the peritoneal cavity of naïve 3 month and 21 month female (♀) and male (♂) C57Bl6 mice was collected and analysed using a cytokine array. The pro- and anti-inflammatory cytokines that exhibited a ≥3-fold change within the peritoneal cavity of aged mice relative to young mice within a sex group are shown. Data was obtained from the mixing of exudate derived from three mice per group, n=1.

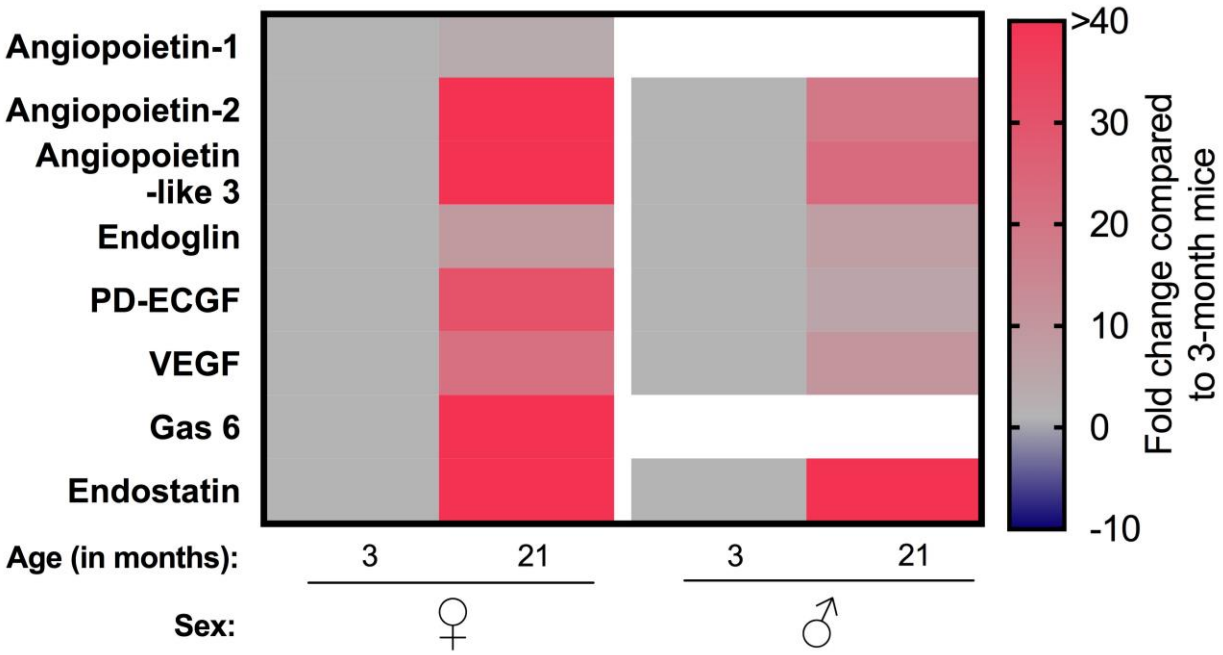

Figure 3-11 Ageing is associated with increased angiogenic factors in the peritoneal cavity

Exudate from the peritoneal cavity of naïve 3 month and 21 month female (♀) and male (♂) C57Bl6 mice was collected and analysed using a cytokine array. The pro- and anti-angiogenic factors that exhibited a ≥3-fold change within the peritoneal cavity of aged mice relative to young mice within a sex group are shown. Data was obtained from the mixing of exudate derived from three mice per group, n=1.

3.2.3 INCREASED PERMEABILITY AND MODULATED STRUCTURE OF THE PERITONEAL MEMBRANE VASCULATURE IN OLDER MICE

As the integrity of blood vessels is reportedly reduced in aged hosts (Chang, Flavahan and Flavahan, 2017; Belmin *et al.*, 1993) and as we observed an age-associated increase in angiogenic mediators within the peritoneal cavity, it was hypothesised that ageing would alter the structure of and increase the permeability of the peritoneal membrane vasculature. To assess this, we administered fluorescent dextran into the bloodstream of young and aged female mice and imaged the peritoneal membrane vasculature using IVM. Following IVM, the PLF was collected to measure the concentration of fluorescent dextran that had leaked from the circulation into the peritoneal cavity.

The young peritoneal membrane vasculature appeared organised with minimal extravascular fluorescence **(Figure 3-12A)**, indicating low levels of dextran leakage from the vasculature into tissue. On the other hand, the aged peritoneal membrane vasculature appeared much more disorganised with more looping structures and increased extravascular fluorescence indicating increased permeability of the vessels **(Figure 3-12B)**. Indeed, quantification of the mean number of grey pixels in the extravascular space of the IVM images confirmed significantly increased levels of extravascular fluorescence in the peritoneal membrane tissue of aged mice compared to young **(Figure 3-13A)**. Quantification of fluorescent dextran concentrations in the PLF of young and aged mice using a plate reader confirmed significantly increased concentrations of 20kDa and 70kDa fluorescent dextrans in the peritoneum of aged mice post-IVM compared young mice **(Figure 3-13B+C)**.

Together, these data suggest that ageing reduces the integrity of the peritoneal membrane vasculature, which may facilitate increased leukocyte trafficking into the peritoneal cavity.

Analysis of the vasculature network using the Angiogenesis Analyzer plug-in on Fiji ImageJ revealed no significant effect of ageing on the number of vessels or total length of the vessels per mm^2 of peritoneal membrane **(Figure 3-14A+B)**, but identified a significant increase in the number of nodes within the aged vasculature compared to young per mm^2 of peritoneal membrane **(Figure 3-14C)**. Furthermore, there was a significant increase in the number of meshes and total mesh area per mm^2 aged peritoneal membrane compared to young mice **(Figure 3-15A+B)**, and a reduction in the mesh index **(Figure 3-15C)**. An increased number of nodes (points of bifurcation) and mesh (looping) structures in the aged peritoneal membrane, including increased mesh area and a reduced mesh index (indicating increased number of vessels involved in the looping structures), suggests that ageing modulates the vasculature structure.

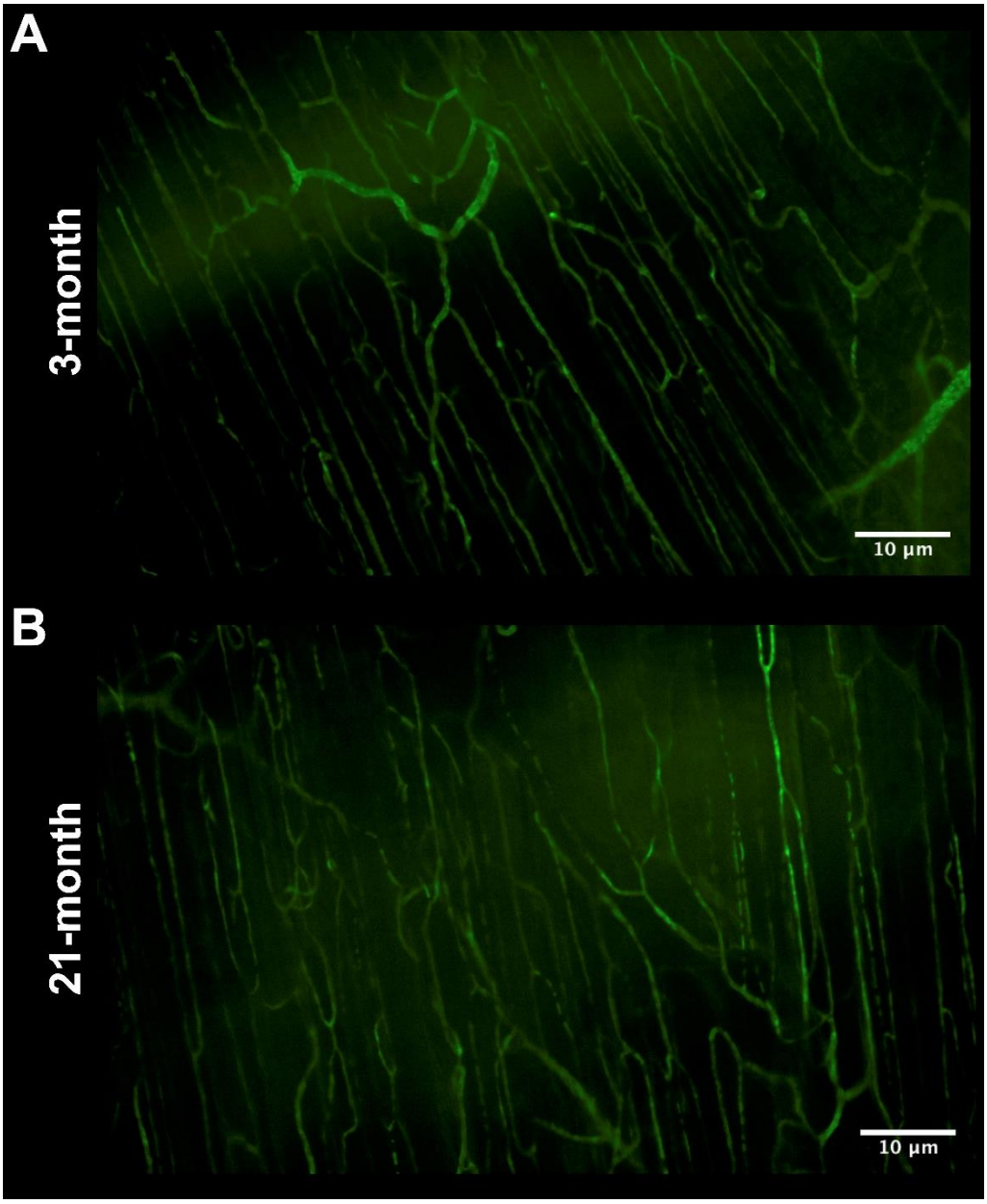

Figure 3-12 Intravital microscopy of the peritoneal membrane vasculature in vivo
Fluorescent dextran (50µl 20 kDa dextran-TRITC and 50µl 70 kDa dextran-FITC) was administered intravenously to young (3 months) and aged (21 months) female mice under terminal anesthesia, the peritoneal membrane was exposed and imaged in real-time at 60 minutes. Representative images of the peritoneal membrane vasculature of **(A)** young and **(B)** aged mice are shown. Scale bar indicates 10µm.

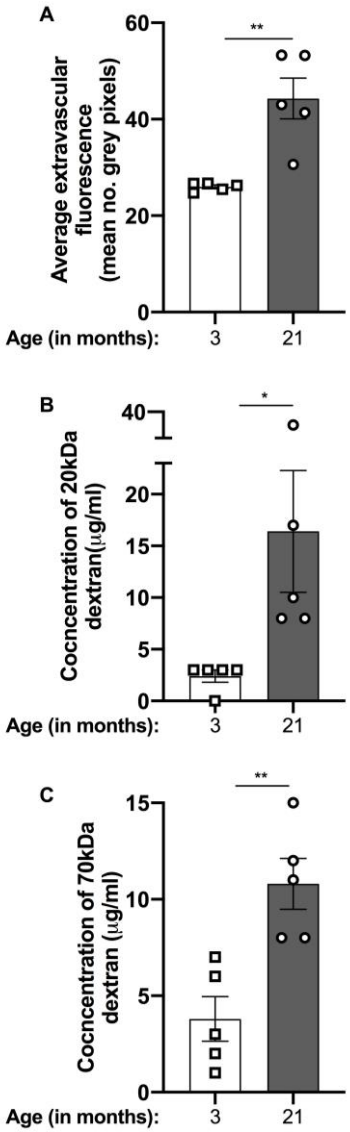

Figure 3-13 Ageing was associated with increased permeability of the peritoneal membrane vasculature

Fluorescent dextran (50µl 20 kDa dextran-TRITC and 50µl 70 kDa dextran-FITC) was administered to young (3 months) and aged (21 months) female mice and the peritoneal membrane vasculature was imaged after 60 minutes. The mean grey pixel values of the extravascular space were obtained using ImageJ to calculate the **(A)** average extravascular fluorescence. Peritoneal lavage fluid was collected from the mice post-imaging and the average concentrations of fluorescent **(B)** 20 kDa and **(C)** 70 kDa dextrans were measured using a plate reader. Data are shown as mean ± SEM for n = 5 independent experiments using 5 different mice per age group. Statistical analysis was performed using an unpaired t-test, *p<0.05, **p<0.01.

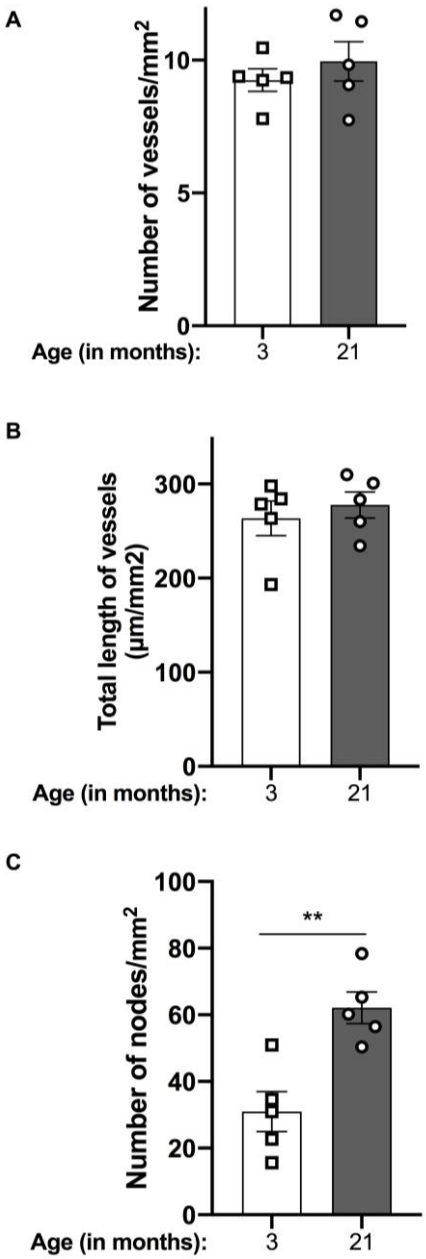

Figure 3-14 Ageing modulates peritoneal vascular structure but not density

Fluorescent dextran (50µl 20 kDa dextran-TRITC and 50µl 70 kDa dextran-FITC) was administered to young (3 months) and aged (21 months) female mice and the peritoneal membrane vasculature was imaged after 60 minutes. Images were processed and analysed using Angiogenesis Analyzer plug-in on ImageJ to provide the **(A)** average number of vessels, **(B)** total length of vessels and the **(C)** number of nodes per mm^2 of membrane. Data are shown as mean±SEM for n = 5 independent experiments using 5 different mice per age group. Statistical analysis was performed using an unpaired t-test, *p<0.05.

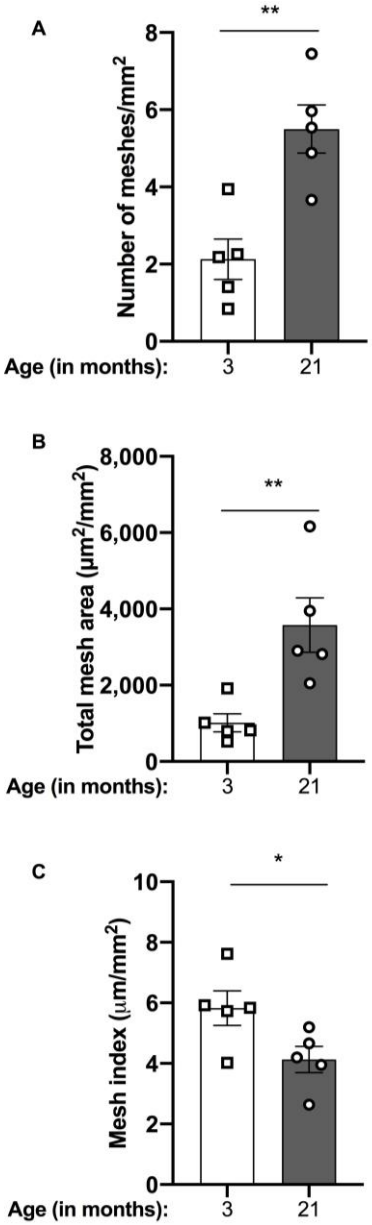

Figure 3-15 Ageing is associated with increased mesh structures within the peritoneal vascular network

Fluorescent dextran (50µl 20 kDa dextran-TRITC and 50µl 70 kDa dextran-FITC) was administered to young (3 months) and aged (21 months) female mice and the peritoneal membrane vasculature was imaged after 60 minutes. Images were processed and analysed using Angiogenesis Analyzer plug-in on ImageJ to provide the **(A)** number of meshes, **(B)** total mesh area and the **(C)** mesh index per mm^2 of membrane. Data are shown as mean ± SEM for n = 5 independent experiments using 5 different mice per age group. Statistical analysis was performed using an unpaired t-test, *p<0.05, **p<0.01.

3.3 DISCUSSION

Homeostatic leukocyte trafficking is key to facilitating immunosurveillance and to maintaining tissue homeostasis (Reglero-Real, Rolas and Nourshargh, 2019). Although growing evidence supports the notion that ageing affects lymphocyte trafficking patterns during inflammation (see Section 1.3.2.4.), few studies have investigated the impact of chronological ageing on homeostatic leukocyte trafficking and even fewer have considered the sexual dimorphism within these age-related changes (see **Table 1-4** and **Table 1-5**). Here, we found ageing was associated with significantly increased numbers of leukocytes in the blood and peritoneum of mice, and significantly decreased numbers of leukocytes in the spleen and inguinal LN. Importantly, these age-related changes occurred in a sex-specific manner. We observed the most prominent age-related changes to leukocyte population numbers within the peritoneal cavity, where 21-month female mice exhibited dramatic increases in peritoneal leukocyte numbers, particularly B-cells, compared to 21-month male mice. Increased peritoneal leukocyte numbers was associated with a pro-inflammatory environment as we observed increased levels of cytokines, chemoattractants/chemokines, leukocyte growth/survival factors and soluble adhesion molecules within the aged cavity, particularly in aged female mice. We observed age-related changes to the peritoneal membrane vasculature of female mice, including increased looping structures within the vasculature network, increased permeability of the vessels, and increased levels of soluble angiogenic factors within the peritoneal cavity, which may have facilitated increased leukocyte trafficking. To the best of our

knowledge, this is the first demonstration of sex-specific age-related changes to leukocyte trafficking patterns to the peritoneal cavity in the steady state.

3.3.1 THE ROLE OF AGEING IN LEUKOCYTE TRAFFICKING TO THE PERITONEAL CAVITY

Studies investigating age-related changes to peritoneal leukocyte populations in the steady state are limited. The data presented in this thesis describe increased numbers of peritoneal leukocytes in aged mice, including increased numbers of neutrophils and B-cells and reduced numbers of macrophages, which agrees with previous reports; where Mogilenko *et al.* demonstrated increased proportions of neutrophils and B-cells, and reduced frequencies of macrophages in the peritoneal cavity of aged (17-24 months) male C57Bl6 mice compared to young (3-6 months) mice using single-cell RNA sequencing (Mogilenko *et al.*, 2021). Linehan *et al.* also described reduced frequencies of peritoneal macrophages in aged (15-20 months) male C57Bl6 mice compared to young (<3 months) mice using flow cytometry (Linehan *et al.*, 2014). Arnardottir *et al.*, however, reported comparable numbers of peritoneal $Ly6G^{+}$ neutrophils and increased numbers of peritoneal $F4/80^{hi}$ macrophages in aged (20 months) male BALBc mice at baseline compared to young (2 months) mice (Arnardottir *et al.*, 2014), which disagrees with the studies using C57Bl/6 mice (including ours). But these differences could be explained by the different strains of mice used in each study. Indeed, there is evidence of differential leukocyte population numbers within the blood (Bernal *et al.*, 2021; Pinchuk and Filipov, 2008), spleen (Pinchuk and Filipov, 2008) and peritoneum (Nossent *et al.*, 2017; Pompeu *et al.*, 1991) of naïve C57Bl6 and

BALBc mice. Therefore, the strain of the mouse used can affect the experimental outcome.

Increased numbers of peritoneal leukocytes in aged mice fits the paradigm of inflammageing, whereby the development of chronic inflammation during the ageing process alters the inflammation status of peripheral tissues (Yue *et al.*, 2021; Lee *et al.*, 2021; Sendama, 2020). Indeed, we observed a significant age-associated reduction in the number of leukocytes residing in the spleen and inguinal LN, and an increase in circulating leukocytes, implying the mobilisation of leukocytes from the lymphoid tissues. This process was also described in a study conducted by Kay *et al.*, whereby increased numbers of circulating $Gr1^{high}$ neutrophils and reduced numbers in the spleen correlated with increased recruitment of neutrophils into the peritoneal cavity during a model of peritonitis (Kay *et al.*, 2015). We observed an age-associated increase in the number of circulating B-cells in naïve mice, which agrees with the work of Pinchuk *et al.* who reported an increased frequency of circulating $CD19^{+}$ B-cells in naïve aged (18 month) C57Bl6 male mice compared to young (1 month) mice using flow cytometric analysis (Pinchuk and Filipov, 2008). Increased circulating B-cell numbers may simply reflect increased trafficking of these cells to the peritoneal cavity in ageing. Collectively, these data suggest an age-related modulation of homeostatic leukocyte trafficking to the peritoneal cavity, however, other factors could explain these changes in leukocyte counts. Ageing may alter peritoneal leukocyte numbers by affecting peritoneal leukocyte proliferation and/or apoptotic rates.

Although there is no literature specific to peritoneal leukocytes, there is an abundance of evidence supporting age-related changes to leukocyte proliferation

(Guidi *et al.*, 1998; Haynes *et al.*, 1999; Yang *et al.*, 2020) and apoptosis (Telford and Miller, 1999; Yang *et al.*, 2020; Fulop *et al.*, 1997; Schindowski *et al.*, 2000) rates across multiple tissues in humans and mice. For example, naïve $CD4^+$ T-cells isolated from the spleens of older (18-20 months) C57Bl6 mice exhibited increased rates of apoptosis in response to antigen stimulation *ex vivo* compared to those isolated from young (2-3 months) mice (Mattoo *et al.*, 2009). Determining proliferation and apoptosis rates in ageing peritoneal leukocytes, by means of assessing the percentage of leukocytes positive for proliferation (e.g. Ki67) and apoptosis (e.g. annexin V, caspase 3) markers using flow cytometry, would be necessary to rule out these possibilities. Alternatively, ageing could influence leukocyte retention within tissues. For example, the shuttling of marginal zone B-cells between the follicle and marginal zone within the spleen is reportedly impaired in aged (>18 months) C57Bl6 mice compared to young (2 months), resulting in B-cell retention in the marginal zones (Turner and Mabbott, 2017). It would therefore be of interest to investigate whether increased numbers of peritoneal leukocytes in aged mice is simply due to increased leukocyte retention within the cavity, through cell tracking or adoptive cell transfer studies.

3.3.2 THE ROLE OF SEX IN LEUKOCYTE TRAFFICKING TO THE PERITONEAL CAVITY

To date, studies investigating age-related changes to peritoneal leukocyte populations have only utilised male mice (Linehan *et al.*, 2014; Arnardottir *et al.*, 2014; Mogilenko *et al.*, 2021). As we know that biological sex influences the immune system (Marquez *et al.*, 2020; Klein and Flanagan, 2016), we hypothesised that any age-related changes to leukocyte population numbers within murine tissues would occur in a sex-specific

manner. We did indeed observe this sexual dimorphism in leukocyte population numbers within the aged peritoneal cavity, and intriguingly, found that the most dramatic age-related changes took place in female mice.

Published datasets regarding the sex-specific differences in peritoneal leukocyte populations of non-inflamed mice have primarily utilised young mice and are usually a by-product of studies focusing on models of inflammation (Scotland *et al.*, 2011; Kay *et al.*, 2015; Bain *et al.*, 2020). The data presented in this thesis demonstrates increased leukocyte numbers, including increased F4/80^{hi} macrophages, in the peritoneal cavity of 3 month female mice compared to 3 month male mice. These data did not reach statistical significance in a two-way ANOVA, likely due to the variation in the data, but are in agreement with previous reports where Kay *et al.* reported increased numbers of peritoneal leukocytes, including F4/80^{hi} macrophages and CD19^{+} B-cells, in young (<3 months) female C57Bl6 mice compared to males (Kay *et al.*, 2015). Scotland *et al.* also reported higher numbers of peritoneal leukocytes in young (<5 months) female C57Bl6 mice compared to young males in the steady state and, importantly, these changes were not due to sex differences in leukocyte apoptosis or proliferation rates but were thought to be due to sex-specific changes in leukocyte trafficking patterns (Scotland *et al.*, 2011). Indeed, ovariectomized female mice had comparable numbers of peritoneal leukocytes to young male mice, suggesting female sex hormones play a direct role in the regulation of leukocyte trafficking to the peritoneal cavity (Scotland *et al.*, 2011). This is interesting as we observed a significant increase in peritoneal leukocyte numbers in the aged female mice compared to young female and aged male mice despite the diminished sex steroid levels that are associated with ageing (reviewed by Horstman *et al.*, 2012).

However, as the ageing process is associated with a multitude of physiological changes (Lopez-Otin *et al.*, 2013) it is likely that reduced sex steroid levels are only one of the factors that affect leukocyte trafficking to the aged peritoneum.

3.3.3 AGE-RELATED MODULATION OF THE PERITONEAL INFLAMMATORY STATUS

Due to the role that inflammageing can play in dysregulated leukocyte trafficking patterns (Hopkin, Lord and Chimen, 2021), we hypothesised that increased numbers of leukocytes within the peritoneal cavity of aged mice would be associated with a pro-inflammatory environment. Indeed, we observed increased levels of multiple pro-inflammatory cytokines, chemoattractants/chemokines, leukocyte growth/survival factors and soluble adhesion molecules within the ageing peritoneal cavity, which suggest that the inflammatory status of the cavity shifts towards a more pro-inflammatory phenotype in ageing. Again, this phenotype was more pronounced for the female mice suggesting sexual dimorphism within the system.

Increased levels of B-cell (e.g. CCL6, CCL21, CXCL13), T-cell (e.g. CX3CL1, CXCL1), DC (e.g. Chemerin, CCL5), and neutrophil (e.g. CXCL1/2) chemoattractants within the ageing peritoneal cavity may have facilitated increased trafficking of these cell types to this tissue in the steady state. Increased levels of CCL22 in the PLF of 21-month female, but not male, mice compared to 3-month counterparts may have promoted the recruitment of monocytes, DC, NK cells and Th2 cells to the peritoneal cavity of these mice. Although CCL22 is inducible upon inflammation, its constitutive expression in tissue can induce immunoregulatory responses such as Treg function and recruitment (Montane *et al.*, 2011; Curiel *et al.*, 2004; Rapp *et al.*, 2019). It is

therefore possible that increased CCL22 expression in the peritoneal cavity of aged female mice is a consequence of the heightened inflammatory status of this tissue, but may also serve as a negative feedback mechanism to promote immunoregulation and tissue homeostasis in the ageing cavity.

The age-associated increase in levels of soluble adhesion molecules (e.g. sP-selectin, sVCAM-1, sICAM-1) within the peritoneal cavity is likely the consequence of increased expression and activity of metalloproteases in the aged tissue. Indeed, metalloproteases are released as part of the SASP, and are able to cleave adhesion molecules off activated EC (Coppe *et al.*, 2010; Conant *et al.*, 2012). Increased expression of soluble adhesion molecules in aged PLF may also reflect increased leukocyte trafficking to the cavity in the steady state. Peritoneal levels of sICAM-1 have been reported to correlate with increased polymorphonuclear cell recruitment to the peritoneal cavity of 27-80 year old adults during episodes of peritonitis (Pruimboom *et al.*, 1995). Whether increased numbers of leukocytes within the peritoneal cavity of aged mice are specifically due to age-related changes to homeostatic leukocyte trafficking patterns needs to be clarified. Another potential mechanism to explain increased leukocyte numbers within the ageing peritoneal cavity could be an age-related increase in the survival and growth of certain leukocyte populations. For example, increased expression of the B-cell survival factor (BAFF) and the haematopoietic cell growth factor (FLT- 3ligand) within the ageing cavity may have promoted the survival of B-cells. Indeed, Amezcua Vesley *et al.* demonstrated that BAFF treatment of peritoneal B1 cells *ex vivo* protected the B-cells from FcγRIIb-mediated apoptosis (Amezcua Vesely *et al.*, 2012). Increased peritoneal BAFF levels

may explain the increased number of B-cells in the peritoneal cavity of aged female mice reported in this thesis.

Ageing resulted in reduced macrophage numbers within the peritoneal cavity of aged male and female mice compared to young, however, M-CSF levels were only reduced in the peritoneal cavity of aged male mice. In fact, we observed a >40-fold increase in M-CSF levels in the peritoneal cavity of aged female mice. As M-CSF promotes macrophage proliferation (Otero *et al.*, 2009), increased M-CSF levels but reduced macrophage numbers in the peritoneal cavity of aged female mice is contradictory. This contradiction could be explained by increased levels of pro-inflammatory mediators, such as TNFα (>15-fold), in the peritoneal cavity of aged female mice compared to aged male mice, which may counteract the proliferation-inducing effects of M-CSF and induce macrophage apoptosis. Indeed, TNFα is able to induce apoptosis of monocyte-derived macrophages *in vitro* when NF-κB signalling is suppressed (Tran *et al.*, 2009). To understand the sexual dimorphic regulation of macrophage populations within the peritoneal cavity of ageing mice further investigation is needed.

The increased expression of IL-6 and IL-12 within the peritoneal cavity of aged male and female mice reported in this thesis is in contrast with previous reports, where Anrnardottir *et al.* demonstrated that the levels of IL-6 and IL-12 within the peritoneal cavity of aged (20 months) male BALBc mice were not significantly different to levels found in young (<2 months) mice, as determined by ELISA (Arnardottir *et al.*, 2014). These differences could be explained by the variation within the published data-set as the baseline peritoneal levels of IL-12 appeared higher in aged mice compared

to young, but did not reach statistical significance in the context of a two-way ANOVA (Arnardottir *et al.*, 2014); or by the different mouse strain and experimental approaches used. Indeed, Chen *et al.* utilised aged (>20 months) male and female C57Bl6 mice and observed increased levels of IL-6 in the muscle, spleen and thymus compared to young (<2 months), as determined by ELISA (Chen *et al.*, 2021b). The results presented in this thesis are therefore in agreement with previous reports that utilised C57Bl6 mice and found that ageing was associated with increased levels of pro-inflammatory mediators across different tissues.

Although ageing was largely associated with increased levels of pro-inflammatory cytokines, chemokines and chemoattractants within the peritoneal cavity, we did observe increased levels of the anti-inflammatory cytokine, IL-10, only in the peritoneal cavity of aged female mice. This does not agree with the work of Linehan *et al.* who reported increased IL-10 production by peritoneal cells derived from aged (>15 months) male C57Bl6 mice *ex vivo* compared to young (<3 months) in the absence of stimulation (Linehan et al., 2014). However, these differences could be explained by the experimental set-up, as Linehan *et al.* removed the peritoneal cells from their physiological environment and placed them into an artificial environment for 24 hours to measure IL-10 production, which may have led to altered cytokine secretion. Indeed, immune responses by leukocytes, such as cytokine secretion, are not isolated events but depend upon, and are the result of, an integration of signals from both the environment and other cells within the tissue (Salvioli *et al.*, 2006). Interestingly, Linehan *et al.* suggest B-cells to be the source of IL-10 production as the depletion of B-cells abolished this age-dependent observation (Linehan *et al.*, 2014). This notion fits with the data presented in this thesis, as we observed a significant increase in the

number of B-cells within the peritoneal cavity of aged female, but not male, mice compared to young, and this was associated with increased peritoneal IL-10 levels.

3.3.4 MODULATED STRUCTURE AND INCREASED PERMEABILITY OF THE AGED PERITONEAL MEMBRANE VASCULATURE

We observed increased levels of several pro-angiogenic factors within the peritoneal cavity of aged mice compared to young, which may induce age-related changes to angiogenic processes in these mice. For example, increased levels of Gas6 in the peritoneal cavity of aged female mice, but not male mice, may have influenced vascular homeostasis. Indeed, Gas6 is a ligand for several protein kinase receptors involved in vascular cell growth and survival, namely Axl, Mer and Tyro3 receptors (Laurance, Lemarie and Blostein, 2012). In retinal microvascular EC, Gas6 plays a crucial role in angiogenic processes by regulating ERK1/2 phosphorylation, thereby stimulating EC proliferation, migration, and tube formation (Kim *et al.*, 2014b). Using IVM, we confirmed that the structure of the peritoneal vasculature in female mice was modified with age, which may reflect age-related changes to angiogenic processes in these mice. However, we report no age-related changes to vascular density.

How ageing affects the vascular density of tissues appears to be tissue-specific. Chen *et al.* reported increased vascular density in the pituitary gland of aged (>13 months) C57Bl6 mice compared to young (<2 months), but reduced vascular density in the testis and pancreas, as determined by quantitative fluorescence microscopy (Chen *et al.*, 2021a). On balance, the high levels of multiple pro-angiogenic factors, such as angiopoietin-2, angiopoietin-like 3 and VEGF, within the peritoneal cavity may have protected the peritoneal membrane from an age-related loss in vessel density.

Indeed, Ahluwalia *et al.* reported impaired angiogenesis of the gastric mucosa of aged (24 months) male Fisher rats in response to ethanol-induced injury compared to young (3 months), and this was partly attributed to an age-related reduction in VEGF expression and an increase in endostatin expression in the aged tissue (Ahluwalia *et al.*, 2013).

As vascular integrity is reportedly reduced with age (Chang, Flavahan and Flavahan, 2017; Belmin *et al.*, 1993; Chen, Zhang and Duan, 2003; Huynh *et al.*, 2011), we hypothesised that increased numbers of leukocytes within the peritoneal cavity of aged mice would be in part due to the increased permeability of the peritoneal membrane vasculature. Indeed, by using an IVM approach, we observed increased permeability of the peritoneal membrane vasculature in aged female mice compared to young. The data presented in this thesis agree with the work of Karaman *et al.*, where intravenous administration of a fluorescent reporter, P20D800, demonstrated increased vascular leakage in the ear skin of aged (18 months) C57Bl6 J-Tyr$^{C\text{-}J}$ albino mice in real-time compared to young (2 months) mice (Karaman *et al.*, 2015). Although the increased permeability of the peritoneal membrane vasculature in aged mice is likely due to several age-related factors, one such possibility is the age-related expansion of the peritoneal mast cell population. Indeed, mast cells secrete a variety of permeability factors such as VEGF and histamine, and their numbers within tissue have been reported to increase with age (Boesiger *et al.*, 1998; Lee *et al.*, 2008; Ashina *et al.*, 2015; Chatterjee and Gashev, 2012; Gunin *et al.*, 2011; Barkaway *et al.*, 2021). Indeed, Barkaway *et al.* reported significantly increased numbers of mast cells in the peritoneal cavity of unchallenged aged (>16 month) C57Bl6 wild-type male mice compared to young (<4 month) mice (Barkaway *et al.*, 2021). It would therefore be of

interest to investigate the relationship between mast cell number and vascular permeability within the naïve peritoneal cavity of old male and female mice.

Increased vascular permeability could promote leukocyte trafficking into the peritoneal cavity through the release of local pro-inflammatory mediators and chemoattractants into the bloodstream. Indeed, Owen-Woods *et al.* reported increased trafficking of neutrophils into the cremaster muscle of young (<3 months) male C57Bl6 mice in response to inflammation-mediated vascular leakage of CXCL1 (Owen-Woods *et al.*, 2020). However, to confirm that increased vascular permeability directly facilitates increased leukocyte trafficking into the aged peritoneal cavity, further experiments such as the fluorescent labelling of circulating leukocytes and imaging their extravasation from the peritoneal membrane vasculature into the cavity in real time are necessary.

3.4 CONCLUSIONS

Homeostatic leukocyte trafficking is an essential part of protective immunity, however, understanding how ageing affects these processes have largely been overlooked. The main aim of this section was to investigate how ageing and biological sex affect leukocyte populations across multiple murine tissues in the steady state to infer age-related and sex-specific changes to homeostatic leukocyte trafficking patterns. A schematic summary of Chapter 3 can be found in **Figure 3-16**. Overall, we found a striking increase in the number of leukocytes in the peritoneal cavity of aged mice, particularly in female mice, and this was associated with a pro-inflammatory environment. We demonstrated increased permeability of the peritoneal membrane vasculature which may aid in increased leukocyte recruitment to the peritoneal cavity

in ageing. To conclude, we have provided evidence that ageing increases leukocyte trafficking to the peritoneal cavity in the steady state, and this occurs in a sexually dimorphic manner.

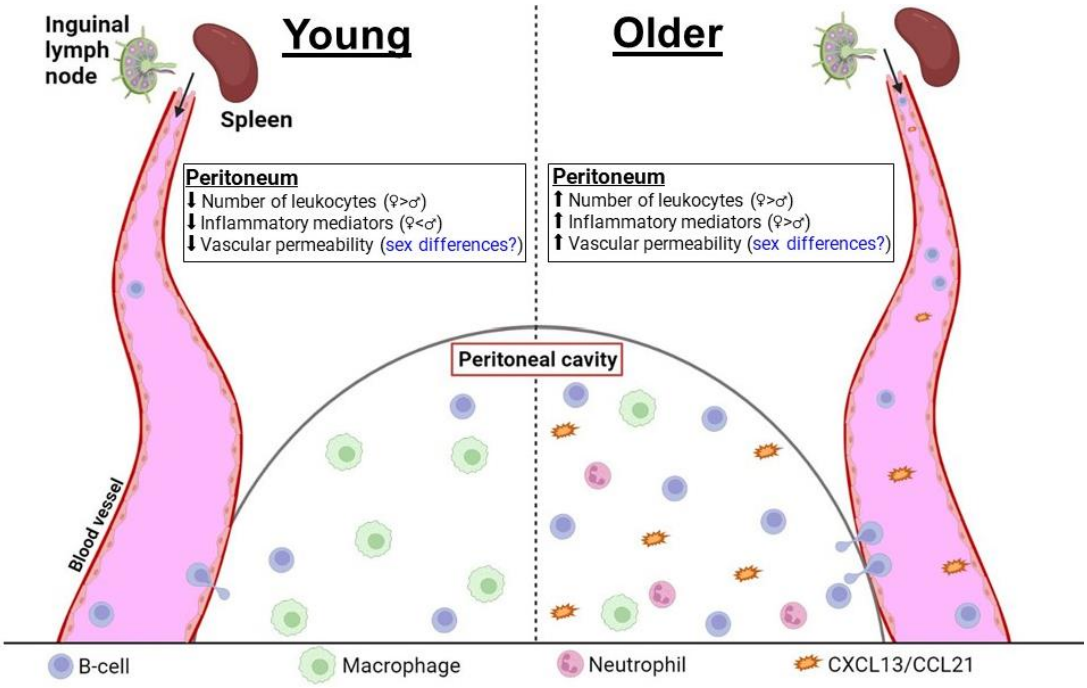

Figure 3-16 Summary of Chapter 3

A schematic depicting the major findings of Chapter 3. We found an age-related increase in the number of leukocytes within the peritoneal cavity of naïve mice, particularly female mice, which were predominantly B-cells. This was accompanied by an increased inflammatory environment within the peritoneal cavity of aged mice, including increased peritoneal levels of chemoattractants, including B-cell chemoattractants CXCL13 and CCL21, growth/survival factors, soluble adhesion molecules, and pro-inflammatory cytokines. Once again, this age-related phenotype was more pronounced in female mice. Intravital microscopy techniques revealed an altered vascular structure and increased vascular permeability within the peritoneal membrane of aged female mice, which may support increased leukocyte extravasation into the cavity with age. Together, these data indicate that ageing affects homeostatic leukocyte trafficking to the peritoneal cavity in a sex-specific fashion. Created with BioRender.com

3.5 LIMITATIONS

Whilst this study provides a first look at the sexual dimorphism in age-related changes to leukocyte populations across multiple murine tissues, this study had its limitations. Firstly, as with most animal studies, this was a cross-sectional study. As of such, only specific ages were investigated. The disproportionate changes in tissue leukocyte counts between 18-month and 21-month mice compared to 3-month mice (e.g. significantly increased numbers of peritoneal leukocytes in 21-month mice compared to 18-month) suggest that a significant change is occurring between these two ages that results in a dramatic change to leukocyte populations across multiple tissue types and warrants further investigation. Secondly, whilst we suggest that the differences in leukocyte population numbers within ageing tissues could reflect age-related changes to homeostatic leukocyte trafficking, there are a number of alternative explanations that we did not investigate. These include age-related changes to leukocyte proliferation/apoptosis rates, leukocyte differentiation fates, and leukocyte retention within tissues. It is also worth noting that, although we investigated several leukocyte populations across multiple murine tissues, we did not consider mast cells or monocytes. It would be interesting to investigate age-related changes to monocyte numbers, particularly in the peritoneum, as monocytes are known to be recruited to the peritoneal cavity during acute inflammation (Newson *et al.*, 2014; Louwe *et al.*, 2021). Currently, we do not know whether inflammageing drives monocyte infiltration of the peritoneal cavity.

The methodology used in this chapter to explore the age-related changes to levels of pro-inflammatory mediators within the peritoneal cavity was largely conducted

using a cytokine array, which only provided relative data for pooled samples. Whilst we had validated the age-related changes to two peritoneal analytes using an ELISA, the lack of quantification of the other analytes meant we could not establish the biological relevance of these age-related changes as determined by cytokine array. Furthermore, the use of pooled samples for the cytokine array prevented us from performing statistical analysis on the data.

We utilised IVM to determine age-related changes to the structure and integrity of the peritoneal membrane vasculature in mice. However, a major limitation was not adjusting the concentration fluorescent dextran based on the weight of the mouse. As aged mice (30.1±1g) were heavier compared to young mice (22.0±1g), a fixed volume of dextran would mean that the aged mice were receiving less fluorescent dextran when taking blood volume into account. Finally, whilst we focus on the sexual dimorphism of age-related changes to the peritoneum in this chapter, we did not assess the structure and integrity of the peritoneal membrane vasculature in male mice due to the limited availability of aged male mice.

CHAPTER 4 – AGE-RELATED CHANGES TO LEUKOCYTE TRAFFICKING DURING ACUTE INFLAMMATION

4.1 INTRODUCTION

Inflammatory leukocyte trafficking processes are evidently modulated by ageing (reviewed by(Hopkin, Lord and Chimen, 2021), yet most studies that have investigated age-related changes to leukocyte trafficking patterns to date have been conducted in mice (see Section 1.3.2.4.). Furthermore, most of the murine studies specifically designed to investigate age-related changes to the inflammatory trafficking of T-cells required lengthy models (>8 days) of acute inflammation (Toapanta and Ross, 2009; Richner *et al.*, 2015; Norian and Allen, 2004). Here, to extrapolate the biological relevance and translatability of mouse models, we sought to investigate the migratory capabilities of PBL derived from young and older donors in the context of acute inflammation using a well-established *in vitro* static adhesion assay (Apta, Chimen and McGettrick, 2017; Rainger and McGettrick, 2017). We also sought to investigate whether ZIP could be used as a shorter model to study inflammatory T-cell trafficking in mice.

4.2 RESULTS

4.2.1 AGEING DOES NOT INFLUENCE THE ABILITY OF PBL TO MIGRATE IN VITRO, BUT SELECTIVELY ENHANCES THE MIGRATION OF SPECIFIC T-CELL SUBSETS

To investigate the effect of age on inflammatory leukocyte trafficking in humans, we isolated PBL from young (20-35 years) and older (60-74 years) adults to use in an *in vitro* transendothelial migration assay. As data previously generated by this lab suggested that an age-related increase in PBL transendothelial migration only

occurred for men and not women (unpublished), we used PBL derived from male donors only in this study. We investigated the ability of PBL to adhere to and migrate across TNFα+IFNγ-stimulated EC and into a collagen matrix over the course of 24 hours using phase-contrast microscopy (Rainger and McGettrick, 2017). We then collected the migrated PBL within the collagen matrix, analysed the migrated PBL using flow cytometry **(Figure 4-1)** and normalised the migrated numbers to the circulating population of the donor (**Appendix I**). Most reports indicate that ageing does not affect the ability of T-cells to migrate *in vitro* (Stohlawetz *et al.*, 1996; Smart, Rao and Cohen, 1993; Callender *et al.*, 2020), however, age-related changes to T-cell expression of integrins (Ritzel *et al.*, 2016; Orme and Roberts, 1998; Ginaldi *et al.*, 2000) and chemokine receptors (Mo *et al.*, 2003; Yung and Mo, 2003; Cane, Ponnappan and Ponnappan, 2012a) have been reported for specific T-cell subsets. It was therefore hypothesised that ageing would enhance the migratory capabilities of specific T-cell subsets *in vitro*.

We observed a significant reduction in PBL total adhesion over time for both donor cohorts, where the total number of adhered PBL was halved by the 24-hour timepoint, with no significant effect of age on PBL adhesion **(Figure 4-2A)**. PBL transmigration across the EC monolayer significantly increased over time and reached >55% for both donor cohorts by the 24 hour timepoint, but was not influenced by the age of the donor **(Figure 4-2B)**. Increased PBL migration was accompanied by increased PBL penetration of the collagen matrix over time for both donor cohorts **(Figure 4-2C)**. Whilst the depth of the collagen matrix did not significantly change with time (data not shown), young PBL reached depths of 62µm and older PBL reached depths of 70µm by the 24 hour timepoint with no significant effect of age on the average

depth of PBL penetration **(Figure 4-2C)**. In contrast, the average migration velocities of young (5.6 µm/min) and older (4.7 µm/min) PBL were not influenced by time nor age but remained constant for the duration of the assay **(Figure 4-2D)**. Together, these data support the notion that chronological ageing does not influence the ability of PBL to adhere to and migrate through cytokine-activated EC *in vitro*.

The total number of PBL adhered to and the percentage of PBL that had migrated across IFNγ+TNFα-stimulated EC were comparable between young and older donors at the 20 minute timepoint **(Figure 4-3A+B)**. In line with this, flow cytometric analysis of the migrated PBL showed that the percentage of migrated T-cells was comparable between young (5.5%) and older donors (8.1%) at the 20-minute time point **(Figure 4-3C)**. However, the percentage of $CD4^+CCR7^+CD45RA^-$ and $CD8^+CCR7^+CD45RA^-$ CM T-cells that had migrated into the collagen matrix was increased for older donors compared to young donors **(Figure 4-3D+E)**. The percentage of migrated $CD4^+KLRG1^+CD57^+$ senescent T-cells was also increased for older donors compared to young donors at the 20 minute time point **(Figure 4-3F)**. The percentage migration of all T-cell subsets assessed for both donor cohorts can be found in **Table 4-1**. These data suggest that ageing does not influence the migration of T-cells overall but enhances the migration of specific T-cell subsets, namely memory and senescent T-cells.

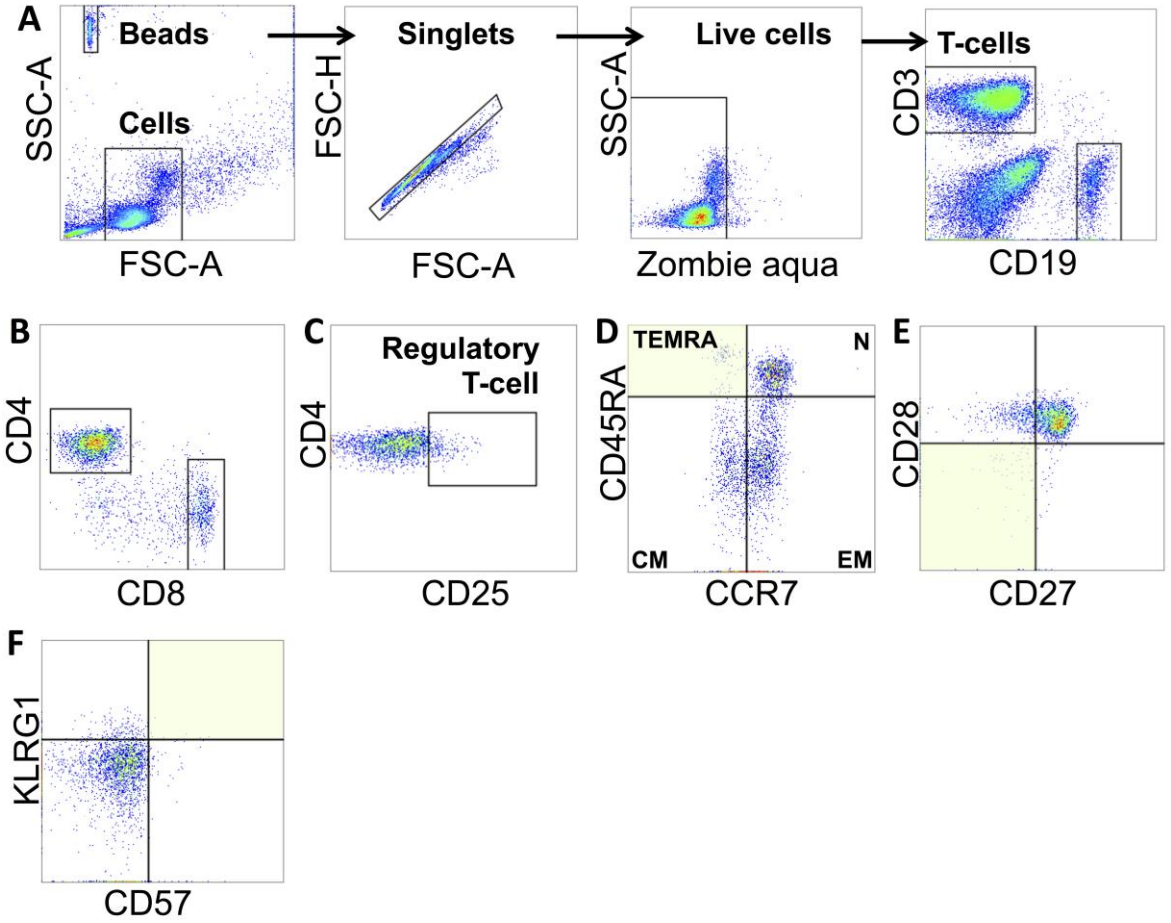

Figure 4-1 Gating strategy to define T-cell subsets within migrated PBL samples

Following the static adhesion assay, the collagen matrix was digested and the PBL that had migrated into the matrix were collected and analysed using flow cytometry. **(A)** The gating strategy used to identify single, live T-cells. T-cells were then distinguished based on **(B)** CD4 and CD8 expression. **(C)** Regulatory T-cells were identified as $CD4^+CD25^+$ cells. **(D)** CD45RA and CCR7 were then used to identify $CD4^+$ and $CD8^+$ naïve (N), effector memory (EM), central memory (CM) and TEMRA T-cells. Senescent T-cells were identified as **(E)** $CD28^-CD27^-$ or **(F)** $KLRG1^+CD57^+$ cells.

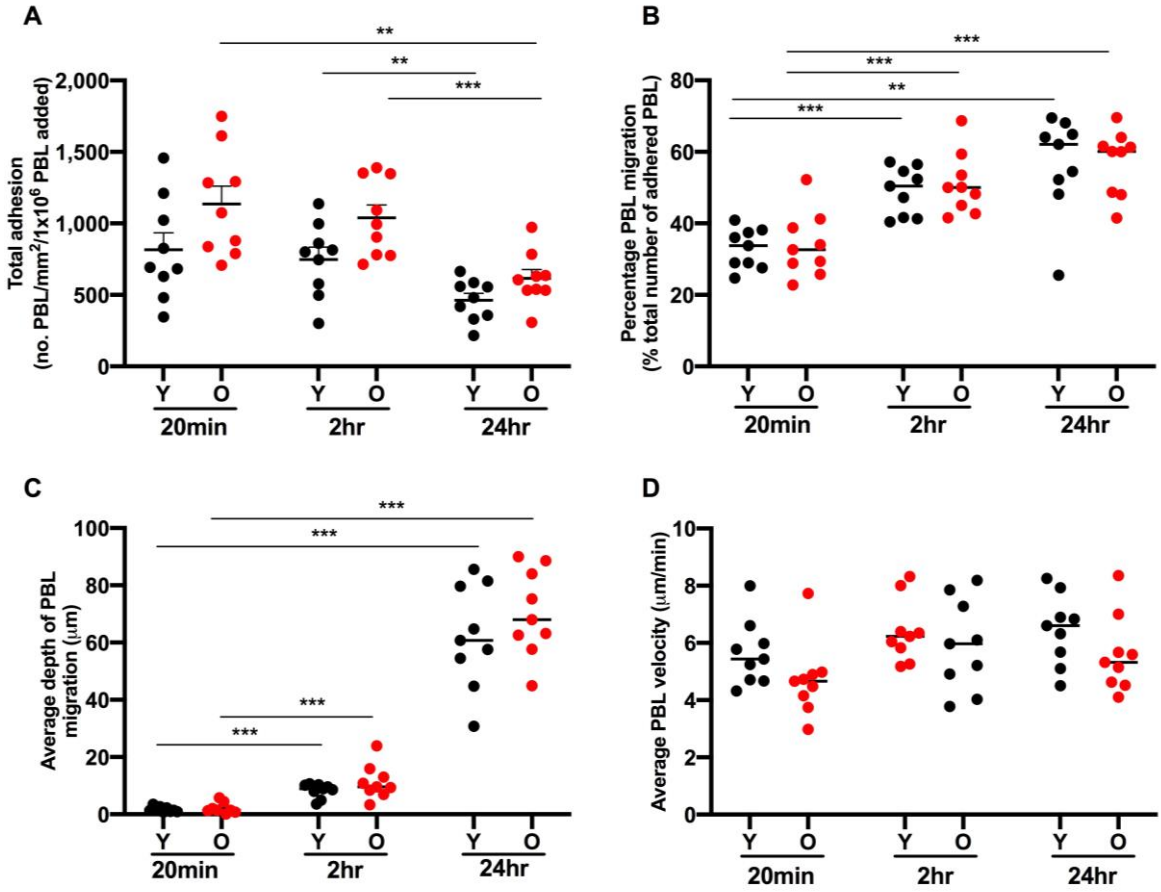

Figure 4-2 Ageing does not affect the migratory capabilities of PBL *in vitro*

PBL ($1x10^6$ cells/ml) were isolated from young (Y, black, n=9) and older (O, red, n=9) donors and added to TNFα (100U/ml) and IFNγ (10ng/ml) stimulated HDBEC for 24 hours at 37°C. At the 20-minute (20min), 2 hour (2hr) and 24 hour (24hr) timepoints digitised images of 5 random fields were captured to assess **(A)** the total number of adhered PBL and **(B)** the percentage of PBL transmigration across HDBEC. Z-stack sequences and 5-minute sequences were also captured at each timepoint to measure the **(C)** average depth of PBL penetration into the collagen matrix and **(D)** average PBL transmigration velocities, respectively. In A-C, two-way ANOVA analysis showed a significant effect of time, but not age, on PBL adhesion ($p<0.001$), percentage migration ($p<0.001$) and average depth of migration ($p<0.001$). Data is shown as mean bar only for n=9 independent experiments using 1 HDBEC donor and 18 different PBL donors. *$p<0.05$, **$p<0.01$, ***$p<0.001$ by Bonferroni multiple comparison post-test.

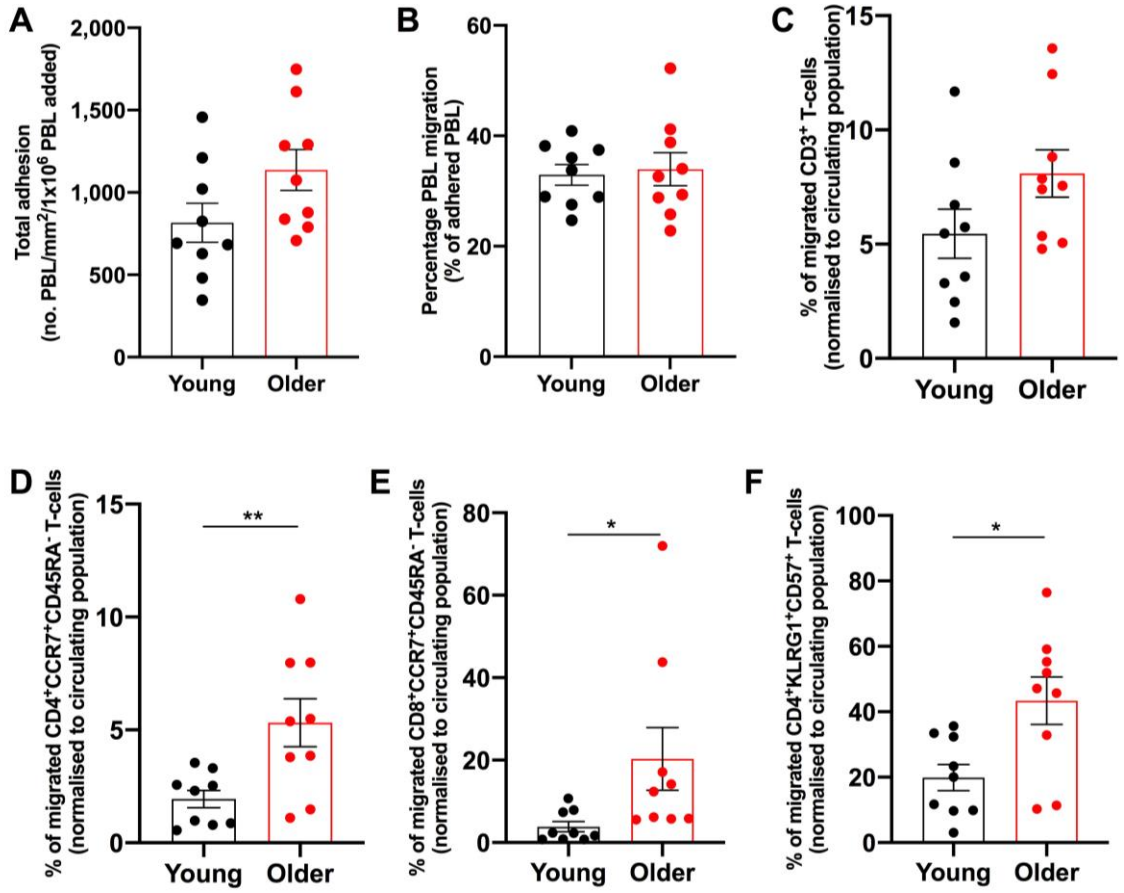

Figure 4-3 Ageing increases the transendothelial migration of memory and senescent T-cell subsets *in vitro*

HDBEC were seeded onto a collagen matrix and stimulated with TNFα (100U/ml) and IFNγ (10ng/ml) for 24 hours. PBL ($1x10^6$ cells/ml) were isolated from young (black, n=9) and older (red, n=9) donors and added to cytokine-activated HDBEC for 20 minutes at 37°C. Digitised images of 5 random fields were captured to assess **(A)** the total number of adhered PBL and **(B)** the percentage of PBL transmigration across HDBEC. The collagen matrix was then collected, digested, and the number of PBL that had migrated across HDBEC and into the collagen matrix were quantified using flow cytometry. The percentage of migrated **(C)** $CD3^+$, **(D)** $CD4^+CCR7^+CD45RA^-$, **(E)** $CD8^+CCR7^+CD45RA^-$, and **(F)** $CD4^+KLRG1^+CD57^+$ T-cells, normalised to the circulating population of the donor, is shown. Data is shown as mean±SEM for n=9 independent experiments using 1 HDBEC donor and 18 different PBL donors. *p<0.05, **p<0.01 by unpaired t-test.

Table 4-1 Percentage of migrated T-cell subsets for young and older blood donors

T-cell subset	Young % migration, normalised to circulating population (mean±SEM)	Older % migration, normalised to circulating population (mean±SEM)	p-value (Young vs Older)
CD4+	5.3 ±1.1	7.7 ±1.2	0.154
CD4+CCR7+CD45RA+ Naive	0.4 ±0.1	0.4 ±0.1	0.995
CD4+CCR7-CD45RA- EM	6.2 ±1.1	13.1 ±2.3	**0.015**
CD4+CCR7-CD45RA+ TEMRA	13.5 ±2.4	22.9 ±4.2	0.066
CD4+CD25+ Treg	3.6 ±1.0	3.3 ±0.6	0.824
CD4+CD27-CD28- Senescent	21.8 ±4.1	20.9 ±4.0	0.869
CD8+	6.2 ±1.3	9.9 ±2.2	0.170
CD8+CCR7+CD45RA+ Naive	0.4 ±0.1	0.4 ±0.1	0.956
CD8+CCR7-CD45RA- EM	6.1 ±0.9	20.7 ±4.1	**0.003**
CD8+CCR7-CD45RA+ TEMRA	10.4 ±2.5	17.4 ±3.9	0.154
CD8+CD27-CD28- Senescent	9.3 ±2.3	23.0 ±5.3	**0.031**
CD8+KLRG1+CD57+ Senescent	15.7 ±4.4	17.8 ±4.2	0.744

Percentage of T-cell subsets that had migrated across cytokine-activated EC and into a collagen matrix, normalised to the circulating population of the donor. The migrated T-cell subsets of young and older donors are shown as mean ± standard error of the mean (SEM). Statistical analysis performed using an unpaired t-test to determine the effects of age on the transendothelial migration of specific T-cell subsets *in vitro*. EM, effector memory; TEMRA, terminally differentiated effector memory T-cells re-expressing CD45RA; Treg, regulatory T-cell.

4.2.2 AGEING EXACERBATES LEUKOCYTE RECRUITMENT TO THE PERITONEAL CAVITY DURING ZYMOSAN-INDUCED PERITONITIS IN A SEX-SPECIFIC MANNER

We next sought to determine the effects of age on lymphocyte trafficking *in vivo*. We used a well-established model of acute inflammation, namely ZIP, to specifically study the recruitment of T-cells to the peritoneal cavity of young and aged mice (Rajakariar *et al.*, 2008; Newson *et al.*, 2014). Forty-eight hours after zymosan challenge, the peritoneal exudate of young and aged mice was collected for the quantification of leukocyte populations by flow cytometry (same gating strategy as **Figure 3-1**). As we observed increased numbers of leukocytes within the peritoneal cavity of naïve aged mice, particularly in aged female mice (see Chapter 3), it was hypothesised that aged mice would have an exacerbated inflammatory response to zymosan-challenge and this would be more pronounced in the aged female mice.

The number of peritoneal leukocytes were >3-fold higher in PBS-treated aged mice compared to PBS-treated young mice **(Figure 4-4)**, which agrees with baseline peritoneal leukocyte counts in Chapter 3 **(Figure 3-2)**. Zymosan-challenge significantly increased the number of leukocytes within the peritoneal cavity of young and aged mice, however, zymosan-challenged aged mice presented with >2-fold more peritoneal leukocytes than zymosan-challenged young mice **(Figure 4-4)**.

Zymosan challenge did not significantly increase the number of peritoneal T-cells in young mice compared to the PBS control mice, but did increase peritoneal T-cell numbers by >4-fold in aged mice **(Figure 4-5)**. Inflamed aged mice presented with >4-fold more T-cells in the peritoneal cavity compared to inflamed young mice **(Figure**

4-5). Zymosan-challenge significantly increased the number of several innate leukocyte subsets in the peritoneal cavity of young and aged mice, including DC and macrophages **(Table 4-2)**. As for the adaptive leukocyte subsets, zymosan-challenge did not significantly affect the number of peritoneal B-cells in young and aged mice, but significantly increased the number of multiple T-cell subsets **(Table 4-2)**. These data demonstrate that ageing exacerbates leukocyte trafficking to the peritoneal cavity in response to acute inflammation.

We next investigated the impact of sex on the trafficking of leukocytes into the peritoneal cavity of young and aged mice post-zymosan challenge. ZIP significantly increased leukocyte numbers in the peritoneal cavity of young male, aged male, and aged female mice but not young female mice **(Figure 4-6)**. Young inflamed male mice had significantly more (2-fold) leukocytes within the peritoneal cavity compared to young inflamed female mice **(Figure 4-6)**. Aged female mice presented with >6-fold more peritoneal leukocytes post-zymosan challenge compared to young inflamed females, whilst aged male mice had comparable numbers of peritoneal leukocyte numbers to young males post-zymosan challenge **(Figure 4-6)**.

We observed increased numbers of T-cells within the peritoneum of young male, aged male, and aged female mice post-zymosan challenge, but did not observe increased T-cell numbers in the peritoneal cavity of inflamed young female mice compared to PBS control mice **(Figure 4-7)**. Aged female mice had >24-fold more T-cells in the peritoneal cavity compared to young females post-zymosan challenge, but the number of T-cells in the peritoneal cavity of inflamed young and aged male mice were comparable **(Figure 4-7)**. Zymosan-challenge led to significant changes to innate

immune cell numbers within the peritoneal cavity of young and aged female and male mice, including increased numbers of peritoneal neutrophils and macrophages **(Table 4-3)**. However, zymosan-challenge only led to significant changes within multiple adaptive immune cell populations in young male, aged male, and aged female mice **(Table 4-4)**. This included increased numbers of B-cells in the peritoneal cavity of young male mice following ZIP, and increased numbers of multiple T-cell subsets in young male, aged male, and aged female mice **(Table 4-4)**. We also quantified the number of leukocyte subsets in the blood, spleen, BM and inguinal LN of inflamed young and aged mice **(Table 4-5** and **Table 4-6)**. Zymosan challenge significantly reduced circulating DC numbers in aged male mice, and significantly reduced the number of circulating ABC in aged female mice **(Table 4-5)**. In the spleen, zymosan-challenge led to reduced T-cell numbers in young female, aged female, and young male mice **(Table 4-5)**. We observed reduced DC numbers in the BM of aged male mice following ZIP, and reduced numbers of B-cells in the BM of young male mice **(Table 4-6)**. In the iLN, we observed a significant increase in the number of senescent T-cells in young male mice following zymosan-challenge **(Table 4-6)**. Together, these data support the hypothesis that age, as well as sex, influence the trafficking of leukocytes in the context of acute inflammation *in vivo*.

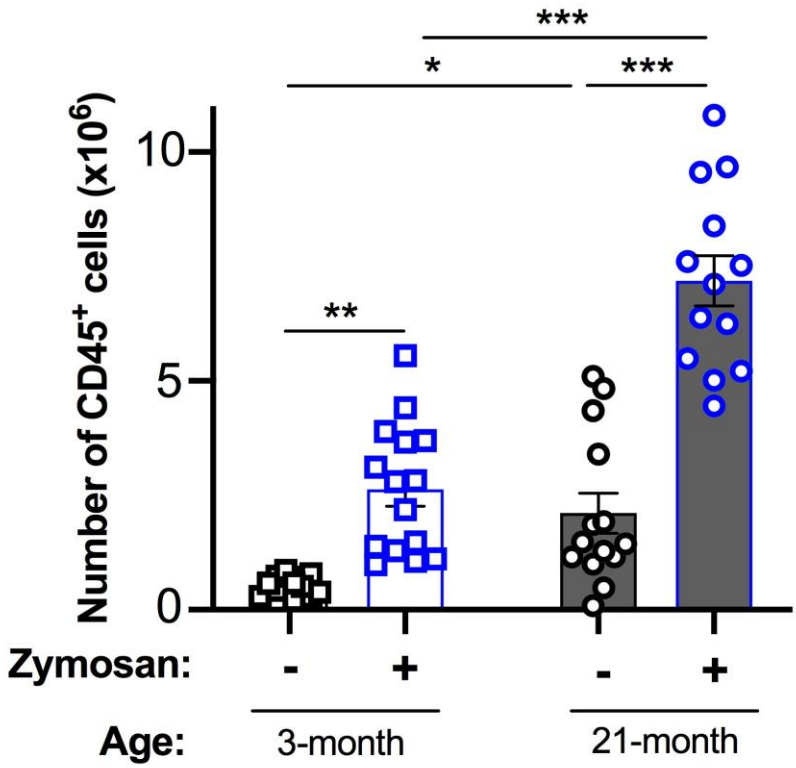

Figure 4-4 Ageing exacerbated leukocyte recruitment to the peritoneal cavity during zymosan-induced peritonitis

Young (3 months) and aged (21 months) C57Bl6 male and female mice received intraperitoneal injection of 0.1mg zymosan (+) to induce peritonitis. Control mice received PBS (-). After 48 hours, the peritoneal cavity exudate was collected and analysed using flow cytometry. The total number of peritoneal $CD45^+$ cells was quantified using CountBright beads. Two-way ANOVA showed a significant effect of age (<0.001) and zymosan challenge (<0.001) on peritoneal leukocyte numbers. Data are presented as mean±SEM for n = 8 independent experiments using n = 14 for 3 month mice and n = 13-14 for 21 month mice. Statistical analysis performed using Bonferroni multiple comparison post-test, ***p<0.001, ** p<0.01, * p<0.05.

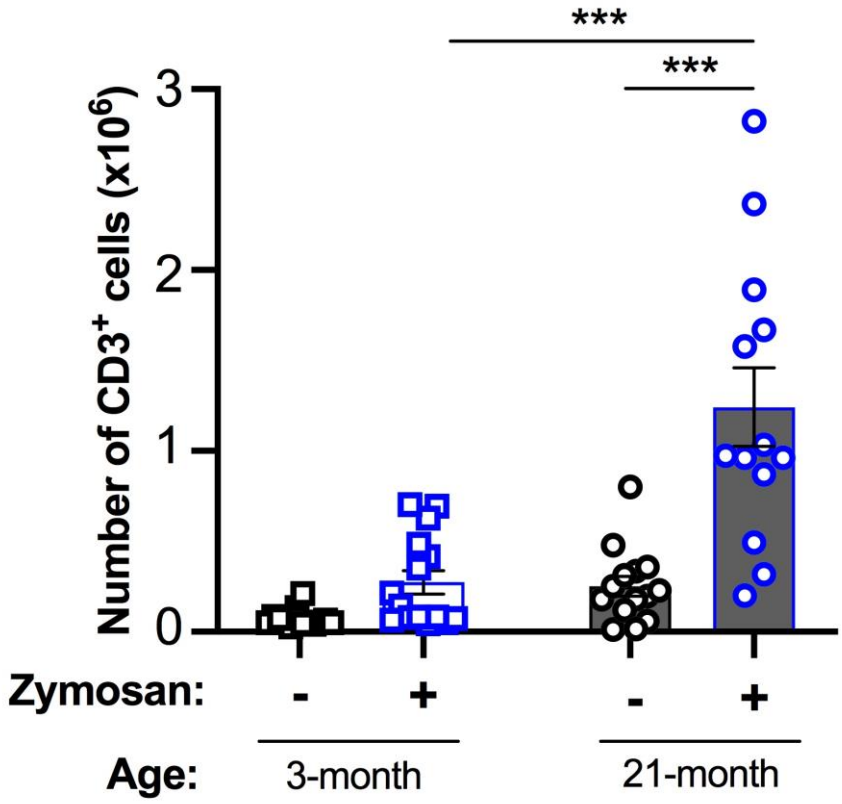

Figure 4-5 Ageing exacerbated T-cell recruitment to the peritoneal cavity during zymosan-induced peritonitis

Young (3 months) and aged (21 months) C57Bl6 male and female mice received intraperitoneal injection of 0.1mg zymosan (+) to induce peritonitis. Control mice received PBS (-). After 48 hours, the peritoneal cavity exudate was collected and analysed using flow cytometry. The total number of peritoneal $CD3^+$ cells was quantified using CountBright beads. Two-way ANOVA showed a significant effect of age (<0.001) and zymosan challenge (<0.001) on peritoneal T-cell numbers. Data are presented as mean±SEM for n = 8 independent experiments using n = 14 for 3 month mice and n = 13-14 for 21 month mice. Statistical analysis performed using Bonferroni multiple comparison post-test, ***p<0.001.

Table 4-2 Leukocyte subsets in the peritoneal cavity of young and aged inflamed mice

	Leukocyte subset	Young PBS (mean±SEM)	Young Zym (mean±SEM)	p-value (Young)	Aged PBS (mean±SEM)	Aged Zym (mean±SEM)	p-value (Aged)	p-value (Young vs Aged Zym)
Innate	DC	32,912 ±3,331	469,100 ±102,104	**0.001**	110,419 ±16,231	534,690 ±79,955	**0.001**	>0,999
	Eosinophils	11,927 ±1,613	327,644 ±51,572	**<0.001**	16,366 ±4,999	144,455 ±37,798	>0.999	**0.002**
	Macrophages	336,297 ±29,210	1,200,764 ±201,480	**0.003**	69,564 ±21,552	1,092,842 ±228,010	**0.013**	>0.999
	Neutrophils	4,937 ±1,909	351,189 ±77,544	**<0.001**	27,542 ±4,681	158,572 ±46,472	0.633	0.051
Adaptive	B-cells	105,982 ±17,118	324,050 ±52,459	>0.999	1,359,328 ±518,902	2,244,924 ±525,869	0.380	**0.002**
	ABCs	6,853 ±1,760	25,426 ±4,424	>0.999	49,776 ±11,245	213,528 ±31,266	**<0.001**	**<0.001**
	$CD4^+$ T-cells	44,643 ±3,652	179,359 ±44,378	0.253	89,274 ±14,343	421,141 ±73,378	**0.003**	**0.001**
	$CD8^+$ T-cells	17,151 ±1,925	92,017 ±20,659	>0.999	138,857 ±26,425	750,020 ±162,107	**<0.001**	**<0.001**
	$CD4^+$ N T-cells	26,567 ±3,806	94,384 ±28,964	0.765	25,386 ±4,694	137,045 ±20,420	**0.023**	0.625
	$CD4^+$ EM T-cells	12,861 ±2,502	59,360 ±11,501	>0.999	25,174 ±6,144	368,137 ±116,632	**0.007**	**0.001**
	$CD4^+$ CM T-cells	4,529 ±664.3	17,692 ±3,699	0.491	10,329 ±2,354	51,472 ±8,630	**0.006**	**<0.001**
	Tregs	4,452 ±475.2	12,882 ±3,481	0.060	5,239 ±856	17,030 ±2,060	**0.004**	>0.999
	$CD8^+$ N T-cells	7,755 ±1,021	38,111 ±10,791	0.918	20,993 ±4,680	174,280 ±31,639	**<0.001**	**<0.001**
	$CD8^+$ EM T-cells	2,456 ±415.7	16,957 ±3,509	>0.999	42,592 ±9,674	175,265 ±43,829	**0.002**	**<0.001**
	$CD8^+$ CM T-cells	6,835 ±1,254	34,412 ±7,701	>0.999	21,099 ±6,137	120,242 ±26,224	**0.004**	**<0.001**
	Senescent T-cells	2,226 ±570.3	9,358 ±1,325	>0.999	49,776 ±11,245	213,528 ±31,266	**<0.001**	**<0.001**

The number of peritoneal leukocyte subsets of young (3 months) and aged (21 months) mice that received intraperitoneal injection of PBS or 0.1mg zymosan A (Zym) treatment. Data are shown as mean ± standard error of the mean (SEM) for innate and adaptive leukocyte subsets. Statistical analysis performed using two-way ANOVA to determine the effects of zymosan-challenge and age on the number of peritoneal leukocyte subsets. ABCs, age-associated B-cells; DC, dendritic cells; N, naïve; EM, effector memory; CM, central memory; Tregs, regulatory T-cells.

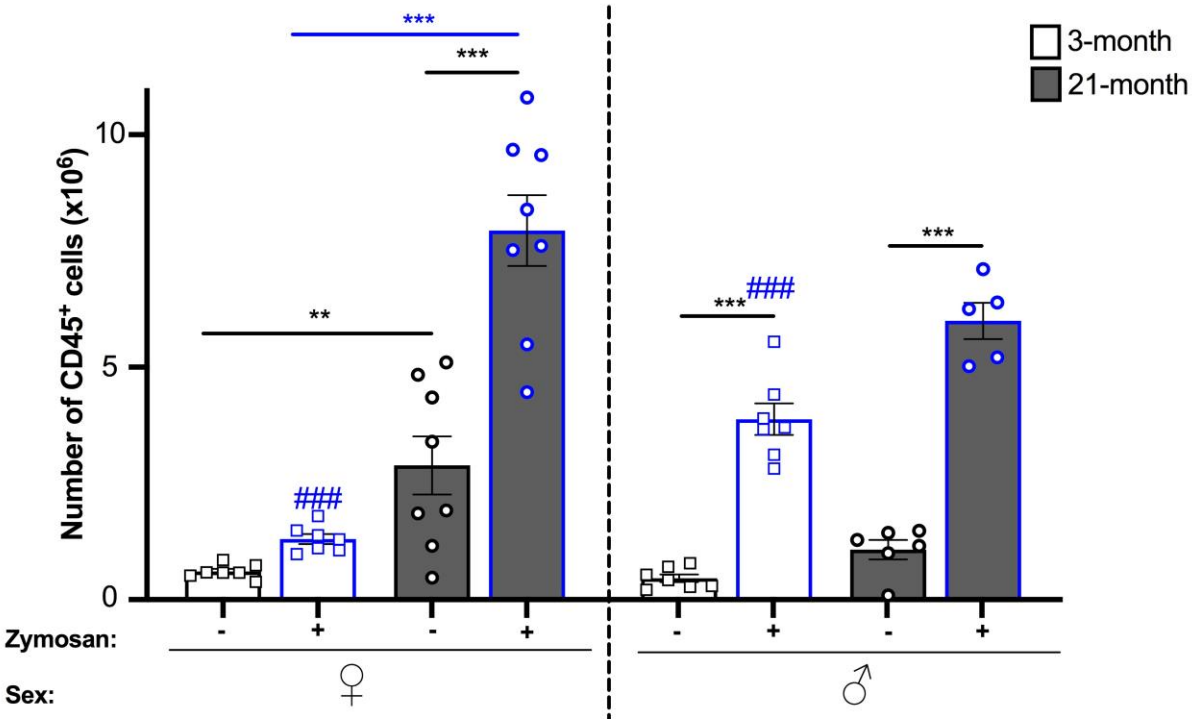

Figure 4-6 Sexual dimorphism of leukocyte recruitment to the peritoneum of young and aged mice during zymosan-induced peritonitis

Young (3 months; white bars) and aged (21 months; grey bars) female (♀) and male (♂) C57Bl6 mice received intraperitoneal injection of 0.1mg zymosan (+) to induce peritonitis. Control mice received PBS (-). After 48 hours, the peritoneal cavity exudate was collected and analysed using flow cytometry. The total number of peritoneal $CD45^+$ leukocytes was quantified using CountBright beads. Three-way ANOVA showed a significant effect of age (<0.001) and zymosan challenge (<0.001), but not sex, on peritoneal $CD45^+$ cell numbers. Data are presented as mean±SEM for n = 8 independent experiments using n = 7 for 3 month mice, n = 5-8 for 21 month mice. Statistically significant changes based on treatment (*), age (*), and sex (#) are depicted. *** or ### p<0.001, ** p<0.01 using Bonferroni multiple comparison post-test.

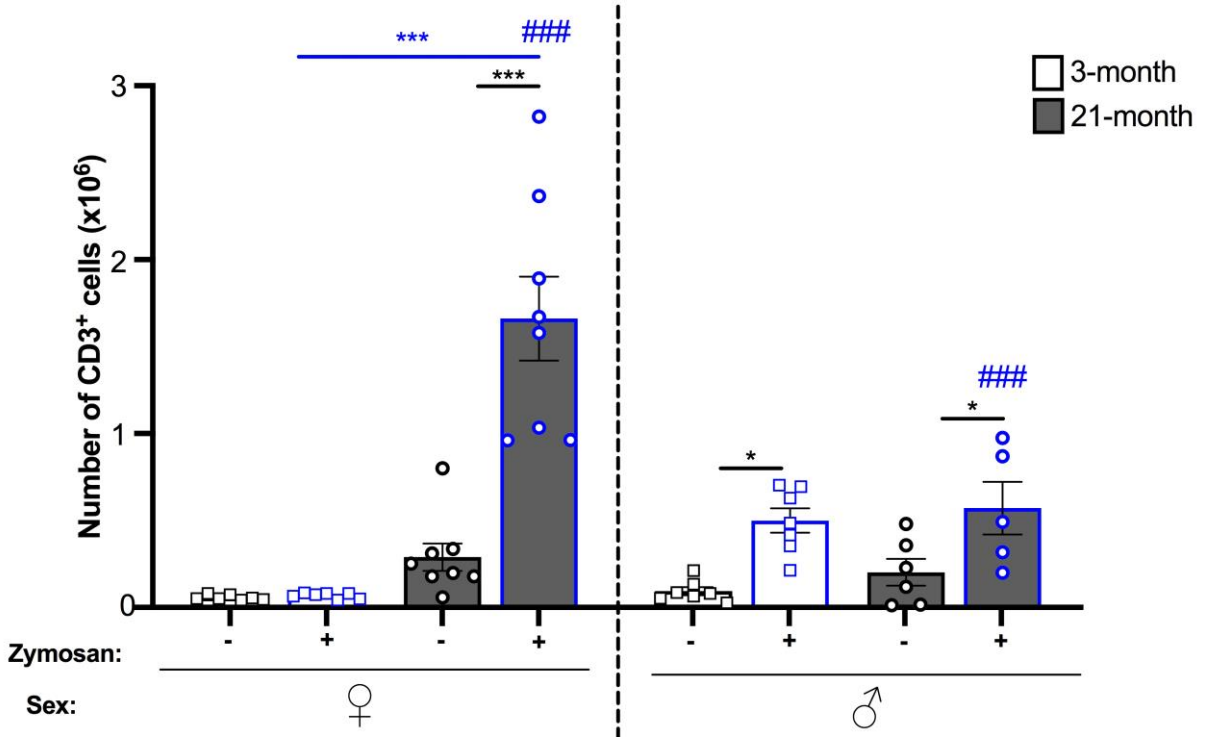

Figure 4-7 Sexual dimorphism of T-cell recruitment to the peritoneum of young and aged mice during zymosan-induced peritonitis

Young (3 months; white bars) and aged (21 months; white bars) female (♀) and male (♂) C57Bl6 mice received intraperitoneal injection of 0.1mg zymosan (+) to induce peritonitis. Control mice received PBS (-). After 48 hours, the peritoneal cavity exudate was collected and analysed using flow cytometry. The total number of peritoneal $CD3^+$ leukocytes was quantified using CountBright beads. Three-way ANOVA showed a significant effect of age (<0.001), zymosan challenge (<0.001), and sex ($p<0.05$) on peritoneal $CD3^+$ cell numbers. Data are presented as mean±SEM for n = 8 independent experiments using n = 7 for 3 month mice, n = 5-8 for 21 month mice. Statistically significant changes based on treatment (*), age (*), and sex (#) are depicted. *** or ### $p<0.001$, ** $p<0.01$ using Bonferroni multiple comparison post-test.

Table 4-3 Innate immune cell populations in the peritoneal cavity of young and aged inflamed male and female mice

	Leukocyte subset (total no.)	YF PBS (mean±SEM)	YF Zym+PBS (mean±SEM)	p-value (YF PBS v Zym+PBS)	AF PBS (mean±SEM)	AF Zym+PBS (mean±SEM)	p-value (AF PBS v Zym+PBS)	YM PBS (mean±SEM)	YM Zym+PBS (mean±SEM)	p-value (YM PBS v Zym+PBS)	AM PBS (mean±SEM)	AM Zym+PBS (mean±SEM)	p-value (AM PBS v Zym+PBS)	p-value (YF v YM Zym)	p-value (AF v AM Zym)	p-value (YF v AF Zym)	p-value (YM v AM Zym)
Innate	DC	26,944 ±2,313	153,503 ±27,372	**<0.001**	105,961 ±22,164	648,154 ±108,256	**<0.001**	38,880 ±5,556	775,529 ±131,168	**<0.001**	115,620 ±25,926	353,148 ±60,501	**<0.001**	**<0.001**	0.083	**0.005**	**0.003**
	Eosinophils	13,936 ±2,244	241,780 ±57,617	**<0.001**	23,173 ±8,351	120,421 ±6,847	**<0.001**	9,918 ±2,212	400,327 ±77,132	**0.001**	8,425 ±2,981	182,910 ±102,039	0.202	0.117	>0.999	0.468	**0.022**
	Macrophages	327,059 ±39,132	603,795 ±114,191	**0.042**	102,168 ±35,691	1,242,576 ±319,075	**0.003**	345,536 ±46,233	1,746,041 ±276,718	**<0.001**	31,525 ±9,726	853,271 ±311,656	**0.024**	**0.003**	>0.999	0.607	0.116
	Neutrophils	1,796 ±432	193,989 ±51,850	**0.001**	26,439 ±5,964	149,400 ±33,286	**<0.001**	5,250 ±3,434	776,057 ±375,189	**0.021**	28,829 ±7,970	216,751 ±112,416	0.306	0.405	>0.999	>0.999	0.953

Innate immune cell populations within the peritoneum of young female (YF), aged female (AF), young male (YM), and aged male (AM) mice that received intraperitoneal injection of PBS or 0.1mg zymosan A (Zym) treatment. Data are shown as mean ± standard error of the mean (SEM) for the number of innate immune cell populations residing in the peritoneal cavity. Statistical analysis performed using three-way ANOVA to determine the effects of zymosan-challenge, sex, and age on the number of peritoneal innate immune cells. DC, dendritic cells.

Table 4-4 Adaptive immune cell populations in the peritoneal cavity of young and aged inflamed male and female mice

	Leukocyte subset (total no.)	YF PBS (mean±SEM)	YF Zym+PBS (mean±SEM)	p-value (YF PBS v Zym+PBS)	AF PBS (mean±SEM)	AF Zym+PBS (mean±SEM)	p-value (AF PBS v Zym+PBS)	YM PBS (mean±SEM)	YM Zym+PBS (mean±SEM)	p-value (YM PBS v Zym+PBS)	AM PBS (mean±SEM)	AM Zym+PBS (mean±SEM)	p-value (AM PBS v Zym+PBS)	p-value (YF v YM Zym)	p-value (AF v AM Zym)	p-value (YF v AF Zym)	p-value (YM v AM Zym)
Adaptive	B-cells	117,556 ±32,463	193,615 ±39,566	0.566	2,328,795 ±810,569	3,549,084 ±371,961	0.330	94,407 ±13,091	438,180 ±71,821	**<0.001**	105,406 ±33,763	158,267 ±60,626	0.889	>0.999	**<0.001**	**<0.001**	>0.999
	ABCs	9,838 ±3,198	20,262 ±6,937	0.718	61,389 ±17,229	249,641 ±39,790	**<0.001**	3,869 ±474	29,945 ±5,572	**<0.001**	36,229 ±13,182	155,746 ±42,847	**0.040**	>0.999	**0.040**	**<0.001**	**0.002**
	$CD4^+$ T-cells	43,301 ±4,046	45,670 ±4,532	>0.999	98,710 ±15,397	536,392 ±95,046	**<0.001**	46,208 ±6,748	296,337 ±56,399	**0.010**	71766 ±25,684	236,740 ±53,746	**0.010**	**0.004**	**0.001**	**<0.001**	>0.999
	$CD8^+$ T-cells	14,712 ±2,138	21,961 ±3,091	0.182	150,480 ±24,630	977,405 ±227,646	**0.002**	19,590 ±3,082	153,316 ±21,050	**<0.001**	125,297 ±52,092	386,204 ±78,086	**0.014**	>0.999	**0.002**	**<0.001**	0.973
	$CD4^+$ N T-cells	27,851 ±3,795	13,582 ±2,390	**0.009**	37,138 ±4,134	153,224 ±17,955	**<0.001**	25,284 ±6,916	156,271 ±38,048	**0.003**	11,636 ±4,540	111,159 ±45,578	**0.020**	**<0.001**	>0.999	**<0.001**	>0.999
	$CD4^+$ EM T-cells	8,112 ±1,350	25,218 ±2,464	**<0.001**	34,127 ±8,549	547,331 ±160,953	**0.006**	18,401 ±4,313	93,973 ±14,825	**<0.001**	14,729 ±7,314	81,427 ±13,134	**0.011**	>0.999	**<0.001**	**<0.001**	>0.999
	$CD4^+$ CM T-cells	5,277 ±1,063	6,629 ±1,292	>0.999	13,603 ±3,011	64,066 ±11,983	**<0.001**	3,781 ±771	27,373 ±4,622	**<0.001**	6,509 ±3,271	31,322 ±3,733	**<0.001**	0.077	**0.003**	**<0.001**	>0.999
	Tregs	3,099 ±228	3,035 ±384	>0.999	5,717 ±832	20,817 ±1,761	**<0.001**	6,030 ±419	21,497 ±4,755	**0.010**	4,681 ±1,651	10,971 ±3,085	0.078	**<0.001**	0.060	**<0.001**	**0.036**
	$CD8^+$ N T-cells	6,857 ±586	5,625 ±1,090	>0.999	25,483 ±3,918	211,377 ±42,585	**<0.001**	8,652 ±1,975	66,535 ±13,727	**<0.001**	15,755 ±9,067	114,923 ±36,040	**0.006**	0.297	**0.027**	**<0.001**	>0.999
	$CD8^+$ EM T-cells	1,719 ±427	4,077 ±524	0.082	48,797 ±8,978	248,509 ±57,287	**0.004**	3,193 ±620	26,362 ±3,228	**<0.001**	41,495 ±15,642	58,075 ±14,675	0.883	>0.999	**<0.001**	**<0.001**	>0.999
	$CD8^+$ CM T-cells	5,035 ±1,094	8,779 ±1,229	0.120	70,899 ±11,691	458,101 ±157,756	**0.039**	8,634 ±2,131	56,841 ±8,201	**<0.001**	35,825 ±10,634	189,323 ±46,974	**0.006**	>0.999	**0.080**	**0.003**	>0.999
	Senescent T-cells	1,529 ±313	5,476 ±1,781	0.059	11,946 ±3,202	72,218 ±8,641	**<0.001**	2,923 ±1,072	12,754 ±823	**<0.001**	28,380 ±9,687	170,840 ±37,957	**<0.001**	>0.999	**<0.001**	**<0.001**	**<0.001**

Adaptive immune cell populations within the peritoneum of young female (YF), aged female (AF), young male (YM), and aged male (AM) mice that received intraperitoneal injection of PBS or 0.1mg zymosan A (Zym) treatment. Data are shown as mean ± standard error of the mean (SEM) for the number of adaptive immune cell populations residing in the peritoneal cavity. Statistical analysis performed using three-way ANOVA to determine the effects of zymosan-challenge, sex, and age on the number of peritoneal adaptive immune cells. ABCs, age-associated B-cells; N, naïve; EM, effector memory; CM, central memory; Tregs, regulatory T-cells.

Table 4-5 Leukocyte populations in the blood and spleens of inflamed young and aged mice

		Leukocyte subset (total no.)	YF PBS (mean±SEM)	YF Zym (mean±SEM)	p-value (YF PBS v Zym)	AF PBS (mean±SEM)	AF Zym (mean±SEM)	p-value (AF PBS v Zym)	YM PBS (mean±SEM)	YM Zym (mean±SEM)	p-value (YM PBS v Zym)	AM PBS (mean±SEM)	AM Zym (mean±SEM)	p-value (AM PBS v Zym)	p-value (YF v YM Zym)	p-value (AF v AM Zym)	p-value (YF v AF Zym)	p-value (YM v AM Zym)
Blood (no. cells/ml)	Innate	DC	37,221 ±2,469	63,743 ±15,419	>0.999	29,194 ±6,632	31,769 ±22,892	>0.999	80,905 ±5,303	96,019 ±15,573	>0.999	350,015 ±95,289	112,417 ±43,025	**0.002**	>0.999	>0.999	>0.999	>0.999
		Eosinophils	12,007 ±5,685	31,540 ±10,497	>0.999	6,009 ±1,780	27,658 ±26,825	>0.999	18,829 ±4,421	56,926 ±18,784	>0.999	93,885 ±19,333	63,131 ±34,301	>0.999	>0.999	>0.999	>0.999	>0.999
		Neutrophils	21,539 ±12,192	82,097 ±43,910	>0.999	31,146 ±14,017	16,455 ±13,658	>0.999	25,871 ±10,146	168,244 ±43,017	>0.999	817,642 ±276,459	390,470 ±159,137	0.149	>0.999	0.368	>0.999	>0.999
	Adaptive	B-cells	130,400 ±55,546	272,365 ±52,017	>0.999	218,127 ±103,980	102,515 ±65,860	>0.999	253,240 ±65,471	406,673 ±157,152	>0.999	837,421 ±151,891	799,797 ±359,395	>0.999	>0.999	**0.031**	>0.999	0.617
		ABCs	4,256 ±1,084	4,216 ±1,302	>0.999	42,069 ±13,974	9,740 ±5,777	**0.028**	13,465 ±3,146	3,338 ±1,472	>0.999	19,049 ±3,582	65,531 ±41,567	0.145	>0.999	0.058	>0.999	**0.016**
		T-cells	148,888 ±53,949	271402 ±49,232	>0.999	74,949 ±12,166	133,401 ±84,274	>0.999	446,624 ±177,617	304,703 ±78,912	>0.999	328,760 ±57,910	204,112 ±51,720	>0.999	>0.999	>0.999	>0.999	>0.999
		Senescent T-cells	2,541 ±1,052	5,270 ±829	>0.999	11,808 ±3,693	6,879 ±3,248	>0.999	10,028 ±2,871	8,385 ±3,927	>0.999	20,696 ±5,133	8,309 ±3,309	0.099	>0.999	>0.999	>0.999	>0.999
Spleen (total no.)	Innate	DC	1,294,787 ±156,815	642,754 ±29,886	>0.999	2,925,504 ±774,668	1,159,441 ±463,580	**0.049**	1,196,014 ±482,754	1,023,994 ±299,024	>0.999	1,434,984 ±196,833	751,516 ±248,878	>0.999	>0.999	>0.999	>0.999	>0.999
		Eosinophils	121,844 ±19,060	85,855 ±4,663	>0.999	675,049 ±515,471	166,402 ±126,886	0.599	168,232 ±78,185	160,785 ±47,403	>0.999	69,526 ±7,422	76,552 ±36,558	>0.999	>0.999	>0.999	>0.999	>0.999
		Macrophages	1,602,428 ±200,226	465,868 ±36,691	>0.999	8,452,275 ±3,015,401	[illegible] ±2,191,60	0.373	1,551,970 ±922,143	995,385 ±442,114	>0.999	1,499,764 ±384,974	1,012,845 ±243,603	>0.999	>0.999	0.923	0.654	>0.999
		Neutrophils	205,201 ±61,340	132,410 ±8,747	>0.999	2,438,416 ±2,000,260	521,704 ±364,921	0.598	136,554 ±71,939	329,536 ±108,519	>0.999	453,541 ±157,951	155,023 ±31,216	>0.999	>0.999	>0.999	>0.999	>0.999
	Adaptive	B-cells	8,507,685 ±1,966,429	2,469,133 ±311,239	0.164	10,572,998 ±2,583,843	1,406,616 ±399,670	**0.004**	7,324,725 ±2,992,563	2,584,163 ±1,001,709	0.515	8,851,202 ±682,382	7,191,210 ±3,039,635	>0.999	>0.999	0.269	>0.999	0.697
		ABCs	207,910 ±43,480	27,455 ±3,448	>0.999	1,153,394 ±276,861	195,727 ±46,520	**<0.001**	88,612 ±26,175	65,861 ±23,535	>0.999	339,127 ±60,817	40,019 ±15,881	>0.999	>0.999	>0.999	>0.999	0.498
		T-cells	9,319,097 ±362,952	4,082,141 ±351,060	**0.007**	6,677,783 ±1,380,723	2,306,244 ±596,203	**0.024**	10,809,573 ±1,818,844	3,946,536 ±885,921	**0.003**	5,446,016 ±297,016	4,384,520 ±1,040,453	>0.999	>0.999	>0.999	>0.999	>0.999
		Senescent T-cells	105,218 ±45,860	64,270 ±3,127	>0.999	388,481 ±58,597	134,242 ±30,897	0.153	431,337 ±184,922	48,333 ±8,366	**0.006**	219,184 ±29,070	156,483 ±44,124	>0.999	>0.999	>0.999	>0.999	0.311

Leukocyte populations within the blood and spleens of young female (YF), aged female (AF), young male (YM), and aged male (AM) mice that received intraperitoneal injection of PBS or 0.1mg zymosan A (Zym) treatment. Data are shown as mean ± standard error of the mean (SEM) for the number of leukocytes in the blood and spleen. Statistical analysis performed using three-way ANOVA to determine the effects of zymosan-challenge, sex, and age on the number of leukocytes. ABCs, age-associated B-cells; DC, dendritic cells.

Table 4-6 Leukocyte populations in the BM and inguinal LN of inflamed young and aged mice

		Leukocyte subset (total no.)	YF PBS (mean±SEM)	YF Zym (mean±SEM)	p-value (YF PBS v Zym)	AF PBS (mean±SEM)	AF Zym (mean±SEM)	p-value (AF PBS v Zym)	YM PBS (mean±SEM)	YM Zym (mean±SEM)	p-value (YM PBS v Zym)	AM PBS (mean±SEM)	AM Zym (mean±SEM)	p-value (AM PBS v Zym)	p-value (YF v YM Zym)	p-value (AF v AM Zym)	p-value (YF v AF Zym)	p-value (YM v AM Zym)
BM (total no.)	Innate	DC	192,098 ±20,380	227,739 ±58,541	>0.999	246,076 ±90,805	304,147 ±55,433	>0.999	91,199 ±19,802	198,011 ±51,764	>0.999	456,813 ±95,494	175,245 ±22,866	**0.021**	>0.999	>0.999	>0.999	>0.999
		Eosinophils	275,460 ±25,805	542,205 ±87,892	0.908	393,949 ±163,470	612,127 ±196,976	>0.999	135,649 ±27,499	300,230 ±55,304	>0.999	409,288 ±109,355	268,510 ±49,687	>0.999	>0.999	0.293	>0.999	>0.999
		Macrophages	2,214,544 ±345,576	2,388,175 ±436,660	>0.999	1,877,790 ±731,235	2,221,140 ±377,334	>0.999	1,007,738 ±343,944	1,650,869 ±290,504	>0.999	3,217,054 ±700,766	1,510,440 ±297,661	0.126	>0.999	>0.999	>0.999	>0.999
		Neutrophils	2,416,272 ±198,146	4,037,483 ±777,055	0.845	2,422,384 ±934,379	3,191,479 ±851,837	>0.999	467,185 ±148,652	3,015,691 ±514,795	0.109	3,817,313 ±1,383,811	2,042,591 ±507,721	>0.999	>0.999	>0.999	>0.999	>0.999
	Adaptive	B-cells	747,109 ±74,481	414,227 ±95,083	>0.999	707,466 ±350,793	792,403 ±191,611	>0.999	2,662,862 ±1,019,168	481,666 ±147,170	**0.006**	933,975 ±352,920	1,097,951 ±232,312	>0.999	>0.999	>0.999	>0.999	>0.999
		ABCs	10,272 ±4,003	7,986 ±1,347	>0.999	47,366 ±22,200	83,616 ±14,300	0.363	52,659 ±17,373	9,400 ±3,965	0.148	47,407 ±14,261	73,144 ±17,001	>0.999	>0.999	>0.999	**0.007**	**0.014**
		T-cells	244,596 ±49,807	111,040 ±17,187	0.684	274,201 ±104,142	352,013 ±64,066	>0.999	76,249 ±21,602	79,745 ±16,758	>0.999	283,604 ±59,451	215,915 ±44,389	>0.999	>0.999	0.643	**0.017**	0.642
		Senescent T-cells	5,968 ±696	6,970 ±738	>0.999	34,921 ±10,180	25,374 ±5,946	>0.999	14,117 ±8,688	5,747 ±1,193	>0.999	27,676 ±7,383	22,154 ±8,478	>0.999	>0.999	>0.999	0.243	0.589
LN (total no.)	Innate	DC	12,766 ±3,840	8,299 ±2,294	>0.999	4,291 ±1,426	16,404 ±5,673	0.100	28,724 ±2,587	17,508 ±1,044	0.158	6,344 ±1,402	2,890 ±1,844	>0.999	0.285	**0.023**	0.498	**0.011**
		Eosinophils	158.8 ±50	314.7 ±136	>0.999	119.9 ±51	376 ±122	0.592	258.5 ±99	101.9 ±40	>0.999	36 ±10	47 ±15	>0.999	0.837	0.098	>0.999	>0.999
		Macrophages	2,463 ±898	5,338 ±1,758	0.783	1,681 ±289	6,501 ±1,780	0.076	2,274 ±448	1,461 ±183	>0.999	834 ±167	1,003 ±410	>0.999	0.173	**0.010**	>0.999	>0.999
		Neutrophils	143.9 ±33	184.5 ±79	>0.999	354 ±91	324.5 ±178	>0.999	535.9 ±424	258 ±14	>0.999	132 ±30	53 ±26	>0.999	>0.999	>0.999	>0.999	>0.999
	Adaptive	B-cells	123,457 ±66,219	154,738 ±101,085	>0.999	10,396 ±6,117	43,990 ±21,033	>0.999	177,639 ±28,761	155,828 ±69,246	>0.999	18,299 ±6,111	8,694 ±2,440	>0.999	>0.999	>0.999	>0.999	0.725
		ABCs	396.5 ±175	478.1 ±264	>0.999	366.1 ±86	766.1 ±242	>0.999	656.3 ±358	472.8 ±170	>0.999	113 ±16	181 ±78	>0.999	>0.999	0.463	>0.999	>0.999
		T-cells	764,092 ±474,905	372,166 ±141,255	>0.999	17,329 ±5,286	60,829 ±19,264	>0.999	748,367 ±88,330	1,065,272 ±108,972	>0.999	43,256 ±9,739	18,453 ±7,407	>0.999	0.060	>0.999	>0.999	**<0.001**
		Senescent T-cells	4,047 ±2,024	2,383 ±701	>0.999	726.6 ±207	1,891 ±643	>0.999	2,030 ±323	10,641 ±2,278	**0.005**	1,563 ±591	740 ±148	>0.999	**0.003**	>0.999	>0.999	**<0.001**

Leukocyte populations within the bone marrow (BM) and inguinal lymph nodes (LN) of young female (YF), aged female (AF), young male (YM), and aged male (AM) mice that received intraperitoneal injection of PBS or 0.1mg zymosan A (Zym) treatment. Data are shown as mean ± standard error of the mean (SEM) for the number of leukocytes in the BM and LN. Statistical analysis performed using three-way ANOVA to determine the effects of zymosan-challenge, sex, and age on the number of leukocytes. ABCs, age-associated B-cells; DC, dendritic cells.

4.3 DISCUSSION

Inflammatory leukocyte trafficking is evidently modulated by the ageing process (reviewed by Hopkin, Lord and Chimen, 2021), yet human studies centred around this research question are limited. Here we found that although ageing did not specifically modify the ability of PBL to adhere to nor migrate across cytokine-activated EC *in vitro*, including the depth and speed of PBL migration, it did affect the composition of migrating PBL. We report no difference in the percentage of T-cell transendothelial migration between young and older donors, as determined by flow cytometry, but we did observe an age-related increase in the proportion of migrated $CD4^+$/$CD8^+$ EM, CM, and some senescent ($CD4^+KLRG1^+CD57^+$ and $CD8^+CD27^-CD28^-$) T-cell subsets.

Several *in vivo* models designed to specifically investigate age-related changes to inflammatory T-cell trafficking exist but are lengthy procedures (Toapanta and Ross, 2009; Richner *et al.*, 2015; Norian and Allen, 2004). As ZIP is a well-characterised murine model to study leukocyte trafficking in the context of acute inflammation (Cash, White and Greaves, 2009), we investigated whether this model could be applied to aged systems to specifically study T-cell trafficking in a short time frame. Here we found that a 48-hour ZIP model was sufficient to induce T-cell recruitment to the peritoneal cavity of young and aged mice. Furthermore, we found that ageing exacerbated T-cell trafficking to the peritoneal cavity during ZIP, and that this occurred in a sex-specific manner.

4.3.1 EFFECT OF AGEING ON LYMPHOCYTE TRAFFICKING IN VITRO

To date, the *in vitro* studies that have investigated age-related changes to T-cell migration have largely relied on isolating specific T-cell subsets from the blood of young and older donors and subjecting the lymphocytes to chemokine-directed transwell-like assays (Kushner *et al.*, 2010; Callender *et al.*, 2020) and transendothelial migration assays (Stohlawetz *et al.*, 1996; Smart, Rao and Cohen, 1993; Lau *et al.*, 2019). To broaden our investigation of age-related changes to T-cell transmigration to multiple T-cell subsets, we used PBL in an *in vitro* transendothelial migration assay and performed flow cytometric analysis of the migrated cells. As data previously generated by this lab suggested an age-related increase in PBL transendothelial migration for male donors only (unpublished), we used PBL derived from men in this study. The data presented in this thesis describe no effect of ageing on the ability of PBL to adhere to and migrate across inflamed EC *in vitro*, but an age-related increase in the transendothelial migration of certain memory and senescent T-cell subsets.

We observed no age-related changes to PBL transendothelial migration, which disagrees with the data previously generated by this lab. This could simply be due to lower n numbers in this thesis, however, several of the published studies investigating age-related changes to lymphocyte transendothelial migration *in vitro* to date have reported no change (Stohlawetz *et al.*, 1996; Smart, Rao and Cohen, 1993; Cane, Ponnappan and Ponnappan, 2012b). Stohlawetz *et al.* observed no difference in the ability of T-cells derived from young (<31 years) and older (>85 years) adults to adhere to nor migrate across IL-1+IFNγ activated HUVEC *in vitro* (Stohlawetz *et al.*, 1996). This was also reported by Smart *et al.* who observed no difference in the ability of T-cells derived from young (<34 years) and older (>70 years) adults to adhere to TNFα-

activated HUVEC *in vitro*, determined by fluorescent quantification of the T-cells using the Rose Bangal stain (Smart, Rao and Cohen, 1993). In contrast, Kushner *et al.* reported reduced migration of T-cells derived from older (>62 years) adults towards VEGF and SDF-1α in a Boyden chamber system compared to T-cells derived from young (<26 years) adults, as determined by calcein staining of the migrated T-cells (Kushner *et al.*, 2010). However, the contrasted findings could be explained by the different experimental set-up used by Kushner *et al.*, as they did not assess T-cell migration across an EC monolayer (Kushner *et al.*, 2010). Furthermore, VEGF and SDF-1α are not effective T-cell chemoattracts, with evidence suggesting SDF-1α actively repulses T-cells away from areas where it is present (Poznansky *et al.*, 2000), and VEGF selectively attracts activated T-cells (Shin *et al.*, 2009). Interestingly, Cane *et al.* reported increased migration of $CD4^+$ T-cells isolated from older (>65 years) donors towards SDF-1α in a transwell system compared to T-cells isolated from young (<30 years) donors, but this was only evident after generating a migration index value (normalised $CD4^+$ T-cell migration towards SDF-1α compared to vehicle control); the percentage of migrating $CD4^+$ T-cells was not significantly different between the different aged donors (Cane, Ponnappan and Ponnappan, 2012b). Overall, the literature suggests that ageing does not affect T-cell migration *in vitro*, which is in agreement with the data presented in this thesis.

We observed a significant age-related increase in the transendothelial migration of $CD4^+$ and $CD8^+$ EM and CM T-cell subsets, which agrees with the work of Lau *et al.* who demonstrated that the memory T-cell subsets, particularly EM T-cells, isolated from older (>53 years) adults exhibited increased levels of migration across HUVEC *in vitro* compared to naïve and TEMRA subsets (Lau *et al.*, 2019). Indeed, memory T-cell

subsets preferentially migrate through cytokine-activated EC *in vitro* (Brezinschek *et al.*, 1995; Lalor *et al.*, 2002; Chimen *et al.*, 2015), but ageing evidently enhances their migratory capabilities. We did not observe any age-related changes to the transendothelial migration of $CD4^+$ and $CD8^+$ TEMRA T-cells, which is in agreement with the works of Callender *et al.* who reported no difference in the migration of $CD4^+$ and $CD8^+$ TEMRA T-cells derived from young (<46 years) and older (>66 years) adults across HUVEC towards a CXCL10/12 gradient *in vitro* (Callender et al., 2020). TEMRA T-cells from young (<46 years) adults exhibit dysfunctional mitochondrial function and reduced migratory capabilities as they cannot meet the energy demands necessary for transmigration (Callender *et al.*, 2020); perhaps that is why ageing does not lead to enhanced migration of this memory T-cell subset.

The use of an *in vitro* assay to assess age-related changes to lymphocyte migration has its caveats, such as the absence of physiological factors that may influence lymphocyte adhesion and migration *in vivo* e.g. local cytokine/chemokine gradients, shear stress, and the presence of other cell types. An artificial environment would limit EC activation and intercellular connectivity through the exclusion of supporting cell types such as pericytes, fibroblasts, and mast cells. Within the microvasculature bed, where leukocyte trafficking takes place, pericytes surround the abluminal surface of the endothelial tube (Geevarghese and Herman, 2014). Pericytes modulate EC activation and vascular permeability through cell-cell contacts and the secretion of soluble factors e.g. VEGF (Kozma *et al.*, 2021; Yamamoto *et al.*, 2015; Zhang *et al.*, 2020b). Fibroblasts are key players in the production and maintenance of extracellular matrix; however, they can propagate and support EC activation during inflammatory events through secreting cytokines, growth factors and proteases

(Enzerink and Vaheri, 2011). In addition to being modulators of immune responses, mast cells can increase vascular permeability through secreting soluble factors such as VEGF and histamine (Boesiger *et al.*, 1998; Lee *et al.*, 2008). It is therefore possible that the lack of additional cell types e.g. pericytes, fibroblasts and mast cells in migration assays changes the physiology of lymphocyte-EC interactions, which may help explain the lack of age-related changes to lymphocyte transendothelial migration observed *in vitro*. Indeed, Agius *et al.* reported reduced memory T-cell recruitment to the skin of older (>70 years) individuals in response to recall antigens compared to younger (<40 years) adults *in vivo* (Agius *et al.*, 2009). This was attributed to defective TNFα production by dermal macrophages in older hosts, which led to reduced activation of dermal EC and reduced recruitment of memory T-cells to the tissue (Agius *et al.*, 2009). It is therefore important to investigate age-related changes to lymphocyte trafficking patterns in a physiological *in vivo* setting.

The sex- and age-mismatch between the EC donor (young female) and PBL donors (young and older males) in the studies outlined in this thesis likely influenced the experimental outcome. It has been well-established that sex influences EC function through the actions of sex steroids (Stanhewicz, Wenner and Stachenfeld, 2018; Patel and Arora, 2008). In men, testosterone binds androgen receptors on EC and promotes NO production and vasodilation (Stanhewicz, Wenner and Stachenfeld, 2018). However, in women, testosterone engagement with the androgen receptors on EC propagates an alternative intracellular signalling cascade that results in suppressed NO production and impaired vasodilation (Stanhewicz, Wenner and Stachenfeld, 2018). EC function is also modulated by the ageing processes (Ting *et al.*, 2021; Donato *et al.*, 2015). The establishment of cellular senescence in EC drives modulated

EC functions, including increased expression of adhesion molecules on EC, reduced vascular integrity, and increased thrombosis (Ting *et al.*, 2021). Therefore, the sex- and age-mismatch of the cell donors remains a major limitation of the *in vitro* studies presented in this thesis and needs to be addressed.

4.3.2 EFFECT OF AGEING ON LYMPHOCYTE TRAFFICKING IN VIVO

Various models of peritonitis have been used to study neutrophil and monocyte trafficking in young and aged mice (Arnardottir *et al.*, 2014; Hornigold *et al.*, 2022), with some studies focusing on sex-specific responses in young mice (Scotland *et al.*, 2011; Kay *et al.*, 2015; Bain *et al.*, 2020). We sought to investigate whether the ZIP model could be used to study T-cell trafficking in mice whilst assessing age-dependent and sex-specific responses within the model. We found that the 48-hour ZIP model was sufficient to investigate T-cell trafficking in young and aged mice. Furthermore, we found that ageing exacerbated T-cell recruitment to the peritoneal cavity in response to zymosan-challenge. This observation was reminiscent of published studies that investigated age-related changes to neutrophil recruitment to the cavity of aged male mice (Arnardottir *et al.*, 2014; Hornigold *et al.*, 2022). Indeed, Arnardottir *et al.* reported increased neutrophil trafficking to the peritoneal cavity of aged (20 months) male BALBc mice 4 hours post-zymosan challenge compared to young (<2 months) mice (Arnardottir *et al.*, 2014). Similarly, Hornigold *et al.* reported increased leukocyte trafficking, including neutrophil trafficking, to the peritoneal cavity of aged (24 months) C57Bl6 male mice compared to young (<3 months) mice following 3-hour septic, thioglycolate- and LPS-induced peritonitis (Hornigold *et al.*, 2022). Importantly, increased neutrophil recruitment to the peritoneal cavity was associated with diminished anti-bacterial immunity in aged mice (Hornigold *et al.*, 2022). Interestingly,

Hornigold *et al.* also reported increased macrophage numbers in the peritoneum of old mice following the thioglycolate- and LPS-induced peritonitis models (Hornigold *et al.*, 2022) suggesting that ageing affects the trafficking of various leukocyte types in the context of acute peritoneal inflammation.

We observed sexual dimorphism within the 48-hour ZIP model, including increased leukocyte trafficking to the peritoneal cavity of young male mice compared to young female mice. This observation is in line with previous studies denoting sex-specific differences in neutrophil recruitment to the peritoneal cavity following various models of peritonitis (Scotland *et al.*, 2011; Kay *et al.*, 2015; Bain *et al.*, 2020). Scotland *et al.* reported increased numbers of neutrophils in the peritoneal cavity of young (<5 months) male C7Bl6 mice compared to females following a 3-hour zymosan-induced and group B streptococcus-induced peritonitis model (Scotland *et al.*, 2011). Similarly, Kay *et al.* reported increased neutrophil recruitment to the peritoneal cavity of young (<3 months) male mice following a 3-hour ZIP compared to females (Kay *et al.*, 2015), and Bain *et al.* reported increased neutrophil recruitment to the peritoneal cavity of young (<4 months) male mice during a 20-hour *S. pneumoniae*-induced peritonitis model compared to females (Bain *et al.*, 2020). Again, increased neutrophil recruitment to the peritoneal cavity during these models of peritonitis was associated with poorer control of the bacterial burden (Scotland *et al.*, 2011; Bain *et al.*, 2020), suggesting that young female mice are more effective at clearing peritoneal infections by restricting neutrophil recruitment to the cavity and limiting peritoneal inflammation. As we observed increased leukocyte trafficking to the peritoneal cavity of aged female mice compared to aged male mice in response to zymosan-challenge, it suggests that ageing is associated with the loss of the protective responses offered by the female

sex in the control of peritoneal inflammation. It would be of interest to determine whether this is due to age-related changes to sex steroid levels in the females, or a knock-on effect of the cumulative biological changes that occur within females during ageing.

4.4 CONCLUSIONS

Several studies have found that ageing is associated with modulated leukocyte trafficking dynamics during inflammatory responses (reviewed by Hopkin, Lord and Chimen, 2021), however, most of these studies neglected to consider the effect of biological sex in their observations and have largely utilised animal models. The first aim of this chapter was to determine whether we could observe age-related changes to human PBL transendothelial migration using an *in vitro* static adhesion assay. We found that, although ageing did not affect the ability of PBL to adhere to nor migrate across inflamed EC, it changed the composition of migrating T-cells **(Figure 4-8)**. The next two aims of this chapter were to determine whether we could utilise a short ZIP model to investigate inflammatory T-cell trafficking, and to determine the effects of age and sex on this model. Indeed, by using a 48-hour ZIP, we observed increased T-cell trafficking into the peritoneal cavity of both young and aged mice following zymosan challenge **(Figure 4-8)**. Importantly, both age and sex influenced inflammatory T-cell trafficking to the cavity, where aged female mice presented with the highest number of recruited T-cells following zymosan-challenge compared to all other cohorts of mice.

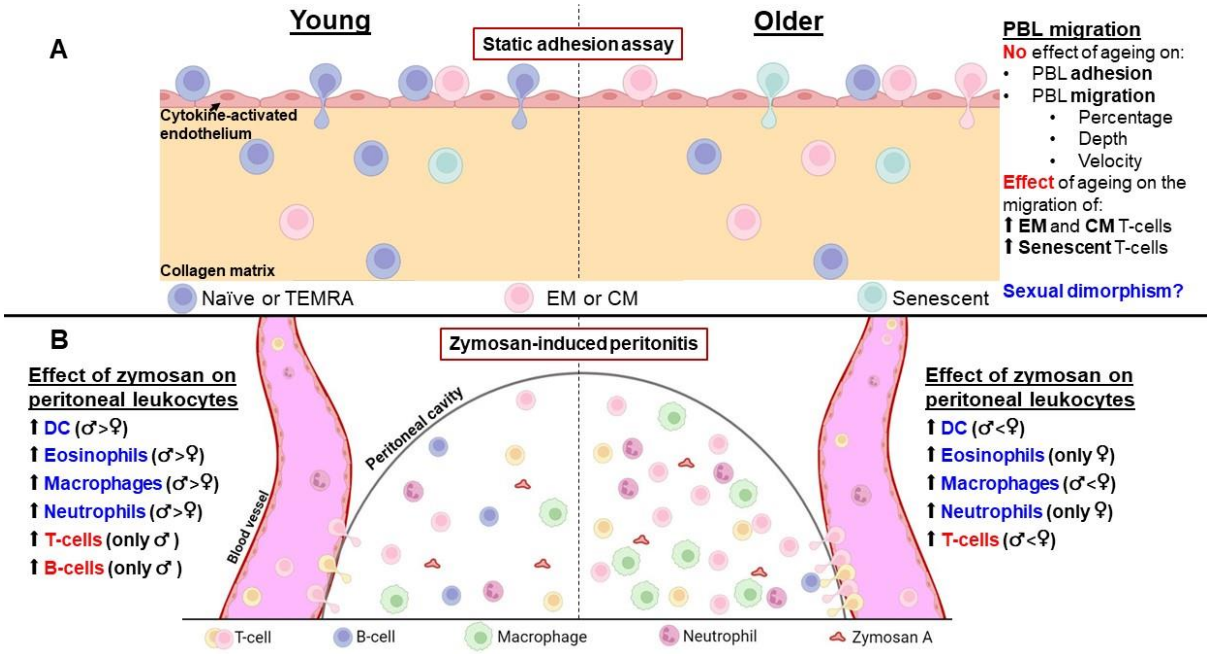

Figure 4-8 Ageing modulates lymphocyte trafficking during acute inflammation

A schematic depicting the major findings of Chapter 4. **(A)** Ageing did not affect the ability of peripheral blood lymphocytes (PBL) to adhere to nor migrate across cytokine-activated endothelial cells *in* vitro. However, ageing did affect the composition of migrating PBL, including enhanced migration of effector memory (EM), central memory (CM), and senescent T-cell subsets. A remaining question is whether there is sexual dimorphism within this age-related phenotype of migrating PBL *in vitro*. **(B)** In a model of zymosan-induced peritonitis (ZIP), we found that zymosan-challenge affected different leukocyte populations in a sex-specific fashion. In young mice, zymosan-challenge increased peritoneal T-cell numbers in male mice only. Ageing exacerbated the inflammatory response to zymosan challenge, with aged mice presenting with significantly more peritoneal leukocytes during ZIP. This age-related phenotype was more pronounced for female mice. Both *in vitro* and *in vivo* models of acute inflammation indicate that ageing influences lymphocyte trafficking kinetics. Created with BioRender.com

4.5 LIMITATIONS

Whilst we observed an age-related exacerbation of lymphocyte trafficking to the site of inflammation *in vivo*, we did not observe this in the human *in vitro* study. This is largely due to the limitations of using *in vitro* models to replicate physiological processes. Firstly, the HDBEC used in this model were derived from young donors and so the lack of age-related changes to PBL migration across EC may be due to the age mismatch of the donor cells. Secondly, the transendothelial migration of PBL *in vitro* occurred in the absence of circulating mediators that may have influenced these interactions. Indeed, it is well documented that older individuals have higher levels of circulating pro-inflammatory mediators (Bruunsgaard *et al.*, 1999; Wei *et al.*, 1992; Mariani *et al.*, 2006; Miles *et al.*, 2008), and so it is possible that their absence may have altered the migratory behaviour of the PBL derived from older individuals. Additional limitations of the *in vitro* static adhesion assay that would influence lymphocyte-EC dynamics include a lack of shear stress, the age- and sex-mismatch of the cell donors, and an isolated cellular environment (i.e. a lack of additional cell types that may have played a role in lymphocyte-EC interactions). Indeed, an *in vitro* assay can never replicate a systemic model of inflammation but can provide some insights into the process.

Whilst we observed significant changes in the number of recruited leukocytes to the peritoneal cavity of aged mice following a 48-hour zymosan challenge, this is only a snapshot of the inflammatory response in these animals. The ZIP model has been well characterised in young mice, where the onset and resolution of inflammation have been studied (Rajakariar *et al.*, 2008; Newson *et al.*, 2014), but this has not been studied in aged mice. It is not yet known how the dynamics of this inflammatory response change with age, whether ageing is associated with delayed resolution of

inflammation, and whether these changes differ between the sexes. It is important to understand how the onset of inflammation, the inflammatory process itself, and the resolution of inflammation changes with age to design therapeutic intervention.

CHAPTER 5 – AGEING ADVERSELY AFFECTS PEPITEM-MEDIATED CONTROL OF LEUKOCYTE TRAFFICKING

5.1 INTRODUCTION

The trafficking of leukocytes to sites of inflammation is necessary to confer protective immunity and reinstate tissue homeostasis (reviewed by Ley *et al.*, 2007 and Reglero-Real, Rolas and Nourshargh, 2019), however, dysregulated leukocyte trafficking can contribute to chronic inflammation and tissue immunopathology (Trowbridge, 1990; Lawrence and Gilroy, 2007; Chakraborty and Lo, 2020). The PEPITEM pathway is a homeostatic immunoregulatory pathway that regulates T-cell trafficking into tissues during inflammatory events (Chimen *et al.*, 2015; Matsubara *et al.*, 2020). The ability of PEPITEM to regulate inflammatory T-cell trafficking in young mice has been reported (Chimen *et al.*, 2015), however, whether PEPITEM is able to regulate inflammatory T-cell trafficking in older hosts has not been investigated. Here, we assessed whether PEPITEM is able to regulate T-cell trafficking in older mice and humans through the use of *in vivo* and *in vitro* models of inflammation. As the PEPITEM pathway is suggested to be dysfunctional in older adults due to an age-related reduction in the expression of AdipoR on circulating B-cells (Chimen *et al.*, 2015), we also assessed the impact of ageing on the functionality of the pathway.

5.2 RESULTS

5.2.1 PEPITEM CONTROLS INFLAMMATORY LEUKOCYTE TRAFFICKING IN AGED MICE

To investigate whether PEPITEM is able to regulate inflammation-induced leukocyte trafficking in aged systems, we first tested whether the peptide could control leukocyte trafficking to the peritoneal cavity during ZIP in young and aged mice. As we have observed sexual dimorphism in the ZIP model (see Chapter 4), we investigated the

effect of PEPITEM treatment in male and female systems. Forty-eight hours after zymosan and PEPITEM treatments, leukocytes were quantified in multiple murine tissues by flow cytometry. The gating strategy to identify murine lymphocytes and myeloid cells was the same as the one used in Chapters 3 and 4 **(Figure 3-1)**. It has previously been reported that PEPITEM can regulate leukocyte trafficking in young mice in the context of several inflammatory models including ZIP (Chimen *et al.*, 2015). As we found that aged mice experienced exacerbated leukocyte recruitment to the peritoneal cavity during ZIP (see Chapter 4), it was hypothesised that PEPITEM would be able regulate leukocyte trafficking to the peritoneal cavity of both young and aged mice in this model.

In response to zymosan challenge, we observed increased $CD45^+$ recruitment to the peritoneal cavity of young and aged mice for both sexes **(Figure 5-1)**. Importantly, PEPITEM treatment suppressed leukocyte recruitment to the peritoneal cavity during ZIP for all groups of mice, where peritoneal leukocyte numbers of zymosan+PEPITEM-treated mice were comparable to PBS-treated mice **(Figure 5-1)**. Furthermore, PEPITEM treatment specifically suppressed inflammatory T-cell recruitment to the peritoneal cavity of young and aged mice, and broadly affected the trafficking of multiple T-cell subsets, including suppressed trafficking of $CD4^+$ CM T-cells, $CD8^+$ naïve T-cells, and Treg **(Figure 5-2** and **Table 5-2)**. However, as T-cell recruitment to the peritoneal cavity did not occur in zymosan-challenged young female mice, PEPITEM treatment did not affect the peritoneal T-cell populations in these mice **(Figure 5-2** and **Table 5-2)**. Interestingly, PEPITEM limited the trafficking of multiple innate immune cell types into the peritoneal cavity of young and aged mice during ZIP, including DC and macrophages **(Table 5-1)**.

We also quantified different leukocyte populations in the blood, spleen, BM and inguinal LN of inflamed mice following PEPITEM treatment, although this data did not reach statistical significance (**Table 5-3** and **Table 5-4**). In the blood, we observed reduced circulating numbers of neutrophils and T-cells in young male and aged female mice following zymosan-challenge and PEPITEM treatment **(Table 5-3)**. We also observed a nonsignificant increase in B-cell numbers in the spleens of inflamed young female, aged female, and young male mice following PEPITEM treatment **(Table 5-3)**. In the BM, PEPITEM treatment reduced the number of T-cells in zymosan-challenged young and aged female mice, whereas splenic T-cell numbers were unchanged for young and aged male mice **(Table 5-4)**. Interestingly, PEPITEM treatment of inflamed mice reduced the number of B-cells in the inguinal LN of young and aged female mice, but increased T-cell numbers in the inguinal LN of young and aged male mice **(Table 5-4)**. Nonetheless, the peritoneal data suggest that PEPITEM is able to regulate the trafficking of multiple immune cell types, including T-cells, to sites of inflammation in young and aged systems.

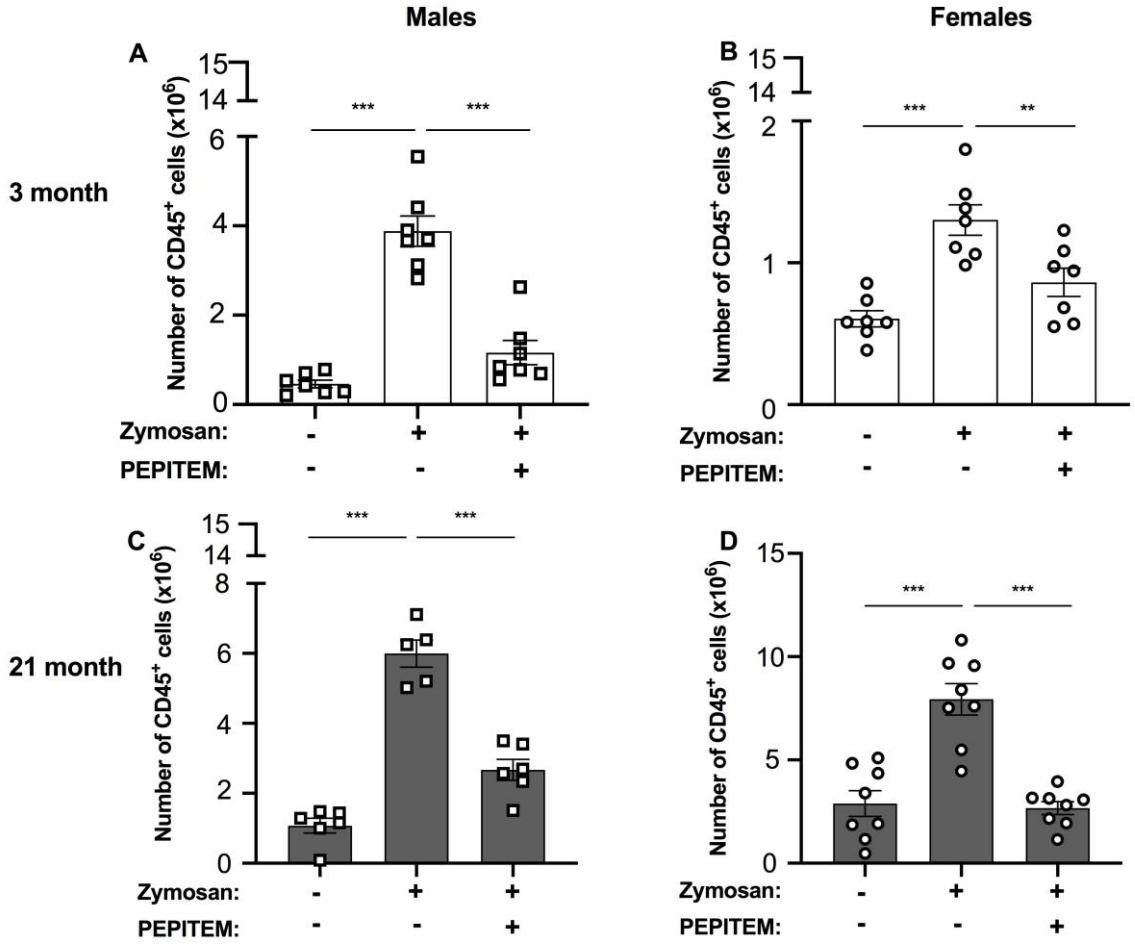

Figure 5-1 PEPITEM reduced leukocyte recruitment to the peritoneal cavity of young and aged mice during zymosan-induced peritonitis

Young (3 months) and aged (21 months) female (♀) and male (♂) C57Bl6 mice received intraperitoneal injection of 0.1mg zymosan (+) to induce peritonitis, control mice received PBS (-). Some mice received PEPITEM treatment (+), some did not (-). After 48 hours, exudate from the peritoneal cavity was collected and analysed using flow cytometry. The total number of $CD45^+$ cells in the peritoneal cavity of **(A+B)** young and **(C+D)** aged **(A+C)** male and **(B+D)** female mice was quantified using CountBright beads. One-way ANOVA showed a significant effect of treatment ($p<0.001$) on peritoneal $CD45^+$ cell numbers for all groups. Data are presented as mean±SEM for n = 13 independent experiments using n=7 for 3 month mice, n=5-8 for 21 month mice. Statistical analysis performed using Bonferroni multiple comparison post-test, ***$p<0.001$, **$p<0.01$.

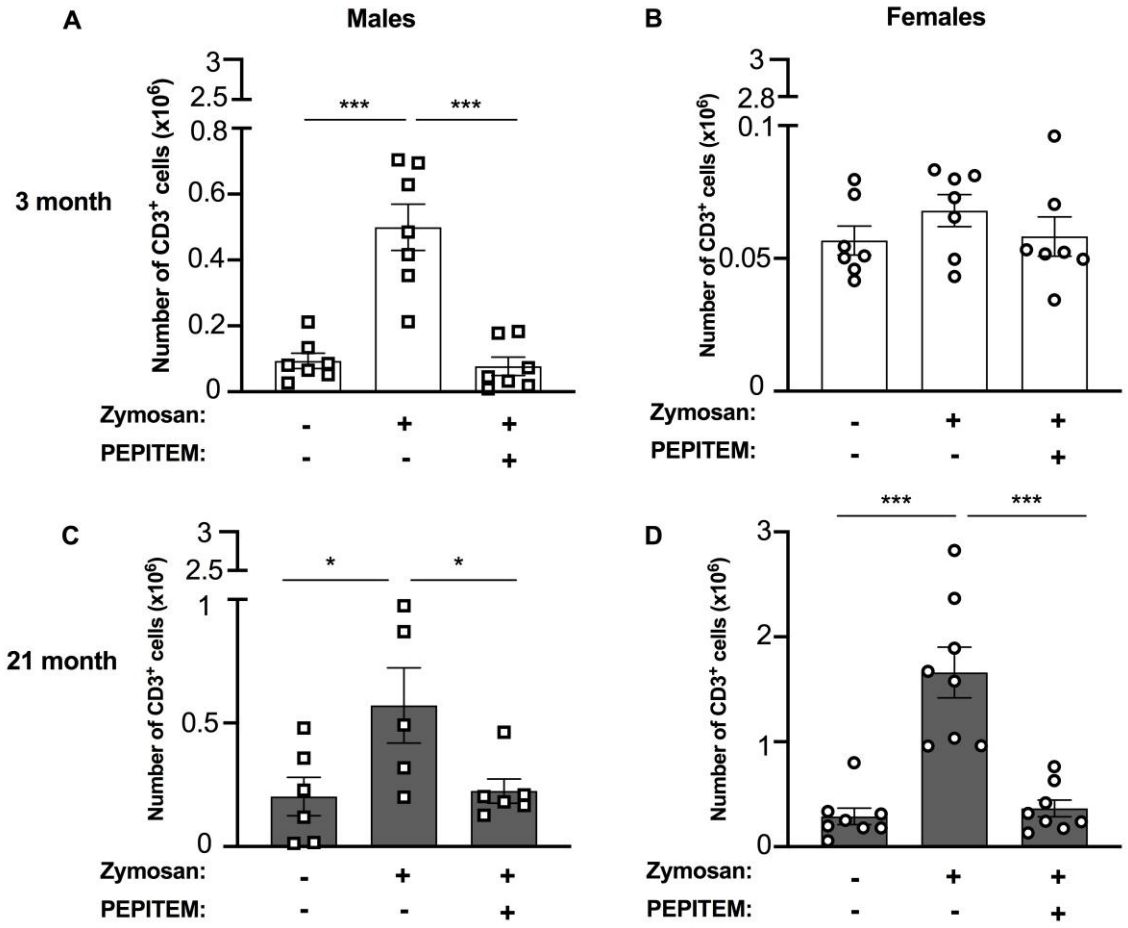

Figure 5-2 PEPITEM reduced T-cell recruitment to the peritoneal cavity of young and aged mice during zymosan-induced peritonitis in a sex-specific manner

Young (3 months) and aged (21 months) female (♀) and male (♂) C57Bl6 mice received intraperitoneal injection of 0.1mg zymosan (+) to induce peritonitis, control mice received PBS (-). Some mice received PEPITEM treatment (+), some did not (-). After 48 hours, exudate from the peritoneal cavity was collected and analysed using flow cytometry. The total number of $CD3^+$ cells in the peritoneal cavity of **(A+B)** young and **(C+D)** aged **(A+C)** male and **(B+D)** female mice was quantified using CountBright beads. One-way ANOVA showed a significant effect of treatment ($p<0.05$) on peritoneal $CD3^+$ cell numbers for young male, aged male and aged female mice. Data are presented as mean±SEM for n = 13 independent experiments using n=7 for 3 month mice, n=5-8 for 21 month mice. Statistical analysis performed using Bonferroni multiple comparison post-test, ***$p<0.001$, *$p<0.05$.

Table 5-1 Innate immune cell populations in the peritoneum of young and aged inflamed mice treated with PEPITEM

	Leukocyte subset (total no.)	YF PBS (mean±SEM)	YF Zym+PBS (mean±SEM)	YF Zym+PEPITEM (mean±SEM)	p-value (YF PBS v Zym+PBS)	p-value (YF Zym+PBS v Zym+PEPITEM)	AF PBS (mean±SEM)	AF Zym+PBS (mean±SEM)	AF Zym+PEPITEM (mean±SEM)	p-value (AF PBS v Zym+PBS)	p-value (AF Zym+PBS v Zym+PEPITEM)	YM PBS (mean±SEM)	YM Zym+PBS (mean±SEM)	YM Zym+PEPITEM (mean±SEM)	p-value (YM PBS v Zym+PBS)	p-value (YM Zym+PBS v Zym+PEPITEM)	AM PBS (mean±SEM)	AM Zym+PBS (mean±SEM)	AM Zym+PEPITEM (mean±SEM)	p-value (AM PBS v Zym+PBS)	p-value (AM Zym+PBS v Zym+PEPITEM)
Innate	DC	26,944 ±2,313	153,503 ±27,372	94,805 ±7,921	**<0.001**	**0.065**	105,961 ±22,164	648,154 ±108,256	207,217 ±16,841	**<0.001**	**<0.001**	38,880 ±5,556	775,529 ±131,168	288,912 ±100,130	**<0.001**	**0.006**	115,620 ±25,926	353,148 ±60,501	180,400 ±17,760	**<0.001**	**0.010**
	Eosinophils	13,936 ±2,244	241,780 ±57,617	106,852 ±20,862	**<0.001**	**0.044**	23,173 ±8,351	120,421 ±6,847	124,312 ±17,447	**<0.001**	>0.999	9,918 ±2,212	400,327 ±77,132	243,786 ±74,147	**0.001**	0.287	8,425 ±2,981	182,910 ±102,039	203,494 ±75,044	0.202	>0.999
	Macrophages	327,059 ±39,132	603,795 ±114,191	239,7946 ±29,861	**0.042**	**0.006**	102,168 ±35,691	1,242,576 ±319,075	640,823 ±67,220	**0.003**	0.154	345,536 ±46,233	1,746,041 ±276,718	695,506 ±122,221	**<0.001**	**<0.001**	31,525 ±9,726	853,271 ±311,656	562,787 ±196,578	**0.024**	0.651
	Neutrophils	1,796 ±432	193,989 ±51,850	115,768 ±19,433	**0.001**	0.302	26,439 ±5,964	149,400 ±33,286	62,625 ±8,958	**<0.001**	**<0.001**	5,250 ±3,434	776,057 ±375,189	67,311 ±32,318	**0.021**	0.061	28,829 ±7,970	216,751 ±112,416	250,748 ±105,779	0.306	>0.999

The number of innate immune cell subsets in the peritoneum of young female (YF), young male (YM), aged female (AF) and aged male (AM) mice treated with PBS, zymosan alone (Zym+PBS) or zymosan in combination with PEPITEM (Zym+PEPITEM) for 48 hours. Data are shown as mean ± standard error of the mean (SEM) for innate leukocyte subsets. Statistical analysis performed using one-way ANOVA to determine the effect of treatment on the number of peritoneal leukocytes within a cohort of mice of the same age and sex. DC, dendritic cells. DC, dendritic cells.

Table 5-2 Adaptive immune cell populations in the peritoneum of young and aged inflamed mice treated with PEPITEM

	Leukocyte subset (total no.)	YF PBS (mean±SEM)	YF Zym+PBS (mean±SEM)	YF Zym+PEPITEM (mean±SEM)	p-value (YF PBS v Zym+PBS)	p-value (YF Zym+PBS v Zym+PEPITEM)	AF PBS (mean±SEM)	AF Zym+PBS (mean±SEM)	AF Zym+PEPITEM (mean±SEM)	p-value (AF PBS v Zym+PBS)	p-value (AF Zym+PBS v Zym+PEPITEM)	YM PBS (mean±SEM)	YM Zym+PBS (mean±SEM)	YM Zym+PEPITEM (mean±SEM)	p-value (YM PBS v Zym+PBS)	p-value (YM Zym+PBS v Zym+PEPITEM)	AM PBS (mean±SEM)	AM Zym+PBS (mean±SEM)	AM Zym+PEPITEM (mean±SEM)	p-value (AM PBS v Zym+PBS)	p-value (AM Zym+PBS v Zym+PEPITEM)
Adaptive	B-cells	117,556 ±32,463	193,615 ±39,566	197,736 ±45,006	0.566	>0.999	2,328,795 ±810,569	3,549,084 ±371,961	1,083,231 ±229,773	0.330	**0.009**	94,407 ±13,091	438,180 ±71,821	105,406 ±33,763	**<0.001**	**<0.001**	105,406 ±33,763	158,267 ±60,626	290,756 ±66,600	0.889	0.318
	ABCs	9,838 ±3,198	20,262 ±6,937	25,326 ±7,190	0.718	>0.999	61,389 ±17,229	249,641 ±39,790	94,185 ±22,108	**<0.001**	**0.004**	3,869 ±474	29,945 ±5,572	6,230 ±1,141	**<0.001**	**<0.001**	36,229 ±13,182	155,746 ±42,847	59,196 ±35,240	**0.040**	0.105
	$CD4^+$ T-cells	43,301 ±4,046	45,670 ±4,532	38,738 ±5,214	>0.999	0.909	98,710 ±15,397	536,392 ±95,046	136,203 ±27,964	**<0.001**	**<0.001**	46,208 ±6,748	296,337 ±56,399	45,927 ±12,576	**0.010**	**<0.001**	71766 ±25,684	236,740 ±53,746	74,465 ±23,539	**0.010**	**0.011**
	$CD8^+$ T-cells	14,712 ±2,138	21,961 ±3,091	19,223 ±2,353	0.182	>0.999	150,480 ±24,630	977,405 ±227,646	186,081 ±41,919	**0.002**	**0.003**	19,590 ±3,082	153,316 ±21,050	32,848 ±10,931	**<0.001**	**<0.001**	125,297 ±52,092	386,204 ±78,086	165,937 ±44,701	**0.014**	**0.038**
	$CD4^+$ N T-cells	27,851 ±3,795	13,582 ±2,390	12,024 ±2,428	**0.009**	>0.999	37,138 ±4,134	153,224 ±17,955	35,189 ±8,943	**<0.001**	**<0.001**	25,284 ±6,916	156,271 ±38,048	15,797 ±3,989	**0.003**	**0.001**	11,636 ±4,540	111,159 ±45,578	21,843 ±4,359	**0.020**	**0.037**
	$CD4^+$ EM T-cells	8,112 ±1,350	25,218 ±2,464	18,436 ±2,193	**<0.001**	0.095	34,127 ±8,549	547,331 ±160,953	48,123 ±10,288	**0.006**	**0.008**	18,401 ±4,313	93,973 ±14,825	26,425 ±6,110	**<0.001**	**<0.001**	14,729 ±7,314	81,427 ±13,134	37,934 ±18,940	**0.011**	0.102
	$CD4^+$ CM T-cells	5,277 ±1,063	6,629 ±1,292	6,451 ±1,086	>0.999	>0.999	13,603 ±3,011	64,066 ±11,983	10,078 ±3,214	**<0.001**	**<0.001**	3,781 ±771	27,373 ±4,622	7,907 ±2,252	**<0.001**	**<0.001**	6,509 ±3,271	31,322 ±3,733	7,465 ±2,483	**<0.001**	**<0.001**
	Tregs	3,099 ±228	3,035 ±384	3,594 ±804	>0.999	>0.999	5,717 ±832	20,817 ±1,761	10,238 ±1,863	**<0.001**	**<0.001**	6,030 ±419	21,497 ±4,755	4,922 ±1,328	**0.010**	**0.003**	4,681 ±1,651	10,971 ±3,085	3,431 ±779	0.078	**0.032**
	$CD8^+$ N T-cells	6,857 ±586	5,625 ±1,090	6,122 ±1,016	>0.999	>0.999	25,483 ±3,918	211,377 ±42,585	25,865 ±6,755	**<0.001**	**<0.001**	8,652 ±1,975	66,535 ±13,727	6,440 ±1,997	**<0.001**	**<0.001**	15,755 ±9,067	114,923 ±36,040	29,515 ±6,674	**0.006**	**0.017**
	$CD8^+$ EM T-cells	1,719 ±427	4,077 ±524	5,304 ±993	0.082	0.682	48,797 ±8,978	248,509 ±57,287	59,287 ±14,353	**0.004**	**0.006**	3,193 ±620	26,362 ±3,228	10,357 ±3,936	**<0.001**	**0.004**	41,495 ±15,642	58,075 ±14,675	43,722 ±12,991	0.883	>0.999
	$CD8^+$ CM T-cells	5,035 ±1,094	8,779 ±1,229	8,476 ±1,259	0.120	>0.999	70,899 ±11,691	458,101 ±157,756	71,771 ±17,377	**0.039**	**0.039**	8,634 ±2,131	56,841 ±8,201	15,066 ±5,273	**<0.001**	**<0.001**	35,825 ±10,634	189,323 ±46,974	84,587 ±26,577	**0.006**	0.054
	Senescent T-cells	1,529 ±313	5,476 ±1,781	3,550 ±549	0.059	0.684	11,946 ±3,202	72,218 ±8,641	18,049 ±2,584	**<0.001**	**<0.001**	2,923 ±1,072	12,754 ±823	5,294 ±2,202	**<0.001**	**0.006**	28,380 ±9,687	170,840 ±37,957	24,147 ±5,794	**<0.001**	**<0.001**

The number of adaptive immune cell subsets in the peritoneum of young female (YF), young male (YM), aged female (AF) and aged male (AM) mice treated with PBS, zymosan alone (Zym+PBS) or zymosan in combination with PEPITEM (Zym+PEPITEM) for 48 hours. Data are shown as mean ± standard error of the mean (SEM) for adaptive leukocyte subsets. Statistical analysis performed using one-way ANOVA to determine the effect of treatment on the number of peritoneal leukocytes within a cohort of mice of the same age and sex. ABCs, age-associated B-cells; N, naïve; EM, effector memory; CM, central memory; Tregs, regulatory T-cells.

Table 5-3 Leukocyte subsets in the blood and spleens of young and aged inflamed mice treated with PEPITEM

		Leukocyte subset (total no.)	YF PBS (mean±SEM)	YF Zym+PBS (mean±SEM)	YF Zym+PEPITEM (mean±SEM)	p-value (YF PBS v Zym+PBS)	p-value (YF Zym+PBS v Zym+PEPITEM)	AF PBS (mean±SEM)	AF Zym+PBS (mean±SEM)	AF Zym+PEPITEM (mean±SEM)	p-value (AF PBS v Zym+PBS)	p-value (AF Zym+PBS v Zym+PEPITEM)	YM PBS (mean±SEM)	YM Zym+PBS (mean±SEM)	YM Zym+PEPITEM (mean±SEM)	p-value (YM PBS v Zym+PBS)	p-value (YM Zym+PBS v Zym+PEPITEM)	AM PBS (mean±SEM)	AM Zym+PBS (mean±SEM)	AM Zym+PEPITEM (mean±SEM)	p-value (AM PBS v Zym+PBS)	p-value (AM Zym+PBS v Zym+PEPITEM)
Blood (no. cells/ml)	Innate	DC	37,221 ±2,469	63,743 ±15,419	128,182 ±22,488	>0.999	>0.999	29,194 ±6,632	31,769 ±22,892	23,651 ±9,877	>0.999	>0.999	80,905 ±5,303	96,019 ±15,573	66,135 ±25,107	>0.999	>0.999	350,015 ±95,289	112,417 ±43,025	213,878 ±75,957	**0.002**	0.0395
		Eosinophils	12,007 ±5,685	31,540 ±10,497	60,175 ±6,760	>0.999	0.745	6,009 ±1,780	27,658 ±26,825	1,401 ±471	>0.999	>0.999	18,829 ±4,421	56,926 ±18,784	26,621 ±11,400	>0.999	0.712	93,885 ±19,333	63,131 ±34,301	57,514 ±18,837	>0.999	>0.999
		Neutrophils	21,539 ±12,192	82,097 ±43,910	92,293 ±20,009	>0.999	>0.999	31,146 ±14,017	16,455 ±13,658	4,787 ±834	>0.999	<0.999	25,871 ±10,146	168,244 ±43,017	83,803 ±41,418	>0.999	>0.999	817,642 ±276,459	390,470 ±159,137	628,684 ±309,579	0.149	0.937
	Adaptive	B-cells	130,400 ±55,546	272,365 ±52,017	43,058 ±95,889	>0.999	>0.999	218,127 ±103,980	102,515 ±65,860	48,927 ±15,547	>0.999	>0.999	253,240 ±65,471	406,673 ±157,152	248,252 ±93,174	>0.999	>0.999	837,421 ±151,891	799,797 ±359,395	729,128 ±149,901	>0.999	>0.999
		ABCs	4,256 ±1,084	4,216 ±1,302	7,395 ±1,979	>0.999	>0.999	42,069 ±13,974	9,740 ±5,777	11,044 ±7,142	**0.028**	>0.999	13,465 ±3,146	3,338 ±1,472	7,315 ±3,8410	>0.999	>0.999	19,049 ±3,582	65,531 ±41,567	49,968 ±12,807	0.145	>0.999
		T-cells	148,888 ±53,949	271,402 ±49,232	276,002 ±88,336	>0.999	>0.999	74,949 ±12,166	133,401 ±84,274	38,784 ±10,508	>0.999	>0.999	446,624 ±177,617	304,703 ±78,912	266,646 ±78,544	>0.999	>0.999	328,760 ±57,910	204,112 ±51,720	249,168 ±53,522	>0.999	>0.999
		Senescent T-cells	2,541 ±1,052	5,270 ±829	6,296 ±1,713	>0.999	>0.999	11,808 ±3,693	6,879 ±3,248	4,937 ±1,156	>0.999	>0.999	10,028 ±2,871	8,385 ±3,927	10,333 ±5,256	>0.999	>0.999	20,696 ±5,133	8,309 ±3,309	19,684 ±3,925	0.099	0.094
Spleen (total no.)	Innate	DC	1,294,787 ±156,815	642,754 ±29,886	829,515 ±297,713	>0.999	>0.999	2,925,504 ±774,668	1,159,441 ±463,580	1,008,140 ±399,504	**0.049**	>0.999	1,196,014 ±482,754	1,023,994 ±299,024	1,093,464 ±308,816	>0.999	>0.999	1,434,984 ±196,833	751,516 ±248,878	743,190 ±155,019	>0.999	>0.999
		Eosinophils	121,844 ±19,060	85,855 ±4,663	145,040 ±54,866	>0.999	>0.999	675,049 ±515,471	166,402 ±126,886	112,315 ±37,880	0.599	>0.999	168,232 ±78,185	160,785 ±47,403	158,126 ±40,472	>0.999	>0.999	69,526 ±7,422	76,552 ±36,558	141,615 ±71,387	>0.999	>0.999
		Macrophages	1,602,428 ±200,226	465,868 ±36,691	526,175 ±148,496	>0.999	>0.999	8,452,275 ±3,015,401	4,082,080 ±2,191,605	2,091,299 ±1,147,322	0.373	>0.999	1,551,970 ±922,143	995,385 ±442,114	763,513 ±228,430	>0.999	>0.999	1,499,764 ±384,974	1,012,845 ±243,603	2,426,436 ±1,741,694	>0.999	>0.999
		Neutrophils	205,201 ±61,340	132,410 ±8,747	135,887 ±49,502	>0.999	>0.999	2,438,416 ±2,000,260	521,704 ±364,921	353,053 ±133,831	0.598	>0.999	136,554 ±71,939	329,536 ±108,519	345,534 ±77,690	>0.999	>0.999	453,541 ±157,951	155,023 ±31,216	609,335 ±411,822	>0.999	>0.999
	Adaptive	B-cells	8,507,685 ±1,966,429	2,469,133 ±311,239	4,004,179 ±810,990	0.164	>0.999	10,572,998 ±2,583,843	1,406,616 ±399,670	4,453,413 ±2,922,334	**0.004**	0.947	7,324,725 ±2,992,563	2,584,163 ±1,001,709	4,303,892 ±1,545,794	0.515	>0.999	8,851,202 ±682,382	7,191,210 ±3,039,635	4,657,781 ±1,075,910	>0.999	>0.999
		ABCs	207,910 ±43,480	27,455 ±3,448	40,577 ±15,142	>0.999	>0.999	1,153,394 ±276,861	195,727 ±46,520	425,077 ±315,541	**<0.001**	0.857	88,612 ±26,175	65,861 ±23,535	63,789 ±17,713	>0.999	>0.999	339,127 ±60,817	40,019 ±15,881	280,328 ±84,149	>0.999	>0.999
		T-cells	9,319,097 ±362,952	4,082,141 ±351,060	3,449,443 ±1,071,736	**0.007**	>0.999	6,677,783 ±1,380,723	2,306,244 ±596,203	3,118,875 ±1,114,117	**0.024**	>0.999	10,809,573 ±1,818,844	3,946,536 ±885,921	3,932,111 ±736,622	**0.003**	>0.999	5,446,016 ±297,016	4,384,520 ±1,040,453	2,627,910 ±459,195	>0.999	0.937
		Senescent T-cells	105,218 ±45,860	64,270 ±3,127	31,389 ±10,856	>0.999	>0.999	388,481 ±58,597	134,242 ±30,897	157,795 ±54,652	0.153	>0.999	431,337 ±184,922	48,333 ±8,366	41,588 ±11,317	**0.006**	>0.999	219,184 ±29,070	156,483 ±44,124	212,424 ±60,925	>0.999	>0.999

The number of leukocyte subsets in the peritoneum of young female (YF), young male (YM), aged female (AF) and aged male (AM) mice treated with PBS, zymosan alone (Zym+PBS) or zymosan in combination with PEPITEM (Zym+PEPITEM) for 48 hours. Data are shown as mean ± standard error of the mean (SEM) for leukocyte subsets. Statistical analysis performed using one-way ANOVA to determine the effect of treatment on the number of peritoneal leukocytes within a cohort of mice of the same age and sex. DC, dendritic cells; ABCs, age-associated B-cells.

Table 5-4 Leukocyte subsets in the bone marrow and inguinal lymph nodes of young and aged inflamed mice treated with PEPITEM

		Leukocyte subset (total no.)	YF PBS (mean±SEM)	YF Zym+PBS (mean±SEM)	YF Zym+PEPITEM (mean±SEM)	p-value (YF PBS v Zym+PBS)	p-value (YF Zym+PBS v Zym+PEPITEM)	AF PBS (mean±SEM)	AF Zym+PBS (mean±SEM)	AF Zym+PEPITEM (mean±SEM)	p-value (AF PBS v Zym+PBS)	p-value (AF Zym+PBS v Zym+PEPITEM)	YM PBS (mean±SEM)	YM Zym+PBS (mean±SEM)	YM Zym+PEPITEM (mean±SEM)	p-value (YM PBS v Zym+PBS)	p-value (YM Zym+PBS v Zym+PEPITEM)	AM PBS (mean±SEM)	AM Zym+PBS (mean±SEM)	AM Zym+PEPITEM (mean±SEM)	p-value (AM PBS v Zym+PBS)	p-value (AM Zym+PBS v Zym+PEPITEM)
BM (total no.)	Innate	DC	192,098 ±20,380	227,739 ±58,541	106,084 ±17,938	>0.999	0.690	246,076 ±90,805	304,147 ±55,433	240,253 ±46,249	>0.999	>0.999	91,199 ±19,802	198,011 ±51,764	306,789 ±57,635	>0.999	0.629	456,813 ±95,494	175,245 ±22,866	247,690 ±50,529	**0.021**	>0.999
		Eosinophils	275,460 ±25,805	542,205 ±87,892	333,959 ±28,545	0.908	0.679	393,949 ±163,470	612,127 ±196,976	416,105 ±67,546	>0.999	0.673	135,649 ±27,499	300,230 ±55,304	462,825 ±87,495	>0.999	0.851	409,288 ±109,355	268,510 ±49,687	241,340 ±25,676	>0.999	>0.999
		Macrophages	2,214,544 ±345,576	2,388,175 ±436,660	1,325,079 ±123,150	>0.999	0.624	1,877,790 ±731,235	2,221,140 ±377,334	2,392,804 ±485,588	>0.999	>0.999	1,007,738 ±343,944	1,650,869 ±290,504	2,576,644 ±522,718	>0.999	0.608	3,217,054 ±700,766	1,510,440 ±297,661	1,766,027 ±575,257	0.126	>0.999
		Neutrophils	2,416,272 ±198,146	4,037,483 ±777,055	2,234,025 ±171,488	0.845	0.495	2,422,384 ±934,379	3,191,479 ±851,837	2,739,282 ±408,139	>0.999	>0.999	467,185 ±148,652	3,015,691 ±514,795	4,258,437 ±854,271	0.109	0.867	3,817,313 ±1,383,811	2,042,591 ±507,721	3,165,602 ±549,299	>0.999	>0.999
	Adaptive	B-cells	747,109 ±74,481	414,227 ±95,083	225,167 ±29,396	>0.999	>0.999	707,466 ±350,793	792,403 ±191,611	365,722 ±130,333	>0.999	>0.999	2,822,387 ±936,581	481,666 ±147,170	527,207 ±108,532	**0.006**	>0.999	933,975 ±352,920	1,097,951 ±232,312	596,943 ±188,587	>0.999	>0.999
		ABCs	10,272 ±4,003	7,986 ±1,347	5,770 ±510	>0.999	>0.999	47,366 ±22,200	83,616 ±14,300	29,800 ±7,269	0.363	0.005	52,659 ±17,373	9,400 ±3,965	12,878 ±2,728	0.148	>0.999	47,407 ±14,261	73,144 ±17,001	40,431 ±8,131	>0.999	0.180
		T-cells	244,596 ±49,807	111,040 ±17,187	51,781 ±4,734	0.684	>0.999	274,201 ±104,142	352,013 ±64,066	250,977 ±59,419	>0.999	0.534	76,249 ±21,602	79,745 ±16,758	79,874 ±13,615	>0.999	>0.999	283,604 ±59,451	215,915 ±44,389	216,141 ±25,456	>0.999	>0.999
		Senescent T-cells	5,968 ±696	6,970 ±738	2,484 ±415	>0.999	>0.999	34,921 ±10,180	25,374 ±5,946	24,557 ±5,879	>0.999	>0.999	14,117 ±8,688	5,747 ±1,193	5,559 ±1,061	>0.999	>0.999	27,676 ±7,383	22,154 ±8,478	20,295 ±4,292	>0.999	>0.999
LN (total no.)	Innate	DC	12,766 ±3,840	8,299 ±2,294	10,619 ±1,345	>0.999	>0.999	4,291 ±1,426	16,404 ±5,673	17,878 ±9,633	0.100	>0.999	28,724 ±2,587	17,508 ±1,044	20,873 ±6,647	0.158	>0.999	6,344 ±1,402	2,890 ±1,844	5,421 ±3,302	>0.999	>0.999
		Eosinophils	159 ±50	315 ±136	380 ±113	>0.999	>0.999	120 ±51	376 ±122	218 ±84	0.592	>0.999	258 ±99	101 ±40	412 ±162	>0.999	0.111	36 ±10	47 ±15	81 ±60	>0.999	>0.999
		Macrophages	2,463 ±898	5,338 ±1,758	5,455 ±937	0.783	>0.999	1,681 ±289	6,501 ±1,780	3,809 ±1,721	0.076	0.430	2,274 ±448	1,461 ±183	5,649 ±1,701	>0.999	0.055	834 ±167	1,003 ±410	921 ±514	>0.999	>0.999
		Neutrophils	144 ±33	185 ±79	178 ±45	>0.999	>0.999	354 ±91	325 ±178	320 ±98	>0.999	>0.999	535 ±424	258 ±14	1,062 ±387	>0.999	**0.005**	132 ±30	53 ±26	112 ±71	>0.999	>0.999
	Adaptive	B-cells	123,457 ±66,219	154,738 ±101,085	78,319 ±19,053	>0.999	>0.999	10,396 ±6,117	43,990 ±21,033	28,677 ±9,893	>0.999	>0.999	177,639 ±28,761	155,828 ±69,246	174,989 ±123,424	>0.999	>0.999	18,299 ±6,111	8,694 ±2,440	15,998 ±12,465	>0.999	>0.999
		ABCs	397 ±175	478 ±264	279 ±62	>0.999	>0.999	366 ±86	766 ±242	875 ±489	>0.999	>0.999	656 ±358	472 ±170	331 ±192	>0.999	>0.999	113 ±16	181 ±78	112 ±25	>0.999	>0.999
		T-cells	764,092 ±474,905	372,166 ±141,255	335,235 ±61,057	>0.999	>0.999	17,329 ±5,286	60,829 ±19,264	36,298 ±16,419	>0.999	>0.999	748,367 ±88,330	1,065,272 ±108,972	622,555 ±240,889	>0.999	0.177	43,256 ±9,739	18,453 ±7,407	15,966 ±8,294	>0.999	>0.999
		Senescent T-cells	4,047 ±2,024	2,383 ±701	2,054 ±509	>0.999	>0.999	727 ±207	1,891 ±643	1,358 ±386	>0.999	>0.999	2,030 ±323	10,641 ±2,278	5,246 ±2,198	**0.005**	0.008	1,563 ±591	740 ±148	754 ±431	>0.999	>0.999

The number of leukocyte subsets in the peritoneum of young female (YF), young male (YM), aged female (AF) and aged male (AM) mice treated with PBS, zymosan alone (Zym+PBS) or zymosan in combination with PEPITEM (Zym+PEPITEM) for 48 hours. Data are shown as mean ± standard error of the mean (SEM) for leukocyte subsets. Statistical analysis performed using one-way ANOVA to determine the effect of treatment on the number of peritoneal leukocytes within a cohort of mice of the same age and sex. DC, dendritic cells; ABCs, age-associated B-cells.

5.2.2 PEPITEM CONTROLS INFLAMMATORY LYMPHOCYTE TRAFFICKING IN HUMANS, BUT THE PATHWAY IS EVIDENTLY IMPAIRED WITH AGE

To investigate whether PEPITEM is able to regulate inflammatory T-cell trafficking in humans, we isolated PBL from the blood of young (23-37 years) and older (60-78 years) men and utilised a well-characterised *in vitro* static adhesion assay to assess the effects of PEPITEM pathway-derived mediators on PBL transendothelial migration (Apta, Chimen and McGettrick, 2017; Rainger and McGettrick, 2017). Work previously generated by our lab suggested that the PEPITEM pathway is functional in older women but dysfunctional in older men compared to younger counterparts (unpublished). To that end, to study the impact of ageing on PEPITEM pathway dysfunction, we only utilised male donors in the following studies. As the expression of AdipoR1/2 on circulating B-cells declines with age (Chimen *et al.*, 2015), it was hypothesised that this would be the driving force behind PEPITEM pathway dysfunction in older men.

Under control conditions, PBL derived from older donors displayed equivalent levels of adhesion to and migration across cytokine-activated HDBEC compared to PBL derived from young donors *in vitro* **(Figure 5-3A+B)**, reminiscent of the data in Chapter 4. The treatment of young PBL with AQ and PEPITEM did not affect their ability to adhere to HDBEC, as compared to the untreated controls, but these treatments significantly reduced the adhesion of older PBL to the EC **(Figure 5-3A)**. Interestingly, AQ treatment significantly reduced the transendothelial migration of young PBL but not older PBL **(Figure 5-3B)**. However, PEPITEM treatment significantly suppressed the transendothelial migration of both young and older PBL **(Figure 5-3B)**. As AQ treatment failed to suppress the transendothelial migration of

older PBL, yet PEPITEM treatment could suppress migration, these data suggest that the PEPITEM pathway is indeed dysregulated in older men and that this is occurring at the initiation phase of the pathway.

To determine whether age-related changes to AdipoR1/2 expression on circulating B-cells could explain the dysregulated AQ responses of older PBL, we measured AdipoR1/2 expression on B-cells isolated from the blood of young and older donors using flow cytometry. We observed a significant but modest reduction in the frequency of B-cells expressing AdipoR1 in older donors compared to young; however, the frequency of AdipoR2-expressing B-cells was unchanged **(Figure 5-4A-C)**. Concomitantly, the MFI of AdipoR1, but not AdipoR2, was significantly reduced on older B-cells compared to young **(Figure 5-4D+E)**. When assessing AdipoR1/2 expression on specific B-cell subsets within the circulating B-cell pool, we observed a significant reduction (~10%) in the frequency of AdipoR1$^+$ naïve mature B-cells in older donors compared to young **(Table 5-5)**. A high frequency of circulating AdipoR1$^+$ B-cells, but not AdipoR2$^+$ B-cells, positively correlated with the percentage inhibition of PBL transendothelial migration in response to AQ treatment, regardless of donor age **(Figure 5-5A+B)**. Although this correlation reached statistical significance, the r^2 value indicated a low level of correlation (r^2=0.0241). However, the frequency of AdipoR1/2$^+$ B-cells did not correlate with the percentage inhibition of PBL transendothelial migration induced by PEPITEM treatment **(Figure 5-5C+D)**. These data indicate an age-related reduction in the expression of AdipoR1, but not AdipoR2, by circulating B-cells which may affect the initiation of the PEPITEM pathway. However, as these changes were only modest, we sought to investigate age-related changes to intracellular signalling events downstream of the AdipoR in B-cells.

We next measured the abundance of APPL1, the adaptor protein immediately downstream of the AdipoR, in the lysates of peripheral blood B-cells derived from young and older donors by western blot. The number of B-cells isolated from young and older donors can be found in **Table 5-6**, whilst the flow cytometry data depicting the purity of the B-cell samples can be found in **Figure 5-6**. On the whole, the abundance of APPL1 appeared reduced in the lysates of older B-cells compared to younger B-cells **(Figure 5-7A)**. To quantify the data, the area under the peak of the protein bands was measured in ImageJ and APPL1 abundance was normalised to actin abundance. The abundance of APPL1 within B-cells did not significantly change upon AQ treatment, regardless of the age of the donor **(Figure 5-7B+C)**. However, under control conditions, APPL1 abundance in B-cells was significantly reduced with age **(Figure 5-7D)**. We then utilised LC/MS to quantify the fold-change in 14-3-3ζ abundance, the PEPITEM parent protein, in B-cells derived from young and older donors following AQ treatment **(Figure 5-7E)**. Interestingly, we observed a significant reduction in the fold-change of 14-3-3ζ in older B-cells compared to young B-cells following AQ-treatment **(Figure 5-7E)**. An unbiased list of the top 30 upregulated proteins in young and old B-cells following AQ treatment can be found in **Table 5-7**. Following AQ treatment, we observed increased expression of proteins involved in fatty acid oxidation (e.g. alcohol dehydrogenase class 3, trifunctional enzyme subunit alpha) in B-cells derived from young donors, and increased expression of proteins involved in actin cytoskeleton rearrangement (e.g. actin, myosin light chain kinase) in B-cells derived from older donors **(Table 5-7)**. Collectively, these data suggest that older B-cells have a diminished capacity to signal downstream of the AdipoR following AQ

stimulation and that this leads to reduced generation of 14-3-3ζ; leading to PEPITEM pathway dysfunction.

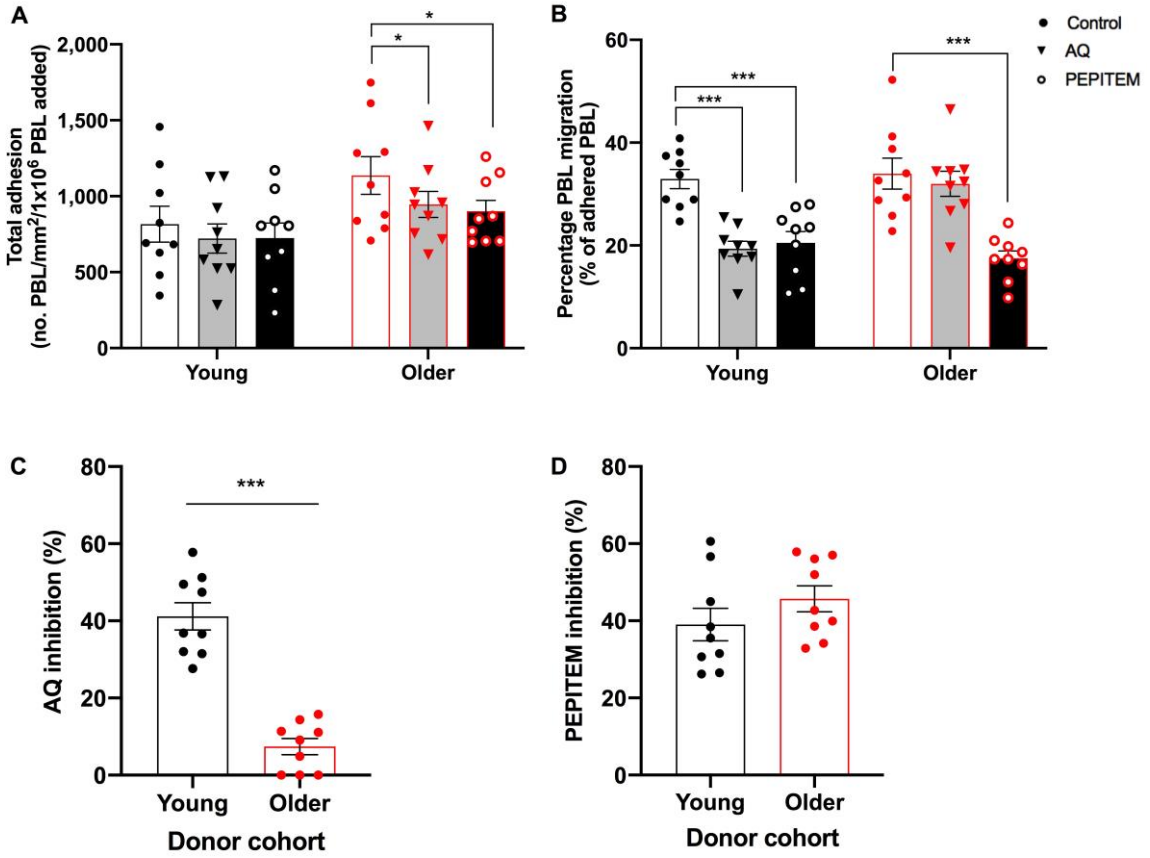

Figure 5-3 Older PBL exhibit dysregulated responses to adiponectin

HDBEC seeded onto a collagen matrix were stimulated with TNFα (100U/ml) and IFNγ (10ng/ml) for 24 hours. PBL were isolated from young (black, n=9) and older (red, n=9) donors and were either left untreated (control), pre-treated with adiponectin (AQ; 10µg/ml), or treated with PEPITEM (20ng/ml) prior to addition to HDBEC for 20 minutes at 37°C. **(A)** The number of PBL adhered to HDBEC expressed as the number of cells/mm^2/number of cells added. **(B)** Proportion of PBL transmigration expressed as the percentage of adhered cells that had transmigrated. The percentage inhibition of PBL transendothelial migration in response to **(C)** AQ and **(D)** PEPITEM treatments, is also shown. In A & B, ANOVA analysis showed a significant effect of treatment, but not age, on PBL adhesion ($p<0.05$) and transmigration ($p<0.001$). Data are shown as mean ± SEM for n=9 independent experiments using 1 HDBEC donor and 18 different PBL donors. *$p<0.05$ and ***$p\leq0.001$ by Dunnett's multiple comparison post-test for A & B, and an unpaired t-test in C & D.

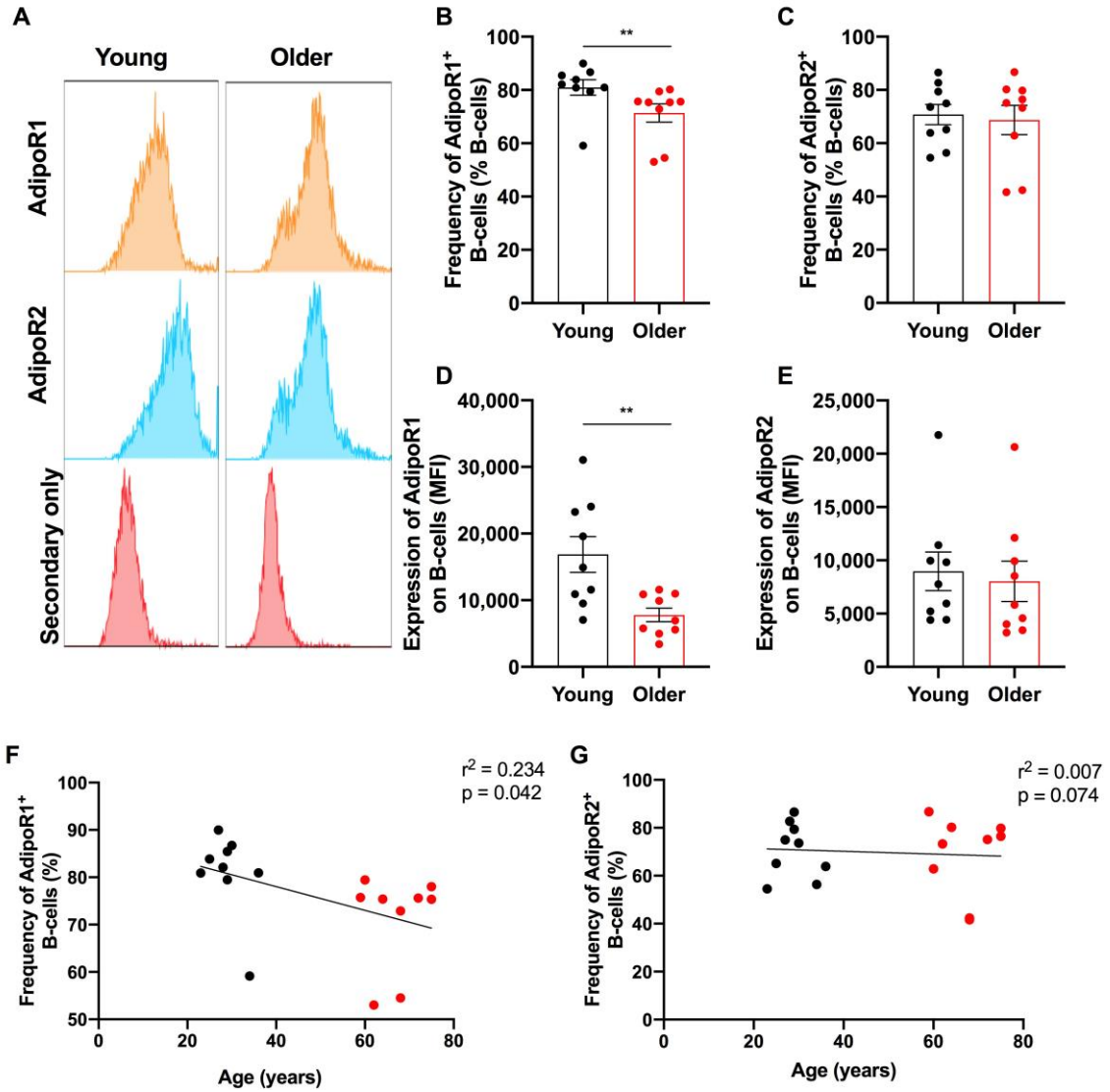

Figure 5-4 Ageing is associated with reduced AdipoR1 expression on circulating B-cells

B-cells were isolated from the blood of young (black, n=9) and older (red, n=9) donors and AdipoR1/2 expression was measured by flow cytometry. **(A)** Representative histograms depicting AdipoR1/2 expression on circulating young and older B-cells and secondary antibody-only control. The **(B+C)** frequency of and **(D+E)** median fluorescent intensity (MFI) values of B-cells expressing **(B+D)** AdipoR1 and **(C+E)** AdipoR2 were determined using flow cytometry. Linear regression analysis of age and expression of AdipoR1 **(F)** and AdipoR2 **(G)** on circulating B-cells. The goodness of fit (r^2) and p-values are indicated for each linear regression. Data are shown as **(B-E)** mean ± SEM and **(F+G)** line graphs for n = 9 independent experiments using 18 different PBL donors. **p≤0.01 by unpaired t-test.

Table 5-5 Adiponectin receptor 1 and 2 expression on B-cell subsets in the blood of young and older men

	Young				Older							
B-cell subset	**AdipoR1+ frequency (%, mean±SEM)**	**AdipoR2+ frequency (%, mean±SEM)**	**AdipoR1 MFI (mean±SEM)**	**AdipoR2 MFI (mean±SEM)**	**AdipoR1+ frequency (%, mean±SEM)**	**AdipoR2+ frequency (%, mean±SEM)**	**AdipoR1 MFI (mean±SEM)**	**AdipoR2 MFI (mean±SEM)**	**p-value (Y v O AdipoR1+ freq)**	**p-value (Y v O AdipoR2+ freq)**	**p-value (Y v O AdipoR1 MFI)**	**p-value (Y v O AdipoR2 MFI)**
Transitional/ Regulatory	77.7 ±4.9	53.7 ±4.9	7,702 ±1,387	4,202 ±773	71.4 ±4.5	61.9 ±6.0	5,214 ±691	4,950 ±965	0.362	0.307	0.131	0.554
Naive mature	90.8 ±1.3	77.6 ±4.1	10,995 ±2,244	6,637 ±1,119	85.3 ±1.3	78.4 ±5.0	7,097 ±1,149	4,460 ±458	**0.011**	0.908	0.144	0.153
Natural effector	90.9 ±1.1	87.3 ±2.4	24,302 ±4,155	16,459 ±2,345	90.3 ±1.4	89.7 ±1.5	19,050 ±2,855	20,166 ±3,738	0.734	0.404	0.315	0.413
Memory non-class switched	76.0 ±2.8	65.2 ±4.1	9,788 ±1,879	6,170 ±1,019	76.1 ±2.9	74.3 ±3.3	9,684 ±1,417	7,336 ±1,217	0.980	0.109	0.965	0.473
B1	66.5 ±5.5	55 ±5.0	12,560 ±2,906	7,141 ±1,400	65.5 ±4.1	60.6 ±8.1	7,200 ±703	9,437 ±2,981	0.885	0.560	0.117	0.496
B10	77.5 ±4.9	65.6 ±5.9	12,521 ±3,015	6,729 ±754	79.4 ±1.5	70.7 ±4.3	10,967 ±1,889	10,421 ±1,496	0.727	0.494	0.669	**0.043**
Senescent	81.0 ±2.4	64.5 ±5.2	8,370 ±1,380	6,366 ±1,257	74.2 ±4.1	74.3 ±2.7	8,464 ±1,598	7,328 ±1,553	0.205	0.126	0.965	0.634

Expression of adiponectin receptor 1 and 2 (AdipoR1/2) on different B-cell subsets in the blood of young (Y) and older (O) donors. Data are shown as mean ± standard error of the mean (SEM) for the percentage of B-cells positive for the expression of AdipoR1/2, as well as median fluorescence intensity (MFI) of both receptors for each B-cell subset per donor cohort. Statistical analysis performed using an unpaired t-test to determine the effect of age on AdipoR1/2 expression by B-cells.

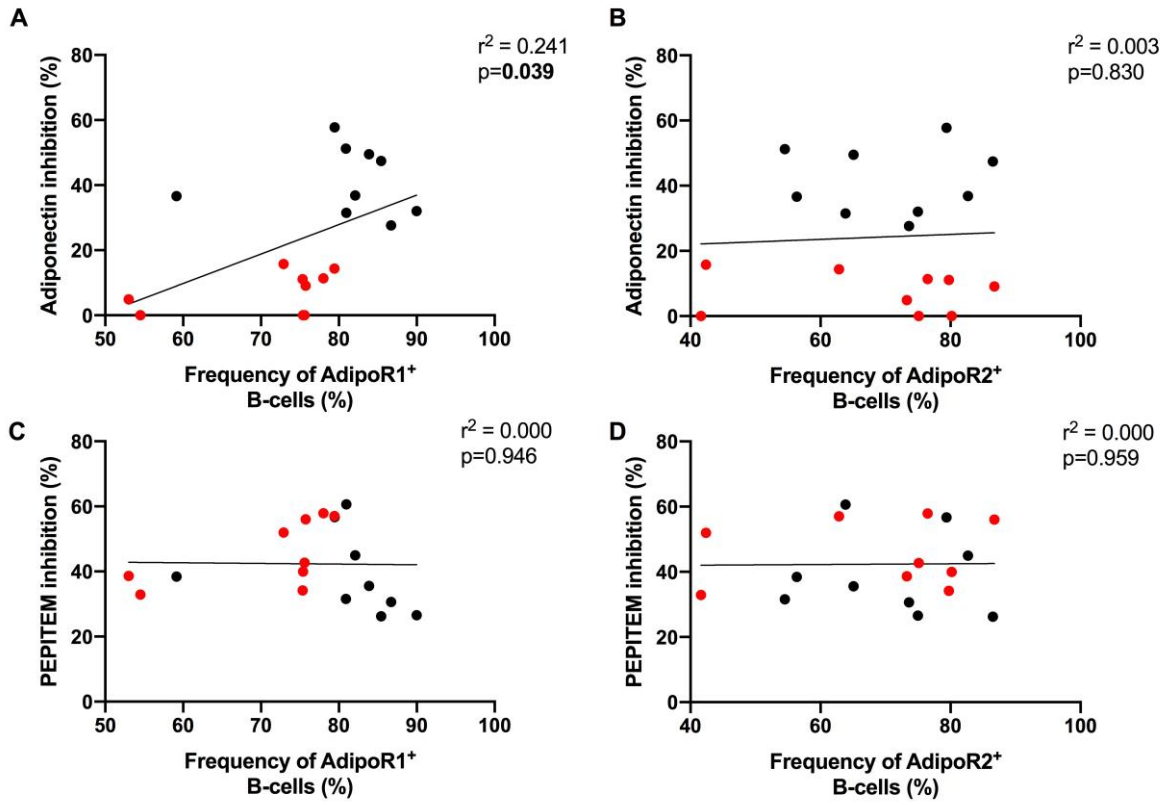

Figure 5-5 A high frequency of AdipoR1+ B-cells was essential for AQ-mediated inhibition of PBL transmigration

PBL were isolated from the blood of young (black dots, n=9) and older (red dots, n=9) donors and AdipoR1/2 expression was measured by flow cytometry. Linear regression analysis of the frequency of **(A+C)** AdipoR1$^+$ and **(B+D)** AdipoR2$^+$ B-cells (from Figure 6-4) and the percentage inhibition of PBL transendothelial migration in response to **(A+B)** AQ and **(C+D)** PEPITEM treatment (from Figure 6-3). The goodness of fit (r^2) and p-values are indicated for each linear regression.

Table 5-6 Number of B-cells isolated from the blood of young and older donors for western blot and LC/MS analysis

Donor	Age (years)	Number of PBMC ($x10^6$)	Number of B-cells ($x10^6$)
Y1	37	127	8.25
Y2	23	98	6.31
Y3	29	81	3.10
Y4	30	79	5.66
Y5	28	128	4.36
A1	74	175	1.13
A2	78	128	1.35
A3	76	121	1.09
A4	65	96	2.24
A5	67	155	0.43

The number of peripheral blood mononuclear cells (PBMC) and subsequent number of B-cells isolated from the blood of young (Y) and older (A) men.

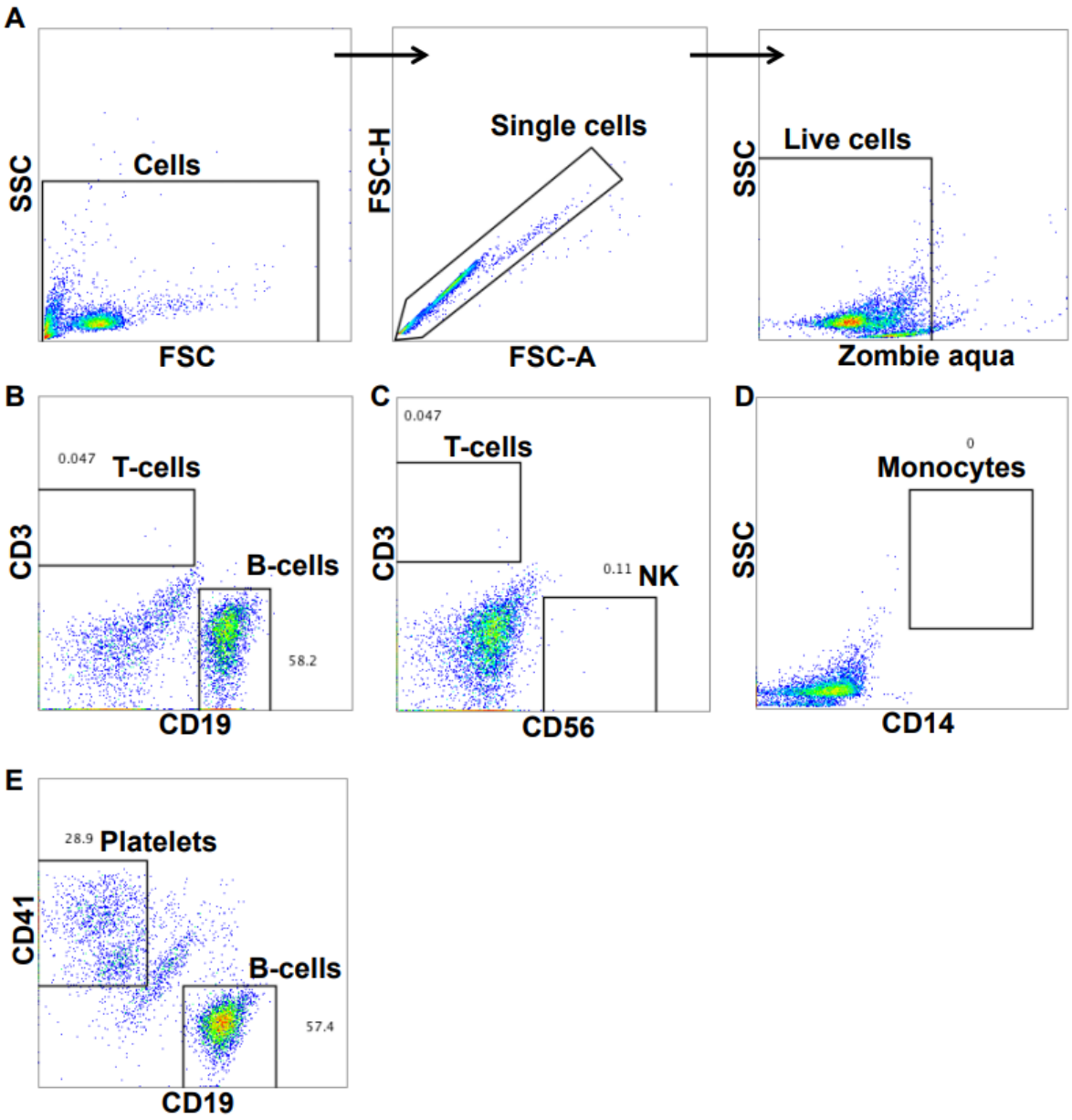

Figure 5-6 Purity of B-cells isolated from the peripheral blood mononuclear cells of young and older donors

Peripheral blood mononuclear cells (PBMC) were isolated from the blood of young and older donors using a histopaque gradient, and B-cells were subsequently isolated from PBMC using an enrichment kit. Flow cytometry data depicting the purity of B-cell samples is shown. **(A)** Gating strategy to identify single, live cells based on forward (FSC) and side scatter (SSC) profiles, cell circularity, and positive zombie aqua staining, respectively. Plots depict frequency of **(B)** $CD3^+$ T-cells, $CD19^+$ B-cells, **(C)** $CD56^+$ natural killer (NK) cells, **(D)** $CD14^+$ monocytes, and **(E)** $CD41^+$ platelets present within the B-cell samples.

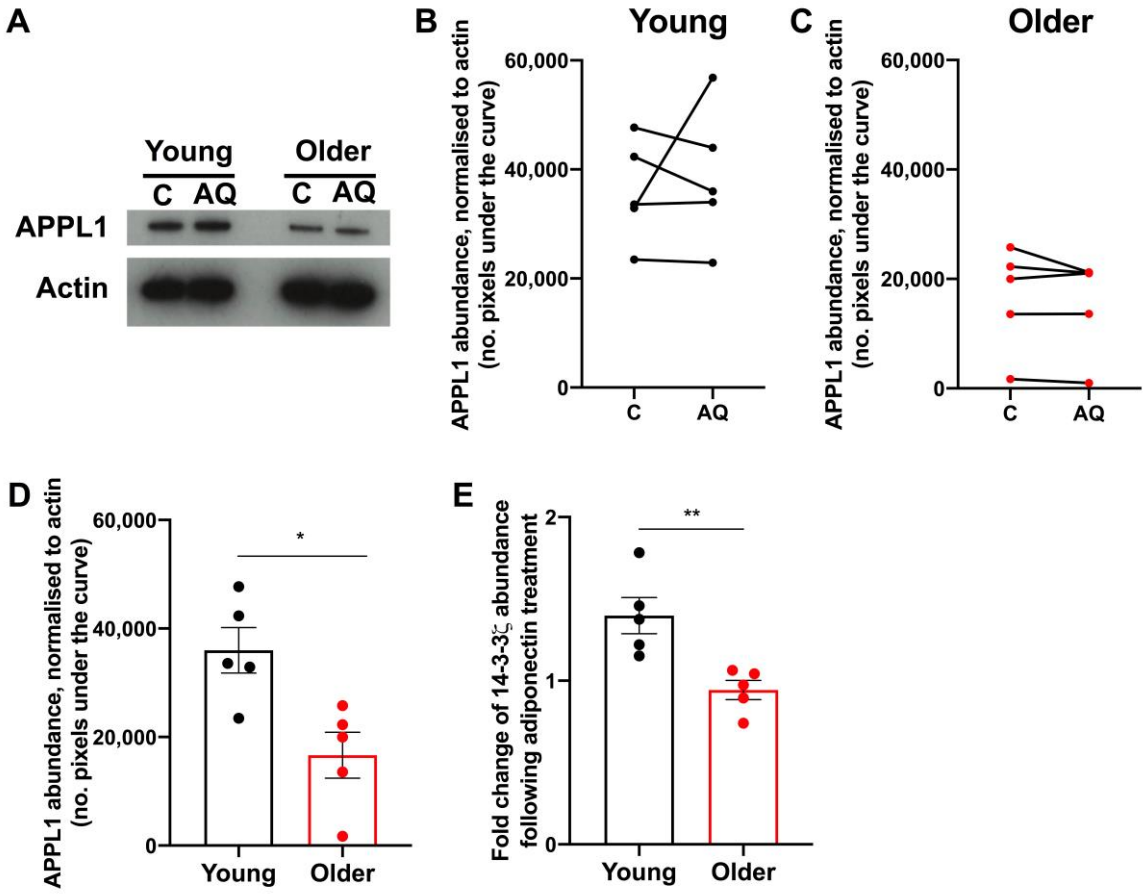

Figure 5-7 Diminished signalling downstream of the AdipoR led to reduced 14-3-3ζ generation by older B-cells

B-cells were isolated from the blood of young (black, n=3) and older (red, n=3) donors and were either left untreated (C) or treated for 15 minutes with adiponectin (AQ). B-cells were then lysed and intracellular proteins were subjected to **(A-D)** western blot and **(E)** LC/MS analysis. **(A)** Representative blots of APPL1 and actin abundance in B-cell lysates. The area under the peak values were calculated for each protein band using Image J and the APPL1 values were normalised to actin values to provide APPL1 abundance for C and AQ-treated B-cell lysates of **(B)** young and **(C)** older donors. **(D)** The abundance of APPL1 normalised to actin for the untreated B-cell lysates of young and older donors. **(E)** The fold-change in 14-3-3ζ abundance in the B-cell lysates of young and older donors in response to AQ-treatment determined by LC/MS. Data are shown as mean ± SEM for n = 3 independent experiments using 6 different B-cell donors. Statistical analysis performed using a paired t-test for B+C, and an unpaired t-test for D+E. *p<0.05

Table 5-7 List of the top 30 upregulated proteins in young and old B-cell following adiponectin treatment

Young donors			Older donors		
UniProt	Description	Average Fold-change	UniProt	Description	Average Fold-change
P84095	Rho-related GTP-binding protein RhoG	38.250	Q9Y251	Heparanase	34.323
Q15691	Microtubule-associated protein RP/EB family member 1	36.751	P46459	Vesicle-fusing ATPase	9.187
Q15848	Adiponectin OS=Homo sapiens	36.238	Q9Y230	RuvB-like 2	3.264
P10515	Dihydrolipoyllysine-residue acetyltransferase component of pyruvate dehydrogenase complex, mitochondrial	35.303	P00390	Glutathione reductase, mitochondrial	2.711
P51149	Ras-related protein Rab-7a	34.996	P48553	Trafficking protein particle complex subunit 10	2.560
Q15181	Inorganic pyrophosphatase	17.169	P98179	RNA-binding protein 3	2.521
O60832	H/ACA ribonucleoprotein complex subunit DKC1	12.237	P22234	Multifunctional protein ADE2	2.170
P10599	Thioredoxin OS=Homo sapiens	9.563	P35232	Prohibitin	2.151
P10599	Thioredoxin	9.563	P61204	ADP-ribosylation factor 3	2.120
P40939	Trifunctional enzyme subunit alpha, mitochondrial	9.477	Q86UE4	Protein LYRIC	1.694
P30041	Peroxiredoxin-6	8.435	P38159	RNA-binding motif protein, X chromosome	1.660
Q96RJ3	Tumor necrosis factor receptor superfamily member 13C	8.411	P18669	Phosphoglycerate mutase 1	1.591
P50995	Annexin A11	7.267	P25789	Proteasome subunit alpha type-4	1.556
P08133	Annexin A6	7.253	P48637	Glutathione synthetase	1.180
P09493	Tropomyosin alpha-1 chain	7.191	P10599	Thioredoxin	1.105
Q16851	UTP--glucose-1-phosphate uridylyltransferase	6.745	P21964	Catechol O-methyltransferase	1.072
O75915	PRA1 family protein 3	6.678	Q9UK53	Inhibitor of growth protein 1	1.029
Q9Y230	RuvB-like 2	6.505	Q9UIA9	Exportin-7	0.942
P42126	Enoyl-CoA delta isomerase 1, mitochondrial	6.344	P85037	Forkhead box protein K1	0.930
O95139	NADH dehydrogenase [ubiquinone] 1 beta subcomplex subunit 6	5.577	Q15404	Ras suppressor protein 1	0.829
P61224	Ras-related protein Rap-1b	2.577	P49137	MAP kinase-activated protein kinase 2	0.801
Q9Y520	Protein PRRC2C	2.490	P59998	Actin-related protein 2/3 complex subunit 4	0.766
P10768	S-formylglutathione hydrolase	2.399	Q15746	Myosin light chain kinase, smooth muscle	0.664
P11766	Alcohol dehydrogenase class-3	2.336	P06753	Tropomyosin alpha-3 chain	0.658
P31943	Heterogeneous nuclear ribonucleoprotein H	2.323	P61158	Actin-related protein 3	0.583
P04439	HLA class I histocompatibility antigen, A alpha chain	2.271	Q9UNH7	Sorting nexin-6	0.499
Q8NBS9	Thioredoxin domain-containing protein 5	1.702	P63261	Actin, cytoplasmic 2	0.465
P07951	Tropomyosin beta chain	1.568	P14854	Cytochrome c oxidase subunit 6B1	0.333
Q99536	Synaptic vesicle membrane protein VAT-1 homolog	1.408	Q13576	Ras GTPase-activating-like protein IQGAP2	0.333
P16109	P-selectin	1.176	Q6UVJ0	Spindle assembly abnormal protein 6 homolog	0.332

A list of the top 30 upregulated proteins in B-cells derived from young and older donors, as determined by unbiased LC/MS analysis. Relative changes in protein abundance between untreated and adiponectin-treated B-cell samples of the same donor were determined using LC/MS and were expressed as relative fold-change. These values were then averaged across donors of the same age group, and the top 30 upregulated proteins determined by unbiased analysis of the LC/MS data are shown (n = 3 donors per age group).

5.3 DISCUSSION

PEPITEM is a regulator of lymphocyte trafficking during inflammation in young hosts (Chimen *et al.*, 2015; Matsubara *et al.*, 2020; Pezhman *et al.*, 2023), but whether PEPITEM regulates lymphocyte trafficking in older hosts had not been explored. Here we showed that PEPITEM limits T-cell trafficking to the peritoneal cavity of young and aged mice during ZIP. We also show that PEPITEM is able to regulate the transmigration of PBL derived from older individuals across cytokine-activated EC *in vitro* to similar levels as PBL derived from young adults.

Previously published work by our lab suggested that the PEPITEM pathway may be dysfunctional in older adults due to an age-related decline in the expression of AdipoR on circulating B-cells (Chimen *et al.*, 2015). Concomitant with those observations, we found that AQ was able to regulate the transendothelial migration of PBL derived from young adults, but not older adults, *in vitro*. Upon further investigation, we found a significant reduction in the frequency of AdipoR1^{+} B-cells in the blood of older adults compared to young. We also found an age-related reduction in the abundance of the adaptor protein immediately downstream of the AdipoR, APPL1, in peripheral blood B-cells. Finally, by using LC/MS techniques, we found older B-cell produced less of the PEPITEM parent protein, 14-3-3ζ, in response to AQ treatment compared to young B-cells. Together, these data indicate that PEPITEM is able to regulate inflammation-driven lymphocyte trafficking in older hosts, but that the pathway becomes dysfunctional with age.

5.3.1 PEPITEM-MEDIATED CONTROL OF LYMPHOCYTE TRAFFICKING DURING INFLAMMATION

PEPITEM has been reported to be a regulator of T-cell trafficking to sites of inflammation in several *in vivo* models, including endotoxin-induced uveitis, a virally induced model of Sjögren's syndrome, a MRL/lpr mouse model of SLE, and obesity (Chimen *et al.*, 2015; Matsubara *et al.*, 2020; Pezhman *et al.*, 2023). Using a model of ZIP, we found that PEPITEM treatment reduced T-cell recruitment to the peritoneal cavity of young mice. This agrees with previously published work by this lab, where Chimen *et al.* reported that PEPITEM treatment reduced T-cell numbers within the peritoneal cavity of young (6-8 weeks) B-cell deficient BALB/c mice during a 48-hour ZIP model (Chimen *et al.*, 2015). However, unlike the data presented in this thesis, Chimen *et al.* reported that PEPITEM treatment did not affect peritoneal $CD19^+$ B-cell, $F4/80^{hi}$ macrophage or $CD11c^+$ DC numbers during the ZIP model (Chimen *et al.*, 2015). These differences could be explained by the different experimental set-up used by Chimen *et al.*, such as the use of a different mouse strain, a higher dose of zymosan (1mg), and an alternative method to quantifying leukocyte populations by flow cytometric analysis (Chimen *et al.*, 2015). Indeed, Matsubara *et al.* reported that PEPITEM-treated young (18 week) MRL/lpr mice presented with fewer numbers of $CD3^+$ T-cells and $F4/80^{hi}$ macrophages in the kidneys compared to control mice, which improved SLE-associated nephritis (Matsubara *et al.*, 2020). Furthermore, Pezhman *et al.* reported that a 6-week PEPITEM treatment resulted in reduced macrophage numbers in the peritoneal cavity of obese C57Bl6 mice compared to untreated mice (Pezhman *et al.*, 2023). Nonetheless, it is clear that PEPITEM can regulate T-cell trafficking *in vivo* in the context of several models of inflammation. However, no studies

have investigated whether PEPITEM is a regulator of T-cell trafficking in ageing. For the first time, we report in this thesis that the PEPITEM-mediated control of T-cell trafficking extends to older hosts in the context of *in vivo* and *in vitro* models of inflammation.

5.3.2 PEPITEM PATHWAY DYSFUCNTION IN AGEING

Studies investigating the effect of ageing on PEPITEM pathway functionality are limited (Chimen *et al.*, 2015). We observed modulated responses of older PBL to AQ treatment *in vitro* compared to younger PBL, where AQ failed to control the transendothelial migration of PBL derived from older individuals. When the expression of AdipoR on circulating B-cells of young and older donors was assessed using flow cytometry, we found an age-related reduction in the frequency of AdipoR1^{+} B-cells. This is in agreement with previously published data by this lab, where Chimen *et al.* reported an age-related reduction in the frequency of AdipoR1^{+} B-cells in healthy adults (Chimen *et al.*, 2015). However, unlike the data reported in this thesis, Chimen *et al.* also reported an age-related reduction in the frequency of AdipoR2-expressing peripheral blood B-cells (Chimen *et al.*, 2015). It is possible that these differences could be explained by a larger sample size (n=40) comprised of male and female donors utilised by Chimen *et al.* compared to the smaller sample size (n=18) and assessment of a single sex in this thesis. Nonetheless, the r^2 values, which measures the strength of the relationship between ageing and AdipoR1 expression on circulating B-cells, was not particularly strong in this thesis (r^2<0.234, **Figure 5-4**), nor within the previously published work (r^2<0.311) (Chimen *et al.*, 2015). To that end, we investigated age-related changes downstream of the AdipoR in B-cells which may have driven modulated responses to AQ.

APPL1 is the intracellular signalling component immediately downstream of the AdipoR (Mao *et al.*, 2006; Cheng *et al.*, 2007), but its expression in B-cells has not been investigated. We therefore assessed the relative protein abundance of APPL1 in B-cells derived from young and older donors by western blotting. We found that B-cells did indeed express the APPL1 protein, and that AQ treatment of the B-cells did not significantly change APPL1 abundance regardless of the age of the B-cell donor. This is in line with the work of Mao *et al.* who found that the abundance of APPL1 in C2C12 myotubes did not change following AQ treatment (Mao *et al.*, 2006). Although it did not reach statistical significance, we observed an age-related decline in the abundance of APPL1 in untreated peripheral blood B-cells. This agrees with the recently published single-cell RNA sequencing data of PBMC, where Zheng *et al.* reported a significant reduction in the gene expression of APPL1 in the circulating B-cells of older (>60 years) adults compared to young (<45 years) adults (Zheng *et al.*, 2020). An age-related reduction in APPL1 abundance would suggest that the signalling downstream of the AdipoR following AQ stimulation would be diminished in older B-cells.

Several of the signalling components downstream of the AdipoR are evidently downregulated with age in terms of expression and/or signalling capacity across multiple cell types (Iemitsu *et al.*, 2002; Poynter and Daynes, 1998; Shin *et al.*, 2016; Salminen, Kaarniranta and Kauppinen, 2016). Piao *et al.* reported reduced protein expression of AdipoR1, AMPK and PPARα in HUVEC that had undergone 18-20 doublings compared to cells that had undergone 5-8 doublings, which led to an age-related inactivation of AQ/AdipoR1 signalling cascade (Piao *et al.*, 2018). The messenger RNA levels of PPARα in upper-inner arm skin samples derived from older (>70 years) men were significantly reduced compared to skin samples of younger (<29

years) men, measured by real-time polymerase chain reaction (Shin *et al.*, 2016). Furthermore, the activity and phosphorylation rates of AMPK were reportedly reduced in the *vatus lateralis* muscle of older (>64 years) healthy men compared to young (<40 years) men, although the physiological relevance of this was not established (Li *et al.*, 2012). Although these studies did not investigate leukocytes specifically, the age-related reduction in the expression and signalling of these components across different cell types suggest a diminished capacity of older cells to signal downstream of the AdipoR. Further investigation is needed to assess the impact of ageing on the abundance and signalling of these signalling components in B-cells in the context of the PEPITEM pathway.

AQ-AdipoR signalling results in the transcription and translation of *YWHAZ* to produce 14-3-3ζ, the parent protein of PEPITEM (see Section 1.4.2). Using an LC/MS approach, we found that older B-cells produced significantly less 14-3-3ζ compared to young B-cells following AQ treatment. Whilst we believe these differences are due to subdued signalling events within older B-cells following AQ-AdipoR engagement, it must be noted that the LC/MS data only provides relative data (i.e. comparing protein abundance between samples from the same donor) and so levels of 14-3-3ζ expression could not be compared between donors. This is of interest as mining the AgeAnno gene knowledgebase (AgeAnno, 2022) revealed that *YWHAZ* gene expression was significantly reduced in naïve B-cells derived from the blood of older (>60 years) adults compared to younger (<59 years) adults in the steady state (Huang *et al.*, 2022). It is therefore possible that the peripheral blood B-cells of older adults generate less 14-3-3ζ prior to and post AQ engagement of the AdipoR. Collectively, these data describe the age-related decline in AQ-AdipoR signalling in B-cells that

leads to reduced 14-3-3ζ production. Reduced levels of the parent protein would indicate reduced production of PEPITEM itself by older B-cells, although it will be necessary to measure PEPITEM production by young and older B-cells to confirm these observations. The data presented in this thesis ultimately describe the dysfunction of the PEPITEM pathway in ageing.

5.4 CONCLUSIONS

The PEPITEM pathway regulates lymphocyte trafficking in the context of inflammation in young hosts (Chimen *et al.*, 2015; Matsubara *et al.*, 2020), however, whether PEPITEM regulates inflammation-mediated lymphocyte trafficking in older hosts had not been investigated. The main aims of this section were to determine whether PEPITEM is able to regulate T-cell trafficking in older mice and humans through the use of *in vivo* and *in vitro* models of inflammation, and to determine whether the ageing process was associated with PEPITEM pathway dysfunction. A schematic summary of Chapter 5 can be found in **Figure 5-8**. Overall, we found that PEPITEM was able to regulate inflammatory T-cell trafficking in young and older hosts. However, ageing was associated with dysregulated responses of PBL to AQ, which resulted in the loss of PEPITEM-mediated control of lymphocyte trafficking. Through various analytical techniques, we found that the circulating B-cells of older adults expressed less of the AdipoR (AdipoR1), less of the AdipoR adaptor protein (APPL1), and generated less of the PEPITEM parent protein (14-3-3ζ) in response to AQ stimulation compared to the B-cells of young adults. Collectively these data indicate that although PEPITEM can control inflammation-driven lymphocyte trafficking in older hosts, its generation is reduced due to the intrinsic changes that occur within ageing B-cells that affect AQ-AdipoR signalling. PEPITEM pathway dysfunction could contribute to dysregulated

lymphocyte trafficking in older individuals, ultimately aiding to the development of age-related inflammatory diseases.

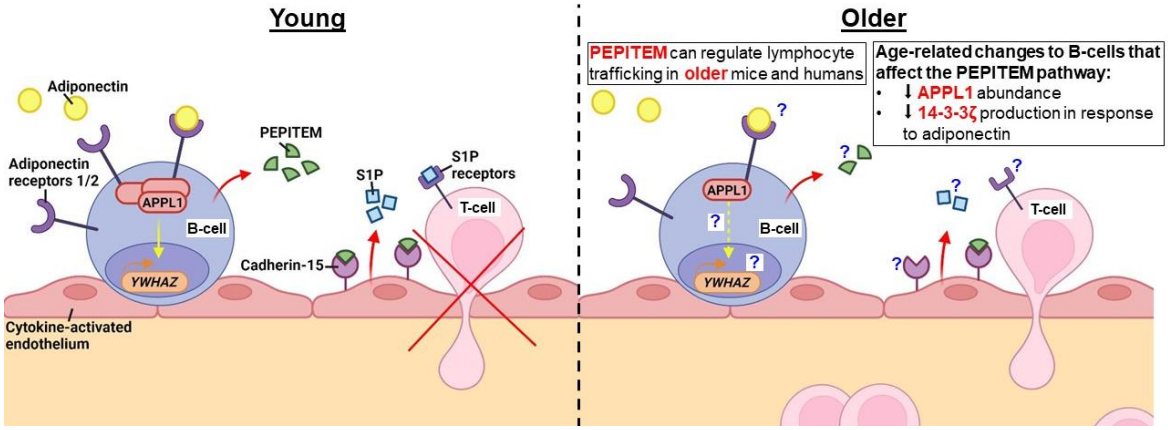

Figure 5-8 Age-related dysfunction of the PEPITEM pathway

A schematic depicting the major findings of Chapter 5. Using the *in vivo* zymosan-induced peritonitis model and *in vitro* static adhesion assay, we found that PEPITEM could regulate lymphocyte trafficking during acute inflammation in older mice and humans. However, the PEPITEM pathway appeared dysfunctional in older adults. Adiponectin could not regulate the transendothelial migration of peripheral blood lymphocytes derived from older donors *in vitro*. We found that B-cells from older donors expressed less adiponectin receptor 1 on the cell surface and less of the intracellular adaptor protein immediately downstream of the adiponectin receptors, APPL1. These age-related changes to B-cells had functional consequences for the PEPITEM pathway, with B-cells derived from older donors generating less of the PEPITEM parent protein, 14-3-3ζ, in response to adiponectin. Collectively these data suggest that the PEPITEM pathway is dysfunctional in older individuals, specifically at the initiation phase, which may contribute to dysregulated lymphocyte trafficking in ageing. Remaining questions (depicted by **?**) include whether ageing modulates: adiponectin-adiponectin receptor binding/signal transduction, signalling downstream of APPL1 in B-cells, the transcription of 14-3-3ζ (*YWHAZ*) in B-cells, PEPITEM production by B-cells, cadherin-15 expression by endothelium, sphingosine-1-phosphate (S1P) generation by endothelium, S1P receptor expression by T-cells, and whether there is sexual dimorphism within the age-related changes to the PEPITEM pathway. Created with BioRender.com

5.5 LIMITAITIONS

Whilst these studies provide a first look at PEPITEM-mediated control of leukocyte trafficking in ageing, they do have limitations. Firstly, the ZIP studies lacked a control peptide group. A control peptide, such as a scrambled version of the PEPITEM amino acid sequence, would have demonstrated that the leukocyte trafficking-suppressing effects of PEPITEM were specific to the peptide and not a consequence of exogenous peptide administration. Secondly, basic measurements of PEPITEM in human and murine samples could not be made due to a lack of sensitivity of current detection methods. The small size (14 amino acids) and low concentration of PEPITEM (approximately 1.5ng/ml in human serum) in biological samples render quantitative methods such as indirect ELISAs and western blotting ineffective, and so the current approach to detect the peptide is LC/MS. However, issues with the sample preparation protocol and instrument set-up have meant that no measurements could be made for the duration of this project. Consequently, we could not gauge age-related changes to circulating levels of PEPITEM in humans/mice, nor age-related changes to PEPITEM production by B-cells.

For the B-cell studies, one limitation was the purity of the B-cell samples. Despite several attempts to optimise kit-based cell isolation protocols, B-cell samples always contained some level of platelet contamination, and this contamination varied between donors (approx. 10-40% contamination). This must be considered when interpreting the data.

CHAPTER 6 – GENERAL DISCUSSION

6.1 SUMMARY OF FINDINGS

The first part of this thesis aimed to explore the effects of age and sex on leukocyte trafficking using *in vitro* and *in vivo* models of homeostasis and inflammation. We were amongst the first to explore the sexually dimorphic immunological changes that occur within the peritoneal cavity of ageing mice, which suggested age-related and sex-specific changes to homeostatic leukocyte trafficking through this tissue. By using *in vivo* and *in vitro* models of acute inflammation, we next investigated age-related changes to lymphocyte trafficking and found that ageing modulated this process in a sex-specific manner. The second part of this thesis aimed to explore PEPITEM-mediated control of inflammatory leukocyte trafficking in ageing, and whether the PEPITEM pathway was affected by the ageing process. We investigated PEPITEM-mediated control of leukocyte trafficking in aged hosts using *in vivo* and *in vitro* models of inflammation, and found an age-related dysregulation of the PEPITEM pathway. To explore the mechanisms driving this dysfunction, we investigated age-related changes to signalling components downstream of the AdipoR in B-cells. The main findings from this thesis are as follows:

- Aged mice had a modulated leukocyte composition within the peritoneal cavity, which was associated with low-grade inflammation. Importantly, this was more prominent in female mice.
- The vasculature within the peritoneal membrane of aged mice displayed increased permeability and had a modulated structure, potentially facilitating increased leukocyte trafficking to the peritoneal cavity of aged mice in the steady state by allowing pro-inflammatory mediators within the cavity to escape.

- Aged mice presented with an exacerbated inflammatory response to zymosan challenge that resulted in increased leukocyte recruitment to the peritoneal cavity. Again, this was more prominent in female mice.
- Ageing did not affect the ability of PBL to adhere to nor migrate across inflamed EC in an *in vitro* static adhesion assay but changed the composition of migrating PBL.
- PEPITEM treatment suppressed lymphocyte trafficking *in vivo* and *in vitro* models of acute inflammation.
- AQ failed to control the transendothelial migration of older PBL *in vitro*, suggesting that ageing is associated with PEPITEM pathway dysfunction.
- Older B-cells had a diminished capacity to signal downstream of the AdipoR, due to reduced expression of AdipoR1 and APPL1, which led to an inability of older B-cells to produce the PEPITEM parent protein, 14-3-3ζ, post-AQ stimulation.

6.2 SIGNIFICANCE OF FINDINGS

Chronic inflammation is one of the major drivers of inflammatory disease (reviewed by Furman *et al.*, 2019). With the establishment of low-grade chronic inflammation in ageing individuals (inflammageing), the risk of developing inflammatory disease increases (Yang *et al.*, 2016; Syed *et al.*, 2022). As of such, several inflammatory diseases affect the older population (Chung *et al.*, 2019). These include T-cell−mediated inflammatory diseases such as RA, inflammatory bowel diseases (IBD), and T1DM (Safiri *et al.*, 2019; Collaborators, 2020; King, Aubert and Herman, 1998; Gregory *et al.*, 2022). Although the etiology of these diseases is not completely understood, inappropriate T-cell activation and aberrant T-cell trafficking into tissue is

thought to play a central role (Barbera Betancourt *et al.*, 2017; Giuffrida and Di Sabatino, 2020). Importantly, some of these diseases display age- and sex-bias. Indeed, RA and IBD primarily affect older women (Safiri *et al.*, 2019; Collaborators, 2020), although the prevalence of RA becomes comparable between men and women with ageing (Goemaere *et al.*, 1990). Interestingly, a study by Kato *et al.* found that the age of RA onset has gradually increased between 2002 and 2013 in Japan and is thought to be a consequence of changes in environmental factors (Kato *et al.*, 2017). With the burden of inflammatory diseases growing amongst older adults worldwide (Safiri *et al.*, 2019; Collaborators, 2020; Gregory *et al.*, 2022), efforts are needed to improve our understanding of basic ageing immunology to maximise the success of therapeutic intervention (reviewed by Ermogenous *et al.*, 2020). For example, understanding how the ageing process affects the trafficking patterns of leukocytes under homeostatic conditions is a prerequisite to understanding how these patterns change upon the induction of inflammation and the establishment of disease. The observations outlined in this thesis not only add to the knowledge of age-related changes to leukocyte trafficking dynamics, but emphasise how sex can also influence these processes. To that end, both age-related and sex-specific changes to immune system function should be considered when prescribing therapeutics for inflammatory diseases to older adults to improve the success of treatment.

Antibodies have long been used in the fight against T-cell−mediated inflammatory diseases, where their therapeutic effects range from interfering with T-cell trafficking patterns (e.g. natalizumab), to inhibiting T-cell activation (e.g. abatacept), to T-cell depletion (e.g. teplizumab) (Kim, Choe and Lee, 2022; Park and Jeen, 2018; Sherry *et al.*, 2011). However, the success of these treatments varies in

terms of efficacy and off-target effects. For example, natalizumab is a humanised monoclonal antibody that binds the α_4 integrin subunit, and is an approved treatment for Crohn's disease (Armuzzi and Felice, 2013). Through binding VLA-4 and LPAM-1 on lymphocytes and blocking their interactions with endothelial-expressed ligands, natalizumab suppresses B- and T-cell entry into the disease site and alleviates disease symptoms (Gordon *et al.*, 2001). However, this biologic has a profound adverse effect. Long-term use of natalizumab can result in the development of a demyelinating disease, namely natalizumab-related progressive multifocal leukoencephalopathy (nrPML), caused by John Cunningham virus (JCV) infiltration of the central nervous system (Tan and Koralnik, 2010). Interestingly the development of nrPML exhibits sex and age bias, with older men more likely to develop the disease due to accelerated JCV seroconversion (Dwyer *et al.*, 2021; Prosperini *et al.*, 2017). The use of this antibody-based therapy is therefore not appropriate for older patients, particularly older male patients.

One of the most successful biologics used in the treatment of RA is abatacept, a modified antibody with a CTLA4 extracellular domain (Malmstrom, Trollmo and Klareskog, 2005). Abatacept blocks the co-stimulation of T-cells by binding CD80/86 on APC, thus inhibiting T-cell activation and subsequently suppressing the generation of autoantibodies that drive disease pathology (Malmstrom, Trollmo and Klareskog, 2005). Importantly, the efficacy of abatacept in patients with RA (~54% response rate) does not differ between men and women (Nourisson *et al.*, 2017). However, despite moderate efficacy, pro-longed abatacept treatment (>12 months) is associated with an increased risk of serious infection (Maxwell and Singh, 2009). Given that older individuals already have an increased risk of infection due to the age-related

senescence of the immune system (Derhovanessian *et al.*, 2008), therapeutics that increase the risk of serious infection are not appropriate for older patients.

Although much progress has been made in the treatment of inflammatory diseases, expanding the arsenal of therapeutics is still necessary to overcome the limitations of available treatments. Antibody-based therapies aid in the treatment of inflammatory disease, but are expensive to produce, have undesirable off-target effects/adverse reactions, and have limited success as a long-term treatment (Samaranayake *et al.*, 2009; Lu *et al.*, 2020). In this thesis we highlight a role for PEPITEM, an immunoregulatory peptide, in the control of inflammatory T-cell trafficking in young and older hosts. Whilst other components of the PEPITEM pathway, such as AQ and S1P, could also offer therapeutic potential in the control of inflammatory T-cell trafficking, they are likely to have several off-target effects due to their broad biological functions (described in Section 1.4). Indeed, AQ plays a central role in metabolic processes, including glucose metabolism and insulin sensitivity (Straub and Scherer, 2019), whilst S1P regulates T-cell trafficking through SLOs (Baeyens *et al.*, 2015). On the other hand, by using an acute *in vivo* model of inflammation, we have shown a high efficacy of PEPITEM in regulating T-cell trafficking in the absence of any obvious undesirable off-target effects or toxicity. This was also shown by others using various models of inflammation and disease (Chimen *et al.*, 2015; Matsubara *et al.*, 2020; Pezhman *et al.*, 2023), however the long-term off-target effects of PEPITEM are not currently known and should be investigated. Whilst considerable research is still needed to explore the therapeutic potential of PEPITEM, we believe that PEPITEM-based therapeutics would be highly desirable. The high potency of PEPITEM and cheaper production costs associated with peptides means

that PEPITEM-based therapeutics would be more cost effective compared to current antibody-based therapies. Importantly, PEPITEM would not operate through the traditional therapeutic paradigm of inhibiting pathological processes, but would re-establish the endogenous homeostatic pathways that control leukocyte trafficking.

PEPITEM-mediated control of leukocyte trafficking was initially described to be specific to T-cells, however, we and others (Matsubara *et al.*, 2020; Pezhman *et al.*, 2023) have shown that the effects of the peptide extend to other leukocyte types. Using a mouse model of SLE, Matsubara *et al.* reported that PEPITEM-treatment reduced the number of T-cells and macrophages in the kidneys of young (18 week) MRL/lpr mice (Matsubara *et al.*, 2020). Furthermore, Pezhman *et al.* reported reduced numbers of macrophages in the peritoneal cavity of obese 8 week-old male C57Bl6 mice following a 6-week treatment with PEPITEM (Pezhman *et al.*, 2023). Indeed, we found that intraperitoneal delivery of PEPITEM reduced the number of T-cells, DC, eosinophils, and macrophages in the peritoneal cavity of mice following acute inflammation. Therefore, PEPITEM evidently affects leukocytes of the myeloid lineage at the site of administration, in an inflammatory context. Part of the basic research into the therapeutic potential of PEPITEM should include investigating how different leukocyte types interact with the peptide under homeostatic and inflammatory conditions, and whether PEPITEM modulates the immune functions of these leukocytes.

We have demonstrated the ability of PEPITEM to regulate the trafficking of older leukocytes *in vivo* an *in vitro*, however, these were just two models of inflammation. Multiple models of acute inflammation, chronic inflammation, and inflammatory disease in older systems are required to scrutinise the ability of PEPITEM to regulate leukocyte

trafficking in older hosts. Importantly, as we have observed sex-specific changes in leukocyte trafficking dynamics, these models should consider biological sex and should assess whether the effects of PEPITEM display sex-specific bias depending on the inflammatory model. Crucially, we cannot yet conclude the effects of ageing on endogenous PEPITEM production. Whilst the data presented in this thesis suggest older B-cells produce less PEPITEM, one of the major limitations of the experimental set-up is the lack of endogenous PEPITEM quantification. Although this limitation was due to technical issues with the PEPITEM detection and quantification methods, this is a fundamental limitation that needs to be addressed to assess the age-related changes to circulating levels of endogenous PEPITEM, and the production of PEPITEM by older B-cells in the context of homeostasis and inflammation.

In vivo data previously generated by our lab revealed that PEPITEM is rapidly cleared by the kidneys (within minutes) upon administration into the circulation (Apta, 2015). Indeed, due to their simple structures, small peptides are vulnerable to proteolytic degradation in the blood, kidneys and liver (Werle and Bernkop-Schnurch, 2006). For PEPITEM to be a viable therapeutic agent, its *in vivo* half-life would need to be dramatically extended to maximise the time it has to exert its effects. This is possible through modifications to its chemical structure, such as pegylation to protect the peptide from enzymatic degradation (Veronese and Pasut, 2005). For this reason, a pegylated version of PEPITEM with similar efficacy to the native peptide (data unpublished) was synthesised and used in the *in vivo* studies outlined in this thesis. We used a fixed amount of pegylated-PEPITEM in these experiments (300µg/dose) to mirror the previously published studies (Chimen *et al.*, 2015), however, a dose-response for the pegylated peptide was not performed and remains a limitation of the

experimental design. Data previously generated by this lab demonstrated that a dose as low as 10µg pegylated-PEPITEM can control neutrophil trafficking during a 4-hour ZIP (unpublished), but the minimal amount of pegylated-PEPITEM needed to control T-cell trafficking during a 48-hour ZIP is currently unknown. Additional pharmacokinetic data is needed for the pegylated version of PEPITEM including the long-term off-target effects/adverse reactions and toxicology.

Finally, to harness the effects of PEPITEM, the active components of the sequence were identified by our lab through amino acid substitution studies, alanine sweeps and peptide truncations (unpublished). Two pharmacophores were identified in the PEPITEM sequence, namely the amino acids SVT and QGA, which displayed greater stability and efficacy compared to the parent peptide (unpublished). Research is currently ongoing to develop these tripeptides as therapeutics. Chemical modifications to peptide sequences, such as substituting amino acids with unnatural analogues (Qvit *et al.*, 2017), forming disulphide bonds within the structure (Furman, Chiu and Hunter, 2015; Hagihara and Saerens, 2014), and acylation (Aicart-Ramos, Valero and Rodriguez-Crespo, 2011), have long been used by drug companies to improve the efficacy and stability of peptide therapeutics. For example, substitution of L-arginine with D-arginine greatly improved the efficacy of desmopressin, a synthetic small peptide derivative of the anti-diuretic hormone vasopressin, compared to the parent peptide by 10-fold (Ozgonenel, Rajpurkar and Lusher, 2007). Therefore, studies investigating how chemical modifications to the tripeptide structures influence their potency, solubility and stability are currently being undertaken. Concomitantly, *in vitro* and *in vivo* models of lymphocyte trafficking are being used to assess the potency,

specificity, and efficacy of these modulated tripeptides compared to the parent protein, PEPITEM.

6.3 SUMMARY OF THE THESIS

In this thesis we explored age-related and sex-specific changes to leukocyte trafficking patterns *in vivo* and *in vitro*. We found that ageing increased leukocyte trafficking through the peritoneal cavity of mice in the steady state, particularly in aged female mice, and is associated with the increased permeability of the peritoneal membrane vasculature. Using ZIP as a model of acute inflammation, we observed an exacerbated inflammatory response to zymosan challenge in aged mice, particularly in aged female mice, where increased numbers of leukocytes were recruited to the inflamed peritoneal cavity. Under inflammatory conditions, we found that PEPITEM could control the trafficking of leukocytes derived from older hosts *in vivo* and *in vitro*. However, the PEPITEM pathway was evidently dysfunctional in older individuals. This was driven by diminished signalling downstream of the AdipoR in older B-cells, leading to reduced production of the PEPITEM parent protein. A graphical summary of this thesis can be found in **Figure 6-1**. In conclusion, we report that the age-related changes to leukocyte trafficking dynamics *in vivo* are sexually dimorphic. We have demonstrated a role for PEPITEM in controlling the trafficking of leukocytes in older mice and humans in the context of inflammation. Finally, we have identified age-related changes to signalling components within the PEPITEM pathway paradigm which may be exploited for therapeutic intervention of inflammatory processes in older adults, such as the treatment of age-related inflammatory diseases.

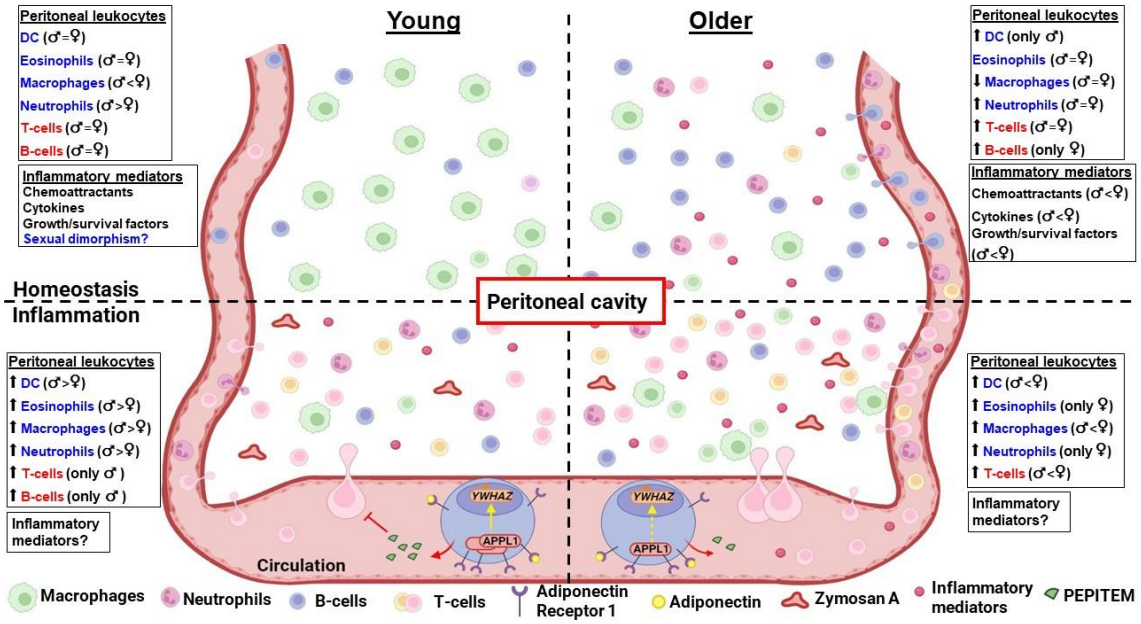

Figure 6-1 Graphical summary of this thesis

Under homeostatic conditions, there are increased numbers of leukocytes and increased levels of inflammatory mediators within the peritoneal cavity of aged mice, particularly aged female mice, compared to young. This was associated with increased permeability of the peritoneal membrane vasculature in aged mice. During acute inflammation (zymosan-induced peritonitis), more leukocytes are recruited the peritoneal cavity of aged mice, particularly aged female mice, compared to young. This could be in part due to the age-related dysregulation of the PEPITEM pathway. B-cells derived from older donors express less adiponectin receptor 1 on the surface and less APPL1 intracellularly compared to young B-cells. Consequently, adiponectin stimulation of the adiponectin receptors leads to reduced production of the PEPITEM parent protein, 14-3-3ζ. Ultimately, the intrinsic age-related changes that occur in B-cells drive PEPITEM pathway dysfunction in ageing. Targeting the PEPITEM pathway may therefore offer a potential therapeutic avenue to treat inflammatory diseases in older adults by restoring regulated leukocyte trafficking. Created with BioRender.com

6.4 FUTURE WORK

Whilst the studies in this thesis were designed to shed light on PEPITEM-mediated control of leukocyte trafficking processes in ageing, additional work is needed to expand upon these findings. We must:

- Validate the cytokine array data by quantifying some of the pro-inflammatory mediators in the peritoneal cavity of young and aged naïve mice.
- Investigate the permeability and structure of the peritoneal membrane vasculature in young and aged male mice.
- Confirm that ageing is associated with increased leukocyte trafficking into the peritoneal cavity in the steady state. This could be visualised in real-time using IVM.
- Determine whether age-related changes to lymphocyte trafficking across activated endothelium can be observed *in vitro* when:
    - The EC are pre-treated with the autologous serum of the donor, given that older individuals have increased circulating levels of pro-inflammatory mediators
    - The EC are derived from an older donor, to age match the PBL and EC donors
    - The EC are senescent, given that there are more senescent cells in older individuals
- Establish whether the kinetics of the ZIP model are different in old mice i.e. assess leukocyte recruitment to the cavity at different time points.

- Validate the effects of PEPITEM on leukocyte trafficking *in vivo* by using a scrambled or control peptide for comparison.
- Investigate whether PEPITEM can modulate homeostatic leukocyte trafficking processes in young and old mice under steady state.
- Perform additional work for the B-cell studies. This includes:
    - Further optimisation to improve the purity of the B-cell samples.
    - Assessing age-related changes to the abundance of signalling of components downstream of APPL1 in B-cells to determine if there are more intrinsic changes that drive PEPITEM pathway dysfunction in ageing.
    - Quantifying PEPITEM production by young and older B-cells following AQ-treatment.
- Investigate whether B-cells derived from older women retain expression of AdipoR1 and APPL1, therefore providing a potential mechanism for the sexual dimorphism in age-related changes to PEPITEM pathway function that we have observed.
- Assess whether circulating levels of PEPITEM are modulated with age in mice and humans.

REFERENCES

Abbas, M. *et al.* (2017) Endothelial Microparticles From Acute Coronary Syndrome Patients Induce Premature Coronary Artery Endothelial Cell Aging and Thrombogenicity: Role of the Ang II/AT1 Receptor/NADPH Oxidase-Mediated Activation of MAPKs and PI3-Kinase Pathways. *Circulation,* 135(3), p 280-296. doi: 10.1161/CIRCULATIONAHA.116.017513.

Adamczak, M. *et al.* (2005) Ageing and plasma adiponectin concentration in apparently healthy males and females. *Clin Endocrinol (Oxf),* 62(1), p 114-118. doi: 10.1111/j.1365-2265.2004.02182.x.

Agace, W. W. (2006) Tissue-tropic effector T cells: generation and targeting opportunities. *Nat Rev Immunol,* 6(9), p 682-692. doi: 10.1038/nri1869.

AgeAnno (2022) Available at: https://relab.xidian.edu.cn/AgeAnno/#/

Agius, E. *et al.* (2009) Decreased TNF-alpha synthesis by macrophages restricts cutaneous immunosurveillance by memory CD4+ T cells during aging. *J Exp Med,* 206(9), p 1929-1940. doi: 10.1084/jem.20090896.

Agrawal, A. *et al.* (2007) Altered innate immune functioning of dendritic cells in elderly humans: a role of phosphoinositide 3-kinase-signaling pathway. *J Immunol,* 178(11), p 6912-6922. doi: 10.4049/jimmunol.178.11.6912.

Ahluwalia, A. *et al.* (2013) An imbalance between VEGF and endostatin underlies impaired angiogenesis in gastric mucosa of aging rats. *Am J Physiol Gastrointest Liver Physiol,* 305(4), p G325-332. doi: 10.1152/ajpgi.00127.2013.

Ahluwalia, A. *et al.* (2014) Aging impairs transcriptional regulation of vascular endothelial growth factor in human microvascular endothelial cells: implications for angiogenesis and cell survival. *J Physiol Pharmacol,* 65(2), p 209-215. doi:

Ahmad, M. *et al.* (1995) Cell type-specific transactivation of the VCAM-1 promoter through an NF-kappa B enhancer motif. *J Biol Chem,* 270(15), p 8976-8983. doi: 10.1074/jbc.270.15.8976.

Ahmed, M. *et al.* (2009) Clonal expansions and loss of receptor diversity in the naive CD8 T cell repertoire of aged mice. *J Immunol,* 182(2), p 784-792. doi: 10.4049/jimmunol.182.2.784.

Ahmed, S. R. *et al.* (2011) Prostaglandin D2 regulates CD4+ memory T cell trafficking across blood vascular endothelium and primes these cells for clearance across lymphatic endothelium. *J Immunol,* 187(3), p 1432-1439. doi: 10.4049/jimmunol.1100299.

Aicart-Ramos, C., Valero, R. A. and Rodriguez-Crespo, I. (2011) Protein palmitoylation and subcellular trafficking. *Biochim Biophys Acta,* 1808(12), p 2981-2994. doi: 10.1016/j.bbamem.2011.07.009.

Ajuwon, K. M. and Spurlock, M. E. (2005) Adiponectin inhibits LPS-induced NF-kappaB activation and IL-6 production and increases PPARgamma2 expression in adipocytes. *Am J Physiol Regul Integr Comp Physiol,* 288(5), p R1220-1225. doi: 10.1152/ajpregu.00397.2004.

Akbar, A. N., Henson, S. M. and Lanna, A. (2016) Senescence of T Lymphocytes: Implications for Enhancing Human Immunity. *Trends Immunol,* 37(12), p 866-876. doi: 10.1016/j.it.2016.09.002.

Al-Attar, A. *et al.* (2016) Data correlations between gender, cytomegalovirus infection and T cells, NK cells, and soluble immune mediators in elderly humans. *Data Brief,* 8(p 536-544. doi: 10.1016/j.dib.2016.06.006.

Allen, S. L. *et al.* (2021) The effect of young and old ex vivo human serum on cellular protein synthesis and growth in an in vitro model of aging. *Am J Physiol Cell Physiol,* 321(1), p C26-C37. doi: 10.1152/ajpcell.00093.2021.

Alon, R. and Nourshargh, S. (2013) Learning in motion: pericytes instruct migrating innate leukocytes. *Nat Immunol,* 14(1), p 14-15. doi: 10.1038/ni.2489.

Alonso Villela, S. M. *et al.* (2020) A protocol for recombinant protein quantification by densitometry. *Microbiologyopen,* 9(6), p 1175-1182. doi: 10.1002/mbo3.1027.

Alpert, A. *et al.* (2019) A clinically meaningful metric of immune age derived from high-dimensional longitudinal monitoring. *Nat Med,* 25(3), p 487-495. doi: 10.1038/s41591-019-0381-y.

Amezcua Vesely, M. C. *et al.* (2012) FcgammaRIIb and BAFF differentially regulate peritoneal B1 cell survival. *J Immunol,* 188(10), p 4792-4800. doi: 10.4049/jimmunol.1102070.

Ancellin, N. *et al.* (2002) Extracellular export of sphingosine kinase-1 enzyme. Sphingosine 1-phosphate generation and the induction of angiogenic vascular maturation. *J Biol Chem,* 277(8), p 6667-6675. doi: 10.1074/jbc.M102841200.

Antonelli, A. *et al.* (2006) Increase of CXC chemokine CXCL10 and CC chemokine CCL2 serum levels in normal ageing. *Cytokine,* 34(1-2), p 32-38. doi: 10.1016/j.cyto.2006.03.012.

Apta, B. H., Chimen, M. and McGettrick, H. M. (2017). *Endocrine Regulation of Lymphocyte Trafficking In Vitro*. In: T-cell Trafficking. Humana Press, New York, 101-119.

Apta, B. H. R. (2015) '*Investigating the structure and function of PEPITEM, a novel inhibitor of T cell transmigration*', PhD thesis, University of Birmingham, Birmingham.

Arita, Y. *et al.* (1999) Paradoxical decrease of an adipose-specific protein, adiponectin, in obesity. *Biochem Biophys Res Commun,* 257(1), p 79-83. doi: 10.1006/bbrc.1999.0255.

Armuzzi, A. and Felice, C. (2013) Natalizumab in Crohn's disease: past and future areas of applicability. *Ann Gastroenterol,* 26(3), p 189-190. doi:

Arnardottir, H. H. *et al.* (2014) Aging delays resolution of acute inflammation in mice: reprogramming the host response with novel nano-proresolving medicines. *J Immunol,* 193(8), p 4235-4244. doi: 10.4049/jimmunol.1401313.

Arsenovic-Ranin, N. *et al.* (2019) Influence of aging on germinal centre reaction and antibody response to inactivated influenza virus antigens in mice: sex-based differences. *Biogerontology,* 20(4), p 475-496. doi: 10.1007/s10522-019-09811-8.

Ashina, K. *et al.* (2015) Histamine Induces Vascular Hyperpermeability by Increasing Blood Flow and Endothelial Barrier Disruption In Vivo. *PLoS One,* 10(7), p e0132367. doi: 10.1371/journal.pone.0132367.

Aspinall, R. and Andrew, D. (2001) Gender-related differences in the rates of age associated thymic atrophy. *Dev Immunol,* 8(2), p 95-106. doi: 10.1155/2001/17064.

Atzmon, G. *et al.* (2008) Adiponectin levels and genotype: a potential regulator of life span in humans. *J Gerontol A Biol Sci Med Sci,* 63(5), p 447-453. doi: 10.1093/gerona/63.5.447.

Azuma, M., Phillips, J. H. and Lanier, L. L. (1992) CD28 co-stimulation of T-cell-mediated cytotoxicity. *Int J Cancer Suppl,* 7(p 33-35. doi:

Baeyens, A. *et al.* (2015) Exit Strategies: S1P Signaling and T Cell Migration. *Trends Immunol,* 36(12), p 778-787. doi: 10.1016/j.it.2015.10.005.

Bahjaoui-Bouhaddi, M. *et al.* (1997) Localized deposition of M-cadherin in the glomeruli of the granular layer during the postnatal development of mouse cerebellum. *J Comp Neurol,* 378(2), p 180-195. doi:

Bahra, P. *et al.* (1998) Each step during transendothelial migration of flowing neutrophils is regulated by the stimulatory concentration of tumour necrosis factor-alpha. *Cell Adhes Commun,* 6(6), p 491-501. doi: 10.3109/15419069809010797.

Bain, C. C. *et al.* (2020) Rate of replenishment and microenvironment contribute to the sexually dimorphic phenotype and function of peritoneal macrophages. *Sci Immunol,* 5(48), p doi: 10.1126/sciimmunol.abc4466.

Balcombe, N. R. and Sinclair, A. (2001) Ageing: definitions, mechanisms and the magnitude of the problem. *Best Pract Res Clin Gastroenterol,* 15(6), p 835-849. doi: 10.1053/bega.2001.0244.

Baldwin, A. L. and Thurston, G. (2001) Mechanics of endothelial cell architecture and vascular permeability. *Crit Rev Biomed Eng,* 29(2), p 247-278. doi: 10.1615/critrevbiomedeng.v29.i2.20.

Barbera Betancourt, A. *et al.* (2017) T Cell-Mediated Chronic Inflammatory Diseases Are Candidates for Therapeutic Tolerance Induction with Heat Shock Proteins. *Front Immunol,* 8(p 1408. doi: 10.3389/fimmu.2017.01408.

Barbosa, M. C., Grosso, R. A. and Fader, C. M. (2018) Hallmarks of Aging: An Autophagic Perspective. *Front Endocrinol (Lausanne),* 9(p 790. doi: 10.3389/fendo.2018.00790.

Barkaway, A. *et al.* (2021) Age-related changes in the local milieu of inflamed tissues cause aberrant neutrophil trafficking and subsequent remote organ damage. *Immunity,* 54(7), p 1494-1510 e1497. doi: 10.1016/j.immuni.2021.04.025.

Barrat, F. *et al.* (1997a) Sex and parity modulate cytokine production during murine ageing. *Clin Exp Immunol,* 109(3), p 562-568. doi: 10.1046/j.1365-2249.1997.4851387.x.

Barrat, F. *et al.* (1997b) Surface antigen expression in spleen cells of C57B1/6 mice during ageing: influence of sex and parity. *Clin Exp Immunol,* 107(3), p 593-600. doi: 10.1046/j.1365-2249.1997.3021199.x.

Barzilai, S. *et al.* (2017) Leukocytes Breach Endothelial Barriers by Insertion of Nuclear Lobes and Disassembly of Endothelial Actin Filaments. *Cell Rep,* 18(3), p 685-699. doi: 10.1016/j.celrep.2016.12.076.

Baumgarth, N. *et al.* (2000) B-1 and B-2 cell-derived immunoglobulin M antibodies are nonredundant components of the protective response to influenza virus infection. *J Exp Med,* 192(2), p 271-280. doi: 10.1084/jem.192.2.271.

Belmin, J. *et al.* (1993) Age-related changes in endothelial permeability and distribution volume of albumin in rat aorta. *Am J Physiol,* 264(3 Pt 2), p H679-685. doi: 10.1152/ajpheart.1993.264.3.H679.

Bernal, A. M. *et al.* (2021) Differential Outcome between BALB/c and C57BL/6 Mice after Escherichia coli O157:H7 Infection Is Associated with a Dissimilar Tolerance Mechanism. *Infect Immun,* 89(5), p doi: 10.1128/IAI.00031-21.

Berner, H. S. *et al.* (2004) Adiponectin and its receptors are expressed in bone-forming cells. *Bone,* 35(4), p 842-849. doi: 10.1016/j.bone.2004.06.008.

Bertoni, A. *et al.* (2018) Integrins in T Cell Physiology. *Int J Mol Sci,* 19(2), p doi: 10.3390/ijms19020485.

Bevilacqua, M. P. *et al.* (1987) Identification of an inducible endothelial-leukocyte adhesion molecule. *Proc Natl Acad Sci U S A,* 84(24), p 9238-9242. doi: 10.1073/pnas.84.24.9238.

Beyersdorf, N. *et al.* (2007) Characterization of mouse CD4 T cell subsets defined by expression of KLRG1. *Eur J Immunol,* 37(12), p 3445-3454. doi: 10.1002/eji.200737126.

Bhayadia, R. *et al.* (2016) Senescence-Induced Oxidative Stress Causes Endothelial Dysfunction. *J Gerontol A Biol Sci Med Sci,* 71(2), p 161-169. doi: 10.1093/gerona/glv008.

Bik, W. *et al.* (2006) The relationship between adiponectin levels and metabolic status in centenarian, early elderly, young and obese women. *Neuro Endocrinol Lett,* 27(4), p 493-500. doi:

BioGPS Available at: http://biogps.org/#goto=genereport&id=36059

Biran, A. *et al.* (2017) Quantitative identification of senescent cells in aging and disease. *Aging Cell,* 16(4), p 661-671. doi: 10.1111/acel.12592.

Blaho, V. A. and Hla, T. (2011) Regulation of mammalian physiology, development, and disease by the sphingosine 1-phosphate and lysophosphatidic acid receptors. *Chem Rev,* 111(10), p 6299-6320. doi: 10.1021/cr200273u.

Blaho, V. A. and Hla, T. (2014) An update on the biology of sphingosine 1-phosphate receptors. *J Lipid Res,* 55(8), p 1596-1608. doi: 10.1194/jlr.R046300.

Boesiger, J. *et al.* (1998) Mast cells can secrete vascular permeability factor/ vascular endothelial cell growth factor and exhibit enhanced release after immunoglobulin E-dependent upregulation of fc epsilon receptor I expression. *J Exp Med,* 188(6), p 1135-1145. doi: 10.1084/jem.188.6.1135.

Bornemann, A. and Schmalbruch, H. (1994) Immunocytochemistry of M-cadherin in mature and regenerating rat muscle. *Anat Rec,* 239(2), p 119-125. doi: 10.1002/ar.1092390202.

Borthwick, N. J. *et al.* (2000) Loss of CD28 expression on CD8(+) T cells is induced by IL-2 receptor gamma chain signalling cytokines and type I IFN, and increases susceptibility to activation-induced apoptosis. *Int Immunol,* 12(7), p 1005-1013. doi: 10.1093/intimm/12.7.1005.

Bradfield, P. F. *et al.* (2007) JAM family and related proteins in leukocyte migration (Vestweber series). *Arterioscler Thromb Vasc Biol,* 27(10), p 2104-2112. doi: 10.1161/ATVBAHA.107.147694.

Brandao, A. P. *et al.* (2004) Persistence of antibody response to pneumococcal capsular polysaccharides in vaccinated long term-care residents in Brazil. *Vaccine,* 23(6), p 762-768. doi: 10.1016/j.vaccine.2004.07.024.

Brenchley, J. M. *et al.* (2003) Expression of CD57 defines replicative senescence and antigen-induced apoptotic death of CD8+ T cells. *Blood,* 101(7), p 2711-2720. doi: 10.1182/blood-2002-07-2103.

Brezinschek, R. I. *et al.* (1995) Phenotypic characterization of CD4+ T cells that exhibit a transendothelial migratory capacity. *J Immunol,* 154(7), p 3062-3077. doi:
Briceno, O. *et al.* (2016) Reduced naive CD8(+) T-cell priming efficacy in elderly adults. *Aging Cell,* 15(1), p 14-21. doi: 10.1111/acel.12384.
Bridges, D. and Moorhead, G. B. (2005) 14-3-3 proteins: a number of functions for a numbered protein. *Sci STKE,* 2005(296), p re10. doi: 10.1126/stke.2962005re10.
Bromley, S. K., Mempel, T. R. and Luster, A. D. (2008) Orchestrating the orchestrators: chemokines in control of T cell traffic. *Nat Immunol,* 9(9), p 970-980. doi: 10.1038/ni.f.213.
Brown, G. D. *et al.* (2003) Dectin-1 mediates the biological effects of beta-glucans. *J Exp Med,* 197(9), p 1119-1124. doi: 10.1084/jem.20021890.
Brown, G. D. *et al.* (2002) Dectin-1 is a major beta-glucan receptor on macrophages. *J Exp Med,* 196(3), p 407-412. doi: 10.1084/jem.20020470.
Brubaker, A. L. *et al.* (2013) Reduced neutrophil chemotaxis and infiltration contributes to delayed resolution of cutaneous wound infection with advanced age. *J Immunol,* 190(4), p 1746-1757. doi: 10.4049/jimmunol.1201213.
Bruunsgaard, H. *et al.* (1999) A high plasma concentration of TNF-alpha is associated with dementia in centenarians. *J Gerontol A Biol Sci Med Sci,* 54(7), p M357-364. doi: 10.1093/gerona/54.7.m357.
Bryl, E. *et al.* (2009) Human CD4low CD25high regulatory T cells indiscriminately kill autologous activated T cells. *Immunology,* 128(1 Suppl), p e287-295. doi: 10.1111/j.1365-2567.2008.02961.x.
Brzezinska, A. *et al.* (2004) Proliferation and apoptosis of human CD8(+)CD28(+) and CD8(+)CD28(-) lymphocytes during aging. *Exp Gerontol,* 39(4), p 539-544. doi: 10.1016/j.exger.2003.09.026.
Buggert, M. *et al.* (2020) The Identity of Human Tissue-Emigrant CD8(+) T Cells. *Cell,* 183(7), p 1946-1961 e1915. doi: 10.1016/j.cell.2020.11.019.
Bulati, M., Caruso, C. and Colonna-Romano, G. (2017) From lymphopoiesis to plasma cells differentiation, the age-related modifications of B cell compartment are influenced by "inflamm-ageing". *Ageing Res Rev,* 36(p 125-136. doi: 10.1016/j.arr.2017.04.001.
Burke-Gaffney, A. and Hellewell, P. G. (1996) Tumour necrosis factor-alpha-induced ICAM-1 expression in human vascular endothelial and lung epithelial cells: modulation by tyrosine kinase inhibitors. *Br J Pharmacol,* 119(6), p 1149-1158. doi: 10.1111/j.1476-5381.1996.tb16017.x.
Bursill, C. A. *et al.* (2003) Adenoviral-mediated delivery of a viral chemokine binding protein blocks CC-chemokine activity in vitro and in vivo. *Immunobiology,* 207(3), p 187-196. doi: 10.1078/0171-2985-00228.
Butcher, E. C. (1991) Leukocyte-endothelial cell recognition: three (or more) steps to specificity and diversity. *Cell,* 67(6), p 1033-1036. doi: 10.1016/0092-8674(91)90279-8.
Callender, L. A. *et al.* (2018) Human CD8(+) EMRA T cells display a senescence-associated secretory phenotype regulated by p38 MAPK. *Aging Cell,* 17(1), p doi: 10.1111/acel.12675.
Callender, L. A. *et al.* (2020) Mitochondrial mass governs the extent of human T cell senescence. *Aging Cell,* 19(2), p e13067. doi: 10.1111/acel.13067.

Campbell, J. J. *et al.* (1998a) 6-C-kine (SLC), a lymphocyte adhesion-triggering chemokine expressed by high endothelium, is an agonist for the MIP-3beta receptor CCR7. *J Cell Biol,* 141(4), p 1053-1059. doi: 10.1083/jcb.141.4.1053.

Campbell, J. J. *et al.* (1998b) Chemokines and the arrest of lymphocytes rolling under flow conditions. *Science,* 279(5349), p 381-384. doi: 10.1126/science.279.5349.381.

Cane, S., Ponnappan, S. and Ponnappan, U. (2012a) Altered regulation of CXCR4 expression during aging contributes to increased CXCL12-dependent chemotactic migration of CD4(+) T cells. *Aging Cell,* 11(4), p 651-658. doi: 10.1111/j.1474-9726.2012.00830.x.

Cane, S., Ponnappan, S. and Ponnappan, U. (2012b) Impairment of non-muscle myosin IIA in human CD4+ T cells contributes to functional deficits in the elderly. *Cell Mol Immunol,* 9(1), p 86-96. doi: 10.1038/cmi.2011.41.

Cao, Y. *et al.* (2009) Endothelial dysfunction in adiponectin deficiency and its mechanisms involved. *J Mol Cell Cardiol,* 46(3), p 413-419. doi: 10.1016/j.yjmcc.2008.10.014.

Carlow, D. A. *et al.* (2009) PSGL-1 function in immunity and steady state homeostasis. *Immunol Rev,* 230(1), p 75-96. doi: 10.1111/j.1600-065X.2009.00797.x.

Carman, C. V. and Springer, T. A. (2004) A transmigratory cup in leukocyte diapedesis both through individual vascular endothelial cells and between them. *J Cell Biol,* 167(2), p 377-388. doi: 10.1083/jcb.200404129.

Carpentier, G. *et al.* (2020) Angiogenesis Analyzer for ImageJ - A comparative morphometric analysis of "Endothelial Tube Formation Assay" and "Fibrin Bead Assay". *Sci Rep,* 10(1), p 11568. doi: 10.1038/s41598-020-67289-8.

Casanova-Acebes, M. *et al.* (2013) Rhythmic modulation of the hematopoietic niche through neutrophil clearance. *Cell,* 153(5), p 1025-1035. doi: 10.1016/j.cell.2013.04.040.

Cash, J. L., White, G. E. and Greaves, D. R. (2009). *Chapter 17 Zymosan-Induced Peritonitis as a Simple Experimental System for the Study of Inflammation*. In: Methods in Enzymology Academic Press, 379-396.

Cattoretti, G. *et al.* (2009) Targeted disruption of the S1P2 sphingosine 1-phosphate receptor gene leads to diffuse large B-cell lymphoma formation. *Cancer Res,* 69(22), p 8686-8692. doi: 10.1158/0008-5472.CAN-09-1110.

Chakraborty, R. and Lo, D. D. (2020) Chronic Inflammation in Mucosal Tissues: Barrier Integrity, Inducible Lymphoid Tissues, and Immune Surveillance. *Curr Top Microbiol Immunol,* 426(p 45-63. doi: 10.1007/82_2020_208.

Chambers, E. S. *et al.* (2021) Recruitment of inflammatory monocytes by senescent fibroblasts inhibits antigen-specific tissue immunity during human aging. *Nat Aging,* 1(p 101-113. doi: 10.1038/s43587-020-00010-6.

Chan-Ling, T. *et al.* (2007) Inflammation and breakdown of the blood-retinal barrier during "physiological aging" in the rat retina: a model for CNS aging. *Microcirculation,* 14(1), p 63-76. doi: 10.1080/10739680601073451.

Chang, F., Flavahan, S. and Flavahan, N. A. (2017) Impaired activity of adherens junctions contributes to endothelial dilator dysfunction in ageing rat arteries. *J Physiol,* 595(15), p 5143-5158. doi: 10.1113/JP274189.

Chaplin, D. D. (2010) Overview of the immune response. *Journal of Allergy and Clinical Immunology,* 125(2 Suppl 2), p S3-23. doi: 10.1016/j.jaci.2009.12.980.

Chatterjee, V. and Gashev, A. A. (2012) Aging-associated shifts in functional status of mast cells located by adult and aged mesenteric lymphatic vessels. *Am J Physiol Heart Circ Physiol,* 303(6), p H693-702. doi: 10.1152/ajpheart.00378.2012.

Chattopadhyay, P. K. *et al.* (2009) The cytolytic enzymes granyzme A, granzyme B, and perforin: expression patterns, cell distribution, and their relationship to cell maturity and bright CD57 expression. *J Leukoc Biol,* 85(1), p 88-97. doi: 10.1189/jlb.0208107.

Chen, D. *et al.* (2008) Protease-activated receptor 1 activation is necessary for monocyte chemoattractant protein 1-dependent leukocyte recruitment in vivo. *J Exp Med,* 205(8), p 1739-1746. doi: 10.1084/jem.20071427.

Chen, J. *et al.* (2021a) Decreased blood vessel density and endothelial cell subset dynamics during ageing of the endocrine system. *EMBO J,* 40(1), p e105242. doi: 10.15252/embj.2020105242.

Chen, J. *et al.* (2003) Aging is associated with increased T-cell chemokine expression in C57BL/6 mice. *J Gerontol A Biol Sci Med Sci,* 58(11), p 975-983. doi: 10.1093/gerona/58.11.b975.

Chen, J. *et al.* (2021b) High-resolution 3D imaging uncovers organ-specific vascular control of tissue aging. *Sci Adv,* 7(6), p doi: 10.1126/sciadv.abd7819.

Chen, K. D. *et al.* (1998) Involvement of p38 mitogen-activated protein kinase signaling pathway in the rapid induction of the 78-kDa glucose-regulated protein in 9L rat brain tumor cells. *J Biol Chem,* 273(2), p 749-755. doi: 10.1074/jbc.273.2.749.

Chen, Y. M., Zhang, J. S. and Duan, X. L. (2003) Changes of microvascular architecture, ultrastructure and permeability of rat jejunal villi at different ages. *World J Gastroenterol,* 9(4), p 795-799. doi: 10.3748/wjg.v9.i4.795.

Cheng, K. K. *et al.* (2007) Adiponectin-induced endothelial nitric oxide synthase activation and nitric oxide production are mediated by APPL1 in endothelial cells. *Diabetes,* 56(5), p 1387-1394. doi: 10.2337/db06-1580.

Cheng, X. *et al.* (2012) Adiponectin induces pro-inflammatory programs in human macrophages and CD4+ T cells. *J Biol Chem,* 287(44), p 36896-36904. doi: 10.1074/jbc.M112.409516.

Chimen, M. (2012) '*Immunomodulation by adipokines in type 1 diabetes*', PhD thesis, University of Birmingham, Birmingham.

Chimen, M. *et al.* (2015) Homeostatic regulation of T cell trafficking by a B cell-derived peptide is impaired in autoimmune and chronic inflammatory disease. *Nat Med,* 21(5), p 467-475. doi: 10.1038/nm.3842.

Chimen, M. *et al.* (2017) Monocyte Subsets Coregulate Inflammatory Responses by Integrated Signaling through TNF and IL-6 at the Endothelial Cell Interface. *J Immunol,* 198(7), p 2834-2843. doi: 10.4049/jimmunol.1601281.

Chiricolo, M. *et al.* (1995) Cell adhesion molecules CD11a and CD18 in blood monocytes in old age and the consequences for immunological dysfunction. Preliminary results. *Gerontology,* 41(4), p 227-234. doi: 10.1159/000213686.

Choi, H. M., Doss, H. M. and Kim, K. S. (2020) Multifaceted Physiological Roles of Adiponectin in Inflammation and Diseases. *Int J Mol Sci,* 21(4), p doi: 10.3390/ijms21041219.

Choi, K. C. *et al.* (2005) Increased expression of 14-3-3varepsilon protein in intrinsically aged and photoaged human skin in vivo. *Mech Ageing Dev,* 126(6-7), p 629-636. doi: 10.1016/j.mad.2004.11.013.

Chong, Y. *et al.* (2005) CD27(+) (memory) B cell decrease and apoptosis-resistant CD27(-) (naive) B cell increase in aged humans: implications for age-related peripheral B cell developmental disturbances. *Int Immunol,* 17(4), p 383-390. doi: 10.1093/intimm/dxh218.

Chou, J. P. and Effros, R. B. (2013) T cell replicative senescence in human aging. *Curr Pharm Des,* 19(9), p 1680-1698. doi: 10.2174/138161213805219711.

Chung, H. Y. *et al.* (2019) Redefining Chronic Inflammation in Aging and Age-Related Diseases: Proposal of the Senoinflammation Concept. *Aging Dis,* 10(2), p 367-382. doi: 10.14336/AD.2018.0324.

Clark, J. A. and Peterson, T. C. (1994) Cytokine production and aging: overproduction of IL-8 in elderly males in response to lipopolysaccharide. *Mech Ageing Dev,* 77(2), p 127-139. doi: 10.1016/0047-6374(94)90020-5.

Clise-Dwyer, K. *et al.* (2007) Environmental and intrinsic factors lead to antigen unresponsiveness in CD4(+) recent thymic emigrants from aged mice. *J Immunol,* 178(3), p 1321-1331. doi: 10.4049/jimmunol.178.3.1321.

Collaborators, G. B. D. A. (2022) Global, regional, and national burden of diseases and injuries for adults 70 years and older: systematic analysis for the Global Burden of Disease 2019 Study. *BMJ,* 376(p e068208. doi: 10.1136/bmj-2021-068208.

Collaborators, G. B. D. I. B. D. (2020) The global, regional, and national burden of inflammatory bowel disease in 195 countries and territories, 1990-2017: a systematic analysis for the Global Burden of Disease Study 2017. *Lancet Gastroenterol Hepatol,* 5(1), p 17-30. doi: 10.1016/S2468-1253(19)30333-4.

Colonna-Romano, G. *et al.* (2009) A double-negative (IgD-CD27-) B cell population is increased in the peripheral blood of elderly people. *Mech Ageing Dev,* 130(10), p 681-690. doi: 10.1016/j.mad.2009.08.003.

Colonna-Romano, G. *et al.* (2008) B cell immunosenescence in the elderly and in centenarians. *Rejuvenation Res,* 11(2), p 433-439. doi: 10.1089/rej.2008.0664.

Colonna-Romano, G. *et al.* (2002) Age- and gender-related values of lymphocyte subsets in subjects from Northern and Southern Italy. *Arch Gerontol Geriatr Suppl,* 8(p 99-107. doi: 10.1016/s0167-4943(02)00109-7.

Conant, K. *et al.* (2012) Matrix metalloproteinase dependent cleavage of cell adhesion molecules in the pathogenesis of CNS dysfunction with HIV and methamphetamine. *Curr HIV Res,* 10(5), p 384-391. doi: 10.2174/157016212802138733.

Coppe, J. P. *et al.* (2010) The senescence-associated secretory phenotype: the dark side of tumor suppression. *Annu Rev Pathol,* 5(p 99-118. doi: 10.1146/annurev-pathol-121808-102144.

Crimmins, E. M. *et al.* (2019) Differences between Men and Women in Mortality and the Health Dimensions of the Morbidity Process. *Clin Chem,* 65(1), p 135-145. doi: 10.1373/clinchem.2018.288332.

Cui, X. B. *et al.* (2012) Insulin decreases myocardial adiponectin receptor 1 expression via PI3K/Akt and FoxO1 pathway. *Cardiovasc Res,* 93(1), p 69-78. doi: 10.1093/cvr/cvr273.

Curbishley, S. M. *et al.* (2005) CXCR 3 activation promotes lymphocyte transendothelial migration across human hepatic endothelium under fluid flow. *Am J Pathol,* 167(3), p 887-899. doi: 10.1016/S0002-9440(10)62060-3.

Curiel, T. J. *et al.* (2004) Specific recruitment of regulatory T cells in ovarian carcinoma fosters immune privilege and predicts reduced survival. *Nat Med,* 10(9), p 942-949. doi: 10.1038/nm1093.

Czesnikiewicz-Guzik, M. *et al.* (2008) T cell subset-specific susceptibility to aging. *Clin Immunol,* 127(1), p 107-118. doi: 10.1016/j.clim.2007.12.002.

da Costa Martins, P. *et al.* (2007) P-selectin glycoprotein ligand-1 is expressed on endothelial cells and mediates monocyte adhesion to activated endothelium. *Arterioscler Thromb Vasc Biol,* 27(5), p 1023-1029. doi: 10.1161/ATVBAHA.107.140442.

Daynes, R. A. *et al.* (1993) Altered regulation of IL-6 production with normal aging. Possible linkage to the age-associated decline in dehydroepiandrosterone and its sulfated derivative. *J Immunol,* 150(12), p 5219-5230. doi:

De Sousa, M. A., Parrott, D. M. and Pantelouris, E. M. (1969) The lymphoid tissues in mice with congenital aplasia of the thymus. *Clin Exp Immunol,* 4(6), p 637-644. doi:

Deepa, S. S. and Dong, L. Q. (2009) APPL1: role in adiponectin signaling and beyond. *Am J Physiol Endocrinol Metab,* 296(1), p E22-36. doi: 10.1152/ajpendo.90731.2008.

Deisher, T. A. *et al.* (1993) The role of protein kinase C in the induction of VCAM-1 expression on human umbilical vein endothelial cells. *FEBS Lett,* 331(3), p 285-290. doi: 10.1016/0014-5793(93)80354-w.

Delaigle, A. M. *et al.* (2004) Induction of adiponectin in skeletal muscle by inflammatory cytokines: in vivo and in vitro studies. *Endocrinology,* 145(12), p 5589-5597. doi: 10.1210/en.2004-0503.

den Braber, I. *et al.* (2012) Maintenance of peripheral naive T cells is sustained by thymus output in mice but not humans. *Immunity,* 36(2), p 288-297. doi: 10.1016/j.immuni.2012.02.006.

Derhovanessian, E. *et al.* (2008) Immunity, ageing and cancer. *Immun Ageing,* 5(p 11. doi: 10.1186/1742-4933-5-11.

Di Bartolo, V. *et al.* (2007) A novel pathway down-modulating T cell activation involves HPK-1-dependent recruitment of 14-3-3 proteins on SLP-76. *J Exp Med,* 204(3), p 681-691. doi: 10.1084/jem.20062066.

Di Giacomo, V. *et al.* (2009) Regulation of CREB activation by p38 mitogen activated protein kinase during human primary erythroblast differentiation. *Int J Immunopathol Pharmacol,* 22(3), p 679-688. doi: 10.1177/039463200902200313.

Di Micco, R. *et al.* (2021) Cellular senescence in ageing: from mechanisms to therapeutic opportunities. *Nat Rev Mol Cell Biol,* 22(2), p 75-95. doi: 10.1038/s41580-020-00314-w.

Diez, J. J. and Iglesias, P. (2003) The role of the novel adipocyte-derived hormone adiponectin in human disease. *Eur J Endocrinol,* 148(3), p 293-300. doi: 10.1530/eje.0.1480293.

DiLillo, D. J., Matsushita, T. and Tedder, T. F. (2010) B10 cells and regulatory B cells balance immune responses during inflammation, autoimmunity, and cancer. *Ann N Y Acad Sci,* 1183(p 38-57. doi: 10.1111/j.1749-6632.2009.05137.x.

Dodd, K. C. and Menon, M. (2022) Sex bias in lymphocytes: Implications for autoimmune diseases. *Frontiers in Immunology,* 13(p doi: 10.3389/fimmu.2022.945762.

Doherty, N. S. *et al.* (1985) Intraperitoneal injection of zymosan in mice induces pain, inflammation and the synthesis of peptidoleukotrienes and prostaglandin E2. *Prostaglandins,* 30(5), p 769-789. doi: 10.1016/0090-6980(85)90006-1.

Donalies, M. *et al.* (1991) Expression of M-cadherin, a member of the cadherin multigene family, correlates with differentiation of skeletal muscle cells. *Proc Natl Acad Sci U S A,* 88(18), p 8024-8028. doi: 10.1073/pnas.88.18.8024.

Donato, A. J. *et al.* (2008) Aging is associated with greater nuclear NF kappa B, reduced I kappa B alpha, and increased expression of proinflammatory cytokines in vascular endothelial cells of healthy humans. *Aging Cell,* 7(6), p 805-812. doi: 10.1111/j.1474-9726.2008.00438.x.

Donato, A. J. *et al.* (2015) Cellular and molecular biology of aging endothelial cells. *J Mol Cell Cardiol,* 89(Pt B), p 122-135. doi: 10.1016/j.yjmcc.2015.01.021.

Dooley, J. and Liston, A. (2012) Molecular control over thymic involution: from cytokines and microRNA to aging and adipose tissue. *Eur J Immunol,* 42(5), p 1073-1079. doi: 10.1002/eji.201142305.

Dougherty, M. K. and Morrison, D. K. (2004) Unlocking the code of 14-3-3. *J Cell Sci,* 117(Pt 10), p 1875-1884. doi: 10.1242/jcs.01171.

Douziech, N. *et al.* (2002) Modulation of human lymphocyte proliferative response with aging. *Exp Gerontol,* 37(2-3), p 369-387. doi: 10.1016/s0531-5565(01)00204-2.

Dudakov, J. A. *et al.* (2009) Withdrawal of sex steroids reverses age- and chemotherapy-related defects in bone marrow lymphopoiesis. *J Immunol,* 182(10), p 6247-6260. doi: 10.4049/jimmunol.0802446.

Dudda, J. C., Simon, J. C. and Martin, S. (2004) Dendritic cell immunization route determines CD8+ T cell trafficking to inflamed skin: role for tissue microenvironment and dendritic cells in establishment of T cell-homing subsets. *J Immunol,* 172(2), p 857-863. doi: 10.4049/jimmunol.172.2.857.

Duggal, N. A. *et al.* (2018) Major features of immunesenescence, including reduced thymic output, are ameliorated by high levels of physical activity in adulthood. *Aging Cell,* 17(2), p doi: 10.1111/acel.12750.

Duggal, N. A. *et al.* (2013) An age-related numerical and functional deficit in CD19(+) CD24(hi) CD38(hi) B cells is associated with an increase in systemic autoimmunity. *Aging Cell,* 12(5), p 873-881. doi: 10.1111/acel.12114.

Dvorak, A. M. and Feng, D. (2001) The vesiculo-vacuolar organelle (VVO). A new endothelial cell permeability organelle. *J Histochem Cytochem,* 49(4), p 419-432. doi: 10.1177/002215540104900401.

Dwyer, C. M. *et al.* (2021) High rates of JCV seroconversion in a large international cohort of natalizumab-treated patients. *Ther Adv Neurol Disord,* 14(p 1756286421998915. doi: 10.1177/1756286421998915.

Eaton, S. M. *et al.* (2004) Age-related defects in CD4 T cell cognate helper function lead to reductions in humoral responses. *J Exp Med,* 200(12), p 1613-1622. doi: 10.1084/jem.20041395.

Effros, R. B. *et al.* (1994) Decline in CD28+ T cells in centenarians and in long-term T cell cultures: a possible cause for both in vivo and in vitro immunosenescence. *Exp Gerontol,* 29(6), p 601-609. doi: 10.1016/0531-5565(94)90073-6.

Engel, P. *et al.* (2011) Therapeutic targeting of B cells for rheumatic autoimmune diseases. *Pharmacol Rev,* 63(1), p 127-156. doi: 10.1124/pr.109.002006.

Enzerink, A. and Vaheri, A. (2011) Fibroblast activation in vascular inflammation. *J Thromb Haemost,* 9(4), p 619-626. doi: 10.1111/j.1538-7836.2011.04209.x.

Ermann, J. *et al.* (2005) Only the CD62L+ subpopulation of CD4+CD25+ regulatory T cells protects from lethal acute GVHD. *Blood,* 105(5), p 2220-2226. doi: 10.1182/blood-2004-05-2044.

Ermogenous, C. *et al.* (2020) Treating age-related multimorbidity: the drug discovery challenge. *Drug Discov Today,* 25(8), p 1403-1415. doi: 10.1016/j.drudis.2020.06.016.

Ernst, D. N. *et al.* (1990) Differences in the expression profiles of CD45RB, Pgp-1, and 3G11 membrane antigens and in the patterns of lymphokine secretion by splenic CD4+ T cells from young and aged mice. *J Immunol,* 145(5), p 1295-1302. doi:

Ershler, W. B. and Keller, E. T. (2000) Age-associated increased interleukin-6 gene expression, late-life diseases, and frailty. *Annu Rev Med,* 51(p 245-270. doi: 10.1146/annurev.med.51.1.245.

Esmaili, S., Hemmati, M. and Karamian, M. (2020) Physiological role of adiponectin in different tissues: a review. *Arch Physiol Biochem,* 126(1), p 67-73. doi: 10.1080/13813455.2018.1493606.

Fabbri, M., Smart, C. and Pardi, R. (2003) T lymphocytes. *Int J Biochem Cell Biol,* 35(7), p 1004-1008. doi: 10.1016/s1357-2725(03)00037-2.

Fagiolo, U. *et al.* (1993) Increased cytokine production in mononuclear cells of healthy elderly people. *Eur J Immunol,* 23(9), p 2375-2378. doi: 10.1002/eji.1830230950.

Fagnoni, F. F. *et al.* (1996) Expansion of cytotoxic CD8+ CD28- T cells in healthy ageing people, including centenarians. *Immunology,* 88(4), p 501-507. doi: 10.1046/j.1365-2567.1996.d01-689.x.

Faint, J. M. *et al.* (2001) Memory T cells constitute a subset of the human CD8+CD45RA+ pool with distinct phenotypic and migratory characteristics. *J Immunol,* 167(1), p 212-220. doi: 10.4049/jimmunol.167.1.212.

Falsey, A. R. *et al.* (2009) Randomized, double-blind controlled phase 3 trial comparing the immunogenicity of high-dose and standard-dose influenza vaccine in adults 65 years of age and older. *J Infect Dis,* 200(2), p 172-180. doi: 10.1086/599790.

Fan, X. *et al.* (2019) 14-3-3 Proteins Are on the Crossroads of Cancer, Aging, and Age-Related Neurodegenerative Disease. *Int J Mol Sci,* 20(14), p doi: 10.3390/ijms20143518.

Fang, J. Y. *et al.* (2016) Skin aging caused by intrinsic or extrinsic processes characterized with functional proteomics. *Proteomics,* 16(20), p 2718-2731. doi: 10.1002/pmic.201600141.

Fann, M. *et al.* (2005) Gene expression characteristics of CD28null memory phenotype CD8+ T cells and its implication in T-cell aging. *Immunol Rev,* 205(p 190-206. doi: 10.1111/j.0105-2896.2005.00262.x.

Ferguson, A. R. and Engelhard, V. H. (2010) CD8 T cells activated in distinct lymphoid organs differentially express adhesion proteins and coexpress multiple chemokine receptors. *J Immunol,* 184(8), p 4079-4086. doi: 10.4049/jimmunol.0901903.

Finger, E. B. *et al.* (1996) Adhesion through L-selectin requires a threshold hydrodynamic shear. *Nature,* 379(6562), p 266-269. doi: 10.1038/379266a0.

Flanagan, S. P. (1966) 'Nude', a new hairless gene with pleiotropic effects in the mouse. *Genet Res,* 8(3), p 295-309. doi: 10.1017/s0016672300010168.

Franceschi, C. and Campisi, J. (2014) Chronic inflammation (inflammaging) and its potential contribution to age-associated diseases. *J Gerontol A Biol Sci Med Sci,* 69 Suppl 1(p S4-9. doi: 10.1093/gerona/glu057.

Frasca, D. (2018) Senescent B cells in aging and age-related diseases: Their role in the regulation of antibody responses. *Exp Gerontol,* 107(p 55-58. doi: 10.1016/j.exger.2017.07.002.

Frasca, D. *et al.* (2017) Human peripheral late/exhausted memory B cells express a senescent-associated secretory phenotype and preferentially utilize metabolic signaling pathways. *Exp Gerontol,* 87(Pt A), p 113-120. doi: 10.1016/j.exger.2016.12.001.

Frommer, K. W. *et al.* (2010) Adiponectin-mediated changes in effector cells involved in the pathophysiology of rheumatoid arthritis. *Arthritis Rheum,* 62(10), p 2886-2899. doi: 10.1002/art.27616.

Fu, H., Subramanian, R. R. and Masters, S. C. (2000) 14-3-3 proteins: structure, function, and regulation. *Annu Rev Pharmacol Toxicol,* 40(p 617-647. doi: 10.1146/annurev.pharmtox.40.1.617.

Fukuhara, S. *et al.* (2012) The sphingosine-1-phosphate transporter Spns2 expressed on endothelial cells regulates lymphocyte trafficking in mice. *J Clin Invest,* 122(4), p 1416-1426. doi: 10.1172/JCI60746.

Fulop, T., Jr. *et al.* (1997) Changes in apoptosis of human polymorphonuclear granulocytes with aging. *Mech Ageing Dev,* 96(1-3), p 15-34. doi: 10.1016/s0047-6374(96)01881-7.

Fulop, T. *et al.* (2017) Immunosenescence and Inflamm-Aging As Two Sides of the Same Coin: Friends or Foes? *Front Immunol,* 8(p 1960. doi: 10.3389/fimmu.2017.01960.

Fulop, T., Larbi, A. and Pawelec, G. (2013) Human T cell aging and the impact of persistent viral infections. *Front Immunol,* 4(p 271. doi: 10.3389/fimmu.2013.00271.

Furman, D. *et al.* (2019) Chronic inflammation in the etiology of disease across the life span. *Nat Med,* 25(12), p 1822-1832. doi: 10.1038/s41591-019-0675-0.

Furman, J. L., Chiu, M. and Hunter, M. J. (2015) Early engineering approaches to improve peptide developability and manufacturability. *AAPS J,* 17(1), p 111-120. doi: 10.1208/s12248-014-9681-9.

Garcia-Guzman, M. *et al.* (1999) Cell adhesion regulates the interaction between the docking protein p130(Cas) and the 14-3-3 proteins. *J Biol Chem,* 274(9), p 5762-5768. doi: 10.1074/jbc.274.9.5762.

Garcia, G. G. and Miller, R. A. (2001) Single-cell analyses reveal two defects in peptide-specific activation of naive T cells from aged mice. *J Immunol,* 166(5), p 3151-3157. doi: 10.4049/jimmunol.166.5.3151.

Garcia, G. G. and Miller, R. A. (2002) Age-dependent defects in TCR-triggered cytoskeletal rearrangement in CD4+ T cells. *J Immunol,* 169(9), p 5021-5027. doi: 10.4049/jimmunol.169.9.5021.

Garg, S. K. *et al.* (2014) Aging is associated with increased regulatory T-cell function. *Aging Cell,* 13(3), p 441-448. doi: 10.1111/acel.12191.

Garris, C. S. *et al.* (2014) Sphingosine-1-phosphate receptor 1 signalling in T cells: trafficking and beyond. *Immunology,* 142(3), p 347-353. doi: 10.1111/imm.12272.

Gassmann, M. *et al.* (2009) Quantifying Western blots: pitfalls of densitometry. *Electrophoresis,* 30(11), p 1845-1855. doi: 10.1002/elps.200800720.
Gavard, J. (2014) Endothelial permeability and VE-cadherin: a wacky comradeship. *Cell Adh Migr,* 8(2), p 158-164. doi: 10.4161/cam.29026.
Gaylo, A. *et al.* (2016) T Cell Interstitial Migration: Motility Cues from the Inflamed Tissue for Micro- and Macro-Positioning. *Front Immunol,* 7(p 428. doi: 10.3389/fimmu.2016.00428.
Geevarghese, A. and Herman, I. M. (2014) Pericyte-endothelial crosstalk: implications and opportunities for advanced cellular therapies. *Transl Res,* 163(4), p 296-306. doi: 10.1016/j.trsl.2014.01.011.
Geginat, J., Lanzavecchia, A. and Sallusto, F. (2003) Proliferation and differentiation potential of human CD8+ memory T-cell subsets in response to antigen or homeostatic cytokines. *Blood,* 101(11), p 4260-4266. doi: 10.1182/blood-2002-11-3577.
Geiger, B. *et al.* (2001) Transmembrane crosstalk between the extracellular matrix--cytoskeleton crosstalk. *Nat Rev Mol Cell Biol,* 2(11), p 793-805. doi: 10.1038/35099066.
Gelinas, D. S. and McLaurin, J. (2005) PPAR-alpha expression inversely correlates with inflammatory cytokines IL-1beta and TNF-alpha in aging rats. *Neurochem Res,* 30(11), p 1369-1375. doi: 10.1007/s11064-005-8341-y.
Gerberick, G. F. *et al.* (1997) Selective modulation of T cell memory markers CD62L and CD44 on murine draining lymph node cells following allergen and irritant treatment. *Toxicol Appl Pharmacol,* 146(1), p 1-10. doi: 10.1006/taap.1997.8218.
Gerberick, G. F., Cruse, L. W. and Ryan, C. A. (1999) Local lymph node assay: differentiating allergic and irritant responses using flow cytometry. *Methods,* 19(1), p 48-55. doi: 10.1006/meth.1999.0826.
Germain, R. N. (2002) T-cell development and the CD4-CD8 lineage decision. *Nat Rev Immunol,* 2(5), p 309-322. doi: 10.1038/nri798.
Germain, R. N. and Stefanova, I. (1999) The dynamics of T cell receptor signaling: complex orchestration and the key roles of tempo and cooperation. *Annu Rev Immunol,* 17(p 467-522. doi: 10.1146/annurev.immunol.17.1.467.
Gibson, K. L. *et al.* (2009) B-cell diversity decreases in old age and is correlated with poor health status. *Aging Cell,* 8(1), p 18-25. doi: 10.1111/j.1474-9726.2008.00443.x.
Ginaldi, L. *et al.* (2000) Immunophenotypical changes of T lymphocytes in the elderly. *Gerontology,* 46(5), p 242-248. doi: 10.1159/000022167.
Giuffrida, P. and Di Sabatino, A. (2020) Targeting T cells in inflammatory bowel disease. *Pharmacol Res,* 159(p 105040. doi: 10.1016/j.phrs.2020.105040.
Goemaere, S. *et al.* (1990) Onset of symptoms of rheumatoid arthritis in relation to age, sex and menopausal transition. *J Rheumatol,* 17(12), p 1620-1622. doi:
Goetzl, E. J. *et al.* (2010) Gender specificity of altered human immune cytokine profiles in aging. *FASEB J,* 24(9), p 3580-3589. doi: 10.1096/fj.10-160911.
Goidl, E. A., Innes, J. B. and Weksler, M. E. (1976) Immunological studies of aging. II. Loss of IgG and high avidity plaque-forming cells and increased suppressor cell activity in aging mice. *J Exp Med,* 144(4), p 1037-1048. doi: 10.1084/jem.144.4.1037.

Goldblatt, D. *et al.* (2009) The immunogenicity of 7-valent pneumococcal conjugate vaccine versus 23-valent polysaccharide vaccine in adults aged 50-80 years. *Clin Infect Dis,* 49(9), p 1318-1325. doi: 10.1086/606046.

Gomez, I. *et al.* (2003) Changes in the expression of CD31 and CXCR3 in CD4+ naive T cells in elderly persons. *Mech Ageing Dev,* 124(4), p 395-402. doi: 10.1016/s0047-6374(03)00014-9.

Goncalves, M. T., Mitchell, T. J. and Lord, J. M. (2016) Immune ageing and susceptibility to Streptococcus pneumoniae. *Biogerontology,* 17(3), p 449-465. doi: 10.1007/s10522-015-9614-8.

Gordon, F. H. *et al.* (2001) A randomized placebo-controlled trial of a humanized monoclonal antibody to alpha4 integrin in active Crohn's disease. *Gastroenterology,* 121(2), p 268-274. doi: 10.1053/gast.2001.26260.

Goronzy, J. J. *et al.* (2015) Naive T cell maintenance and function in human aging. *J Immunol,* 194(9), p 4073-4080. doi: 10.4049/jimmunol.1500046.

Goronzy, J. J. and Weyand, C. M. (2019) Mechanisms underlying T cell ageing. *Nat Rev Immunol,* 19(9), p 573-583. doi: 10.1038/s41577-019-0180-1.

Gowans, J. L. (1959) The recirculation of lymphocytes from blood to lymph in the rat. *J Physiol,* 146(1), p 54-69. doi: 10.1113/jphysiol.1959.sp006177.

Gregg, R. *et al.* (2005) The number of human peripheral blood CD4+ CD25high regulatory T cells increases with age. *Clin Exp Immunol,* 140(3), p 540-546. doi: 10.1111/j.1365-2249.2005.02798.x.

Gregory, G. A. *et al.* (2022) Global incidence, prevalence, and mortality of type 1 diabetes in 2021 with projection to 2040: a modelling study. *Lancet Diabetes Endocrinol,* 10(10), p 741-760. doi: 10.1016/S2213-8587(22)00218-2.

Griffin, D. O., Holodick, N. E. and Rothstein, T. L. (2011) Human B1 cells in umbilical cord and adult peripheral blood express the novel phenotype CD20+ CD27+ CD43+ CD70. *J Exp Med,* 208(1), p 67-80. doi: 10.1084/jem.20101499.

Grolleau-Julius, A. *et al.* (2008) Impaired dendritic cell function in aging leads to defective antitumor immunity. *Cancer Res,* 68(15), p 6341-6349. doi: 10.1158/0008-5472.CAN-07-5769.

Groom, J. R. *et al.* (2012) CXCR3 chemokine receptor-ligand interactions in the lymph node optimize CD4+ T helper 1 cell differentiation. *Immunity,* 37(6), p 1091-1103. doi: 10.1016/j.immuni.2012.08.016.

Gubbels Bupp, M. R. (2015) Sex, the aging immune system, and chronic disease. *Cell Immunol,* 294(2), p 102-110. doi: 10.1016/j.cellimm.2015.02.002.

Guidi, L. *et al.* (1998) Changes in the amount and level of phosphorylation of p56(lck) in PBL from aging humans. *Mech Ageing Dev,* 102(2-3), p 177-186. doi: 10.1016/s0047-6374(97)00144-9.

Gunin, A. G. *et al.* (2011) Age-related changes in proliferation, the numbers of mast cells, eosinophils, and cd45-positive cells in human dermis. *J Gerontol A Biol Sci Med Sci,* 66(4), p 385-392. doi: 10.1093/gerona/glq205.

Gunn, M. D. *et al.* (1998) A chemokine expressed in lymphoid high endothelial venules promotes the adhesion and chemotaxis of naive T lymphocytes. *Proc Natl Acad Sci U S A,* 95(1), p 258-263. doi: 10.1073/pnas.95.1.258.

Hagihara, Y. and Saerens, D. (2014) Engineering disulfide bonds within an antibody. *Biochim Biophys Acta,* 1844(11), p 2016-2023. doi: 10.1016/j.bbapap.2014.07.005.

Hainz, U. *et al.* (2005) Insufficient protection for healthy elderly adults by tetanus and TBE vaccines. *Vaccine,* 23(25), p 3232-3235. doi: 10.1016/j.vaccine.2005.01.085.

Halin, C. *et al.* (2005) The S1P-analog FTY720 differentially modulates T-cell homing via HEV: T-cell-expressed S1P1 amplifies integrin activation in peripheral lymph nodes but not in Peyer patches. *Blood,* 106(4), p 1314-1322. doi: 10.1182/blood-2004-09-3687.

Hamann, A. and Syrbe, U. (2000) T-cell trafficking into sites of inflammation. *Rheumatology (Oxford),* 39(7), p 696-699. doi: 10.1093/rheumatology/39.7.696.

Hamann, D. *et al.* (1997) Phenotypic and functional separation of memory and effector human CD8+ T cells. *J Exp Med,* 186(9), p 1407-1418. doi: 10.1084/jem.186.9.1407.

Hampton, H. R. and Chtanova, T. (2019) Lymphatic Migration of Immune Cells. *Front Immunol,* 10(p 1168. doi: 10.3389/fimmu.2019.01168.

Han, D. C., Rodriguez, L. G. and Guan, J. L. (2001) Identification of a novel interaction between integrin beta1 and 14-3-3beta. *Oncogene,* 20(3), p 346-357. doi: 10.1038/sj.onc.1204068.

Hansen, T. *et al.* (2009) Visceral adipose tissue, adiponectin levels and insulin resistance are related to atherosclerosis as assessed by whole-body magnetic resonance angiography in an elderly population. *Atherosclerosis,* 205(1), p 163-167. doi: 10.1016/j.atherosclerosis.2008.11.007.

Hao, Y. *et al.* (2011) A B-cell subset uniquely responsive to innate stimuli accumulates in aged mice. *Blood,* 118(5), p 1294-1304. doi: 10.1182/blood-2011-01-330530.

Hargreaves, D. C. *et al.* (2001) A coordinated change in chemokine responsiveness guides plasma cell movements. *J Exp Med,* 194(1), p 45-56. doi: 10.1084/jem.194.1.45.

Hausser, A. *et al.* (1999) Protein kinase C mu is negatively regulated by 14-3-3 signal transduction proteins. *J Biol Chem,* 274(14), p 9258-9264. doi: 10.1074/jbc.274.14.9258.

Hayflick, L. and Moorhead, P. S. (1961) The serial cultivation of human diploid cell strains. *Exp Cell Res,* 25(p 585-621. doi: 10.1016/0014-4827(61)90192-6.

Haynes, L. *et al.* (2003) CD4 T cell memory derived from young naive cells functions well into old age, but memory generated from aged naive cells functions poorly. *Proc Natl Acad Sci U S A,* 100(25), p 15053-15058. doi: 10.1073/pnas.2433717100.

Haynes, L. *et al.* (1999) Interleukin 2, but not other common gamma chain-binding cytokines, can reverse the defect in generation of CD4 effector T cells from naive T cells of aged mice. *J Exp Med,* 190(7), p 1013-1024. doi: 10.1084/jem.190.7.1013.

Hazeldine, J. and Lord, J. M. (2015) Innate immunesenescence: underlying mechanisms and clinical relevance. *Biogerontology,* 16(2), p 187-201. doi: 10.1007/s10522-014-9514-3.

He, W. *et al.* (2018) Circadian Expression of Migratory Factors Establishes Lineage-Specific Signatures that Guide the Homing of Leukocyte Subsets to Tissues. *Immunity,* 49(6), p 1175-1190 e1177. doi: 10.1016/j.immuni.2018.10.007.

Heath, J. J. and Grant, M. D. (2020) The Immune Response Against Human Cytomegalovirus Links Cellular to Systemic Senescence. *Cells,* 9(3), p doi: 10.3390/cells9030766.

Henderson, R. B. *et al.* (2003) Rapid recruitment of inflammatory monocytes is independent of neutrophil migration. *Blood,* 102(1), p 328-335. doi: 10.1182/blood-2002-10-3228.
Heng, T. S. *et al.* (2005) Effects of castration on thymocyte development in two different models of thymic involution. *J Immunol,* 175(5), p 2982-2993. doi: 10.4049/jimmunol.175.5.2982.
Heng, T. S. *et al.* (2012) Impact of sex steroid ablation on viral, tumour and vaccine responses in aged mice. *PLoS One,* 7(8), p e42677. doi: 10.1371/journal.pone.0042677.
Henson, S. M. and Akbar, A. N. (2009) KLRG1--more than a marker for T cell senescence. *Age (Dordr),* 31(4), p 285-291. doi: 10.1007/s11357-009-9100-9.
Henson, S. M. *et al.* (2015) Blockade of PD-1 or p38 MAP kinase signaling enhances senescent human CD8(+) T-cell proliferation by distinct pathways. *Eur J Immunol,* 45(5), p 1441-1451. doi: 10.1002/eji.201445312.
Hirokawa, K. *et al.* (2013) Slower immune system aging in women versus men in the Japanese population. *Immun Ageing,* 10(1), p 19. doi: 10.1186/1742-4933-10-19.
Hla, T. (2003) Signaling and biological actions of sphingosine 1-phosphate. *Pharmacol Res,* 47(5), p 401-407. doi: 10.1016/s1043-6618(03)00046-x.
Hla, T. *et al.* (2001) Lysophospholipids--receptor revelations. *Science,* 294(5548), p 1875-1878. doi: 10.1126/science.1065323.
Hoffman, W., Lakkis, F. G. and Chalasani, G. (2016) B Cells, Antibodies, and More. *Clin J Am Soc Nephrol,* 11(1), p 137-154. doi: 10.2215/CJN.09430915.
Holland, W. L. *et al.* (2011) Receptor-mediated activation of ceramidase activity initiates the pleiotropic actions of adiponectin. *Nat Med,* 17(1), p 55-63. doi: 10.1038/nm.2277.
Hollnagel, A. *et al.* (2002) The cell adhesion molecule M-cadherin is not essential for muscle development and regeneration. *Mol Cell Biol,* 22(13), p 4760-4770. doi: 10.1128/MCB.22.13.4760-4770.2002.
Hopkin, S., Lord, J. M. and Chimen, M. (2021) Dysregulation of leukocyte trafficking in ageing: Causal factors and possible corrective therapies. *Pharmacol Res,* 163(p 105323. doi: 10.1016/j.phrs.2020.105323.
Hornigold, K. *et al.* (2022) Age-related decline in the resistance of mice to bacterial infection and in LPS/TLR4 pathway-dependent neutrophil responses. *Front Immunol,* 13(p 888415. doi: 10.3389/fimmu.2022.888415.
Horstman, A. M. *et al.* (2012) The role of androgens and estrogens on healthy aging and longevity. *J Gerontol A Biol Sci Med Sci,* 67(11), p 1140-1152. doi: 10.1093/gerona/gls068.
Hossin, M. Z. (2021) The male disadvantage in life expectancy: can we close the gender gap? *Int Health,* 13(5), p 482-484. doi: 10.1093/inthealth/ihaa106.
Hu, L. *et al.* (2017) Epidermal Dysfunction Leads to an Age-Associated Increase in Levels of Serum Inflammatory Cytokines. *J Invest Dermatol,* 137(6), p 1277-1285. doi: 10.1016/j.jid.2017.01.007.
Huang, A. J. *et al.* (1993) Endothelial cell cytosolic free calcium regulates neutrophil migration across monolayers of endothelial cells. *J Cell Biol,* 120(6), p 1371-1380. doi: 10.1083/jcb.120.6.1371.
Huang, K. *et al.* (2022) AgeAnno: a knowledgebase of single-cell annotation of aging in human. *Nucleic Acids Res,* p doi: 10.1093/nar/gkac847.

Huang, M. C. *et al.* (2011) Preferential enhancement of older human T cell cytokine generation, chemotaxis, proliferation and survival by lenalidomide. *Clin Immunol,* 138(2), p 201-211. doi: 10.1016/j.clim.2010.11.002.

Huang, Z. *et al.* (2021) Effects of sex and aging on the immune cell landscape as assessed by single-cell transcriptomic analysis. *Proc Natl Acad Sci U S A,* 118(33), p doi: 10.1073/pnas.2023216118.

Hun, M. L. *et al.* (2020) Gender Disparity Impacts on Thymus Aging and LHRH Receptor Antagonist-Induced Thymic Reconstitution Following Chemotherapeutic Damage. *Front Immunol,* 11(p 302. doi: 10.3389/fimmu.2020.00302.

Huynh, J. *et al.* (2011) Age-related intimal stiffening enhances endothelial permeability and leukocyte transmigration. *Sci Transl Med,* 3(112), p 112ra122. doi: 10.1126/scitranslmed.3002761.

Iemitsu, M. *et al.* (2002) Aging-induced decrease in the PPAR-alpha level in hearts is improved by exercise training. *Am J Physiol Heart Circ Physiol,* 283(5), p H1750-1760. doi: 10.1152/ajpheart.01051.2001.

ImageJ (2012) Available at: https://imagej.nih.gov/ij/docs/guide/146-30.html

Inadera, H. *et al.* (1999) Increase in circulating levels of monocyte chemoattractant protein-1 with aging. *J Interferon Cytokine Res,* 19(10), p 1179-1182. doi: 10.1089/107999099313127.

Irintchev, A. *et al.* (1994) Expression pattern of M-cadherin in normal, denervated, and regenerating mouse muscles. *Dev Dyn,* 199(4), p 326-337. doi: 10.1002/aja.1001990407.

Isobe, T. *et al.* (2005) Influence of gender, age and renal function on plasma adiponectin level: the Tanno and Sobetsu study. *Eur J Endocrinol,* 153(1), p 91-98. doi: 10.1530/eje.1.01930.

Iwabu, M. *et al.* (2015) Adiponectin/adiponectin receptor in disease and aging. *NPJ Aging Mech Dis,* 1(p 15013. doi: 10.1038/npjamd.2015.13.

Iwabu, M. *et al.* (2010) Adiponectin and AdipoR1 regulate PGC-1alpha and mitochondria by Ca(2+) and AMPK/SIRT1. *Nature,* 464(7293), p 1313-1319. doi: 10.1038/nature08991.

Iwata, M. *et al.* (2004) Retinoic acid imprints gut-homing specificity on T cells. *Immunity,* 21(4), p 527-538. doi: 10.1016/j.immuni.2004.08.011.

Jackson, D. G. (2019) Leucocyte Trafficking via the Lymphatic Vasculature-Mechanisms and Consequences. *Front Immunol,* 10(p 471. doi: 10.3389/fimmu.2019.00471.

James, M. J. *et al.* (2003) Anergic T cells exert antigen-independent inhibition of cell-cell interactions via chemokine metabolism. *Blood,* 102(6), p 2173-2179. doi: 10.1182/blood-2003-02-0637.

Jameson, S. C. and Masopust, D. (2018) Understanding Subset Diversity in T Cell Memory. *Immunity,* 48(2), p 214-226. doi: 10.1016/j.immuni.2018.02.010.

Jayanthi, P., Joshua, E. and Ranganathan, K. (2010) Ageing and its implications. *J Oral Maxillofac Pathol,* 14(2), p 48-51. doi: 10.4103/0973-029X.72500.

Jeon, H., Mun, G. I. and Boo, Y. C. (2012) Analysis of serum cytokine/chemokine profiles affected by aging and exercise in mice. *Cytokine,* 60(2), p 487-492. doi: 10.1016/j.cyto.2012.07.014.

Jia, G. *et al.* (2019) Endothelial cell senescence in aging-related vascular dysfunction. *Biochim Biophys Acta Mol Basis Dis,* 1865(7), p 1802-1809. doi: 10.1016/j.bbadis.2018.08.008.

Johnson, S. A., Rozzo, S. J. and Cambier, J. C. (2002) Aging-dependent exclusion of antigen-inexperienced cells from the peripheral B cell repertoire. *J Immunol,* 168(10), p 5014-5023. doi: 10.4049/jimmunol.168.10.5014.

Kaech, S. M., Wherry, E. J. and Ahmed, R. (2002) Effector and memory T-cell differentiation: implications for vaccine development. *Nat Rev Immunol,* 2(4), p 251-262. doi: 10.1038/nri778.

Kaminski, D. A. *et al.* (2012) Advances in human B cell phenotypic profiling. *Front Immunol,* 3(p 302. doi: 10.3389/fimmu.2012.00302.

Kang, I. *et al.* (2004) Age-associated change in the frequency of memory CD4+ T cells impairs long term CD4+ T cell responses to influenza vaccine. *J Immunol,* 173(1), p 673-681. doi: 10.4049/jimmunol.173.1.673.

Kansas, G. S. *et al.* (1993) Regulation of leukocyte rolling and adhesion to high endothelial venules through the cytoplasmic domain of L-selectin. *J Exp Med,* 177(3), p 833-838. doi: 10.1084/jem.177.3.833.

Karaman, S. *et al.* (2015) Decline of lymphatic vessel density and function in murine skin during aging. *Angiogenesis,* 18(4), p 489-498. doi: 10.1007/s10456-015-9479-0.

Karim, M. R. and Wang, Y. F. (2019) Phenotypic identification of CD19(+)CD5(+)CD1d(+) regulatory B cells that produce interleukin 10 and transforming growth factor beta1 in human peripheral blood. *Arch Med Sci,* 15(5), p 1176-1183. doi: 10.5114/aoms.2018.77772.

Kasinski, A. *et al.* (2014) Transcriptional regulation of YWHAZ, the gene encoding 14-3-3zeta. *PLoS One,* 9(4), p e93480. doi: 10.1371/journal.pone.0093480.

Kato, E. *et al.* (2017) The age at onset of rheumatoid arthritis is increasing in Japan: a nationwide database study. *Int J Rheum Dis,* 20(7), p 839-845. doi: 10.1111/1756-185X.12998.

Kaufmann, U. *et al.* (1999) M-cadherin and its sisters in development of striated muscle. *Cell Tissue Res,* 296(1), p 191-198. doi: 10.1007/s004410051280.

Kawahara, A. *et al.* (2009) The sphingolipid transporter spns2 functions in migration of zebrafish myocardial precursors. *Science,* 323(5913), p 524-527. doi: 10.1126/science.1167449.

Kay, E. *et al.* (2015) Sexual dimorphisms in leukocyte trafficking in a mouse peritonitis model. *J Leukoc Biol,* 98(5), p 805-817. doi: 10.1189/jlb.3A1214-601RR.

Keller, B. *et al.* (2021) The expansion of human T-bet(high)CD21(low) B cells is T cell dependent. *Sci Immunol,* 6(64), p eabh0891. doi: 10.1126/sciimmunol.abh0891.

Ketani, S. *et al.* (2016) Expression of ICAM-1 in the Aorta of Wistar Albino Rats. *International Journal of Morphology,* 34(4), p 1482. doi: 10.4067/S0717-95022016000400049.

Khan, S. Y. *et al.* (2017) Premature senescence of endothelial cells upon chronic exposure to TNFalpha can be prevented by N-acetyl cysteine and plumericin. *Sci Rep,* 7(p 39501. doi: 10.1038/srep39501.

Kharroubi, I. *et al.* (2003) Expression of adiponectin receptors in pancreatic beta cells. *Biochem Biophys Res Commun,* 312(4), p 1118-1122. doi: 10.1016/j.bbrc.2003.11.042.

Kim, H. S. *et al.* (2014a) Redox regulation of 14-3-3zeta controls monocyte migration. *Arterioscler Thromb Vasc Biol,* 34(7), p 1514-1521. doi: 10.1161/ATVBAHA.114.303746.
Kim, M., Choe, Y. H. and Lee, S. I. (2022) Lessons From the Success and Failure of Targeted Drugs for Rheumatoid Arthritis: Perspectives for Effective Basic and Translational Research. *Immune Netw,* 22(1), p e8. doi: 10.4110/in.2022.22.e8.
Kim, T. H. *et al.* (2021) Korean Red ginseng prevents endothelial senescence by downregulating the HO-1/NF-kappaB/miRNA-155-5p/eNOS pathway. *J Ginseng Res,* 45(2), p 344-353. doi: 10.1016/j.jgr.2020.08.002.
Kim, Y. *et al.* (2018) Globular adiponectin acts as a melanogenic signal in human epidermal melanocytes. *Br J Dermatol,* 179(3), p 689-701. doi: 10.1111/bjd.16488.
Kim, Y. S. *et al.* (2014b) Gas6 stimulates angiogenesis of human retinal endothelial cells and of zebrafish embryos via ERK1/2 signaling. *PLoS One,* 9(1), p e83901. doi: 10.1371/journal.pone.0083901.
King, H., Aubert, R. E. and Herman, W. H. (1998) Global burden of diabetes, 1995-2025: prevalence, numerical estimates, and projections. *Diabetes Care,* 21(9), p 1414-1431. doi: 10.2337/diacare.21.9.1414.
Kishore, M. *et al.* (2012) Primed T cell responses to chemokines are regulated by the immunoglobulin-like molecule CD31. *PLoS One,* 7(6), p e39433. doi: 10.1371/journal.pone.0039433.
Kissebah, A. H. *et al.* (2000) Quantitative trait loci on chromosomes 3 and 17 influence phenotypes of the metabolic syndrome. *Proc Natl Acad Sci U S A,* 97(26), p 14478-14483. doi: 10.1073/pnas.97.26.14478.
Kitahara, K. *et al.* (2009) Adiponectin stimulates IL-8 production by rheumatoid synovial fibroblasts. *Biochem Biophys Res Commun,* 378(2), p 218-223. doi: 10.1016/j.bbrc.2008.11.017.
Kizer, J. R. *et al.* (2012) Associations of total and high-molecular-weight adiponectin with all-cause and cardiovascular mortality in older persons: the Cardiovascular Health Study. *Circulation,* 126(25), p 2951-2961. doi: 10.1161/CIRCULATIONAHA.112.135202.
Kjaergaard, A. G. *et al.* (2013) Soluble adhesion molecules correlate with surface expression in an in vitro model of endothelial activation. *Basic Clin Pharmacol Toxicol,* 113(4), p 273-279. doi: 10.1111/bcpt.12091.
Klein, S. L. and Flanagan, K. L. (2016) Sex differences in immune responses. *Nat Rev Immunol,* 16(10), p 626-638. doi: 10.1038/nri.2016.90.
Kleiveland, C. R. (2015) Peripheral Blood Mononuclear Cells. *In:* VERHOECKX, K., COTTER, P., LOPEZ-EXPOSITO, I., KLEIVELAND, C., LEA, T., MACKIE, A., REQUENA, T., SWIATECKA, D. & WICHERS, H. (eds.) *The Impact of Food Bioactives on Health: in vitro and ex vivo models.* Cham (CH).
Kline, G. H., Hayden, T. A. and Klinman, N. R. (1999) B cell maintenance in aged mice reflects both increased B cell longevity and decreased B cell generation. *J Immunol,* 162(6), p 3342-3349. doi:
Koch, S. *et al.* (2008) Multiparameter flow cytometric analysis of CD4 and CD8 T cell subsets in young and old people. *Immun Ageing,* 5(p 6. doi: 10.1186/1742-4933-5-6.

Kohler, S. *et al.* (2005) Post-thymic in vivo proliferation of naive CD4+ T cells constrains the TCR repertoire in healthy human adults. *Eur J Immunol,* 35(6), p 1987-1994. doi: 10.1002/eji.200526181.

Kosco, M. H. *et al.* (1989) Antibody-forming cell induction during an early phase of germinal centre development and its delay with ageing. *Immunology,* 68(3), p 312-318. doi:

Kozma, M. *et al.* (2021) Cerebral Pericytes and Endothelial Cells Communicate through Inflammasome-Dependent Signals. *Int J Mol Sci,* 22(11), p doi: 10.3390/ijms22116122.

Kruger-Genge, A. *et al.* (2019) Vascular Endothelial Cell Biology: An Update. *Int J Mol Sci,* 20(18), p doi: 10.3390/ijms20184411.

Kuilman, T. *et al.* (2010) The essence of senescence. *Genes Dev,* 24(22), p 2463-2479. doi: 10.1101/gad.1971610.

Kumar, B. V., Connors, T. J. and Farber, D. L. (2018) Human T Cell Development, Localization, and Function throughout Life. *Immunity,* 48(2), p 202-213. doi: 10.1016/j.immuni.2018.01.007.

Kuniyasu, Y. *et al.* (2000) Naturally anergic and suppressive CD25(+)CD4(+) T cells as a functionally and phenotypically distinct immunoregulatory T cell subpopulation. *Int Immunol,* 12(8), p 1145-1155. doi: 10.1093/intimm/12.8.1145.

Kushner, E. J. *et al.* (2010) Human aging and CD31+ T-cell number, migration, apoptotic susceptibility, and telomere length. *J Appl Physiol (1985),* 109(6), p 1756-1761. doi: 10.1152/japplphysiol.00601.2010.

Kusunoki, N. *et al.* (2010) Adiponectin stimulates prostaglandin E(2) production in rheumatoid arthritis synovial fibroblasts. *Arthritis Rheum,* 62(6), p 1641-1649. doi: 10.1002/art.27450.

Kuwana, T., Peterson, P. A. and Karlsson, L. (1998) Exit of major histocompatibility complex class II-invariant chain p35 complexes from the endoplasmic reticulum is modulated by phosphorylation. *Proc Natl Acad Sci U S A,* 95(3), p 1056-1061. doi: 10.1073/pnas.95.3.1056.

Lagerwaard, B. *et al.* (2021) Matrisome, innervation and oxidative metabolism affected in older compared with younger males with similar physical activity. *J Cachexia Sarcopenia Muscle,* 12(5), p 1214-1231. doi: 10.1002/jcsm.12753.

Lages, C. S. *et al.* (2008) Functional regulatory T cells accumulate in aged hosts and promote chronic infectious disease reactivation. *J Immunol,* 181(3), p 1835-1848. doi: 10.4049/jimmunol.181.3.1835.

Lai, K. P. *et al.* (2013) Targeting thymic epithelia AR enhances T-cell reconstitution and bone marrow transplant grafting efficacy. *Mol Endocrinol,* 27(1), p 25-37. doi: 10.1210/me.2012-1244.

Lalor, P. A. (1991) An evolutionarily-conserved role for murine Ly-1 B cells in protection against bacterial infections. *Autoimmunity,* 10(1), p 71-76. doi: 10.3109/08916939108997150.

Lalor, P. F. *et al.* (2002) Recruitment of lymphocytes to the human liver. *Immunol Cell Biol,* 80(1), p 52-64. doi: 10.1046/j.1440-1711.2002.01062.x.

Langer, H. F. and Chavakis, T. (2009) Leukocyte-endothelial interactions in inflammation. *J Cell Mol Med,* 13(7), p 1211-1220. doi: 10.1111/j.1582-4934.2009.00811.x.

Larbi, A. and Fulop, T. (2014) From "truly naive" to "exhausted senescent" T cells: when markers predict functionality. *Cytometry A,* 85(1), p 25-35. doi: 10.1002/cyto.a.22351.
Lau, E. Y. M. *et al.* (2019) Type 2 diabetes is associated with the accumulation of senescent T cells. *Clin Exp Immunol,* 197(2), p 205-213. doi: 10.1111/cei.13344.
Laurance, S., Lemarie, C. A. and Blostein, M. D. (2012) Growth arrest-specific gene 6 (gas6) and vascular hemostasis. *Adv Nutr,* 3(2), p 196-203. doi: 10.3945/an.111.001826.
Lawrence, M. B. *et al.* (1997) Threshold levels of fluid shear promote leukocyte adhesion through selectins (CD62L,P,E). *J Cell Biol,* 136(3), p 717-727. doi: 10.1083/jcb.136.3.717.
Lawrence, T. and Gilroy, D. W. (2007) Chronic inflammation: a failure of resolution? *Int J Exp Pathol,* 88(2), p 85-94. doi: 10.1111/j.1365-2613.2006.00507.x.
Lazuardi, L. *et al.* (2009) Microarray analysis reveals similarity between CD8+CD28- T cells from young and elderly persons, but not of CD8+CD28+ T cells. *Biogerontology,* 10(2), p 191-202. doi: 10.1007/s10522-008-9167-1.
Le Garff-Tavernier, M. *et al.* (2010) Human NK cells display major phenotypic and functional changes over the life span. *Aging Cell,* 9(4), p 527-535. doi: 10.1111/j.1474-9726.2010.00584.x.
Lechleitner, S. *et al.* (1998) Interferon enhances tumor necrosis factor-induced vascular cell adhesion molecule 1 (CD106) expression in human endothelial cells by an interferon-related factor 1-dependent pathway. *J Exp Med,* 187(12), p 2023-2030. doi: 10.1084/jem.187.12.2023.
Ledgerwood, L. G. *et al.* (2008) The sphingosine 1-phosphate receptor 1 causes tissue retention by inhibiting the entry of peripheral tissue T lymphocytes into afferent lymphatics. *Nat Immunol,* 9(1), p 42-53. doi: 10.1038/ni1534.
Lee, K. S. *et al.* (2008) Mast cells can mediate vascular permeability through regulation of the PI3K-HIF-1alpha-VEGF axis. *Am J Respir Crit Care Med,* 178(8), p 787-797. doi: 10.1164/rccm.200801-008OC.
Lee, M. J. *et al.* (1999) Vascular endothelial cell adherens junction assembly and morphogenesis induced by sphingosine-1-phosphate. *Cell,* 99(3), p 301-312. doi: 10.1016/s0092-8674(00)81661-x.
Lee, S. K. (2018) Sex as an important biological variable in biomedical research. *BMB Rep,* 51(4), p 167-173. doi: 10.5483/bmbrep.2018.51.4.034.
Lee, Y. I. *et al.* (2021) Cellular Senescence and Inflammaging in the Skin Microenvironment. *Int J Mol Sci,* 22(8), p doi: 10.3390/ijms22083849.
Lefebvre, J. S. *et al.* (2012) The aged microenvironment contributes to the age-related functional defects of CD4 T cells in mice. *Aging Cell,* 11(5), p 732-740. doi: 10.1111/j.1474-9726.2012.00836.x.
Lerner, A., Yamada, T. and Miller, R. A. (1989) Pgp-1hi T lymphocytes accumulate with age in mice and respond poorly to concanavalin A. *Eur J Immunol,* 19(6), p 977-982. doi: 10.1002/eji.1830190604.
Ley, K. *et al.* (2007) Getting to the site of inflammation: the leukocyte adhesion cascade updated. *Nat Rev Immunol,* 7(9), p 678-689. doi: 10.1038/nri2156.
Ley, K. and Reutershan, J. (2006) Leucocyte-endothelial interactions in health and disease. *Handb Exp Pharmacol,* 176 Pt 2), p 97-133. doi: 10.1007/3-540-36028-x_4.

Ley, K., Tedder, T. F. and Kansas, G. S. (1993) L-selectin can mediate leukocyte rolling in untreated mesenteric venules in vivo independent of E- or P-selectin. *Blood,* 82(5), p 1632-1638. doi:

Li, M. *et al.* (2012) Reduced AMPK-ACC and mTOR signaling in muscle from older men, and effect of resistance exercise. *Mech Ageing Dev,* 133(11-12), p 655-664. doi: 10.1016/j.mad.2012.09.001.

Li, N. *et al.* (2021) Adiponectin preserves metabolic fitness during aging. *Elife,* 10(p doi: 10.7554/eLife.65108.

Li, Z. *et al.* (1999) Increased expression of matrix metalloproteinase-2 in the thickened intima of aged rats. *Hypertension,* 33(1), p 116-123. doi: 10.1161/01.hyp.33.1.116.

Lim, H. W., Hillsamer, P. and Kim, C. H. (2004) Regulatory T cells can migrate to follicles upon T cell activation and suppress GC-Th cells and GC-Th cell-driven B cell responses. *J Clin Invest,* 114(11), p 1640-1649. doi: 10.1172/JCI22325.

Lin, Y. *et al.* (2016) Changes in blood lymphocyte numbers with age in vivo and their association with the levels of cytokines/cytokine receptors. *Immun Ageing,* 13(p 24. doi: 10.1186/s12979-016-0079-7.

Linehan, E. *et al.* (2014) Aging impairs peritoneal but not bone marrow-derived macrophage phagocytosis. *Aging Cell,* 13(4), p 699-708. doi: 10.1111/acel.12223.

Linton, P. J. *et al.* (2005) Intrinsic versus environmental influences on T-cell responses in aging. *Immunol Rev,* 205(p 207-219. doi: 10.1111/j.0105-2896.2005.00266.x.

Lischner, H. W. and DiGeorge, A. M. (1969) Role of the thymus in humoral immunity. *Lancet,* 2(7629), p 1044-1049. doi: 10.1016/s0140-6736(69)90647-3.

Liu, D. *et al.* (1995) Crystal structure of the zeta isoform of the 14-3-3 protein. *Nature,* 376(6536), p 191-194. doi: 10.1038/376191a0.

Liu, M. *et al.* (2021) Specialized immune responses in the peritoneal cavity and omentum. *J Leukoc Biol,* 109(4), p 717-729. doi: 10.1002/JLB.5MIR0720-271RR.

Ljubicic, V. and Hood, D. A. (2009) Diminished contraction-induced intracellular signaling towards mitochondrial biogenesis in aged skeletal muscle. *Aging Cell,* 8(4), p 394-404. doi: 10.1111/j.1474-9726.2009.00483.x.

Lopez-Otin, C. *et al.* (2013) The hallmarks of aging. *Cell,* 153(6), p 1194-1217. doi: 10.1016/j.cell.2013.05.039.

Lopez-Otin, C. *et al.* (2023) Hallmarks of aging: An expanding universe. *Cell,* 186(2), p 243-278. doi: 10.1016/j.cell.2022.11.001.

Lord, J. M. (2013) The effect of ageing of the immune system on vaccination responses. *Hum Vaccin Immunother,* 9(6), p 1364-1367. doi: 10.4161/hv.24696.

Lou, O. *et al.* (2007) CD99 is a key mediator of the transendothelial migration of neutrophils. *J Immunol,* 178(2), p 1136-1143. doi: 10.4049/jimmunol.178.2.1136.

Louwe, P. A. *et al.* (2021) Recruited macrophages that colonize the post-inflammatory peritoneal niche convert into functionally divergent resident cells. *Nat Commun,* 12(1), p 1770. doi: 10.1038/s41467-021-21778-0.

Lu, J. *et al.* (2009) 14-3-3zeta Cooperates with ErbB2 to promote ductal carcinoma in situ progression to invasive breast cancer by inducing epithelial-mesenchymal transition. *Cancer Cell,* 16(3), p 195-207. doi: 10.1016/j.ccr.2009.08.010.

Lu, R. M. *et al.* (2020) Development of therapeutic antibodies for the treatment of diseases. *J Biomed Sci,* 27(1), p 1. doi: 10.1186/s12929-019-0592-z.
Luckheeram, R. V. *et al.* (2012) CD4(+)T cells: differentiation and functions. *Clin Dev Immunol,* 2012(p 925135. doi: 10.1155/2012/925135.
Luu, N. T., Rainger, G. E. and Nash, G. B. (2000) Differential ability of exogenous chemotactic agents to disrupt transendothelial migration of flowing neutrophils. *J Immunol,* 164(11), p 5961-5969. doi: 10.4049/jimmunol.164.11.5961.
Lynch, H. E. *et al.* (2009) Thymic involution and immune reconstitution. *Trends Immunol,* 30(7), p 366-373. doi: 10.1016/j.it.2009.04.003.
Maceyka, M. *et al.* (2012) Sphingosine-1-phosphate signaling and its role in disease. *Trends Cell Biol,* 22(1), p 50-60. doi: 10.1016/j.tcb.2011.09.003.
Mackall, C. L. *et al.* (1995) Age, thymopoiesis, and CD4+ T-lymphocyte regeneration after intensive chemotherapy. *N Engl J Med,* 332(3), p 143-149. doi: 10.1056/NEJM199501193320303.
Mackay, C. R., Marston, W. L. and Dudler, L. (1990) Naive and memory T cells show distinct pathways of lymphocyte recirculation. *J Exp Med,* 171(3), p 801-817. doi: 10.1084/jem.171.3.801.
MacLennan, I. C. *et al.* (2003) Extrafollicular antibody responses. *Immunol Rev,* 194(p 8-18. doi: 10.1034/j.1600-065x.2003.00058.x.
Maier, J. A. *et al.* (1990) Extension of the life-span of human endothelial cells by an interleukin-1 alpha antisense oligomer. *Science,* 249(4976), p 1570-1574. doi: 10.1126/science.2218499.
Malmstrom, V., Trollmo, C. and Klareskog, L. (2005) Modulating co-stimulation: a rational strategy in the treatment of rheumatoid arthritis? *Arthritis Res Ther,* 7 Suppl 2(Suppl 2), p S15-20. doi: 10.1186/ar1505.
Mao, X. *et al.* (2006) APPL1 binds to adiponectin receptors and mediates adiponectin signalling and function. *Nat Cell Biol,* 8(5), p 516-523. doi: 10.1038/ncb1404.
Mariani, E. *et al.* (2006) Simultaneous evaluation of circulating chemokine and cytokine profiles in elderly subjects by multiplex technology: relationship with zinc status. *Biogerontology,* 7(5-6), p 449-459. doi: 10.1007/s10522-006-9060-8.
Marlovits, S. *et al.* (2000) Effect on diphtheria immunity of combined tetanus and diphtheria booster vaccination in adults. *Eur J Clin Microbiol Infect Dis,* 19(7), p 506-513. doi: 10.1007/s100960000305.
Marquez, E. J. *et al.* (2020) Sexual-dimorphism in human immune system aging. *Nat Commun,* 11(1), p 751. doi: 10.1038/s41467-020-14396-9.
Martin, M. D. and Badovinac, V. P. (2018) Defining Memory CD8 T Cell. *Front Immunol,* 9(p 2692. doi: 10.3389/fimmu.2018.02692.
Masopust, D. and Schenkel, J. M. (2013) The integration of T cell migration, differentiation and function. *Nat Rev Immunol,* 13(5), p 309-320. doi: 10.1038/nri3442.
Masopust, D., Sivula, C. P. and Jameson, S. C. (2017) Of Mice, Dirty Mice, and Men: Using Mice To Understand Human Immunology. *J Immunol,* 199(2), p 383-388. doi: 10.4049/jimmunol.1700453.
Matloubian, M. *et al.* (2004) Lymphocyte egress from thymus and peripheral lymphoid organs is dependent on S1P receptor 1. *Nature,* 427(6972), p 355-360. doi: 10.1038/nature02284.
Matsubara, H. *et al.* (2020) PEPITEM/Cadherin 15 Axis Inhibits T Lymphocyte Infiltration and Glomerulonephritis in a Mouse Model of Systemic Lupus

Erythematosus. *J Immunol,* 204(8), p 2043-2052. doi: 10.4049/jimmunol.1900213.
Matsushita, T. *et al.* (2008) Regulatory B cells inhibit EAE initiation in mice while other B cells promote disease progression. *J Clin Invest,* 118(10), p 3420-3430. doi: 10.1172/JCI36030.
Mattoo, H. *et al.* (2009) Naive CD4 T cells from aged mice show enhanced death upon primary activation. *Int Immunol,* 21(11), p 1277-1289. doi: 10.1093/intimm/dxp094.
Mauro, L. *et al.* (2015) Estrogen receptor-alpha drives adiponectin effects on cyclin D1 expression in breast cancer cells. *FASEB J,* 29(5), p 2150-2160. doi: 10.1096/fj.14-262808.
Maxwell, L. and Singh, J. A. (2009) Abatacept for rheumatoid arthritis. *Cochrane Database Syst Rev,* 2009(4), p CD007277. doi: 10.1002/14651858.CD007277.pub2.
Mayr, B. and Montminy, M. (2001) Transcriptional regulation by the phosphorylation-dependent factor CREB. *Nat Rev Mol Cell Biol,* 2(8), p 599-609. doi: 10.1038/35085068.
McGettrick, H. M. *et al.* (2009a) Direct observations of the kinetics of migrating T cells suggest active retention by endothelial cells with continual bidirectional migration. *J Leukoc Biol,* 85(1), p 98-107. doi: 10.1189/jlb.0508301.
McGettrick, H. M. *et al.* (2009b) Fibroblasts from different sites may promote or inhibit recruitment of flowing lymphocytes by endothelial cells. *Eur J Immunol,* 39(1), p 113-125. doi: 10.1002/eji.200838232.
McGettrick, H. M. *et al.* (2017). *Mesenchymal Stromal Cells as Active Regulators of Lymphocyte Recruitment to Blood Vascular Endothelial Cells*. In: T-cell Trafficking. Humana Press, New York, 121-142.
McGowan, J. *et al.* (2019) 14-3-3zeta-A Novel Immunogen Promotes Inflammatory Cytokine Production. *Front Immunol,* 10(p 1553. doi: 10.3389/fimmu.2019.01553.
Mehrpour, M. *et al.* (2010) Autophagy in health and disease. 1. Regulation and significance of autophagy: an overview. *Am J Physiol Cell Physiol,* 298(4), p C776-785. doi: 10.1152/ajpcell.00507.2009.
Mellado, M. *et al.* (2015) T Cell Migration in Rheumatoid Arthritis. *Front Immunol,* 6(p 384. doi: 10.3389/fimmu.2015.00384.
Merino, J. *et al.* (1998) Progressive decrease of CD8high+ CD28+ CD57- cells with ageing. *Clin Exp Immunol,* 112(1), p 48-51. doi: 10.1046/j.1365-2249.1998.00551.x.
Mhawech, P. (2005) 14-3-3 proteins--an update. *Cell Res,* 15(4), p 228-236. doi: 10.1038/sj.cr.7290291.
Miguel-Hidalgo, J. J. *et al.* (2007) Distribution of ICAM-1 immunoreactivity during aging in the human orbitofrontal cortex. *Brain Behav Immun,* 21(1), p 100-111. doi: 10.1016/j.bbi.2006.05.001.
Miles, E. A. *et al.* (2008) Age-related increases in circulating inflammatory markers in men are independent of BMI, blood pressure and blood lipid concentrations. *Atherosclerosis,* 196(1), p 298-305. doi: 10.1016/j.atherosclerosis.2006.11.002.
Miles, E. A. *et al.* (2001) Influence of age and dietary fish oil on plasma soluble adhesion molecule concentrations. *Clin Sci (Lond),* 100(1), p 91-100. doi:

Millan, J. *et al.* (2006) Lymphocyte transcellular migration occurs through recruitment of endothelial ICAM-1 to caveola- and F-actin-rich domains. *Nat Cell Biol,* 8(2), p 113-123. doi: 10.1038/ncb1356.
Millan, J. and Ridley, A. J. (2005) Rho GTPases and leucocyte-induced endothelial remodelling. *Biochem J,* 385(Pt 2), p 329-337. doi: 10.1042/BJ20041584.
Miller, C. and Kelsoe, G. (1995) Ig VH hypermutation is absent in the germinal centers of aged mice. *Journal of Immunology,* 155(7), p 3377-3384. doi:
Mittelbrunn, M. and Kroemer, G. (2021) Hallmarks of T cell aging. *Nat Immunol,* 22(6), p 687-698. doi: 10.1038/s41590-021-00927-z.
Miyamoto, S. *et al.* (1995) Integrin function: molecular hierarchies of cytoskeletal and signaling molecules. *J Cell Biol,* 131(3), p 791-805. doi: 10.1083/jcb.131.3.791.
Mo, R. *et al.* (2003) T cell chemokine receptor expression in aging. *J Immunol,* 170(2), p 895-904. doi: 10.4049/jimmunol.170.2.895.
Mogilenko, D. A. *et al.* (2021) Comprehensive Profiling of an Aging Immune System Reveals Clonal GZMK(+) CD8(+) T Cells as Conserved Hallmark of Inflammaging. *Immunity,* 54(1), p 99-115 e112. doi: 10.1016/j.immuni.2020.11.005.
Montane, J. *et al.* (2011) Prevention of murine autoimmune diabetes by CCL22-mediated Treg recruitment to the pancreatic islets. *J Clin Invest,* 121(8), p 3024-3028. doi: 10.1172/JCI43048.
Montecino-Rodriguez, E., Berent-Maoz, B. and Dorshkind, K. (2013) Causes, consequences, and reversal of immune system aging. *J Clin Invest,* 123(3), p 958-965. doi: 10.1172/JCI64096.
Monti, B., Berteotti, C. and Contestabile, A. (2005) Dysregulation of memory-related proteins in the hippocampus of aged rats and their relation with cognitive impairment. *Hippocampus,* 15(8), p 1041-1049. doi: 10.1002/hipo.20099.
Morisaki, N. *et al.* (1997) New indices of ischemic heart disease and aging: studies on the serum levels of soluble intercellular adhesion molecule-1 (ICAM-1) and soluble vascular cell adhesion molecule-1 (VCAM-1) in patients with hypercholesterolemia and ischemic heart disease. *Atherosclerosis,* 131(1), p 43-48. doi: 10.1016/s0021-9150(97)06083-8.
Morley, J. E. (2003) Hormones and the aging process. *J Am Geriatr Soc,* 51(7 Suppl), p S333-337. doi: 10.1046/j.1365-2389.2003.51344.x.
Moroy, T. and Karsunky, H. (2000) Regulation of pre-T-cell development. *Cell Mol Life Sci,* 57(6), p 957-975. doi: 10.1007/PL00000737.
Morrison, D. K. and Cutler, R. E. (1997) The complexity of Raf-1 regulation. *Curr Opin Cell Biol,* 9(2), p 174-179. doi: 10.1016/s0955-0674(97)80060-9.
Mould, A. P. and Humphries, M. J. (2004) Regulation of integrin function through conformational complexity: not simply a knee-jerk reaction? *Curr Opin Cell Biol,* 16(5), p 544-551. doi: 10.1016/j.ceb.2004.07.003.
Mun, G. I. and Boo, Y. C. (2010) Identification of CD44 as a senescence-induced cell adhesion gene responsible for the enhanced monocyte recruitment to senescent endothelial cells. *Am J Physiol Heart Circ Physiol,* 298(6), p H2102-2111. doi: 10.1152/ajpheart.00835.2009.
Munier, C. C., Ottmann, C. and Perry, M. W. D. (2021) 14-3-3 modulation of the inflammatory response. *Pharmacol Res,* 163(p 105236. doi: 10.1016/j.phrs.2020.105236.

Munir, H. *et al.* (2015) Analyzing the effects of stromal cells on the recruitment of leukocytes from flow. *J Vis Exp,* 95), p e52480. doi: 10.3791/52480.
Murciano, C. *et al.* (2008) Influence of aging on murine neutrophil and macrophage function against Candida albicans. *FEMS Immunol Med Microbiol,* 53(2), p 214-221. doi: 10.1111/j.1574-695X.2008.00418.x.
Muslin, A. J. *et al.* (1996) Interaction of 14-3-3 with signaling proteins is mediated by the recognition of phosphoserine. *Cell,* 84(889-897), p doi:
Nacka-Aleksić, M. *et al.* (2020) Sex as a confounding factor in the effects of ageing on rat lymph node T cell compartment. *Exp Gerontol,* 142(p 111140. doi: 10.1016/j.exger.2020.111140.
Nagasawa, M. *et al.* (2018) High plasma adiponectin levels are associated with frailty in a general old-old population: The Septuagenarians, Octogenarians, Nonagenarians Investigation with Centenarians study. *Geriatr Gerontol Int,* 18(6), p 839-846. doi: 10.1111/ggi.13258.
Nagel, J. E. *et al.* (1988) Decreased proliferation, interleukin 2 synthesis, and interleukin 2 receptor expression are accompanied by decreased mRNA expression in phytohemagglutinin-stimulated cells from elderly donors. *J Clin Invest,* 81(4), p 1096-1102. doi: 10.1172/JCI113422.
Naghavi, M. *et al.* (2015) Global, regional, and national age-sex specific all-cause and cause-specific mortality for 240 causes of death, 1990-2013: a systematic analysis for the Global Burden of Disease Study 2013. *Lancet,* 385(9963), p 117-171. doi: 10.1016/S0140-6736(14)61682-2.
Nakajima, T. *et al.* (2002) T-cell-mediated lysis of endothelial cells in acute coronary syndromes. *Circulation,* 105(5), p 570-575. doi: 10.1161/hc0502.103348.
Nations, U. (2019) Available at: https://www.un.org/en/development/desa/population/publications/pdf/ageing/WorldPopulationAgeing2019-Highlights.pdf
Naylor, K. *et al.* (2005) The influence of age on T cell generation and TCR diversity. *J Immunol,* 174(11), p 7446-7452. doi: 10.4049/jimmunol.174.11.7446.
Nechamen, C. A. *et al.* (2004) Human follicle-stimulating hormone (FSH) receptor interacts with the adaptor protein APPL1 in HEK 293 cells: potential involvement of the PI3K pathway in FSH signaling. *Biol Reprod,* 71(2), p 629-636. doi: 10.1095/biolreprod.103.025833.
Newson, J. *et al.* (2014) Resolution of acute inflammation bridges the gap between innate and adaptive immunity. *Blood,* 124(11), p 1748-1764. doi: 10.1182/blood-2014-03-562710.
Nguyen, T. M. D. (2020) Adiponectin: Role in Physiology and Pathophysiology. *Int J Prev Med,* 11(p 136. doi: 10.4103/ijpvm.IJPVM_193_20.
Nicoletti, C. *et al.* (1991) Repertoire diversity of antibody response to bacterial antigens in aged mice. II. Phosphorylcholine-antibody in young and aged mice differ in both VH/VL gene repertoire and in specificity. *J Immunol,* 147(8), p 2750-2755. doi:
Nikolich-Zugich, J. (2008) Ageing and life-long maintenance of T-cell subsets in the face of latent persistent infections. *Nat Rev Immunol,* 8(7), p 512-522. doi: 10.1038/nri2318.
Niwa, Y. *et al.* (1989) Neutrophil chemotaxis, phagocytosis and parameters of reactive oxygen species in human aging: cross-sectional and longitudinal studies. *Life Sci,* 44(22), p 1655-1664. doi: 10.1016/0024-3205(89)90482-7.

Nomellini, V. *et al.* (2012) Dysregulation of neutrophil CXCR2 and pulmonary endothelial icam-1 promotes age-related pulmonary inflammation. *Aging Dis,* 3(3), p 234-247. doi:

Noren Hooten, N. and Evans, M. K. (2017) Techniques to Induce and Quantify Cellular Senescence. *J Vis Exp,* 123), p doi: 10.3791/55533.

Norian, L. A. and Allen, P. M. (2004) No intrinsic deficiencies in CD8+ T cell-mediated antitumor immunity with aging. *J Immunol,* 173(2), p 835-844. doi: 10.4049/jimmunol.173.2.835.

Nossent, A. Y. *et al.* (2017) CCR7-CCL19/CCL21 Axis is Essential for Effective Arteriogenesis in a Murine Model of Hindlimb Ischemia. *J Am Heart Assoc,* 6(3), p doi: 10.1161/JAHA.116.005281.

Nourisson, C. *et al.* (2017) Impact of gender on the response and tolerance to abatacept in patients with rheumatoid arthritis: results from the 'ORA' registry. *RMD Open,* 3(2), p e000515. doi: 10.1136/rmdopen-2017-000515.

Nourshargh, S. and Alon, R. (2014) Leukocyte migration into inflamed tissues. *Immunity,* 41(5), p 694-707. doi: 10.1016/j.immuni.2014.10.008.

Nourshargh, S., Hordijk, P. L. and Sixt, M. (2010) Breaching multiple barriers: leukocyte motility through venular walls and the interstitium. *Nat Rev Mol Cell Biol,* 11(5), p 366-378. doi: 10.1038/nrm2889.

Nourshargh, S., Krombach, F. and Dejana, E. (2006) The role of JAM-A and PECAM-1 in modulating leukocyte infiltration in inflamed and ischemic tissues. *J Leukoc Biol,* 80(4), p 714-718. doi: 10.1189/jlb.1105645.

Nutt, S. L. *et al.* (2015) The generation of antibody-secreting plasma cells. *Nat Rev Immunol,* 15(3), p 160-171. doi: 10.1038/nri3795.

Obeid, S. and Hebbard, L. (2012) Role of adiponectin and its receptors in cancer. *Cancer Biol Med,* 9(4), p 213-220. doi: 10.7497/j.issn.2095-3941.2012.04.001.

Ochando, J. C. *et al.* (2005) Lymph node occupancy is required for the peripheral development of alloantigen-specific Foxp3+ regulatory T cells. *J Immunol,* 174(11), p 6993-7005. doi: 10.4049/jimmunol.174.11.6993.

Oh, D. J. *et al.* (2018) Association of Up-Regulated Plasma Adiponectin With Risk of Incident Depression in a Community-Dwelling Elderly Population. *J Clin Psychiatry,* 79(3), p doi: 10.4088/JCP.17m11695.

Ohashi, K. *et al.* (2010) Adiponectin promotes macrophage polarization toward an anti-inflammatory phenotype. *J Biol Chem,* 285(9), p 6153-6160. doi: 10.1074/jbc.M109.088708.

Okada, R. *et al.* (2008) Phenotypic classification of human CD4+ T cell subsets and their differentiation. *Int Immunol,* 20(9), p 1189-1199. doi: 10.1093/intimm/dxn075.

Olsen, N. J. *et al.* (2001) Androgen receptors in thymic epithelium modulate thymus size and thymocyte development. *Endocrinology,* 142(3), p 1278-1283. doi: 10.1210/endo.142.3.8032.

Onyema, O. O. *et al.* (2015) Aging-associated subpopulations of human CD8+ T-lymphocytes identified by their CD28 and CD57 phenotypes. *Arch Gerontol Geriatr,* 61(3), p 494-502. doi: 10.1016/j.archger.2015.08.007.

Oo, M. L. *et al.* (2011) Engagement of S1P(1)-degradative mechanisms leads to vascular leak in mice. *J Clin Invest,* 121(6), p 2290-2300. doi: 10.1172/JCI45403.

Orme, I. M. and Roberts, A. D. (1998) Changes in integrin/adhesion molecule expression, but not in the T-cell receptor repertoire, in old mice infected with tuberculosis. *Mech Ageing Dev,* 105(1-2), p 19-29. doi: 10.1016/s0047-6374(98)00079-7.

Otero, K. *et al.* (2009) Macrophage colony-stimulating factor induces the proliferation and survival of macrophages via a pathway involving DAP12 and beta-catenin. *Nat Immunol,* 10(7), p 734-743. doi: 10.1038/ni.1744.

Ouchi, N. *et al.* (1999) Novel modulator for endothelial adhesion molecules: adipocyte-derived plasma protein adiponectin. *Circulation,* 100(25), p 2473-2476. doi: 10.1161/01.cir.100.25.2473.

Ouchi, N. and Walsh, K. (2007) Adiponectin as an anti-inflammatory factor. *Clin Chim Acta,* 380(1-2), p 24-30. doi: 10.1016/j.cca.2007.01.026.

Ouedraogo, R. *et al.* (2007) Adiponectin deficiency increases leukocyte-endothelium interactions via upregulation of endothelial cell adhesion molecules in vivo. *J Clin Invest,* 117(6), p 1718-1726. doi: 10.1172/JCI29623.

Ouyang, Q. *et al.* (2003) Age-associated accumulation of CMV-specific CD8+ T cells expressing the inhibitory killer cell lectin-like receptor G1 (KLRG1). *Exp Gerontol,* 38(8), p 911-920. doi: 10.1016/s0531-5565(03)00134-7.

Owen-Woods, C. *et al.* (2020) Local microvascular leakage promotes trafficking of activated neutrophils to remote organs. *J Clin Invest,* 130(5), p 2301-2318. doi: 10.1172/JCI133661.

Ozgonenel, B., Rajpurkar, M. and Lusher, J. M. (2007) How do you treat bleeding disorders with desmopressin? *Postgrad Med J,* 83(977), p 159-163. doi: 10.1136/pgmj.2006.052118.

Ozinsky, A. *et al.* (2000) The repertoire for pattern recognition of pathogens by the innate immune system is defined by cooperation between toll-like receptors. *Proc Natl Acad Sci U S A,* 97(25), p 13766-13771. doi: 10.1073/pnas.250476497.

Pajvani, U. B. *et al.* (2003) Structure-function studies of the adipocyte-secreted hormone Acrp30/adiponectin. Implications fpr metabolic regulation and bioactivity. *J Biol Chem,* 278(11), p 9073-9085. doi: 10.1074/jbc.M207198200.

Pang, T. T. and Narendran, P. (2008) The distribution of adiponectin receptors on human peripheral blood mononuclear cells. *Ann N Y Acad Sci,* 1150(p 143-145. doi: 10.1196/annals.1447.021.

Pangrazzi, L. and Weinberger, B. (2020) T cells, aging and senescence. *Exp Gerontol,* 134(p 110887. doi: 10.1016/j.exger.2020.110887.

Papadopoulou, A. S. *et al.* (2011) The thymic epithelial microRNA network elevates the threshold for infection-associated thymic involution via miR-29a mediated suppression of the IFN-alpha receptor. *Nat Immunol,* 13(2), p 181-187. doi: 10.1038/ni.2193.

Paramanik, V. and Thakur, M. K. (2013) Role of CREB signaling in aging brain. *Arch Ital Biol,* 151(1), p 33-42. doi: 10.4449/aib.v151i1.1461.

Park, S. C. and Jeen, Y. T. (2018) Anti-integrin therapy for inflammatory bowel disease. *World J Gastroenterol,* 24(17), p 1868-1880. doi: 10.3748/wjg.v24.i17.1868.

Parliment, U. (2021) Available at: https://commonslibrary.parliament.uk/research-briefings/cbp-9239/

Parry, H. M. *et al.* (2021) PD-1 is imprinted on cytomegalovirus-specific CD4+ T cells and attenuates Th1 cytokine production whilst maintaining cytotoxicity. *PLoS Pathog,* 17(3), p e1009349. doi: 10.1371/journal.ppat.1009349.

Patel, P. D. and Arora, R. R. (2008) Endothelial dysfunction: a potential tool in gender related cardiovascular disease. *Ther Adv Cardiovasc Dis,* 2(2), p 89-100. doi: 10.1177/1753944707088904.

Paul-Clark, M. J. *et al.* (2004) 15-epi-lipoxin A4-mediated induction of nitric oxide explains how aspirin inhibits acute inflammation. *J Exp Med,* 200(1), p 69-78. doi: 10.1084/jem.20040566.

Pennington, K. L. *et al.* (2018) The dynamic and stress-adaptive signaling hub of 14-3-3: emerging mechanisms of regulation and context-dependent protein-protein interactions. *Oncogene,* 37(42), p 5587-5604. doi: 10.1038/s41388-018-0348-3.

Pereira, B. I. *et al.* (2020) Sestrins induce natural killer function in senescent-like CD8(+) T cells. *Nat Immunol,* 21(6), p 684-694. doi: 10.1038/s41590-020-0643-3.

Pezhman, L. *et al.* (2023) PEPITEM modulates leukocyte trafficking to reduce obesity-induced inflammation. *Clin Exp Immunol,* 212(1), p 1-10. doi: 10.1093/cei/uxad022.

Pfister, G. *et al.* (2006) Naive T cells in the elderly: are they still there? *Ann N Y Acad Sci,* 1067(p 152-157. doi: 10.1196/annals.1354.018.

Phillipson, M. *et al.* (2006) Intraluminal crawling of neutrophils to emigration sites: a molecularly distinct process from adhesion in the recruitment cascade. *J Exp Med,* 203(12), p 2569-2575. doi: 10.1084/jem.20060925.

Piali, L. *et al.* (1998) The chemokine receptor CXCR3 mediates rapid and shear-resistant adhesion-induction of effector T lymphocytes by the chemokines IP10 and Mig. *Eur J Immunol,* 28(3), p 961-972. doi: 10.1002/(SICI)1521-4141(199803)28:03<961::AID-IMMU961>3.0.CO;2-4.

Piao, L. *et al.* (2018) Adiponectin/AdiopR1 signal inactivation contributes to impaired angiogenesis in mice of advanced age. *Int J Cardiol,* 267(p 150-155. doi: 10.1016/j.ijcard.2018.05.089.

Pido-Lopez, J., Imami, N. and Aspinall, R. (2001) Both age and gender affect thymic output: more recent thymic migrants in females than males as they age. *Clin Exp Immunol,* 125(3), p 409-413. doi: 10.1046/j.1365-2249.2001.01640.x.

Pieper, K., Grimbacher, B. and Eibel, H. (2013) B-cell biology and development. *J Allergy Clin Immunol,* 131(4), p 959-971. doi: 10.1016/j.jaci.2013.01.046.

Pilling, D. *et al.* (1996) CD4+ CD45RA+ T cells from adults respond to recall antigens after CD28 ligation. *Int Immunol,* 8(11), p 1737-1742. doi: 10.1093/intimm/8.11.1737.

Pinchuk, L. M. and Filipov, N. M. (2008) Differential effects of age on circulating and splenic leukocyte populations in C57BL/6 and BALB/c male mice. *Immun Ageing,* 5(p 1. doi: 10.1186/1742-4933-5-1.

Plunkett, F. J. *et al.* (2007) The loss of telomerase activity in highly differentiated CD8+CD28-CD27- T cells is associated with decreased Akt (Ser473) phosphorylation. *J Immunol,* 178(12), p 7710-7719. doi: 10.4049/jimmunol.178.12.7710.

Polito, R. *et al.* (2019) Adiponectin Receptors and Pro-inflammatory Cytokines Are Modulated in Common Variable Immunodeficiency Patients: Correlation With Ig

Replacement Therapy. *Front Immunol,* 10(p 2812. doi: 10.3389/fimmu.2019.02812.

Pompeu, M. L. *et al.* (1991) Granulocytes in the inflammatory process of BALB/c mice infected by Leishmania amazonensis. A quantitative approach. *Acta Trop,* 48(3), p 185-193. doi: 10.1016/0001-706x(91)90046-m.

Porte, Y., Buhot, M. C. and Mons, N. (2008) Alteration of CREB phosphorylation and spatial memory deficits in aged 129T2/Sv mice. *Neurobiol Aging,* 29(10), p 1533-1546. doi: 10.1016/j.neurobiolaging.2007.03.023.

Poynter, M. E. and Daynes, R. A. (1998) Peroxisome proliferator-activated receptor alpha activation modulates cellular redox status, represses nuclear factor-kappaB signaling, and reduces inflammatory cytokine production in aging. *J Biol Chem,* 273(49), p 32833-32841. doi: 10.1074/jbc.273.49.32833.

Poznansky, M. C. *et al.* (2000) Active movement of T cells away from a chemokine. *Nat Med,* 6(5), p 543-548. doi: 10.1038/75022.

Prosperini, L. *et al.* (2017) Age as a risk factor for early onset of natalizumab-related progressive multifocal leukoencephalopathy. *J Neurovirol,* 23(5), p 742-749. doi: 10.1007/s13365-017-0561-9.

Pruimboom, W. M. *et al.* (1995) Levels of soluble intercellular adhesion molecule 1, eicosanoids and cytokines in ascites of patients with liver cirrhosis, peritoneal cancer and spontaneous bacterial peritonitis. *Int J Immunopharmacol,* 17(5), p 375-384. doi: 10.1016/0192-0561(95)00015-t.

Puddu, P. *et al.* (2012) Relationships among hyperuricemia, endothelial dysfunction and cardiovascular disease: molecular mechanisms and clinical implications. *J Cardiol,* 59(3), p 235-242. doi: 10.1016/j.jjcc.2012.01.013.

Pulsatelli, L. *et al.* (2000) Chemokine production by peripheral blood mononuclear cells in elderly subjects. *Mech Ageing Dev,* 121(1-3), p 89-100. doi: 10.1016/s0047-6374(00)00200-1.

Pyo, J. O. *et al.* (2013) Overexpression of Atg5 in mice activates autophagy and extends lifespan. *Nat Commun,* 4(p 2300. doi: 10.1038/ncomms3300.

Qvit, N. *et al.* (2017) Peptidomimetic therapeutics: scientific approaches and opportunities. *Drug Discov Today,* 22(2), p 454-462. doi: 10.1016/j.drudis.2016.11.003.

Rahman, A. *et al.* (1998) E-selectin expression in human endothelial cells by TNF-alpha-induced oxidant generation and NF-kappaB activation. *Am J Physiol,* 275(3), p L533-544. doi: 10.1152/ajplung.1998.275.3.L533.

Rainger, G. E. and McGettrick, H. M. (2017) T-Cell Trafficking Methods and Protocols Second Edition Preface. *T-Cell Trafficking: Methods and Protocols, 2nd Edition.*

Rainger, G. E. *et al.* (2001) A novel system for investigating the ability of smooth muscle cells and fibroblasts to regulate adhesion of flowing leukocytes to endothelial cells. *J Immunol Methods,* 255(1-2), p 73-82. doi: 10.1016/s0022-1759(01)00427-6.

Rajakariar, R. *et al.* (2008) Novel biphasic role for lymphocytes revealed during resolving inflammation. *Blood,* 111(8), p 4184-4192. doi: 10.1182/blood-2007-08-108936.

Ramachandran, H. *et al.* (2012) Optimal thawing of cryopreserved peripheral blood mononuclear cells for use in high-throughput human immune monitoring studies. *Cells,* 1(3), p 313-324. doi: 10.3390/cells1030313.

Ramello, M. C. *et al.* (2021) Polyfunctional KLRG-1(+)CD57(+) Senescent CD4(+) T Cells Infiltrate Tumors and Are Expanded in Peripheral Blood From Breast Cancer Patients. *Front Immunol,* 12(p 713132. doi: 10.3389/fimmu.2021.713132.

Rao, T. S. *et al.* (1994) In vivo characterization of zymosan-induced mouse peritoneal inflammation. *J Pharmacol Exp Ther,* 269(3), p 917-925. doi:

Rapp, M. *et al.* (2019) CCL22 controls immunity by promoting regulatory T cell communication with dendritic cells in lymph nodes. *J Exp Med,* 216(5), p 1170-1181. doi: 10.1084/jem.20170277.

Ratliff, M. *et al.* (2013) In senescence, age-associated B cells secrete TNFalpha and inhibit survival of B-cell precursors. *Aging Cell,* 12(2), p 303-311. doi: 10.1111/acel.12055.

Reglero-Real, N. *et al.* (2016) Endothelial Cell Junctional Adhesion Molecules: Role and Regulation of Expression in Inflammation. *Arterioscler Thromb Vasc Biol,* 36(10), p 2048-2057. doi: 10.1161/ATVBAHA.116.307610.

Reglero-Real, N., Rolas, L. and Nourshargh, S. (2019) Leukocyte Trafficking: Time to Take Time Seriously. *Immunity,* 50(2), p 273-275. doi: 10.1016/j.immuni.2019.01.013.

Ren, Z. *et al.* (2009) Effect of age on susceptibility to Salmonella Typhimurium infection in C57BL/6 mice. *J Med Microbiol,* 58(Pt 12), p 1559-1567. doi: 10.1099/jmm.0.013250-0.

Reznick, R. M. *et al.* (2007) Aging-associated reductions in AMP-activated protein kinase activity and mitochondrial biogenesis. *Cell Metab,* 5(2), p 151-156. doi: 10.1016/j.cmet.2007.01.008.

Richards, A. A. *et al.* (2006) Adiponectin multimerization is dependent on conserved lysines in the collagenous domain: evidence for regulation of multimerization by alterations in posttranslational modifications. *Mol Endocrinol,* 20(7), p 1673-1687. doi: 10.1210/me.2005-0390.

Richner, J. M. *et al.* (2015) Age-Dependent Cell Trafficking Defects in Draining Lymph Nodes Impair Adaptive Immunity and Control of West Nile Virus Infection. *PLoS Pathog,* 11(7), p e1005027. doi: 10.1371/journal.ppat.1005027.

Richter, V. *et al.* (2003) Circulating vascular cell adhesion molecules VCAM-1, ICAM-1, and E-selectin in dependence on aging. *Gerontology,* 49(5), p 293-300. doi: 10.1159/000071710.

Riddell, N. E. *et al.* (2015) Multifunctional cytomegalovirus (CMV)-specific CD8(+) T cells are not restricted by telomere-related senescence in young or old adults. *Immunology,* 144(4), p 549-560. doi: 10.1111/imm.12409.

Riley, R. L., Kruger, M. G. and Elia, J. (1991) B cell precursors are decreased in senescent BALB/c mice, but retain normal mitotic activity in vivo and in vitro. *Clin Immunol Immunopathol,* 59(2), p 301-313. doi: 10.1016/0090-1229(91)90026-7.

Ritzel, R. M. *et al.* (2016) Age-Associated Resident Memory CD8 T Cells in the Central Nervous System Are Primed To Potentiate Inflammation after Ischemic Brain Injury. *J Immunol,* 196(8), p 3318-3330. doi: 10.4049/jimmunol.1502021.

Rivera-Nieves, J. *et al.* (2006) Critical role of endothelial P-selectin glycoprotein ligand 1 in chronic murine ileitis. *J Exp Med,* 203(4), p 907-917. doi: 10.1084/jem.20052530.

Roberts, A. D., Ely, K. H. and Woodland, D. L. (2005) Differential contributions of central and effector memory T cells to recall responses. *J Exp Med,* 202(1), p 123-133. doi: 10.1084/jem.20050137.

Rodriguez-Zhurbenko, N. *et al.* (2019) Human B-1 Cells and B-1 Cell Antibodies Change With Advancing Age. *Front Immunol,* 10(p 483. doi: 10.3389/fimmu.2019.00483.

Rodriguez, I. J. *et al.* (2020) Immunosenescence Study of T Cells: A Systematic Review. *Front Immunol,* 11(p 604591. doi: 10.3389/fimmu.2020.604591.

Rodriguez, L. G. and Guan, J. L. (2005) 14-3-3 regulation of cell spreading and migration requires a functional amphipathic groove. *J Cell Physiol,* 202(1), p 285-294. doi: 10.1002/jcp.20122.

Rom, I. and Scalia, R. (2013) Aging-associated Calpain Activation Increases Leukocyte Trafficking in the Microcirculation. *The FASEB Journal,* 27(687), p 16-687. doi: 10.1096/fasebj.27.1_supplement.687.16.

Romagnani, S. (2000) T-cell subsets (Th1 versus Th2). *Ann Allergy Asthma Immunol,* 85(1), p 9-18; quiz 18, 21. doi: 10.1016/S1081-1206(10)62426-X.

Rose, O. *et al.* (1995) Contactus adherens, a special type of plaque-bearing adhering junction containing M-cadherin, in the granule cell layer of the cerebellar glomerulus. *Proc Natl Acad Sci U S A,* 92(13), p 6022-6026. doi: 10.1073/pnas.92.13.6022.

Rosenkranz, D. *et al.* (2007) Higher frequency of regulatory T cells in the elderly and increased suppressive activity in neurodegeneration. *J Neuroimmunol,* 188(1-2), p 117-127. doi: 10.1016/j.jneuroim.2007.05.011.

Rossi, M. I. *et al.* (2003) B lymphopoiesis is active throughout human life, but there are developmental age-related changes. *Blood,* 101(2), p 576-584. doi: 10.1182/blood-2002-03-0896.

Roviezzo, F. *et al.* (2011) Sphingosine-1-phosphate modulates vascular permeability and cell recruitment in acute inflammation in vivo. *J Pharmacol Exp Ther,* 337(3), p 830-837. doi: 10.1124/jpet.111.179168.

Roy, A. *et al.* (2013) Regulation of cyclic AMP response element binding and hippocampal plasticity-related genes by peroxisome proliferator-activated receptor alpha. *Cell Rep,* 4(4), p 724-737. doi: 10.1016/j.celrep.2013.07.028.

Rubtsov, A. V. *et al.* (2011) Toll-like receptor 7 (TLR7)-driven accumulation of a novel CD11c(+) B-cell population is important for the development of autoimmunity. *Blood,* 118(5), p 1305-1315. doi: 10.1182/blood-2011-01-331462.

Rubtsova, K. *et al.* (2015) Age-Associated B Cells: A T-bet-Dependent Effector with Roles in Protective and Pathogenic Immunity. *J Immunol,* 195(5), p 1933-1937. doi: 10.4049/jimmunol.1501209.

Ruby, C. E. and Weinberg, A. D. (2009) OX40-enhanced tumor rejection and effector T cell differentiation decreases with age. *J Immunol,* 182(3), p 1481-1489. doi: 10.4049/jimmunol.182.3.1481.

Rufer, N. *et al.* (1999) Telomere fluorescence measurements in granulocytes and T lymphocyte subsets point to a high turnover of hematopoietic stem cells and memory T cells in early childhood. *J Exp Med,* 190(2), p 157-167. doi: 10.1084/jem.190.2.157.

Rufer, N. *et al.* (2003) Ex vivo characterization of human CD8+ T subsets with distinct replicative history and partial effector functions. *Blood,* 102(5), p 1779-1787. doi: 10.1182/blood-2003-02-0420.

Safiri, S. *et al.* (2019) Global, regional and national burden of rheumatoid arthritis 1990-2017: a systematic analysis of the Global Burden of Disease study 2017. *Ann Rheum Dis,* 78(11), p 1463-1471. doi: 10.1136/annrheumdis-2019-215920.

Sakaguchi, S. (2005) Naturally arising Foxp3-expressing CD25+CD4+ regulatory T cells in immunological tolerance to self and non-self. *Nat Immunol,* 6(4), p 345-352. doi: 10.1038/ni1178.

Salminen, A. and Kaarniranta, K. (2012) AMP-activated protein kinase (AMPK) controls the aging process via an integrated signaling network. *Ageing Res Rev,* 11(2), p 230-241. doi: 10.1016/j.arr.2011.12.005.

Salminen, A., Kaarniranta, K. and Kauppinen, A. (2016) Age-related changes in AMPK activation: Role for AMPK phosphatases and inhibitory phosphorylation by upstream signaling pathways. *Ageing Res Rev,* 28(p 15-26. doi: 10.1016/j.arr.2016.04.003.

Salvioli, S. *et al.* (2006) Inflamm-aging, cytokines and aging: state of the art, new hypotheses on the role of mitochondria and new perspectives from systems biology. *Curr Pharm Des,* 12(24), p 3161-3171. doi: 10.2174/138161206777947470.

Samaranayake, H. *et al.* (2009) Challenges in monoclonal antibody-based therapies. *Ann Med,* 41(5), p 322-331. doi: 10.1080/07853890802698842.

Sandor, A. M., Jacobelli, J. and Friedman, R. S. (2019) Immune cell trafficking to the islets during type 1 diabetes. *Clin Exp Immunol,* 198(3), p 314-325. doi: 10.1111/cei.13353.

Sansoni, P. *et al.* (1993) Lymphocyte subsets and natural killer cell activity in healthy old people and centenarians. *Blood,* 82(9), p 2767-2773. doi:

Santoro, M. M., Gaudino, G. and Marchisio, P. C. (2003) The MSP receptor regulates alpha6beta4 and alpha3beta1 integrins via 14-3-3 proteins in keratinocyte migration. *Dev Cell,* 5(2), p 257-271. doi: 10.1016/s1534-5807(03)00201-6.

Sanz, I. *et al.* (2019) Challenges and Opportunities for Consistent Classification of Human B Cell and Plasma Cell Populations. *Front Immunol,* 10(p 2458. doi: 10.3389/fimmu.2019.02458.

Sapey, E. *et al.* (2014) Phosphoinositide 3-kinase inhibition restores neutrophil accuracy in the elderly: toward targeted treatments for immunosenescence. *Blood,* 123(2), p 239-248. doi: 10.1182/blood-2013-08-519520.

Sato, I. *et al.* (1993) Reduction of nitric oxide producing activity associated with in vitro aging in cultured human umbilical vein endothelial cell. *Biochem Biophys Res Commun,* 195(2), p 1070-1076. doi: 10.1006/bbrc.1993.2153.

Schaum, N. *et al.* (2020) Ageing hallmarks exhibit organ-specific temporal signatures. *Nature,* 583(7817), p 596-602. doi: 10.1038/s41586-020-2499-y.

Scheiermann, C., Kunisaki, Y. and Frenette, P. S. (2013) Circadian control of the immune system. *Nat Rev Immunol,* 13(3), p 190-198. doi: 10.1038/nri3386.

Schenkel, A. R. *et al.* (2002) CD99 plays a major role in the migration of monocytes through endothelial junctions. *Nat Immunol,* 3(2), p 143-150. doi: 10.1038/ni749.

Schenkel, A. R., Mamdouh, Z. and Muller, W. A. (2004) Locomotion of monocytes on endothelium is a critical step during extravasation. *Nat Immunol,* 5(4), p 393-400. doi: 10.1038/ni1051.

Schindowski, K. *et al.* (2000) Age-related changes of apoptotic cell death in human lymphocytes. *Neurobiol Aging,* 21(5), p 661-670. doi: 10.1016/s0197-4580(00)00171-8.

Scotland, R. S. *et al.* (2011) Sex differences in resident immune cell phenotype underlie more efficient acute inflammatory responses in female mice. *Blood,* 118(22), p 5918-5927. doi: 10.1182/blood-2011-03-340281.

Sempowski, G. D. *et al.* (2000) Leukemia inhibitory factor, oncostatin M, IL-6, and stem cell factor mRNA expression in human thymus increases with age and is associated with thymic atrophy. *J Immunol,* 164(4), p 2180-2187. doi: 10.4049/jimmunol.164.4.2180.

Sempowski, G. D. *et al.* (2002) Leukemia inhibitory factor is a mediator of Escherichia coli lipopolysaccharide-induced acute thymic atrophy. *Eur J Immunol,* 32(11), p 3066-3070. doi: 10.1002/1521-4141(200211)32:11<3066::AID-IMMU3066>3.0.CO;2-J.

Sendama, W. (2020) The effect of ageing on the resolution of inflammation. *Ageing Res Rev,* 57(p 101000. doi: 10.1016/j.arr.2019.101000.

Seo, S. B. *et al.* (2018) 14-3-3beta Depletion Drives a Senescence Program in Glioblastoma Cells Through the ERK/SKP2/p27 Pathway. *Mol Neurobiol,* 55(2), p 1259-1270. doi: 10.1007/s12035-017-0407-8.

Setoguchi, R. (2016) IL-15 boosts the function and migration of human terminally differentiated CD8+ T cells by inducing a unique gene signature. *Int Immunol,* 28(6), p 293-305. doi: 10.1093/intimm/dxw004.

Shamri, R. *et al.* (2005) Lymphocyte arrest requires instantaneous induction of an extended LFA-1 conformation mediated by endothelium-bound chemokines. *Nat Immunol,* 6(5), p 497-506. doi: 10.1038/ni1194.

Shanley, D. P. *et al.* (2009) An evolutionary perspective on the mechanisms of immunosenescence. *Trends Immunol,* 30(7), p 374-381. doi: 10.1016/j.it.2009.05.001.

Shapiro, L. and Scherer, P. E. (1998) The crystal structure of a complement-1q family protein suggests an evolutionary link to tumor necrosis factor. *Curr Biol,* 8(6), p 335-338. doi: 10.1016/s0960-9822(98)70133-2.

Sharma, S., Dominguez, A. L. and Lustgarten, J. (2006) High accumulation of T regulatory cells prevents the activation of immune responses in aged animals. *J Immunol,* 177(12), p 8348-8355. doi: 10.4049/jimmunol.177.12.8348.

Shaw, S. K. *et al.* (2001) Real-time imaging of vascular endothelial-cadherin during leukocyte transmigration across endothelium. *J Immunol,* 167(4), p 2323-2330. doi: 10.4049/jimmunol.167.4.2323.

Sherry, N. *et al.* (2011) Teplizumab for treatment of type 1 diabetes (Protege study): 1-year results from a randomised, placebo-controlled trial. *Lancet,* 378(9790), p 487-497. doi: 10.1016/S0140-6736(11)60931-8.

Shevach, E. M. (2002) CD4+ CD25+ suppressor T cells: more questions than answers. *Nat Rev Immunol,* 2(6), p 389-400. doi: 10.1038/nri821.

Shevach, E. M. (2009) Mechanisms of foxp3+ T regulatory cell-mediated suppression. *Immunity,* 30(5), p 636-645. doi: 10.1016/j.immuni.2009.04.010.

Shimatani, K. *et al.* (2009) PD-1+ memory phenotype CD4+ T cells expressing C/EBPalpha underlie T cell immunodepression in senescence and leukemia. *Proc Natl Acad Sci U S A,* 106(37), p 15807-15812. doi: 10.1073/pnas.0908805106.

Shimomura, A. *et al.* (1996) Calmodulin-dependent protein kinase II potentiates transcriptional activation through activating transcription factor 1 but not cAMP

response element-binding protein. *J Biol Chem,* 271(30), p 17957-17960. doi: 10.1074/jbc.271.30.17957.
Shin, J. Y. *et al.* (2009) Vascular endothelial growth factor-induced chemotaxis and IL-10 from T cells. *Cell Immunol,* 256(1-2), p 72-78. doi: 10.1016/j.cellimm.2009.01.006.
Shin, M. H. *et al.* (2016) Activation of Peroxisome Proliferator-Activated Receptor Alpha Improves Aged and UV-Irradiated Skin by Catalase Induction. *PLoS One,* 11(9), p e0162628. doi: 10.1371/journal.pone.0162628.
Shirakawa, K. *et al.* (2016) Obesity accelerates T cell senescence in murine visceral adipose tissue. *J Clin Invest,* 126(12), p 4626-4639. doi: 10.1172/JCI88606.
Shlomchik, M. J. and Weisel, F. (2012) Germinal center selection and the development of memory B and plasma cells. *Immunol Rev,* 247(1), p 52-63. doi: 10.1111/j.1600-065X.2012.01124.x.
Shulman, Z. *et al.* (2009) Lymphocyte crawling and transendothelial migration require chemokine triggering of high-affinity LFA-1 integrin. *Immunity,* 30(3), p 384-396. doi: 10.1016/j.immuni.2008.12.020.
Silva, G. C. *et al.* (2017) Replicative senescence promotes prothrombotic responses in endothelial cells: Role of NADPH oxidase- and cyclooxygenase-derived oxidative stress. *Exp Gerontol,* 93(p 7-15. doi: 10.1016/j.exger.2017.04.006.
Simon, A. K., Hollander, G. A. and McMichael, A. (2015) Evolution of the immune system in humans from infancy to old age. *Proceedings of the Royal Society B: Biological Sciences,* 282(1821), p 20143085. doi: 10.1098/rspb.2014.3085.
Sims, G. P. *et al.* (2005) Identification and characterization of circulating human transitional B cells. *Blood,* 105(11), p 4390-4398. doi: 10.1182/blood-2004-11-4284.
Sixt, M. *et al.* (2001) Endothelial cell laminin isoforms, laminins 8 and 10, play decisive roles in T cell recruitment across the blood-brain barrier in experimental autoimmune encephalomyelitis. *J Cell Biol,* 153(5), p 933-946. doi: 10.1083/jcb.153.5.933.
Smart, B. A., Rao, K. M. and Cohen, H. J. (1993) Age-related increase in phorbol myristate acetate-induced lymphocyte adhesion to vascular endothelium. *Mech Ageing Dev,* 72(1), p 77-87. doi: 10.1016/0047-6374(93)90133-c.
Solana, R. *et al.* (2012) CMV and Immunosenescence: from basics to clinics. *Immun Ageing,* 9(1), p 23. doi: 10.1186/1742-4933-9-23.
Song, H., Chan, J. and Rovin, B. H. (2009) Induction of chemokine expression by adiponectin in vitro is isoform dependent. *Transl Res,* 154(1), p 18-26. doi: 10.1016/j.trsl.2009.04.003.
Song, H. J. *et al.* (2014) Gender differences in adiponectin levels and body composition in older adults: Hallym aging study. *BMC Geriatr,* 14(p 8. doi: 10.1186/1471-2318-14-8.
Spaulding, C. C., Walford, R. L. and Effros, R. B. (1997) Calorie restriction inhibits the age-related dysregulation of the cytokines TNF-alpha and IL-6 in C3B10RF1 mice. *Mech Ageing Dev,* 93(1-3), p 87-94. doi: 10.1016/s0047-6374(96)01824-6.
Spiegel, S. and Milstien, S. (2011) The outs and the ins of sphingosine-1-phosphate in immunity. *Nat Rev Immunol,* 11(6), p 403-415. doi: 10.1038/nri2974.
Stall, A. M., Wells, S. M. and Lam, K. P. (1996) B-1 cells: unique origins and functions. *Semin Immunol,* 8(1), p 45-59. doi: 10.1006/smim.1996.0007.

Stanhewicz, A. E., Wenner, M. M. and Stachenfeld, N. S. (2018) Sex differences in endothelial function important to vascular health and overall cardiovascular disease risk across the lifespan. *Am J Physiol Heart Circ Physiol,* 315(6), p H1569-H1588. doi: 10.1152/ajpheart.00396.2018.

Stanworth, R. D. and Jones, T. H. (2008) Testosterone for the aging male; current evidence and recommended practice. *Clin Interv Aging,* 3(1), p 25-44. doi: 10.2147/cia.s190.

Staples, J. E. *et al.* (1999) Estrogen receptor alpha is necessary in thymic development and estradiol-induced thymic alterations. *J Immunol,* 163(8), p 4168-4174. doi:

Stark, K. *et al.* (1999) Seroprevalence and determinants of diphtheria, tetanus and poliomyelitis antibodies among adults in Berlin, Germany. *Vaccine,* 17(7-8), p 844-850. doi:

Stephan, R. P., Sanders, V. M. and Witte, P. L. (1996) Stage-specific alterations in murine B lymphopoiesis with age. *Int Immunol,* 8(4), p 509-518. doi: 10.1093/intimm/8.4.509.

Stephens, L. A. *et al.* (2001) Human CD4+CD25+ thymocytes and peripheral T cells have immune suppressive activity in vitro. *Eur J Immunol,* 31(4), p 1247-1254. doi: 10.1002/1521-4141(200104)31:4<1247::aid-immu1247>3.0.co;2-m.

Stern, D. M. *et al.* (1991) Endothelium and regulation of coagulation. *Diabetes Care,* 14(2), p 160-166. doi: 10.2337/diacare.14.2.160.

Steven, J. L. (1892) Metchnikoff on the Comparative Pathology of Inflammation. *Glasgow Med J,* 38(3), p 195-205. doi:

Stichel, C. C. and Luebbert, H. (2007) Inflammatory processes in the aging mouse brain: participation of dendritic cells and T-cells. *Neurobiol Aging,* 28(10), p 1507-1521. doi: 10.1016/j.neurobiolaging.2006.07.022.

Stohlawetz, P. *et al.* (1996) The effect of age on the transendothelial migration of human T lymphocytes. *Scand J Immunol,* 44(5), p 530-534. doi: 10.1046/j.1365-3083.1996.d01-331.x.

Stott, D. J. *et al.* (2009) Adipocytokines and risk of stroke in older people: a nested case-control study. *Int J Epidemiol,* 38(1), p 253-261. doi: 10.1093/ije/dyn215.

Straub, L. G. and Scherer, P. E. (2019) Metabolic Messengers: Adiponectin. *Nat Metab,* 1(3), p 334-339. doi: 10.1038/s42255-019-0041-z.

Su, Y. W. *et al.* (2011) 14-3-3sigma regulates B-cell homeostasis through stabilization of FOXO1. *Proc Natl Acad Sci U S A,* 108(4), p 1555-1560. doi: 10.1073/pnas.1017729108.

Sundd, P. *et al.* (2011) Biomechanics of leukocyte rolling. *Biorheology,* 48(1), p 1-35. doi: 10.3233/BIR-2011-0579.

Sung, B. *et al.* (2004) Modulation of PPAR in aging, inflammation, and calorie restriction. *J Gerontol A Biol Sci Med Sci,* 59(10), p 997-1006. doi: 10.1093/gerona/59.10.b997.

Suri, A. *et al.* (2005) Natural peptides selected by diabetogenic DQ8 and murine I-A(g7) molecules show common sequence specificity. *J Clin Invest,* 115(8), p 2268-2276. doi: 10.1172/JCI25350.

Sutherland, J. S. *et al.* (2005) Activation of thymic regeneration in mice and humans following androgen blockade. *J Immunol,* 175(4), p 2741-2753. doi: 10.4049/jimmunol.175.4.2741.

Syed, M. A. *et al.* (2022) Optimising the selection of outcomes for healthy ageing trials: a mixed methods study. *Geroscience,* 44(6), p 2585-2609. doi: 10.1007/s11357-022-00690-5.
Szakal, A. K. *et al.* (1990) Kinetics of germinal center development in lymph nodes of young and aging immune mice. *Anat Rec,* 227(4), p 475-485. doi: 10.1002/ar.1092270411.
Tabula Muris, C. (2020) A single-cell transcriptomic atlas characterizes ageing tissues in the mouse. *Nature,* 583(7817), p 590-595. doi: 10.1038/s41586-020-2496-1.
Takemura, Y. *et al.* (2007) Adiponectin modulates inflammatory reactions via calreticulin receptor-dependent clearance of early apoptotic bodies. *J Clin Invest,* 117(2), p 375-386. doi: 10.1172/JCI29709.
Tan, C. S. and Koralnik, I. J. (2010) Progressive multifocal leukoencephalopathy and other disorders caused by JC virus: clinical features and pathogenesis. *Lancet Neurol,* 9(4), p 425-437. doi: 10.1016/S1474-4422(10)70040-5.
Tang, C. H. *et al.* (2007) Adiponectin enhances IL-6 production in human synovial fibroblast via an AdipoR1 receptor, AMPK, p38, and NF-kappa B pathway. *J Immunol,* 179(8), p 5483-5492. doi: 10.4049/jimmunol.179.8.5483.
Tang, Q. and Bluestone, J. A. (2008) The Foxp3+ regulatory T cell: a jack of all trades, master of regulation. *Nat Immunol,* 9(3), p 239-244. doi: 10.1038/ni1572.
Telford, W. G. and Miller, R. A. (1999) Aging increases CD8 T cell apoptosis induced by hyperstimulation but decreases apoptosis induced by agonist withdrawal in mice. *Cell Immunol,* 191(2), p 131-138. doi: 10.1006/cimm.1998.1422.
Thomas, R., Wang, W. and Su, D. M. (2020) Contributions of Age-Related Thymic Involution to Immunosenescence and Inflammaging. *Immun Ageing,* 17(p 2. doi: 10.1186/s12979-020-0173-8.
Thome, J. J. *et al.* (2016) Longterm maintenance of human naive T cells through in situ homeostasis in lymphoid tissue sites. *Sci Immunol,* 1(6), p doi: 10.1126/sciimmunol.aah6506.
Thornton, A. M. and Shevach, E. M. (2000) Suppressor effector function of CD4+CD25+ immunoregulatory T cells is antigen nonspecific. *J Immunol,* 164(1), p 183-190. doi: 10.4049/jimmunol.164.1.183.
Tian, Y. *et al.* (2017) Unique phenotypes and clonal expansions of human CD4 effector memory T cells re-expressing CD45RA. *Nat Commun,* 8(1), p 1473. doi: 10.1038/s41467-017-01728-5.
Ting, K. K. *et al.* (2021) The aging endothelium. *Vasc Biol,* 3(1), p R35-R47. doi: 10.1530/VB-20-0013.
Toapanta, F. R. and Ross, T. M. (2009) Impaired immune responses in the lungs of aged mice following influenza infection. *Respir Res,* 10(p 112. doi: 10.1186/1465-9921-10-112.
Tonegawa, S. (1983) Somatic generation of antibody diversity. *Nature,* 302(5909), p 575-581. doi: 10.1038/302575a0.
Topp, M. S. *et al.* (2003) Restoration of CD28 expression in CD28- CD8+ memory effector T cells reconstitutes antigen-induced IL-2 production. *J Exp Med,* 198(6), p 947-955. doi: 10.1084/jem.20021288.
Tortorella, C. *et al.* (2004) Role of defective ERK phosphorylation in the impaired GM-CSF-induced oxidative response of neutrophils in elderly humans. *Mech Ageing Dev,* 125(8), p 539-546. doi: 10.1016/j.mad.2004.06.001.

Tousoulis, D. *et al.* (2012) The role of nitric oxide on endothelial function. *Curr Vasc Pharmacol,* 10(1), p 4-18. doi: 10.2174/157016112798829760.
Tran, T. M. *et al.* (2009) TNFalpha-induced macrophage death via caspase-dependent and independent pathways. *Apoptosis,* 14(3), p 320-332. doi: 10.1007/s10495-009-0311-4.
Trowbridge, H. O. (1990) Immunological aspects of chronic inflammation and repair. *J Endod,* 16(2), p 54-61. doi: 10.1016/S0099-2399(06)81564-5.
True, A. L., Rahman, A. and Malik, A. B. (2000) Activation of NF-kappaB induced by H(2)O(2) and TNF-alpha and its effects on ICAM-1 expression in endothelial cells. *Am J Physiol Lung Cell Mol Physiol,* 279(2), p L302-311. doi: 10.1152/ajplung.2000.279.2.L302.
Tsai, J. S. *et al.* (2013) Plasma adiponectin levels correlate positively with an increasing number of components of frailty in male elders. *PLoS One,* 8(2), p e56250. doi: 10.1371/journal.pone.0056250.
Tsao, T. S. *et al.* (2003) Role of disulfide bonds in Acrp30/adiponectin structure and signaling specificity. Different oligomers activate different signal transduction pathways. *J Biol Chem,* 278(50), p 50810-50817. doi: 10.1074/jbc.M309469200.
Tsuchida, A. *et al.* (2004) Insulin/Foxo1 pathway regulates expression levels of adiponectin receptors and adiponectin sensitivity. *J Biol Chem,* 279(29), p 30817-30822. doi: 10.1074/jbc.M402367200.
Turner, V. M. and Mabbott, N. A. (2017) Ageing adversely affects the migration and function of marginal zone B cells. *Immunology,* 151(3), p 349-362. doi: 10.1111/imm.12737.
Uryga, A. K. and Bennett, M. R. (2016) Ageing induced vascular smooth muscle cell senescence in atherosclerosis. *J Physiol,* 594(8), p 2115-2124. doi: 10.1113/JP270923.
Vaena, S. *et al.* (2021) Aging-dependent mitochondrial dysfunction mediated by ceramide signaling inhibits antitumor T cell response. *Cell Rep,* 35(5), p 109076. doi: 10.1016/j.celrep.2021.109076.
Valenzuela, H. F. and Effros, R. B. (2002) Divergent telomerase and CD28 expression patterns in human CD4 and CD8 T cells following repeated encounters with the same antigenic stimulus. *Clin Immunol,* 105(2), p 117-125. doi: 10.1006/clim.2002.5271.
van der Geest, K. S. *et al.* (2014) Aging disturbs the balance between effector and regulatory CD4+ T cells. *Exp Gerontol,* 60(p 190-196. doi: 10.1016/j.exger.2014.11.005.
van Deursen, J. M. (2014) The role of senescent cells in ageing. *Nature,* 509(7501), p 439-446. doi: 10.1038/nature13193.
Verma, K. *et al.* (2017) Human CD8+ CD57- TEMRA cells: Too young to be called "old". *PLoS One,* 12(5), p e0177405. doi: 10.1371/journal.pone.0177405.
Veronese, F. M. and Pasut, G. (2005) PEGylation, successful approach to drug delivery. *Drug Discov Today,* 10(21), p 1451-1458. doi: 10.1016/S1359-6446(05)03575-0.
Vignali, D. A., Collison, L. W. and Workman, C. J. (2008) How regulatory T cells work. *Nat Rev Immunol,* 8(7), p 523-532. doi: 10.1038/nri2343.

Voehringer, D. *et al.* (2001) Viral infections induce abundant numbers of senescent CD8 T cells. *J Immunol,* 167(9), p 4838-4843. doi: 10.4049/jimmunol.167.9.4838.
Voehringer, D., Koschella, M. and Pircher, H. (2002) Lack of proliferative capacity of human effector and memory T cells expressing killer cell lectinlike receptor G1 (KLRG1). *Blood,* 100(10), p 3698-3702. doi: 10.1182/blood-2002-02-0657.
Voigt, E. A. *et al.* (2019) Sex Differences in Older Adults' Immune Responses to Seasonal Influenza Vaccination. *Front Immunol,* 10(p 180. doi: 10.3389/fimmu.2019.00180.
Voisin, M. B., Probstl, D. and Nourshargh, S. (2010) Venular basement membranes ubiquitously express matrix protein low-expression regions: characterization in multiple tissues and remodeling during inflammation. *Am J Pathol,* 176(1), p 482-495. doi: 10.2353/ajpath.2010.090510.
von Andrian, U. H. *et al.* (1991) Two-step model of leukocyte-endothelial cell interaction in inflammation: distinct roles for LECAM-1 and the leukocyte beta 2 integrins in vivo. *Proc Natl Acad Sci U S A,* 88(17), p 7538-7542. doi: 10.1073/pnas.88.17.7538.
Waki, H. *et al.* (2005) Generation of globular fragment of adiponectin by leukocyte elastase secreted by monocytic cell line THP-1. *Endocrinology,* 146(2), p 790-796. doi: 10.1210/en.2004-1096.
Walling, B. L. and Kim, M. (2018) LFA-1 in T Cell Migration and Differentiation. *Front Immunol,* 9(p 952. doi: 10.3389/fimmu.2018.00952.
Wang, C. *et al.* (2008a) GPR30 contributes to estrogen-induced thymic atrophy. *Mol Endocrinol,* 22(3), p 636-648. doi: 10.1210/me.2007-0359.
Wang, C. *et al.* (2014) Rapamycin antagonizes TNF induction of VCAM-1 on endothelial cells by inhibiting mTORC2. *J Exp Med,* 211(3), p 395-404. doi: 10.1084/jem.20131125.
Wang, C. *et al.* (2009) Deleting the 14-3-3 protein Bmh1 extends life span in Saccharomyces cerevisiae by increasing stress response. *Genetics,* 183(4), p 1373-1384. doi: 10.1534/genetics.109.107797.
Wang, M. *et al.* (2021) Programmed PPAR-alpha downregulation induces inflammaging by suppressing fatty acid catabolism in monocytes. *iScience,* 24(7), p 102766. doi: 10.1016/j.isci.2021.102766.
Wang, S. *et al.* (2006) Venular basement membranes contain specific matrix protein low expression regions that act as exit points for emigrating neutrophils. *J Exp Med,* 203(6), p 1519-1532. doi: 10.1084/jem.20051210.
Wang, Y. *et al.* (2008b) Post-translational modifications of adiponectin: mechanisms and functional implications. *Biochem J,* 409(3), p 623-633. doi: 10.1042/BJ20071492.
Watson, C. *et al.* (1996) IL-6 acts on endothelial cells to preferentially increase their adherence for lymphocytes. *Clin Exp Immunol,* 105(1), p 112-119. doi: 10.1046/j.1365-2249.1996.d01-717.x.
Wegmann, F. *et al.* (2006) ESAM supports neutrophil extravasation, activation of Rho, and VEGF-induced vascular permeability. *J Exp Med,* 203(7), p 1671-1677. doi: 10.1084/jem.20060565.
Wei, J. *et al.* (1992) Increase of plasma IL-6 concentration with age in healthy subjects. *Life Sci,* 51(25), p 1953-1956. doi: 10.1016/0024-3205(92)90112-3.

Wei, S., Kryczek, I. and Zou, W. (2006) Regulatory T-cell compartmentalization and trafficking. *Blood,* 108(2), p 426-431. doi: 10.1182/blood-2006-01-0177.
Weltevrede, M. *et al.* (2016) Cytomegalovirus persistence and T-cell immunosenescence in people aged fifty and older: A systematic review. *Exp Gerontol,* 77(p 87-95. doi: 10.1016/j.exger.2016.02.005.
Weninger, W. *et al.* (2001) Migratory properties of naive, effector, and memory CD8(+) T cells. *J Exp Med,* 194(7), p 953-966. doi: 10.1084/jem.194.7.953.
Wenisch, C. *et al.* (2000) Effect of age on human neutrophil function. *J Leukoc Biol,* 67(1), p 40-45. doi: 10.1002/jlb.67.1.40.
Werle, M. and Bernkop-Schnurch, A. (2006) Strategies to improve plasma half life time of peptide and protein drugs. *Amino Acids,* 30(4), p 351-367. doi: 10.1007/s00726-005-0289-3.
Westera, L. *et al.* (2015) Lymphocyte maintenance during healthy aging requires no substantial alterations in cellular turnover. *Aging Cell,* 14(2), p 219-227. doi: 10.1111/acel.12311.
Weyand, C. M. *et al.* (1998) Functional properties of CD4+ CD28- T cells in the aging immune system. *Mech Ageing Dev,* 102(2-3), p 131-147. doi: 10.1016/s0047-6374(97)00161-9.
Wiggin, G. R. *et al.* (2002) MSK1 and MSK2 are required for the mitogen- and stress-induced phosphorylation of CREB and ATF1 in fibroblasts. *Mol Cell Biol,* 22(8), p 2871-2881. doi: 10.1128/MCB.22.8.2871-2881.2002.
Wilker, E. and Yaffe, M. B. (2004) 14-3-3 Proteins--a focus on cancer and human disease. *J Mol Cell Cardiol,* 37(3), p 633-642. doi: 10.1016/j.yjmcc.2004.04.015.
Willinger, T. *et al.* (2005) Molecular signatures distinguish human central memory from effector memory CD8 T cell subsets. *J Immunol,* 175(9), p 5895-5903. doi: 10.4049/jimmunol.175.9.5895.
Wilson, D. *et al.* (2020) Frailty Is Associated With Neutrophil Dysfunction Which Is Correctable With Phosphoinositol-3-Kinase Inhibitors. *J Gerontol A Biol Sci Med Sci,* 75(12), p 2320-2325. doi: 10.1093/gerona/glaa216.
Wing, K. *et al.* (2002) Characterization of human CD25+ CD4+ T cells in thymus, cord and adult blood. *Immunology,* 106(2), p 190-199. doi: 10.1046/j.1365-2567.2002.01412.x.
Wolf, A. M. *et al.* (2004) Adiponectin induces the anti-inflammatory cytokines IL-10 and IL-1RA in human leukocytes. *Biochem Biophys Res Commun,* 323(2), p 630-635. doi: 10.1016/j.bbrc.2004.08.145.
Wols, H. A. *et al.* (2010) Migration of immature and mature B cells in the aged microenvironment. *Immunology,* 129(2), p 278-290. doi: 10.1111/j.1365-2567.2009.03182.x.
Xiong, Y. and Hla, T. (2014) S1P control of endothelial integrity. *Curr Top Microbiol Immunol,* 378(p 85-105. doi: 10.1007/978-3-319-05879-5_4.
Xu, W. and Larbi, A. (2017) Markers of T Cell Senescence in Humans. *Int J Mol Sci,* 18(8), p doi: 10.3390/ijms18081742.
Yadav, R. *et al.* (2003) Migration of leukocytes through the vessel wall and beyond. *Thromb Haemost,* 90(4), p 598-606. doi: 10.1160/TH03-04-0220.
Yager, E. J. *et al.* (2008) Age-associated decline in T cell repertoire diversity leads to holes in the repertoire and impaired immunity to influenza virus. *J Exp Med,* 205(3), p 711-723. doi: 10.1084/jem.20071140.

Yamaguchi, N. *et al.* (2005) Adiponectin inhibits Toll-like receptor family-induced signaling. *FEBS Lett,* 579(30), p 6821-6826. doi: 10.1016/j.febslet.2005.11.019.
Yamamoto, S. *et al.* (2015) Inflammation-induced endothelial cell-derived extracellular vesicles modulate the cellular status of pericytes. *Sci Rep,* 5(p 8505. doi: 10.1038/srep08505.
Yamauchi, T. *et al.* (2014) Adiponectin receptors: a review of their structure, function and how they work. *Best Pract Res Clin Endocrinol Metab,* 28(1), p 15-23. doi: 10.1016/j.beem.2013.09.003.
Yamauchi, T. *et al.* (2003) Cloning of adiponectin receptors that mediate antidiabetic metabolic effects. *Nature,* 423(6941), p 762-769. doi: 10.1038/nature01705.
Yamauchi, T. *et al.* (2002) Adiponectin stimulates glucose utilization and fatty-acid oxidation by activating AMP-activated protein kinase. *Nat Med,* 8(11), p 1288-1295. doi: 10.1038/nm788.
Yamauchi, T. *et al.* (2007) Targeted disruption of AdipoR1 and AdipoR2 causes abrogation of adiponectin binding and metabolic actions. *Nat Med,* 13(3), p 332-339. doi: 10.1038/nm1557.
Yan, J. *et al.* (2010) The effect of ageing on human lymphocyte subsets: comparison of males and females. *Immun Ageing,* 7(p 4. doi: 10.1186/1742-4933-7-4.
Yanaba, K. *et al.* (2008) A regulatory B cell subset with a unique CD1dhiCD5+ phenotype controls T cell-dependent inflammatory responses. *Immunity,* 28(5), p 639-650. doi: 10.1016/j.immuni.2008.03.017.
Yanaba, K. *et al.* (2009) The development and function of regulatory B cells expressing IL-10 (B10 cells) requires antigen receptor diversity and TLR signals. *J Immunol,* 182(12), p 7459-7472. doi: 10.4049/jimmunol.0900270.
Yang, J. *et al.* (2016) Discover the network underlying the connections between aging and age-related diseases. *Sci Rep,* 6(p 32566. doi: 10.1038/srep32566.
Yang, X. *et al.* (2020) Age-Related Gene Alteration in Naive and Memory T cells Using Precise Age-Tracking Model. *Front Cell Dev Biol,* 8(p 624380. doi: 10.3389/fcell.2020.624380.
Yang, Y. and Wilson, J. M. (1996) CD40 ligand-dependent T cell activation: requirement of B7-CD28 signaling through CD40. *Science,* 273(5283), p 1862-1864. doi: 10.1126/science.273.5283.1862.
Yi, H. S. *et al.* (2019) T-cell senescence contributes to abnormal glucose homeostasis in humans and mice. *Cell Death Dis,* 10(3), p 249. doi: 10.1038/s41419-019-1494-4.
Yoda-Murakami, M. *et al.* (2001) Change in expression of GBP28/adiponectin in carbon tetrachloride-administrated mouse liver. *Biochem Biophys Res Commun,* 285(2), p 372-377. doi: 10.1006/bbrc.2001.5134.
Yokota, T. *et al.* (2000) Adiponectin, a new member of the family of soluble defense collagens, negatively regulates the growth of myelomonocytic progenitors and the functions of macrophages. *Blood,* 96(5), p 1723-1732. doi:
Yoshida, S. *et al.* (2020) The CD153 vaccine is a senotherapeutic option for preventing the accumulation of senescent T cells in mice. *Nat Commun,* 11(1), p 2482. doi: 10.1038/s41467-020-16347-w.
Yousef, H. *et al.* (2019) Aged blood impairs hippocampal neural precursor activity and activates microglia via brain endothelial cell VCAM1. *Nat Med,* 25(6), p 988-1000. doi: 10.1038/s41591-019-0440-4.

Yousefzadeh, M. J. *et al.* (2018) Circulating levels of monocyte chemoattractant protein-1 as a potential measure of biological age in mice and frailty in humans. *Aging Cell,* 17(2), p doi: 10.1111/acel.12706.
Yu, X. *et al.* (2008) Neutralizing antibodies derived from the B cells of 1918 influenza pandemic survivors. *Nature,* 455(7212), p 532-536. doi: 10.1038/nature07231.
Yue, Z. *et al.* (2021) Tissue-resident macrophage inflammaging aggravates homeostasis dysregulation in age-related diseases. *Cell Immunol,* 361(p 104278. doi: 10.1016/j.cellimm.2020.104278.
Yung, R. L. and Mo, R. (2003) Aging is associated with increased human T cell CC chemokine receptor gene expression. *J Interferon Cytokine Res,* 23(10), p 575-582. doi: 10.1089/107999003322485071.
Zhang, N. and Bevan, M. J. (2011) CD8(+) T cells: foot soldiers of the immune system. *Immunity,* 35(2), p 161-168. doi: 10.1016/j.immuni.2011.07.010.
Zhang, Y. *et al.* (2020a) Recombinant Adiponectin Induces the Production of Pro-Inflammatory Chemokines and Cytokines in Circulating Mononuclear Cells and Fibroblast-Like Synoviocytes From Non-Inflamed Subjects. *Front Immunol,* 11(p 569883. doi: 10.3389/fimmu.2020.569883.
Zhang, Z. S. *et al.* (2020b) Research advances in pericyte function and their roles in diseases. *Chin J Traumatol,* 23(2), p 89-95. doi: 10.1016/j.cjtee.2020.02.006.
Zhao, J. *et al.* (2011) Age-related increases in PGD(2) expression impair respiratory DC migration, resulting in diminished T cell responses upon respiratory virus infection in mice. *J Clin Invest,* 121(12), p 4921-4930. doi: 10.1172/JCI59777.
Zhao, L. *et al.* (2007) Changes of CD4+CD25+Foxp3+ regulatory T cells in aged Balb/c mice. *J Leukoc Biol,* 81(6), p 1386-1394. doi: 10.1189/jlb.0506364.
Zhen, X. *et al.* (1999) Age-associated impairment in brain MAPK signal pathways and the effect of caloric restriction in Fischer 344 rats. *J Gerontol A Biol Sci Med Sci,* 54(12), p B539-548. doi: 10.1093/gerona/54.12.b539.
Zheng, Y. *et al.* (2020) A human circulating immune cell landscape in aging and COVID-19. *Protein Cell,* 11(10), p 740-770. doi: 10.1007/s13238-020-00762-2.
Zou, L. *et al.* (2004) Bone marrow is a reservoir for CD4+CD25+ regulatory T cells that traffic through CXCL12/CXCR4 signals. *Cancer Res,* 64(22), p 8451-8455. doi: 10.1158/0008-5472.CAN-04-1987.
Zou, Y. *et al.* (2006) Upregulation of aortic adhesion molecules during aging. *J Gerontol A Biol Sci Med Sci,* 61(3), p 232-244. doi: 10.1093/gerona/61.3.232.

APPENDIX I

T-cell subset	Young % parent population (mean±SEM)	Older % parent population (mean±SEM)	p-value
T-cells (% PBMC)	59.2 ±3.5	57.0 ±1.6	0.573
CD4+ (% T-cells)	62.3 ±6.6	60.9 ±3.8	0.859
CD4+CCR7+CD45RA+ Naive (% CD4+ T-cells)	8.8 ±3.6	4.6 ±1.9	0.319
CD4+CCR7-CD45RA- EM (% CD4+ T-cells)	20.9 ±5.1	19.3 ±1.5	0.759
CD4+CCR7+CD45RA- CM (% CD4+ T-cells)	30.5 ±4.3	50.8 ±6.5	**0.023**
CD4+CCR7-CD45RA+ TEMRA (% CD4+ T-cells)	13.5 ±2.4	22.9 ±4.2	0.066
CD4+CD25+ Treg (% CD4+ T-cells)	3.9 ±0.7	4.8 ±0.3	0.314
CD4+CD27-CD28- Senescent (% CD4+ T-cells)	8.1 ±2.9	6.8 ±2.8	0.754
CD4+CD57+KLRG1+ Senescent (% CD4+ T-cells)	4.3 ±2.1	4.5 ±1.3	0.940
CD8+ (% T-cells)	23.0 ±4.0	21.2 ±6.7	0.822
CD8+CCR7+CD45RA+ Naive (% CD8+ T-cells)	44.7 ±9.1	7.4 ±1.6	**0.002**
CD8+CCR7-CD45RA- EM (% CD8+ T-cells)	33.7 ±10.0	65.7 ±4.7	**0.016**
CD8+CCR7+CD45RA- CM (% CD8+ T-cells)	7.2 ±1.6	11.9 ±2.1	0.114
CD8+CCR7-CD45RA+ TEMRA (% CD8+ T-cells)	10.5 ±1.6	15.1 ±2.6	0.168
CD8+CD27-CD28- Senescent (% CD8+ T-cells)	24.1 ±4.0	36.2 ±5.8	0.117
CD8+KLRG1+CD57+ Senescent (% CD8+ T-cells)	21.9 ±8.5	30.7 ±5.2	0.396

Percentage of T-cell subsets in the PBMC of young and aged donors, determined by flow cytometry. The percentage of circulating T-cells are shown as mean ± standard error of the mean (SEM) of the parent gate population i.e. PBMC, T-cells or $CD4^+$/$CD8^+$ T-cells. Statistical analysis performed using an unpaired t-test to determine the effects of age on circulating T-cell populations. EM, effector memory; CM, central memory; TEMRA, terminally differentiated effector memory T-cells re-expressing CD45RA; Treg, regulatory T-cell.